Low temperature aqueous phase oxidation of alkanes with metal doped zeolites prepared by chemical vapour infiltration

MICHAEL M FORDE

Summary

The low temperature oxidation of methane, ethane and propane to useful oxygenates in the aqueous phase using neat hydrogen peroxide is explored. High catalytic activity of metal doped zeolite catalysts in the target transformation of C1-C3 alkanes to their corresponding alcohols, aldehydes and carboxylic acids with low selectivity to carbon oxides (over-oxidation products) has been achieved. Chemical vapour infiltration has been employed as the technique of choice to prepare metal doped zeolites used in this work with new methods to tune both selectivity to oxygenates and catalytic activity of these materials for alkane oxidation being presented. These new materials represent a step change in the design and application of zeolite catalysts for lower alkane oxidation from both a materials and oxidative chemistry perspective. The preparation technique has wider applicability in catalyst preparation and reproducibly affords very well dispersed and minute nanoparticles on a variety of support materials by an easily accessible methodology. Finally a new and innovative technique of catalyst preparation, with beneficial effects in alkane oxidation, dubbed "The Hybrid Method" is presented.

Declaration

I, Michael M Forde, declare that the work presented herein was performed by myself in the fulfilment of this PhD at Cardiff University. Contributions to this thesis made by other colleagues and taken from previous work have been referenced in the text, to the best of my knowledge.

Acknowledgements

I, Michael M Forde, take pleasure in acknowledging the following persons for their varied contributions to my PhD studies and writing of this thesis:

- Prof. G J Hutchings for the opportunity to study and work in his group, especially on this challenging project that I'd say turned out fantastic.

- The Dow Chemical Company for funding the Methane Challenge and keeping close ties with us during the project.

- Members of the Hutchings Group at Cardiff, the Kiely Group at Leigh and the Dr. Murphy's EPR Group members for academic, technical and personal support in a relaxed and productive environment. Mention must especially be made of Qian for his excellent microscopy work, Emma at Cardiff for recording EPR spectra on my behalf and my team members Hasbi and Ceri for their work in the project.

- My former post-docs and industrial collaborators- Nikos Dmitratos, Antonio Sanchez, Henk Hagen, Eric Stangand, Joo Kang amongst others who have really helped with the development of this work and hours on end of discussions and speculations...and great leads! In a special way thanks to Nikos for corrections on this thesis amidst an extremely busy schedule and helping many other colleagues with their corrections.

- My parents, close friends and beautiful wife for support in every way possible and pestering me daily to write this thesis... it really helped me do get the job done.

Dedication

This thesis is dedicated to the Divine One who moves within us all and allows humankind to search out all mysteries...even low temperature methane oxidation! It is also dedicated to my parents and siblings without whom I would not have reached this stage of development, and to my beautiful wife which is the source of balance and joy in my life.

Contents

List of Tables

List of Figures

Abbreviations

CVI- chemical vapour deposition

LNG- liquefied natural gas

MTBE- methyl tertiary butylether

ATP- adenosine triphosphate

sMMO- soluble methane mono-oxygenase

pMMO- particulate methane mono-oxygenase

NADH- nicotinamide adenine dinucleotide

DFT- density functional theory

PCET- proton coupled electron transfer

EPR- electron paramagnetic resonance

M-OOH - metal hydro-peroxy species

ROS- reactive oxygen species

TBHP- tertiary butyl hydrogen peroxide

TS-1- titanium silicalite-1

TOF- turn over frequency

NMR- nuclear magnetic resonance

TEM- transmission electron microscopy

XPS- X-Ray Photoelectron Spectroscopy

UV-VIS - Ultra Violet Visible Electromagnetic Radiation Spectroscopy

XRD- X-Ray Diffraction Spectroscopy

XANES- X-ray Absorption Near Edge Structure

EXAFS- Extended X-Ray Absorption Fine Structure

T_d - tetrahedral

O_h- octahedral

HTS- hydrothermal synthesis

IMP- wet impregnation

SI- sol immobilisation

ICP- inductively coupled plasma

LC- liquid chromatography

GC- gas chromatograpy

MS-mass spectrometry

EDX- energy dispersive X-ray spectroscopy

CO_x- carbon oxides

C1- one carbon alkane/molecule

C2- 2 carbon alkane/molecule

C3- three carbon alkane/molecule

Oxy.- oxygenate

Prod.- productivity

Abstract

The global use of energy and consumer products places ever an increasing demand on energy and chemical resources. Natural gas is said to be both abundant and cheap and contains methane and ethane as its major components. Utilisation of these simple hydrocarbons remains a challenge if we consider the less than ideal industrial processes used in current application for converting lower alkanes into useful oxygenated products. Finding methods for atom efficient, less energy intensive, economical and environmentally friendly natural gas conversion technologies is highly desirable. Heterogeneous catalysis offers the unique ability to satisfy all of these goals if suitable catalysts are discovered. The work presented in the thesis lays a foundation for the design and understanding of the application of old materials, zeolites, with new twists.

The excellent ability of iron and copper containing zeolites to oxidise methane, ethane and propane at low temperature in water using neat hydrogen peroxide is detailed. In comparison to the reference enzymatic system of soluble methane mono-oxygenase, found in biological methanotrophic bacteria , these ZSM-5 materials are many times more active (4-5 times for methane and more than 10 times for ethane) with high selectivity to oxygenates in reactions at 50°C. In terms of turn over frequency or volumetric productivity these materials are on par with the

best reported catalytic (synthetic) systems such as Periana's platinum based homogeneous catalysts, which represent a significant move forward for truly heterogeneous catalysis in methane oxidation at mild temperature.

The identification of methyl hydroperoxide as the primary reaction intermediate for reactions performed with ZSM-5 along with assignment of the observed activity to trace impurities of Fe in commercial ZSM-5 formed the basis of systematic catalytic testing of metal doped zeolites in this report. It is postulated that for ZSM-5 the active site is an isolated iron-oxo-hydroxo dimer similar in structure to the active site of sMMO and the iron species postulated to be involved in benzene to phenol conversion over nitrous oxide treated ZSM-5. When using metal doped (Fe and Cu) ZSM-5(30) the catalysis proceeds using multiple metal sites in the catalyst, including the proposed active site (isolated iron-oxo dimers), and involves the intermediacy of multiple reaction pathways. Interestingly, though hydroxyl radicals and reactive oxygen species derived from methyl hydroperoxide may play a part in the catalysis, the reaction proceeds with low selectivity to carbon oxides which is atypical of the involvement of free radical chemistry for methane oxidation. This suggests a level of control exists in the system which may be linked to the structure of the zeolite (confinement) or the nature of the surface metal species.

There any many areas of this system which merits further investigation, but sufficient understanding of the reaction mechanism has been gained allowing the development of tuned catalysts which can selectively produce desired oxygenated products from their corresponding alkane in high selectivity and appreciable yield. The new preparation techniques developed, i.e. chemical vapour infiltration (CVI) and the "hybrid method", in this thesis is pivotal to further development of these materials for high yield applications. Furthermore, the results show that an industrial application of this catalytic system for ethane oxidation to ethanol or acetic acid, in particular, is possible and only when using catalysts prepared by the CVI technique.

Chapter 1

Introduction

1.1. Methane as a chemical feedstock

The global consumption of energy and hydrocarbon related commodities, synthetic or naturally produced, has and will continue to increase even in the case of a global population plateau or decline. Modern civilisation has progressively looked towards finite non-renewable hydrocarbon resources for everything from fuels to materials used in consumer goods in varied industries. Though there is debate as to the future reserves of petroleum upon which we all heavily rely, it is well known that eventually this feedstock will be depleted if other chemical feedstocks and renewable energy technologies are not found and utilised more aggressively. Natural gas whose principal component is methane (CH_4) is abundant, cheap and has a comparatively lower CO_2 emissions footprint than petroleum.[1] These factors place natural gas, and by extension methane, as a principal candidate for replacing petroleum as a chemical feedstock besides renewable biomass resources.

The estimated global natural gas reserves are set at *ca.* 6,675 trillion cubic feet according to the US Energy Information Administration [2] thus methane is abundant. The uses of methane are variable with a large portion currently being used for fuel and heating purposes in domestic and industrial settings either directly in gaseous form or as liquefied natural gas (LNG).[3] It is also used as a coolant and in several food related processes. A significant amount of methane is used for methanol (CH_3OH) production, a higher valued chemical. Methanol in turn is used to produce methyl tertiary butylether (MTBE) [3], a gasoline additive, as a hydrogen carrier for fuel cells and to make primary chemicals such as formaldehyde (using iron oxide and silver catalysts at high temperature)[4] and acetic acid (carbonylation in the Monstano or Cativa Process using Rh and Ir catalysts).[5,6] These primary chemicals then enter

the chemical chain as feedstocks for downstream chemicals which range from plastics to pigments. [4,5] The growing area of biodiesel trans-esterification is also dependant on methanol as key component of that process. In terms of emerging technologies it seems that using methanol for electricity generation, fuel cell technology and as a direct transportation fuel is gaining in the marketplace. These gains stem from the fact that the atom content of methane is much more useful in the form of methanol [3] which is not hard to grasp considering the widespread uses of methanol and also its ease of transportation as opposed to natural gas or LNG. This is evident in the huge global capacity for methanol production (75 million metric tonnes) and the current global demand (45.6 million tonnes in 2010 with estimated increasing demand in 2011).[3] Across the 90 methanol plants globally [3] the "syn gas" process is used which is summarised as[7] :

$$CH_4 + H_2O \rightarrow CO + 2 H_2 \text{ (Ni catalyst , 40atm, 850}^{o}\text{C)} \quad \text{Eq. 1}$$

$$2CH_4 + O_2 \rightarrow 2CO + 4H_2 \text{ (exothermic)} \quad \text{Eq. 2}$$

$$CO + H_2 \rightarrow CH_3OH \text{ (Cu ZnO/Al}_2\text{O}_3 \text{ catalyst, 250}^{o}\text{C, 50-100 atm)} \quad \text{Eq. 3}$$

$$CO_2 + 3H_2 \rightarrow CH_3OH \quad \text{Eq. 4}$$

$$CO + H_2O \rightarrow CO_2 + H_2 \text{ (water gas shift reaction)} \quad \text{Eq.5}$$
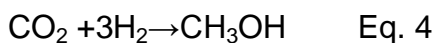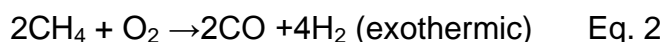
In this scheme partial methane oxidation (equation 2) is coupled to the methane steam reformed reaction (equation 1) to provide some of the heat energy needed as the steam reforming is highly endothermic. Carbon monoxide and hydrogen reacts to from methanol usually over $Cu/ZnO/Al_2O_3$ type catalysts (equation 3) but carbon dioxide originating from the water gas shift reaction (necessary to adjust the ratios of carbon monoxide and hydrogen) can also be transformed to methanol using

hydrogen.[7] The entire process is highly energy intensive and thus costly. It is desirable to convert methane to methanol *via* a direct low temperature process preferably with O_2 as the oxidant. This seemingly simple process can be outlined as

$$CH_4 + \frac{1}{2} O_2 \rightarrow CH_3OH \qquad\qquad Eq.\ 6$$
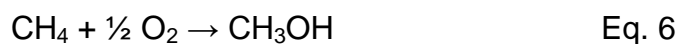
but is technically challenging due to the strong C-H bond (435kJ/mol) [8], lack of polarisability of the C-H bond in CH_4 and the decreasing bond C-H bond strength in the oxygenated products rendering the product (CH_3OH) more easily oxidised than the substrate. Thus direct oxidation of methane to methanol in an energy efficient process has remained an elusive target. However, there have been approaches of academic but not industrial importance and notably nature has solved the issue of selective low temperature methane oxidation by the use of highly evolved enzymatic systems.

1.2. Biological Methane Oxidation

Methanotrophic bacteria have evolved to use methane as an energy source by converting it to methanol and subsequently to formaldehyde and adenosine triphosphate (ATP) *via* various enzymatic processes. Methane mono-oxygenases (MMO's) responsible for the CH_4 to CH_3OH conversion have been long identified and studied. Key work on the study of MMO performed in 1977 by Dalton *et al.* showed the versatility of this enzyme for alkane, alkene, ether and aromatic hydrocarbon oxidations [9].

It was reported that the soluble form of MMO (sMMO) could oxidise C1-C8 hydrocarbons efficiently to the corresponding alcohol. The MMO mechanism [10] (Figure 1) utilises a di-iron hydroxylase subunit (MMOH) to activate O_2 forming an intermediate Q which subsequently inserts and O atom into the C-H bond of CH_4 producing CH_3OH. This entire process relies on reductase subunit (MMOR) which shuttles electrons from reduced nicotinamide adenine dinucleotide (NADH) to the MMOH prior to O_2 activation. A third subunit (MMOB, a regulatory protein) is a key player in production of the peroxo-diiron intermediate (H peroxo) which is a precursor to intermediate Q. This complex system based on the concerted effort of three protein subunits and a cofactor is still not fully understood as the action of the MMOB in forming H-peroxo and the manner in which intermediate Q actually inserts O into a C-H bond has remained elusive. For the latter DFT [10-14] studies propose an initial H abstraction from CH_4 with a one electron reduction of $Fe^{(IV)}$ to $Fe^{(III)}$ followed by C-O bond formation with a one electron reduction of the second $Fe^{(IV)}$ to $Fe^{(III)}$ through a rebound or concerted mechanism. This proposal should be kept in mind for the

discussion of the unexpected methane oxidation activity of catalysts reported in Chapters 3, 4, 5.
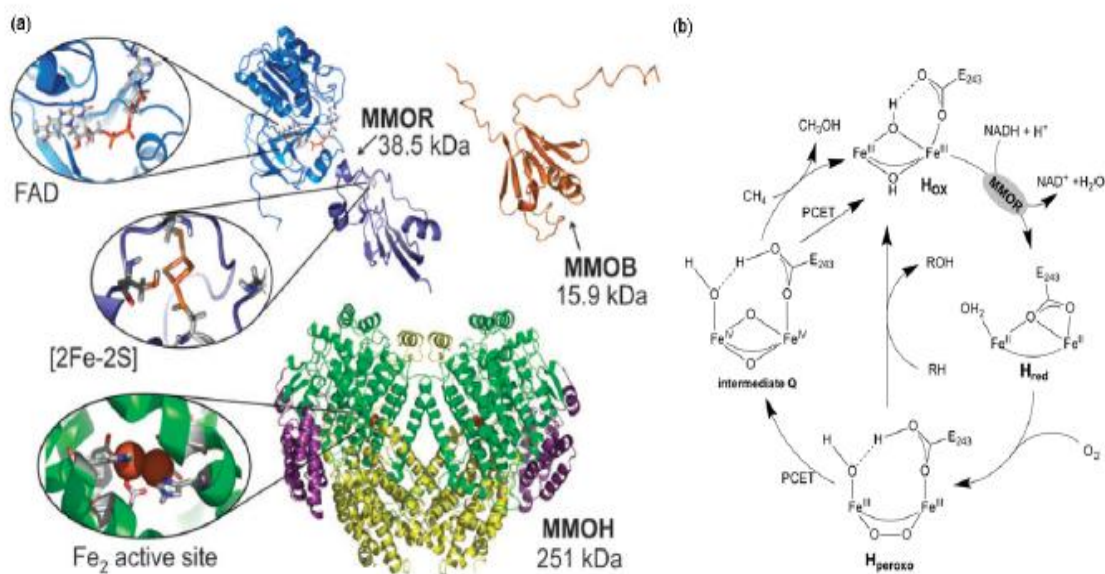
Figure 1 (a) Crystal Structure of sMMO(Bath) and (b) proposed mechanism for methane hydroxylation by PCET- proton coupled electron transfer. This figure is reproduced from ref. 9.

The assayed activity of the full intact sMMO in the studies of Dalton *et al.* for methane oxidation was 5.05 mol(CH$_3$OH) kg(protein)$^{-1}$ h^{-1} [9] and this represents an academic target for low temperature methane oxidation. Interestingly when the NADH is not used as a cofactor, hydrogen peroxide (H$_2$O$_2$) can be used as the oxidant in place of O$_2$ and the activity for methane oxidation drops to a *ca.* 0.08 mol(CH$_3$OH) kg(protein)$^{-1}$ h^{-1} (N.B. best calculation based on experimental details in reference) [15]. We will come back to the point of O$_2$ vs H$_2$O$_2$ as an oxidant in section 1.4.

A second variant of MMO is the membrane bound version, pMMO, which uses Cu as its hydroxylase active transition metal. pMMO is much more prevalent than sMMO but is even more difficult to express, characterise and has only been shown to hydroxylate C1-C5 substrates effectively.[16,17] Based on its crystal structure pMMO utilises a di-copper moiety at its hydroxylase active site [18], though there is some evidence for a tri-copper cluster based on the work of Chan and Yu.[19] It was proposed that this tricopper cluster has eluded investigators in crystal structure studies but can be characterised using redox potentiometry and EPR but other work by Dalton *et al.* [20] suggests the tricopper cluster is not associated with hydroxylase activity but a one Cu^{+2} plus Fe^{+3} combination is actually the active component. Furthermore evidence for both a mononuclear copper and copper containing cluster was provided by Liberman *et al.* [21] The mechanism is not well understood but the di-copper cluster proposed has some merit based on parallels with other active Cu sites used in alkane and other oxidations.

Though both pMMO and sMMO have been studied somewhat extensively there are no commercial applications for these systems owing mainly to the difficulty in expressing and purifying these proteins and the fact that the primary product (methanol) is utilised for further oxidation reactions (to formaldehyde) which is an integral component of respiration processes of bacteria containing MMO. Efforts have been focused to turn off the subsequent oxidation using enzyme inhibitors but in this case only low a yield to methanol was achieved, e.g. a 13.2 mM CH_3OH solution resulted. [21] Using the purely enzymatic system for methane oxidation does not seem viable with current technology due to the many disadvantages such as limited reaction temperature regime, cost of producing and purifying the necessary enzymes and long term stability under demanding conditions.

Any discussion on biological methane activation would not be completed without mentioning the ability of bacteria using gold [23] as the active metal for alkane oxidation and the ability of P450 enzymes. The former has not been extensively used but there are reports on the ability of both the auric-enzymes and synthetic analogues to effectively oxidise methane to methanol at low temperature using O_2 as the oxidant and this system even releases measurable H_2O_2 under some conditions .[24] Again the motif of an Au---Au site featured in the active site.

Unlike MMO, P450 which is ubiquitous in nature has an active site using coordination *via* N donors of a porphyrin moiety and S of a cysteine resides, *i.e.* thiolate heme complex.[25] The heme active site activates O_2 by a reductive mechanism after the substrate is bound by displacing water from the original complex followed by a series of electron transfer and protonation steps to generate an oxy-ferryl porphyrin radical intermediate. The next step is the insertion of O atom by this intermediate into the C-H bond *via* abstraction-radical rebound mechanism to give the hydroxylated product and the regenerated active site (Fig. 2). [25-28] P450 can generally use terminal oxidants such as $H_2O_2,$ unlike MMO, and there exist many P450 systems which use peroxides specifically (*i.e.* peroxidase enzymes). [25-28]
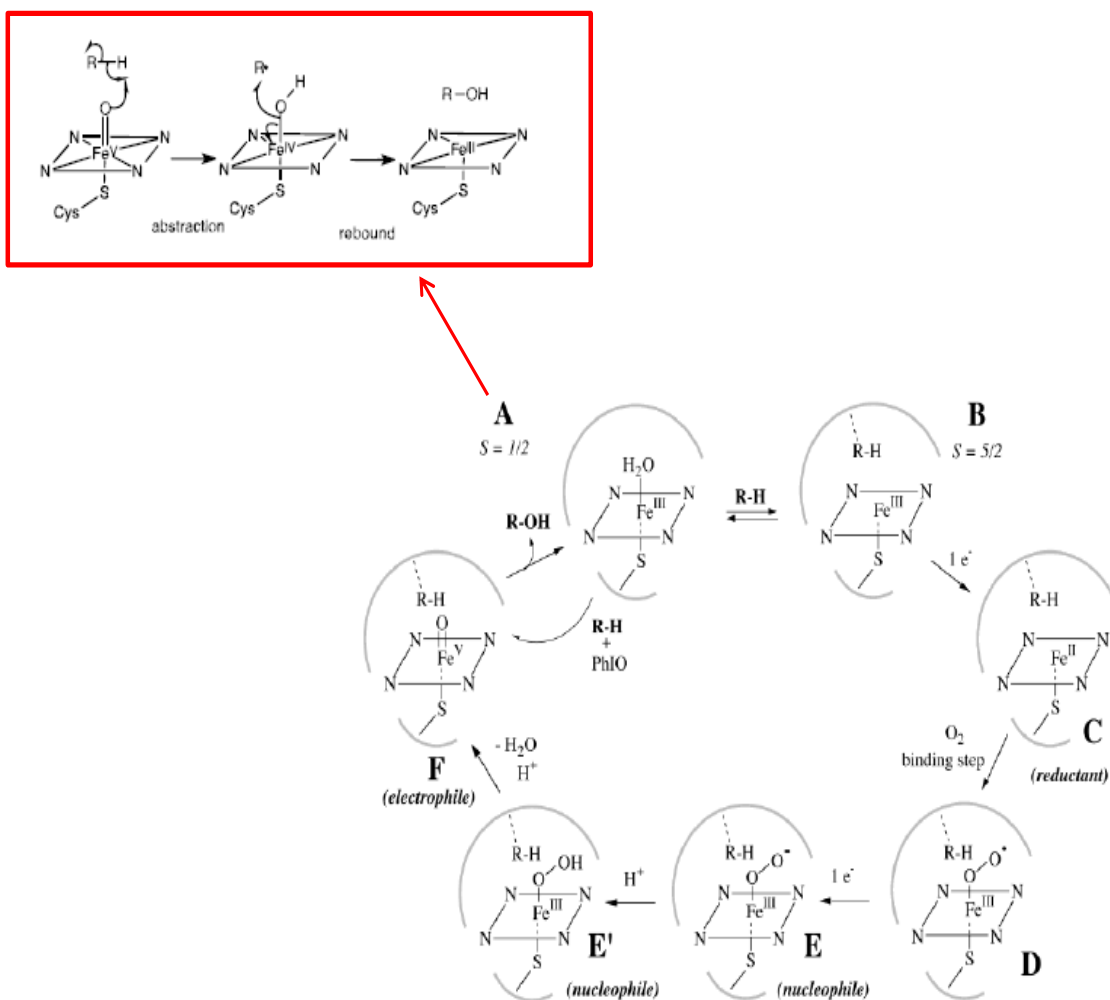
Fig 2 Schematic representation of the species (**A** to **F**) proposed to be involved in the mechanism of alkane hydroxylation using P450 and the scheme for the radical abstraction rebound step (insert in red upper left corner). Figure complied from refs. 27,28.

1.3. Academic approaches to liquid phase methane oxidation

The heading implies that all the approaches reported have only gained academic and not industrial status hence the issue of methane to methanol oxidation is still considered the "holy grail" of catalysis. Examples of the main work in this field are given in Tables 1.1 and 1.2. As is evident the early work in Table 1 is based on homogeneous catalysis though some promising heterogeneous systems have also been described. The basis of much of this work started with the discovery of primary C-H bond activation by a Pt salt in aqueous solution by Shilov *et al.* [29] In this autocatalytic system the C-H bond is "activated" by insertion into the Pt complex to form a Pt-C bond. This activation is based on the ability of the d-electrons Pt complex to donate in the anti-bonding orbitals of the C-H bond thereby weakening the C-H bond. A number of redox steps, characteristic of this type of chemistry, followed by hydrolysis leads to the hydroxylated product. This idea has been extended by others and was optimised by Periana *et al.* [30,31] first with Hg(II) salts and then using a Pt-bipyridimine complex in oleum to achieve high conversion levels as shown in Figure 1.3. The mechanism is hinged on the very electrophilic nature of the redox metal center in strongly acid solvents.

In many studies strong acid solvents were employed so as to form acid salts (e.g. methyl bisulphate) which can then be subsequently hydrolysed, the reason being the prevention of over oxidation of the desired alcohol. Pd, Cu and Rh [32-34] have also been used in similar ways. Utilisation of strong acids has the associated issues of reactor corrosion, handling hazards and an open loop due to the eventual formation of dilute acid solvents in which the oxidation process cannot be maintained. Furthermore from an industrial standpoint, the formation of dilute aqueous methanol

solutions is not highly desirable due to the energy input required to distill such a mixture to produce pure methanol.
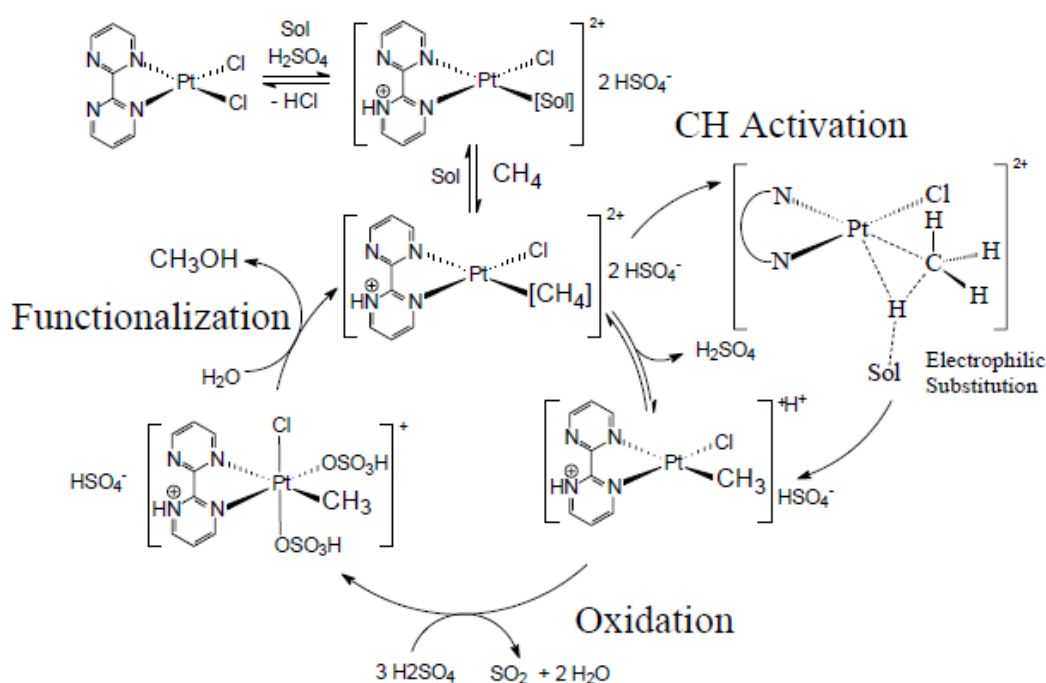
Figure 1.3 Methane oxidation in the Periana Pt based system. Oleum is used and the product, methyl bis-sulphate has to be hydrolysed to produce methanol. Diagram taken from ref. 35.

In more recent efforts other non-noble metals have been used. Fe has been of major interest as its use in Fenton's type chemistry is well known and hydroxylation of organic molecules *via* radical reactions can be achieved.[36] This issue of producing dilute methanol solutions and facile over-oxidation pathways cannot be avoided in these systems. Hence many groups report substantial formic acid and carbon dioxide selectivity with these types of catalysts. However, the detection of methyl

hydroxyperoxide (CH_3OOH) in these systems is a key discovery since it is considered the real primary product and precursor to methanol in systems involving metal hydro-peroxy species (M-OOH) as the reactive oxygen species (ROS). Thus understanding how to produce this molecule efficiently and control its decomposition to methanol is pivotal to any attempt at methane conversion to methanol with high selectivity. Though Shul'pin has carried out significant work on this area using homogeneous catalysts for a variety of alkane transformations and demonstrates the experimental process for quantification of CH_3OOH as a reaction intermediate [37-39], there are no reports of this intermediate in the biological strategies to methane oxidation. The generation of CH_3OOH by radical processes may proceed by the following equations:

$$\bullet CH_3 + O_2 \rightarrow CH_3OO\bullet \qquad \text{Eq. 7}$$

$$CH_3OO\bullet + H_2O_2 \rightarrow CH_3OOH + \bullet OOH \qquad \text{Eq. 8}$$

$$\bullet CH_3 + \bullet OOH \rightarrow CH_3OOH \qquad \text{Eq. 9}$$
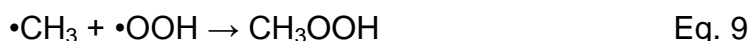
These pathways rely on the production of methyl radicals ($\bullet CH_3$) formed *via* reactive intermediates [Fe(IV)=O] which may arise from the interaction of Fe salts with H_2O_2 [39] and hydro-peroxy radicals ($\bullet OOH$) which may be formed by:

$$Fe^{2+} + H_2O_2 \rightarrow \bullet OH + OH^- + Fe^{3+} \qquad \text{Eq.10}$$

$$Fe^{3+} + H_2O_2 \rightarrow Fe^{2+} + \bullet OOH + H^+ \qquad \text{Eq.11}$$
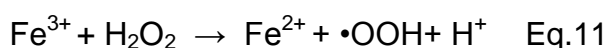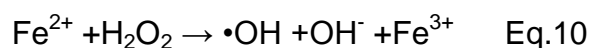
Methyl radicals can also produce methanol directly by interaction with hydroxyl radicals although the major pathway is through the hydro-peroxy intermediate especially when O_2 is present, even in minute amounts.[36] These types of catalytic

systems have the ability to activate O_2 at low temperatures, avoid the use of strong acids and are tuneable but in generally only low overall yields can be achieved.

Truly heterogeneous processes for methane oxidation at mild temperature are few. Interestingly Fe has only featured in two of these approaches being based on phthalocyanine complexes and said to be "bio-mimetic". The encapsulation approach adopted by Raja et al. [41,42] is reported to increase catalyst stability with the "support" material providing some level of substrate confinement which assists in bringing the substrate into contact with the active species. Though this work as been extended to other hydroxylation and epoxidation studies in the case of methane oxidation there are doubts as to the contribution of background solvent oxidation (except where H_2O was used as the solvent) and the assertion of O_2 activation and incorporation into the products. However, they report 4.9% conversion of methane with 52.6% methanol selectivity in 12h using $TBHP/O_2$. On the other hand the work of A. Sorokin et al. [43, 44] with a grafted N-bridged di-iron phthalocyanine elegantly shows CH_3OOH as a reactive intermediate and attributes the observation of formaldehyde and formic acid to over-oxidation reactions. Under optimal conditions this catalyst was reported to have 0.12% methane conversion with formic acid and formaldehyde as the only products after 20h. Sorokin and co-workers noted the presence of a proportion of C2 products derived from the decomposition of the catalyst. Recent work performed by myself shows this complex to be unstable under reaction conditions.[45] At very low oxidant levels in short reaction times or in the presence of dilute acids the catalysis proceeds selectively but the prevalence of catalyst decomposition leads to dissolution of Fe which may contribute to all observed products via Fenton's type chemistry. This catalyst was not re-useable, even when used under acid conditions.

Table 1.1 Key approaches to methane oxidation using homogeneous catalysis

System	Oxidant	Reference
Pt salts in aqueous solution, autocatalytic. H_2O required to form CH_3OH	$[PtCl_6]^{2-}$	29
$Pd(O_2CC_2H_5)_2$ complex as catalyst in aqueous solution, tri-fluroacetic acid anhydride is necessary	H_2O_2	32
Hg(II) in concentrated H_2SO_4 as catalyst at 180°C forming methyl bisulphate. Hydrolysis of product gives methanol. One pass yield of ~ 43% with 90% selectivity	SO_3	30
$EuCl_3$/Zn(0) catalyst in tri-fluoroacetic acid(H-donor) . 0.8% yield under standard conditions but tuneable. CO_2 is produced from the donor-solvent and not from CH_4	O_2	46
Fuming H_2SO_4 as the reagent with addition of $K_2S_2O_8$, $HgSO_4$, $CeSO_4$ or $PdSO_4$ as a radical initiator. Product only isolated as CH_3SO_3H and CH_3OSO_3H.	SO_3	47
$[NBu_4]VO_3$- pyrazine-2-carboxylic acid catalyst with H_2O_2 as a promoter. First identification of methyl hydroperoxide as a primary reaction product. •OH radicals from H_2O_2 initiate the reaction by C-H bond cleavage to give H_3C• with reacts rapidly with O_2 to form CH_3OOH. Temperatures below 100°C used.	O_2/H_2O_2	48
Pt-bipyrimidine complex catalyst, fuming H_2SO_4 media used to give CH_3OSO_3H as the product in 70% yield	SO_3	31
Di-iron silicotungstate catalyst, H_2O solvent. Low yields and substantial CO_2 made	H_2O_2	49
Au(III) catalyst, sulphuric acid solvent, up to 0.6M CH_3OH produced with >90% selectivity	Se^{6+}	48
Various Fe complexes, C1-C4 substrates, Fenton's type chemistry, alkylhydroperoxy species observed	H_2O_2	38
Pd(II) complexes in trifluoroacetic acid anhydride,CF_3COOCH_3 as product which can be hydrolysed to CH_3OH	O_2	34
Various metal chlorides including $HAuCl_3$ and $OsCl_3$ which were the best for CH_4 oxidation, substantial CO_2 observed	H_2O_2	50
$Ru(OAc)_2Salen_2$, acetone-water solvent. 27mM methanol with 2.4mM formaldehyde solution formed in 3h. No additives or acid promoter. Re-use of catalyst not reported. Rate slows after 1h and consecutive oxidation of methanol to formaldehyde begins	O_2	51

Table 1.2 Key heterogeneous approaches used in methane oxidation

System	Oxidant	Reference
Pd/C or Al_2O_3, Pd black, Pt/C catalyst. CO is the reductant in place of H_2 and the reaction proceeds by in situ H_2O_2 formation and use as the oxidant.	O_2	53
$H_4PVMo_{11}O_{40}$ catalyst in $(CF_3CO)_2O$ solvent (and others). 33% conversion achieved under optimal conditions at 80°C. Major product was methylformate and formic acid.	H_2O_2	54
Fe or Cu phthalocyanine encapsulated in zeolite Na-X and Na-Y. Various oxidant and solvent combination studied.	H_2O_2 or $TBHP/O_2$	41
TS-1 catalyst. Very low conversion levels obtained. Ti-OOH is the proposed active species	H_2O_2 or TBHP	55
Biomimetic approach using N-bridged di-iron-t-butylphthalocyanine grafted to SiO_2.Evidence from Fe-OOH and Fe)IV)=O as active species presented. Formic acid is the main product and CO_2 produced is not reported.	H_2O_2	43,44
Gas phase reaction. Fe/ZSM5 catalyst. α-oxygen species is the active oxidant. Final product is COx unless hydrolysis with H_2O is performed after the reaction. Not a closed catalytic cycle. Cu in FeZSM5 shown to markedly tune selectivity to methanol over CO_x	N_2O	56,57
Pt-CTF catalyst, H_2SO_4 solvent, 215°C reaction temperature. Ester is produced. Heterogeneous version of the Periana catalyst.	SO_3	58
Cu/ZSM5 catalyst. High temperature O_2 treatment produces a Cu_2O_2 species with performs methane oxidation at low temperature (<100°C) after catalyst treatment. Not a closed catalytic cycle, low yields.	O_2	59
Co/ZSM5 used a catalyst with O_2 pre-treatment to produce the active species and subsequent CH_4 oxidation at 150°C. Not a closed catalytic cycle.	O_2	60

It has been demonstrated that TS-1 interacts with H_2O_2 to produce Ti^{3+}-OOH. This metal hydroperoxy species is responsible for methane oxidation, as well as other hydrocarbons, but in very low yields (1.1µmoles in 20h).[62] Interestingly, this active species is reasonably stable and is it is detected on the catalyst surface for many hours after it is formed. If the catalyst is pre-treated with H_2O_2 and then dried mildly it can still hydroxylate alkanes under mild conditions even in the absence of further addition of H_2O_2 because of these long lived metal hydroperoxy species. Again a key point is the observation of CH_3OOH from methane, which may be produced by mechanisms which are not strictly by radical based. Since all these approaches utilised an "ex-situ" oxidant (H_2O_2 or TBHP) the idea of generating hydroperoxy species from $O_2 + H_2$ while simultaneously performing alkane oxidation should be viable. Though this has been demonstrated, in principle, by Lin and Sen in 1992 the work has not been further extended.[53] An important part of that study (see the following section) was the necessity of a weak acid to the catalytic activity and the absence of methyl radicals in the reaction mechanism when probed with CO as a methyl radical trap. This hinted at a mechanism which had a different mechanistic pathway from that typically observed with Fe based oxidation (Fenton's chemistry using H_2O_2).

More recently the work of Palkovits *et al.* [58] which successfully created a heterogeneous analogue of the Periana Pt- bipyridimine catalyst [31] was reported. Pt was incorporated into a covalent tri-azine framework for use as a solid catalyst. This recyclable catalyst displayed similar product amounts to the original Pt-bipyrimidine system when using sulphur trioxide in oleum. The same drawbacks mentioned

previously for the Periana system apply here with the exception that the catalyst can be recovered and recycled with no loss of activity.

Finally, it is worth mentioning that towards the end of this PhD period a report of Fe/ZSM-5 for CH_4 oxidation using H_2O_2 surfaced [62]. In that work the authors used, in a broad sense, the same system which is the subject of this thesis. However, it is clear from their account that the control of selectivity was not achieved and the real active site was not probed. It is useful at this point to compare the actual activity of key systems reported to date for methane activation. In Table 3 comparison is made based on a number of factors such as TOF (h^{-1}), volumetric productivity (moles products cm^{-3} s^{-1}) and oxygenate productivity (moles products $kg(cat)^{-1}$ h^{-1}). It is clear that only the Periana system [31] (entry 2 Table 1.3, also its heterogeneous analogue) and a recent report by Khokhar *et al.* [52] (entry 3 Table 1.3) has high volumetric productivity and high methanol selectivity. In the former case the actual reaction product methyl bis-sulphate has to be hydrolysed to produce methanol whilst methanol and formaldehyde is formed in the latter report but the catalyst seems to deactivate after 3h reaction. sMMO shows a volumetric productivity 2 orders of magnitude lower than the Periana system but has highest TOF(95 h^{-1}). It would be interesting to scale that reaction to a larger volume and higher overall methane pressure to investigate whether or not sMMO can attain commercially viable rates. All other systems, including the homogeneous iron catalysed approach, shows low TOF and low volumetric productivity, entries 4-8.

Table 1.3 Comparison of some methane oxidation approaches based on TOF and volumetric productivity

Entry	Catalyst	Catalytic Details	Methanol selec. %[a]	TOF/ h-1[b]	Volum. Prod. / Mol cm^{-3} s^{-1} [c]	Ref.
1	sMMO	2ml, H_2O solvent, 0.2h, 45°C	100	95.0	2.8×10^{-9}	9
2	(bpym)PtCl$_2$/ oleum	80ml, 220°C, 2.5h, SO_3 in oleum. Product as CH_3OSO_3H	81*	36	2.3×10^{-7}	31
3	Ru(OAc)$_2$Salen	Acetone-water solvent, 30°C, 3h. Catalyst shuts down after 3h	92	19.6	1.6×10^{-7}	52
4	FeCl$_3$ (aqueous)	10ml H_2O solvent, 90°C,1h, H_2O_2 . CO_2 is the major product	7	7.2	1.9×10^{-9}	51
5	OsCl$_3$ (aqueous)	10ml H_2O solvent, 90°C,1h, H_2O_2	30	12.0	3.3×10^{-9}	51
5	FeCl$_{16}$Pc-Na-X	0.75g catalyst, 100ml CH_3CN solvent, 12h, TBHP,O_2	52.6	4.7	2.9×10^{-10}	41,42
6	(Fe^{t}BuPc)$_2$N/SiO$_2$	2ml, 60°C, 20h, 0.075M H_2SO_4, H_2O_2 . Formic acid is the major product	0	5.6	1.5×10^{-9}	43,44
7	H-ZSM5	1.5g catalyst, 70ml H_2O solvent, 5h, 100°C, H_2O_2 . Formic acid is the major product	0.1	n/a*	1.78×10^{-8}	62
8	Pd/C	40mg catalyst, 5ml, 70-100°C, CO , O_2. Formic acid and CO_2 are major products	n/a	8**	1.1×10^{-9}**	53

[a] Calculated as moles (MeOH) / moles (produced) × 100; [b] calculated as moles (products) / (mole (metal) x reaction time) ; [c] calculated as moles (liquid phase oxygenates) / (reaction volume x reaction time) *Specific details not available from the reference ** estimated based on highest quoted TON for methane to formic acid of 160, and using authors calculation of TON based on moles of surface Pd on the catalyst and estimated time of 20h reaction.

1.4. Approaches to methane oxidation within the Dow Methane Challenge

The work described in the chapters which follow was part of the wider Dow Methane Challenge [63] project at Cardiff Catalysis Institute. Early work by Edwards *et al.* on hydrogen peroxide synthesis from hydrogen and oxygen in a tri-phasic system using Au-Pd catalysts [64-68] provided well studied catalytic system for the production of a "green oxidant" which could possibly be used *in situ* for methane oxidation without the need for acid additives. The *in situ* concept was based on the capture of hydroperoxy species derived from molecular oxygen and hydrogen to hydroxylate methane and other lower alkanes. The demonstration that small metal nanoparticles can activate molecular oxygen to produce hydrogen peroxide and that catalytic turnover of oxygen in epoxidation reactions also occur when these particles were employed [69] showed promise for general alkane activation with these types of catalysts.

It was mentioned previously that methane and ethane had been successfully converted by Lin and Sen [53] to their corresponding alcohols by noble metal catalysts comprised of Pd or Pt supported on carbon. Carbon monoxide was used in a water gas shift reaction at the noble metal site to produce hydrogen, which was then reacted with molecular oxygen to produce H_2O_2 "in situ". In that work of it was reported that the direct use of hydrogen, instead of using a water gas shift reaction, resulted in a much higher rate of H_2O_2 production with an accompanying issue of high rate of hydrogen peroxide hydrogenation/decomposition. This led to lower productivity of the catalysts because the rate of H_2O_2 production was not comparable with the rate at which the alkane substrate was oxidised. Further work by this group and also Park and co-workers [70] showed that the system could be tuned to

selectively produce methanol if aqueous copper salts were added to the reaction mixture and trifluoroacetic acid used as a co-solvent. The presence of Cu (presumably Cu^{+1} was the active state) tuned the selectivity of the system and the trifluoroacetic acid replaced the HCl component in which Cl^- was thought to be essential to the oxidation reaction.

Further proof of concept studies showed the primary C-H bonds could be oxidised with molecular O_2 without the formation of carbon oxides.[71] Within our group it was observed that during benzyl alcohol oxidation using Au-Pd/TiO_2 catalysts and molecular oxygen that toluene was initially produced as a by-product of the reaction and subsequently oxidised to given benzoic acid. [71, 72] Later studies on solvent free toluene oxidation were performed and as shown by Kesavan *et al.* [70] careful control of particle size for Au-Pd supported on TiO_2 or C realised almost complete conversion of toluene without the formation of carbon oxides. Moreover, an unexpected pathway to benzyl benzoate through a hemi-acetal was observed and the catalytic activity varied depending on the support and this was linked to the shape of the metal nanoparticles which existed as random alloy structures on the support surface.

These studies paved the way for methane oxidation primarily using Au-Pd/TiO_2 catalysts by Mohd Ab Rahim. [73] The same catalysts as used by Edwards *et al.* for hydrogen peroxide synthesis [64,65] were employed in methane oxidation using hydrogen peroxide. These materials were prepared by a wet impregnation procedure followed by calcination and the Au-Pd particles on the surface had core-shell structure in which an Au rich core is surrounded by a Pd/PdO shell and the entire

particle had high interaction with the TiO_2 surface[a]. Catalysts prepared by sol immobilisation techniques were not used in this work due to their high hydrogen peroxide decomposition ability which is linked to the smaller particle size (2-4nm) and metallic state of the Au and Pd. The oxidation reactions proceeded even at 2^oC with the addition of hydrogen peroxide or its production from the reaction gas mixture of methane, hydrogen and oxygen (with nitrogen diluents). Though methanol was the major product (high oxygenate selectivity) the productivity of the system was low. Using a flow reactor system improved the productivity of the catalyst and it was identified that poor activity was related to hydrogen peroxide decomposition without oxidation of the substrate (i.e. hydrogen peroxide transformation to water and oxygen) hence low contact time improved catalytic activity. The data presented cannot be compared to sMMO [9] or other systems like the Periana [31] work but is the first extensive study of the ability of very small noble metal nanoparticles to perform selective methane oxidation in water at low temperature.

In order to increase the catalytic activity the need for new catalysts is highlighted. The ability to produce hydrogen peroxide and the activation of C-H bonds by Au-Pd nanoparticles is not enough to build a highly active and selective catalytic system. A review of the literature reveals the following:

1) Biological systems utilise confined spaces in which to oxidise a wide variety of substrates selectively. Notably heterogeneous systems which have metals in confined spaces are typically zeolites.

2) In all cases acidity is an important element. The MMO biological system has carboxylate acid groups of amino acids flanking the active site which donate

---

[a] This is observed as a "wetting" or spill over effect of the particle on the titania surface and changes the regular spherical shape to a truncated cubo-octahedral one.

protons during the reaction while most homogeneous systems only work in strong acid solvents.

3) Fe, Cu and Au feature as promising metals for methane oxidation based on biological reference systems in which case activation of molecular oxygen is usually the first and most important step in the oxidation, and not C-H activation as it is a result of forming a highly reactive oxygen species. In this way the formation of a "bio-mimetic" active site should proceed by first ensuring that a highly reactive oxygen species, *e.g.* Fe(IV)=O species, can be formed by the interaction of the active site with molecular oxygen and has sufficient lifetime to allow interaction with the substrate. This has already been postulated for benzene to phenol and methane to methanol (after hydrolysis) oxidation with Fe/ZSM-5 and N_2O. Other reactive oxygen species may also effectively hydroxylate alkanes.

4) Systems which can produce methyl hydroxyperoxide (CH_3OOH) are promising candidates for a lower energy pathway for the reaction and may also be achieved through non-radical processes thereby allowing control of overall selectivity to primary oxygenated products.

1.5. Introduction to Chemical Vapour Infiltration (CVI) and Zeolites

The work in this thesis is based on the important concepts outlined in the previous section. The development of catalysts which can selectively oxidise lower alkane substrates with appreciable rates and high oxygenate selectivity at low temperature under mild conditions is disclosed. To achieve this target a vapour deposition method was employed to deposit metals on a variety of support materials and specifically on ZSM-5, an MFI type zeolite. The technique was chosen as a tool to develop catalysts with excellent metal dispersion and very small nanoparticles with narrow size distribution. It was desired that the synthesis could be a simple reproducible route without the need for solvents/ inorganic deposits/ organic stabilisers.

Chemical vapour deposition (CVD) has been used for a number of years for many applications ranging from synthesis of thin films, microelectronics and in micro-fabrication for a variety of metal, non-metallic and semiconductor species. The technique itself was demonstrated in 1890 by Mond *et al.* for the preparation of pure nickel films using nickel tetracarbonyl complex.[74] In recent years there has been a concentration of research efforts, and by extension industrial applications, for the use of CVD techniques in nanofabrication applications in the creation of exciting new materials. With many of these materials there are a number of other synthesis routes to the desired product but CVD is said to offer strict and tailored control of the architecture of the deposits.[75] This level of control can be achieved by tuning the parameters utilised in the technique (temperature, precursor choice, carrier gas choice, pressure, deposition time) and represents one of the major advantages of using CVD techniques. Furthermore, the ease of synthesis scale-up, reproducibility,

tolerance to a wide range of precursors (certain criteria must still be met) and the ability to have experimental "add-ons" to monitor the reaction *in situ* as it proceeds makes CVD even more attractive. However, the vapour deposition technique has not been so frequently employed to prepare catalysts as compared to the other more common preparation methods. This is largely due to the high cost of commercial vapour deposition equipment and the expertise needed to prepare suitable catalysts.

In the area of heterogeneous catalysis using micro/meso-structured materials, and most recently carbon nanotubes (CNT'S), CVD has emerged as a powerful tool for both the synthesis of the materials and loading it with metal nanoparticles and this is primarily due to the prospects of morphological control and ease of varying architectural features.[76] A very early work, relative to the use of CVD for making active nanoparticulate catalysts, showed that CVD can be used to make Au nanoparticles (on TiO_2) smaller than 2nm in diameter with similar activity to analogous catalysts made by other methods for CO oxidation.[77] As noted by Haruta and others [74,78] the size of nanoparticles, the material on which they are dispersed and the level of dispersion matters greatly in heterogeneous catalysis. This is also true for catalysis by gold nanoparticles on various supports.

The method is based on the sublimation of a metal precursor under low vacuum conditions onto a support material (usually a wafer) followed by the thermal decomposition of the sublimed precursor under controlled conditions. It may also be achieved by the sputtering ion technique where a metal source is bombarded with a dense ion beam and ejects charged ions (similar to ionisation chambers of mass spectrometers). These ions are moved towards the target wafer or support surface by an electric field. The type of ions produced can be varied by varying the beam intensity or energy and also the vacuum conditions but ions may be selected based

on mass in a similar way to how a mass spectrometer works.[79] Extensive experimentation is required to be able to tune the amount of metal deposited on a surface and it is clear that for powdered samples this is not possible using sputtering ion deposition.

One development in the field surrounds the use of relatively volatile metal precursors which are organometallic compounds. This has given rise to the term Organometallic Chemical Vapour Deposition (OMCVD) which is primarily used in the electronics/ semiconductor industry.[74] Thin films are routinely deposited on substrates at much lower temperature than traditional vapour deposition techniques. The precursor vapour is sublimed at a lower temperature than the support/substrate is held at. Once the vapour interacts with the support the precursor is thermally decomposed leaving behind the metal ions/atoms deposited on the surface. Thus the film content and size can be easily controlled by the choice of metal precursors, the deposition temperature and time. In practice a carrier gas is used to move the vapour uniformly onto the substrate.

The use of OMCVD was extended to include powdered substrates in Fluidised Bed OMCVD (FB-OMCVD) [80] with the first demonstration of the preparation of controlled bimetallic nanoparticles being reported by Hierso *et al.* in 1998.[81,82] This adaptation included the use of a 'hot' carrier gas to both vapourize and transport the organometallic precursor to the support material in a rotating cylinder. In this way more uniform deposition of the metal is achieved and the process can be more easily controlled since the carrier gas temperature and flow rate determines the amount of precursor available for deposition. Haruta and co-workers employed the vapour deposition technique to prepare highly active Au supported nanoparticles for CO oxidation on a variety of support materials. [83] The precursor was dimethylgold (III)

acetylacetonate which has a high vapour pressure at room temperature and low decomposition temperature. This precursor affords very clean films and small particulate size (a special property of the decomposition profile of the molecule). The as-prepared gold nanoparticles were active for CO oxidation in the absence of any spectator ligands/ inorganic species. The preparation had the advantage that supports which could not be previously accessed by wet methods (for example, silica cannot be used in co-precipitation or deposition precipitation of gold and wet impregnation leads to particles above 20nm) and showed that the Au nanoparticles were active once there was a strong support- nanoparticle interaction regardless of the support material. That study highlighted the versatility in the technique being able to deposit metals on a variety of supports and produce similar particle size regardless of the support.

Sivakumar[84] and Dal Santo[85] also performed OMCVD using powdered support materials but in this case the support and precursor was loaded into a vacuum flask connected to a Schlenk line under static bed or rotary bed conditions respectively. This adaptation allowed the large scale preparation of catalysts using simple laboratory equipment and for the first time the precursor and support were intimately mixed at one temperature (as opposed to the two components being held at different temperatures). In this way a material can be loaded with a metal precursor and then heat treated to produce supported metal nanoparticles at a later stage. The modified technique has been used to prepare catalysts used for alkane oxidation in this thesis due to the ease of preparation and ability to scale up the preparation reliably. In the results chapters it will be shown that small particle size (<5nm) without carbon deposits is afford by the technique and that superior catalysts using ZSM-5 as a support have been prepared (i.e. as compared to ion exchange methods).

It would be fitting at this point to also introduce the reader to a general background on zeolites. The term zeolite has been applied to any microporous crystalline aluminosilicate material. This is not strictly so as there are zeolites completely devoid of aluminium ions in their structure, but maintain the same physical properties (crystallite size, pore dimensions, pore volumes and shapes) as their aluminosilicate counterparts. A case in point would be titaniumilicate-1 and silicalite-1 (TS-1 and Sil-1 respectively) which are both zeolites with the MFI (mordenite framework inverted) structure but contain no Al^{3+} ions. Technically all of these materials belong to a class called porous tectosilicates.[86]

There are 133 types of zeolitic framework structures and around 40 natural zeolites are known.[87] Natural zeolites are commonly used in cosmetic applications (e.g. facial masks) due to their propensity to detoxify the skin by removing molecules from the skin surface. They are also used in industrial applications as sorbents, for ion exchange and storage in agricultural and water treatment systems, and as feed additives for livestock.[88] Commercially produced zeolites on the other hand find widespread use in catalysis, especially for hydrocarbon based processes, and in detergents (largest application by mass of material).[89] This is based on the shape-size selectivity property of zeolites, which is related to their intrinsic structures.

The structure of a zeolite is made up on TO_4 tetrahedra (T = Si, Al) joined by –O atoms in rings which connect to build a 2-D or 3-D framework.[89] The positive charge on aluminium (Al^{3+}) being different from the formal +4 charge on the Si atoms renders a charged framework which necessitates the inclusion of a counterion (e.g. Na^+, NH_4^+, H^+, Li^+, K^+) for overall neutrality. The presence of cations in the structure translates into an ion-exchange capacity and in this way metal loaded zeolites are prepared by ion exchanging the counterion for a metal ion (usually from nitrate

source in the aqueous phase). Another useful property is the acidity of zeolitic materials. When Si^{4+} is replaced by a heteroatom (such as Al^{3+}) the bridging O atom becomes a Bronsted acidic hydroxyl group (silanols, Si-O(H)---Al) when located close to the Lewis acidic Al^{3+} atom.[90] Additionally, if a heteroatom is removed from the framework it may form a counterion species (called extra-framework species) to allow charge balance. This extra-framework species is a Lewis acid and in general the formation of Lewis acid sites in the zeolite is facilitated by a loss of Bronsted acid sites (silanols, H^+ and NH_4^+). Acidity is an important feature of zeolites and in some materials such as ZSM-5 this property can be fine tuned to produce active catalysts for acid catalysed reactions.

Three examples of the importance of the acidity of zeolites and diffusion properties can be had in Mordenite, Zeolite Y (or X or USY) and ZSM-5. Mordenite has, in practice, a 12-member ring structure with a one dimensional pore whose aperture of 6.7-7.0 A^o means that it can accommodate larger molecules.[89] Mordenite is used for alkylation of biphenyl with propene and it has been shown that only the regions near the pore openings are utilised in this reaction.[91] The material is active for this reaction due to its acidity (proton transfer property) and the ability to stabilise organic radical cations. Zeolite Y or ZSM-5 would not be used in this way due to the larger and small pore apertures respectively. The former is utilised in catalytic cracking of petroleum due to its large cavities which are accessible in 3 dimensions.[92] ZSM-5 (Figure 1.4), on the other hand, displays a 10 and 5-membered connected ring structure with a pore aperture of 5.6 A^o and contains straight and sinusoidal channels in the structure.[93] Molecules can diffuse in two directions in ZSM-5 because of the cavity formed at the intersection of the two types of channels which allows "hopping" from one type of channel to the next.[89] The usefulness of ZSM-5 is

related to the pore size (only small molecules can be involved in catalysis inside the channels), the ability to tune the acidity by a variety of methods and also to be able to introduce heteroatoms (Fe, Zn, Ga, Ge, Pb) into the framework.[94] The latter is very important for catalysis if extra-framework metal species are necessary for the reaction and has been extensively explored due to the relative ease of preparing ZSM-5.

Additionally, the ability to ion-exchange extra-framework counterions with metal ions from a solution or gas phase translates into the ability to load zeolite channels with metal species. These species can be exchanged at the so-called 'cation exchange sites' commonly to replace NH_4^+ or H^+ thereby stabilising the negative charge of the framework. As di- or trivalent counterions (Fe^{3+}, Zn^{2+}, Co^{2+} etc) are being included in the ZSM-5 structure it goes without saying that charge balance necessitates that new structural features are formed. Heteroatoms such as Fe^{3+} have been said to occupy the framework positions of Al^{3+} causing expansion of the lattice. Though it is debated that incorporation of framework iron occurs when Fe^{3+} is introduced by post-synthesis modifications, it is clear that for FeSil-1 (iron incorporated into aluminium free ZSM-5 analogue during hydrothermal synthesis) Fe^{3+} ions actually occupy the tetrahedral positions in the building units.[95] Like Al^{3+} these ions are Lewis acids and can undergo modification by heat treatment whereby they are dislodged to from extra-framework species.
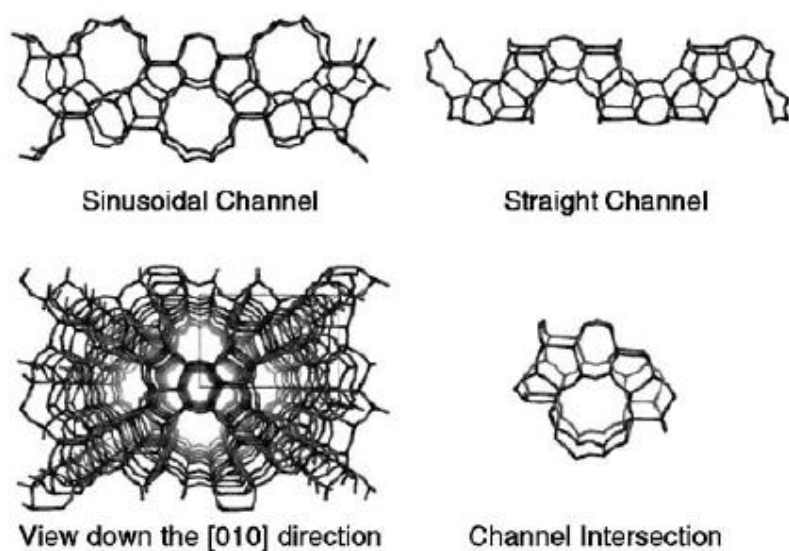
Figure 1.4 Structure of ZSM-5 showing two channel types and their intersection.

The nature of these extra-framework Fe species has been extensively studied. It is suggested that dimeric iron-oxo-hydroxo clusters, iron-oxo oligomers, pure iron clusters and small oxidic iron cluster (diameter below 0.5nm) are to be found in ZSM-5 channels (see front page of Chapter 3 for a pictorial representation of this).[102-108] ZSM-5 has also been used in the activation of benzene and methane to produce phenol and methanol respectively, using N_2O as an oxidant. It has been shown that trace impurities of iron in ZSM-5 was the active metal for the hydroxylation which only occurred after the formation of Fe(IV)=O (ferryl) species upon the interaction of Fe^{2+} sites with N_2O and loss of nitrogen.[109] In the oxidation of methane, ethane and propane presented in Chapter 3-5, ZSM-5 has been used as the metal support material since it has the ability to facilitate the high dispersion of metal species (exchange capacity) and was shown to be itself catalytically active for the oxidation of methane using hydrogen peroxide by C. Hammond.

References

1. Speight, J.G. <u>Natural Gas: A Basic Handbook</u> , Gulf Publishing, Texas (2007).

2. *International Energy Outlook 2011* DOE/EIA-0484(2011), United States Department of Energy and Energy Information Administration, p 64. Accessed at www.tnqtn.com. (October 2011)

3. Methanol Institute, www.methanol.org (October 2011).

4. Reuss,G.; Distledorf, W.; Gamer, A.O.; Hilt, A. " Formaldehyde", <u>Ulmann's Encyclopaedia of Industrial Chemistry</u>, Wiley-VCH, Weinheim (2000).

5. Cheung, H.; Tanke, S.R.; Torrence, P. " Acetic Acid", <u>Ulmann's Encyclopaedia of Industrial Chemistry</u>, Wiley-VCH, Weinheim (2000).

6. Jones, H. *Platinum Metals Rev.* 44, 94-105 (2000).

7. Waugh, K.C. *Catalysis Today* 15 (1), 51-75 (1992).

8. Blanksby, S.J.; Ellison, G.B. *Acc. Chem. Res.* 36, 225-263 (2003).

9. Colby, J.; Stirling, D. I.; Dalton, H. *Biochem. J.* 165, 395-402 (1977).

10. Merkx, M.; *et al. Angew. Chem. Int. Ed.* 40, 2782-2807 (2001).

11. Baik, M. H.; Newcomb, M. N.; Friesner, R. A.; Lippard, S. *J. Chem. Rev.* 103, 2385-2419 (2003).

12. Musaev, D.G.; Basch,H.; Morokuma, K. *J. Am. Chem. Soc.* 124, 4135-4148 (2002).

13. Seigbahn, P.E.M *J.Bio.Inorg.Chem.* 6, 27-45 (2001)

14. Gherman, B.F.; Dunietz, B.D.; Whillington, D.A.; Lippard, S.J.; *J. Am. Chem. Soc.* 123, 3539-3837(2001).

15. Jiang, Y.; Wilkins, P. C.; Dalton, H. *Biochimica et Biophysica Acta, Protein Structure and Molecular Enzymology* 1163, 105-112 (1993).

16. Burrows, K.J.; Cornish, A.S.; Scott, D.; Higgins, I.J. *Microbiology* 3327-3333 (1984).

17. Sullivan,J.P.; Dickinson, D.; Chase, A.A. *Crit. Rev. Microbio.* 24, 335-373 (1998).

18. Lieberman, R. L.; Rosenzweig, A. C. *Nature* 434, 177-182 (2005).

19. Chan, S.I.; Yu, S.S. *Acc. Chem. Res* 41, 969-979 (2008).

20. Basu, P.; Katterle, B.; Anderson, K. K.; Dalton, H. *Biochem. J.* 369, 417-427 (2003).

21. Liberman, R.; *et al. PNAS* 100, 3820-3825 (2003).

22. Lee, S.G.; et al. *Biotech. Lett.* 26, 947-950 (2004).

23.Levchenko, L.A.; *et al. Dokl. Biochem. Biophys.* 377, 123-124(2001).

24.Levchenko, L.A.; et al. *Dokl. Chem.* 430, 50-53 (2010).

25. Denisov, I.G.; Markis, T.M.; Sligar, S.G.; Schlichting, I. *Chem. Rev.* 105, 2253-2277 (2005).

26. Groves, J.T. *J. Chem. Educ.* 62, 928-931(1985).

27. Newcomb, B.; Toy, P.H. *Acc. Chem. Res.* 33, 449-455 (2000).

28. Meunier, B.; Visser, S.P.; Shaik, S. *Chem. Rev.* 104, 3947-3980 (2004).

29. Kusch, L. A.; Lavrushko, V. V.; Misharin. Y. S.; Moravsky, A.P.; Shilov, A. E. *New. J. Chem.* 7, 729-733 (1983).

30. Periana, R.A.; *et al. Science* 259, 340-349 (1993).

31. Periana, R. A.; *et al. Science* 280, 560-564 (1998).

32. Kao, L.; Hutson, A. C.; Sen, A. *J. Am. Chem. Soc.* 113, 700-701 (1991).

33. Lin, M.; Sen, A. *Nature* 368, 613-615 (1994).

34. An, Z.; Pan, X.; Liu, X.; Han, X.; Bao, X. *J. Am. Chem. Soc* 128, 16028-16029 (2006).

35. Periana, R. A.; *et al. J.Mol. Catal A: Chemical* 220, 7-25 (2004).

36. Sawyer, D. T.; Sobkowiak, A.; Matsushita, T. *Acc. Chem. Res.* 29, 409-416 (1996).

37. Nizova, G. V.; Suss-Fink, G.; Shul'piin, G. B. *Chem. Commun.* 397-398 (1997).

38. Shul'pin, G. B., Nizova, G. V., Kozlov, Y. N., Cuervo, L. G. & Suss-Fink, G. *Adv. Synth. Catal.* 246, 317-332 (2004).

39. Shul'pin, G. B. *J. Mol. Catal A: Chem.* 189, 39-66 (2002).

40. Ensing, B.; Buda, F.; Blöchl, P.E.; Baerends, E.J. *Phys. Chem. Chem. Phys.* 3619-3627 (2002).

41. Raja, R.; Ratnasamy, P. *App. Catal. A: General* 158, L7-L15 (1997).

42. Ratnasamy, P.; Srinivas, D. *Catalysis Today* 141, 3-11 (2009).

43. Sorokin, A. B.; Kudrik, E. V.; Bouchu, D. *Chem. Comm.* 2562-2564 (2008).

44. Sorokin, A. B.; *et al. Catal.Today* 157, 149-154 (2010).

45. Forde, M.M.; *et al. J. Catal.* 290, 177-185 (2012).

46. Yamanaka, I.; Soma, M; Otsuka, K. *Chem.Commun.* 2235-2236 (1995).

47. Basickes,N.; Hogan,T.E.; Sen,A. *J. Am. Chem. Soc.* 118, 13111-13112 (1996).

48. Nizova, G.A.; Suss-Fink, G.; Shul'pin, G.B. *Chem.Commun.* 397-398 (1997).

49. Mizuno, N.; Seki, Y.; Nishiyama, Y.; Kiyoto, I.; Misono, M. *J.Catal.* 184, 550-552 (1999).

50. Jones, C. J.; *et al. Angew. Chem. Int. Ed.* 43, 4620-1629 (2004).

51. Wang, Y.; Otsuka, K. *J.Catal.* 155, 256-267 (1995).

52. Khokhar, M.D.; Shukla, R.S.; Jasra, R.V. *J. Mol. Catal A: Chemical* 299, 108-116 (2009).

53. Lin, M.; Sen, A. *J. Am. Chem. Soc.* 114, 7308-7310 (1992).

54. Seki,Y.; Mizuno,N.; Misono, M. *App.Catal. A: General* 158, L47-L51 (1997).

55. Shul'pin, G. B.; Mishra, G. S.; Shul'pina, L. S.; Strelkova, T. V.; Pombeiro, A. J. L. *Catal. Comm.* 8, 1516-1520 (2007).

56. Panov, G.; Sheveleva, G. A.; Kharitonov, A. S.; Rommikov, V. N.; Vostrikova, L. A. *App. Catal. A: General* 82, 31 (1992).

57. Wood, B. R.; Reimer, J. A.; Bell, A. T.; Janicke, M. T.; Ott, K. C. *J. Catal.* 225, 300-306 (2004).

58. Palkovits, R.; Antonietti, M.; Kuhn, P.; Thomas, A.; Schuth, F. *Angew. Chem. Int. Ed.* 48, 6909-6912 (2009).

59. Groothaert, M.H.; Smeets, P.J.; Sels, B.; Jacobs,P.A.; Schoonheydt, R.A. *J. Am. Chem. Soc.* 127, 1394-1395 (2005).

60. Beznis, N. V.; Weckhuysen, B. M.; Bitter, J. H. *Catal. Lett.* 136, 52-56 (2010).

61. Shul'pin, G. B.; Sooknoi, T.; Romakh, V.; Suss-Fink, G.; Shul'pina, L. S. Tetrahedron Letters 47, 3071-3075 (2006).

62. Rahman, A. K. M. L.; Kumashiro, M.; Ishihara, T. *Catal. Commun.* 12, 1198 (2011).

63. www.dow.com/news/corporate/2008/20080124a.htm, accessed October 2011.

64. Edwards, J.K.; *et al. J. Catal.* 236, 69-79 (2005).

65. Edwards, J.K.; *et al. J. Mater. Chem.* 15, 4595-4600 (2005).

66. Lopez- Sanchez, J.A.; *et al. Phys. Chem. Chem. Phys.* 10, 1921-1930 (2008).

67. Landon, P.; *et al. Phys. Chem. Chem. Phys.* 5, 1917-1923 (2003).

68. Landon, P.; Collier, P.J.; Papworth, A.J.; Kiely, C.J.; Hutchings, G.J. *Chem. Commun.* 2058 -2059 (2002).

69. Hughes, M. D.; *et al. Nature* 437, 1132 - 1135 (2005).

70. Park, E.D.; Choi, S.H.; Lee, J. S. *J.Catal* 194, 33-44 (2000).

71. Kesavan, L. *et al. Science* 331, 195-199 (2011).

72. Enache, D.I. *et al. Science* 311, 362-365 (2006).

73. Ab Rahim, M.H Submitted thesis , Cardiff University (2011).

74. Serp, P.; Kalck, P. ; Feurer, R. *Chem. Rev.* 102, 3085-3128 (2002).

75. Teo, K.B.K; *et al.* Nature 437, 968 (2005).

76. Terranova, M.I.; Sessa, V.; Rossi, M.; *Chem. Vap. Deposition* 12, 315-325 (2006).

77. Valden, M.; Lai, X.; Goodman, W. *Science* 281,1647-1650 (1998)

78. Haruta, M. *CATTECH* 6(3), 102-115 (2002).

79. Bessergenev, V. *J. Phys. Condens. Matter* 16, S531-S552 (2004).

80. Serp, P.; Feurer, R.; Morancho, R.; Kalck, P. *J.Catal.* 157, 294-300 (1995).

81. Hierso, J.C.; Feurer, R.; Poujardieu, J.; Kihn, Y.; Kalck, P. *J. Mol. Catal A:Chemical* 135, 321-325 (1998).

82. Hierso, J.C.; Serp, P.; Feurer, R.; Kalck, P. *App. Organomet. Chem.* 12, 161 (1998).

83. Okumura, M.; *et al. Catal. Lett.* 51, 53-58 (1998).

84. Sivakumar,P.; Ishak, R.;Tricoli, V. *Electrochimica Acta,* 50, 3312-3319 (2005).

85. Santo, V.D.; Mondelli, C.; Grandi,V.D.; Gallo, A.; Recchia, S.; Sordelli, L.; Psaro, R. *Applied Catalysis A: General,* 346, 126-133 (2008).

86. Liebau,F.; Gies, H.; Gunawardne, R.P.; Marles. B. *Zeolites* 6, 373–377 (1986).

87. Baerlocher,C.H.; Meier,W.M.; Holson, D. Atlas of Zeolite Framework Types. Elsevier, Amsterdam (2001).

88. Flanigen, E.M. *Pure Appl. Chem.* 52, 2191–2211 (1980).

89. Lobo, R.F. in Handbook of Zeolite Science and Technology (Auerbatch, S.M.; Carrado, K.A.; Dutta, P.K. eds.) Marcel Dekker, NY (2003)

90. Van Santen R.A. *Studies in Surface Science and Catalysis* 85, 273- 294 (1994)

91. Maesen,T.L.M.; Marcus, B. Introduction to Zeolite Science and Practice, 2nd ed. (Bekkum, H.V.; Flanigen, E.M.; Jacobs, P.A.; Jansen,J,C, eds.) 137, Elsevier, Amsterdam (2001).

92. Garces, J.M.; Kuperman, A.; Millar, D.M.; Olken,M.M.; Pyzik,A.J.; Rafaniello. W. *Adv. Mater.* 12, 1725-1735 (2000).

93. Kokotailo, G.T.; Lawton, S.L; Olson, D.H.; Meier, W.M. *Nature* 272, 437–438 (1978).

94. To, J.; Sokol, A.A.; French, S.A.; Catlow, C.R.A.; Sherwood, P.; Huub, J.J. van Dam *Angew. Chem. Int. Ed.* 45, 1633-1638 (2006).

95. Brodiga, S.; *et al. J. Catal.* 158, 486-501 (1996).

96. Panov, G.; Sheveleva, G. A.; Kharitonov, A. S.; Rommikov, V. N.; Vostrikova, L. A. *App. Catal. A: General* 82, 31 (1992).

97. Panov, G.; Sobolev, V. I.; Kharitonov, A. S. *J. Mol. Catal A: Chemical* 61, 85-97 (1990).

98. Jia, J. F.; Pillai, K. S.; Sachtler, W. H. M. *J. Catal.* 221, 119-126 (2004).

99. Hensen, E. J. M.; *et al.* *J. Catal.* 221, 560-574 (2004).

100. Wang, Y. *Res. Chem. Intermed.* 32, 235-251 (2006).

101. Kubánek, P.; Wichterlová, B.; Sobalik, Z. *J. Catal.* 211, 109-118 (2002).

102. Panov, G.; Sheveleva, G. A.; Kharitonov, A. S.; Rommikov, V. N.; Vostrikova, L. A. *App. Catal. A: General* 82, 31 (1992).

103. Panov, G.; Sobolev, V. I.; Kharitonov, A. S. *J. Mol. Catal A: Chemical* 61, 85-97 (1990).

104. Jia, J. F.; Pillai, K. S.; Sachtler, W. H. M. *J. Catal.* 221, 119-126 (2004).

105. Hensen, E. J. M.; *et al.* *J. Catal.* 221, 560-574 (2004).

106. Wang, Y. *Res. Chem. Intermed.* 32, 235-251 (2006).

107. Kubánek, P.; Wichterlová, B.; Sobalik, Z. *J. Catal.* 211, 109-118 (2002).

108. Zecchina, A.; Rivallan, M.; Berlier, G.; Lamberti, C.; Ricchiardi, G. *et al. Phys. Chem. Chem. Phys.* 9, 3483-3499 (2007)

109. Wood, B. R.; Reimer, J. A.; Bell, A. T.; Janicke, M. T.; Ott, K. C. *J. Catal.* 225, 300-306 (2004).

Chapter 2

Experimental Details

2.1. Materials

Commercial samples of ZSM5(x) [x = 23, 30, 80, 280, referring to SiO_2:Al_2O_3 ratio and Ferrerite (SiO_2:Al_2O_3 =20) were obtained from Zeolyst International and used as obtained. Zeolyte Y was obtained from PZ Zeolytes. MCM-41, Al-MCM-41 and alumina was purchased from Sigma-Aldrich and used as received. TiO_2 (P25 Degussa) and high surface area SiO_2 (Degussa) were used as supplied. TS-1 was supplied by DOW Chemical Co. and Silicalite-1 was prepared using hydrothermal synthesis by C.Hammond.

For catalyst preparation iron (III) acetylacetonate ($Fe(acac)_3$, 99.99%), copper acetylacetonate ($Cu(acac)_2$, 99.99%), gallium acetylacetonate ($Ga(acac)_3$, 99.99%) aluminium acetylacetonate ($Al(acac)_3$, 99.999%), zinc acetylacetonate ($Zn(acac)_2$, 99.995%) ferrocene (98%) were obtained from Sigma-Aldrich and used without further purification. $HAuCl_4$ $\cdot 3H_2O$ (99.99% purity) was supplied by Johnson Matthey. Bis(cyclopentadienyl) ruthenium (99.99%) was used as supplied from Strem Chemicals.

Stabilised 50% H_2O_2 in water and 1000 ppm metal atomic absorption standards were obtained from Sigma-Aldrich. All gases were obtained from BOC Gases or Air Products Ltd. Purity of gases was as follows:

Methane 99.995%, ethane 99.9%, propane (purity not confirmed), 1% C_2H_4/N_2, pure oxygen 99.99%, 25% O_2/N_2 99.99%, 5% H_2/N_2 99.99%, 5% H_2/Ar 99.95%, pure H_2 99.99%,He 99.99%, Nitrogen (O_2 free) 99.95%.

For EPR studies 5,5'-dimethyl-1-pyrroline-N-oxide (>97%) was purchased from Sigma and stored at low temperature during use.

2.2. Catalysis Preparation

2.2.1. Impregnation method

Typically, the synthesis of a Au impregnation catalyst was performed by slowly adding the support (TiO$_2$, 1.95 g) to a gold solution (5 mL, HAuCl$_4$(aq) of concentration 12.25mg Au/ml) with vigorous stirring. The slurry was kept in the oven for 16 hrs at 110 ^{o}C and when appropriate the as prepared catalyst was calcined at 400 ^{o}C for 3 h in static air.

2.2.3. Chemical Vapour Infiltration (CVI)

2.2.3.1. General Preparation for amorphous materials

This technique was modified after the work of Sivakumar [1] and Dal Santo [2]. The preparation was performed in a vacuum flask connected to a Schlenk line. Usually 1 g of the support material (TiO$_2$, Al$_2$O$_3$, SiO$_2$) and the desired amount of organometallic precursor (corresponding to the metal loading required) were placed in the flask with a magnetic stirrer bar and mixed until uniform in appearance. The flask was then evacuated (lowest pressure 10^{-3} mbar) and its contents heated under dynamic vacuum for 1-2 h at 140-175 ^{o}C [see Table 2.1 for details]. The sample was removed after cooling and attaining atmospheric pressure, and then heat treated in static air or in flowing 5%H$_2$/Ar. An upright Carbolyte furnace fitted with a quartz tube connected to a gas manifold was also used for heat treatment. This set up allowed exact measurement of gas flow using digital flow controllers and was generally used for H$_2$, 50% H$_2$/He or O$_2$ treatments.

2.2.3.2. CVI on microporous and mesoporous materials

For zeolite based samples the support (ZSM-5, ferrerite, ZeoY, TS-1, Sil-1, MCM-41, Al-MCM-41) was first heat treated at 150 ^{o}C for 2 h under vacuum prior to addition of the organometallic precursor and catalyst preparation as above. Care was taken to thoroughly mix the treated support and the metal precursor well before heating under reduced pressure. This was carried out by manually shaking the contents in a capped vial vigorously for 1-2 minutes or sifting the mixture two to three times through a sieve and then manually mixing. To prepare bimetallic catalysts the deposition temperature[a] of the component with higher deposition temperature was used. Catalysts were also prepared on a 5 g scale with these methods by using a larger Schlenk tube or a 250 ml round bottom flask.

2.2.3.4. Washing of CVI samples made on micro & mesoporous supports

Acetone washing- the as-prepared Fe(acac)$_3$@ZSM-5(30) (1g) was stirred briefly in 250ml acetone then filtered, washed with 2-3x 100 ml acetone and dried in air followed by drying under dynamic vacuum at 50°C for 3h prior to heat treatment.

Acid washing – prior to heat treatment the as-prepared sample (1g) was stirred in HNO$_3$ (5ml conc. in 50ml water) at 50 ^{o}C for 10 minutes followed by filtering and water washing with 100-250 ml of water as needed (i.e. until the filtrate ran clear). The solvent went red in a few minutes with loss of the

---

[a] Deposition of the volatile precursor occurs in the Schlenk tube at the temperatures specified in Table 2.1. Thermal decomposition of the precursor occurs during calcination separately.

original orange colour of the sample as evidence by the light cream residue after filtration.

H_2O_2 washing – prior to heat treatment the as-prepared sample (1g) was stirred in aqueous H_2O_2 (10ml, 50% H_2O_2 in 50ml water) at room temperature for 30 minutes followed by filtering and water washing. Copious evolution of gas was observed within minutes with the catalyst retaining its orange colour. These washes were followed by regular calcination of the material or heat treatment under H_2/Ar.

2.2.3.5. Preparation of "hybrid catalysts"

"Hybrid" catalysts were prepared by first depositing one metal using the impregnation method (or sol immobilisation) and followed by vapour deposition of a second metal onto the dried impregnation sample with subsequent heat treatments. This method was also applied to Au deposited by sol-immobilisation. The catalyst is denoted $M1@M2/S_{CVI@IMP \ or \ SI}$ where M1 is the metal deposited by CVI, M2 the metal deposited by impregnation or sol immobilisation, S the support. Fe@Au, Cu@Au were prepared with TiO_2 and ZSM-5(30) as supports in this way.

Table 2.1 Parameters for Preparation of Catalysts

Metal	Precursor	Deposition Temp./ ^{o}C	Deposition Time/h	Notes
Fe	Fe(acac)$_3$	150	1-2	Usually above 85% of the precursor is deposited
Fe	Ferrocene	100	2	Usually above 85% of the precursor is deposited. Colour when mixed with ZSM-5 is blue and not orange-red. Above 100°C ferrocene decomposes under vacuum.
Cu	Cu(acac)$_2$	140	1	Conditions need to be carefully controlled. Long deposition times lead to inactive catalysts
Ru	Ru(C$_5$H$_5$)$_2$	120	1	Sensitive to moisture
Al	Al(acac)$_3$	150	1	Not very effective at this temperature. Higher temperature leads to a lot of the precursor on the flask walls
Ga	Ga(acac)$_3$	150	2	Longer deposition time needed. A higher percentage of the precursor observed on the flask walls
Zn	Zn(acac)$_2$	150	2	Un-sublimed precursor observed at the base of the support.

2.3. Reactor Design

All catalytic reactions were performed in a custom built Parr Autoclave reactor set-up which included individual gas burettes connected to each reactor for gas mixing. Figure 2.1 outlines the design. The standard internal volume of the each autoclave with Teflon liner inserted was 35 cm^3 and this could be replaced by a larger autoclave to achieve and internal volume of 70 cm^3. In general the maximum allowed temperature was 250 ^{o}C and maximum gas pressure of 150 bars. Heating and stirring was typically controlled by a pre-set program (electronic) using software but this could also be done manually. The liquid sampling line was not used in the course of this work but fitted with a second alkane/ labelled $^{18}O_2$ source on some autoclaves for pressurising the reactors while avoiding gas contamination issues.
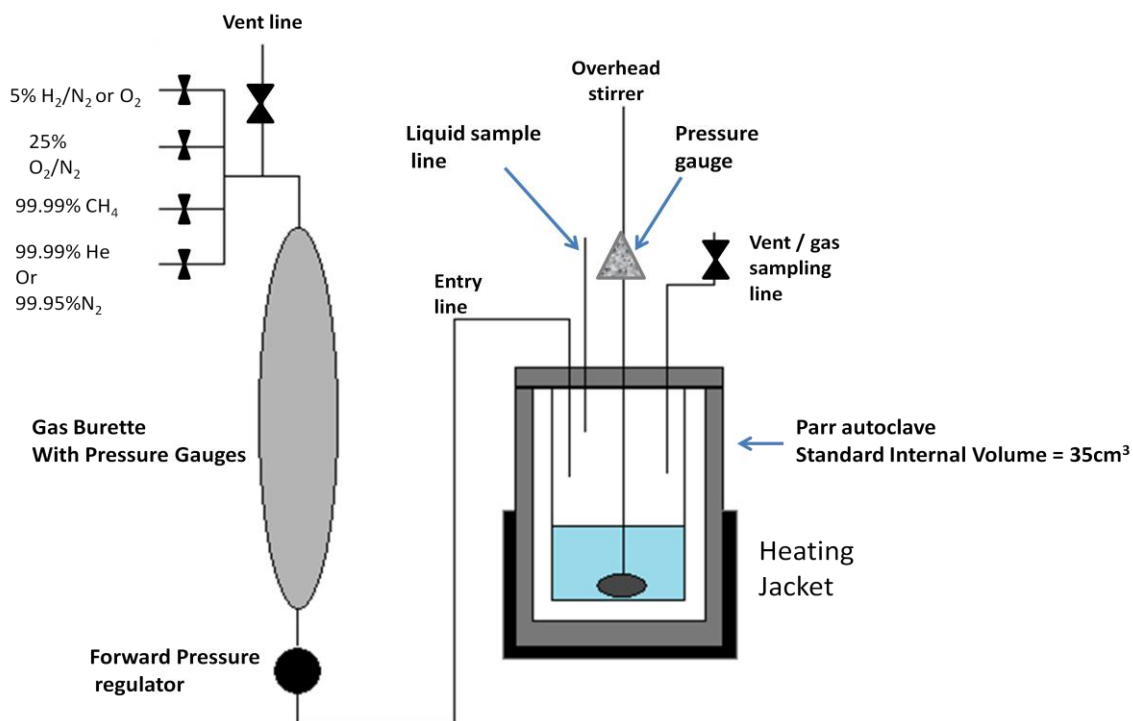
Figure 2.1 Schematic of the reactor system used for catalytic reactions

2.4. Catalytic Testing

The catalytic oxidation of methane was carried out using a stainless-steel autoclave (Parr reactor) containing a Teflon liner vessel with total volume of 50 ml (working volume of 35ml). In a typical experiment, catalyst (27 mg) was added to pure water (10ml) containing a measured amount of H_2O_2 (50 wt% H_2O_2). The system was pressurized with methane to a fixed pressure (30.5bar, 0.0305 mol) after air in the reactor was removed by purging three times with methane. The autoclave was heated to the desired reaction temperature (30-70 °C). Once the reaction temperature was attained the solution was vigorously stirred at 1500 rpm and maintained at the reaction temperature for a fixed period (0.5 h to 20 h). At the end of the reaction the autoclave was cooled in ice to a temperature below 10 °C to minimise loss of volatile products and the reaction gas was removed for analysis using a gas sampling bag fitted to the outlet line. The reaction mixture was filtered and analysed by ^{1}H-NMR using D_2O as a solvent and a calibrated TMS in $CDCl_3$ insert. In some cases the methanol amount was also verified by GC and LC-MS analysis to compare with NMR data.

Some reactions were also performed in 20ml water and details of other parameters are given where these results are discussed in the following chapters. This procedure was also followed for ethane, propane and ethylene oxidation studies. In the case of the addition on O_2 or H_2 the gases were mixed in the desired proportions in the burette prior to introduction into the reactor. For isotopic labelling studies the labelled gas feed was connected directly to the autoclave to avoid loss of substrate and contamination issues.

2.5. Analysis of products

Gas phase CO_2 was determined by GC analysis on Varian 450-GC equipped with FID & TCD detectors, methaniser and CP-SiL5CB column (50m, 0.33mm diameter, He carrier gas). Liquid phase products could be analysed by liquid GC injection using the same equipment but it was not sensitive enough to detect the low levels of HCOOH and CH_3COOH produced in some reactions. For this reason ^{1}H-NMR was the method of choice for liquid analysis. However, CO_2 in the liquid phase was suitably analysed using our GC-FID method. To carry out this analysis the initial water solvent was degassed with N_2 until a steady peak for CO_2 was observed upon GC analysis of the water. An aliquot (10 ml) was used as detailed above for the reaction. The reaction mixture was analysed immediately after depressurisation once enough filtrate had been collected for analysis (usually within one minute). For this procedure the gas and liquid injection ports of the instrument were first flushed with N_2 and kept under low N_2 flow to prevent injection of ambient air which would contribute significantly to the CO_2 in the analysis. A standard saturated solution of CO_2 in water was prepared by stirring water in a pressurised atmosphere of CO_2/N_2 to confirm the CO_2 in water assignment. Sample data for this method is given in Table 2.2. For CO_2 quantification a calibration curve was obtain with four CO_2/N_2 standard obtained from BOC gases.

^{1}H-NMR (500MHz Bruker spectrometer) unambiguously identified all major liquid phase reaction products. Formaldehyde and acetylaldehyde were observed as their hydrates, depending on the concentration. An internal standard containing 1% TMS in $CDCl_3$ was placed in a sealed tube and used to quantify the product amount after calibration against known methanol standards. Calibration against formic acid and

ethanol was also performed. All oxygenated species identified are given in Table 5 along with the shifts observed in parts per million (only the peak used in quantification is reported) and a sample spectrum is given in Figure 4. Note ethyl hydroperoxide was observed and quantified in other work but was not detected in any ethane reactions using zeolite based catalysts.

Table 2.2 Results of using the two protocols for total CO_2 analysis

Entry	Experiment	Products/ µmol		Ratio CO_2 liq. to gas
		CO_2 in liquid	CO_2 in gas [a]	
1	GC analysis of reaction liquid + gas	5.31[b]	55.74	1:10.5
2	Out gassing of reaction mixture. Gas only analysis	6.61[c]	63.7	1:9.6

Catalyst: acidified $Fe(NO_3)_3$(aq), 10ml water, 0.5M H_2O_2, 0.5h, 30 bar CH_4, 1500rpm[a] Measured by GC-FID method using first reaction gas extracted; [b] measured by modified liquid analysis under a N_2 atmosphere; [c] estimated by the sum total of CO_2 in the reaction gas mixture after 4 degassing steps. Note these data do not include the analysis of oxygenated liquid phase products Entries 1 and 2 were performed separately using the same experimental as described. pH of the final reaction mixture was 3-4.

Table 2.3 Liquid phase oxygenated products analysed by 1H-NMR for methane and ethane oxidation (only peak used in quantification displayed)

Species	Abbreviation	δ/ppm
Methanol	CH_3OH	3.35, s
Methylhydroxyperoxide	CH_3OOH	3.9,s
Formic acid	$HCOOH$	8.4,s
Ethanol	EtOH	1.2,t
Acetic acid	CH_3COOH	2.1,s
Hydrated formaldehyde	$(CH_2O)OH_2$	5.1,s
Hydrated acetylaldehyde	$(CH_3CHO)OH_2$	1.3,d
Acetylaldehyde	CH_3CHO	2.35,s
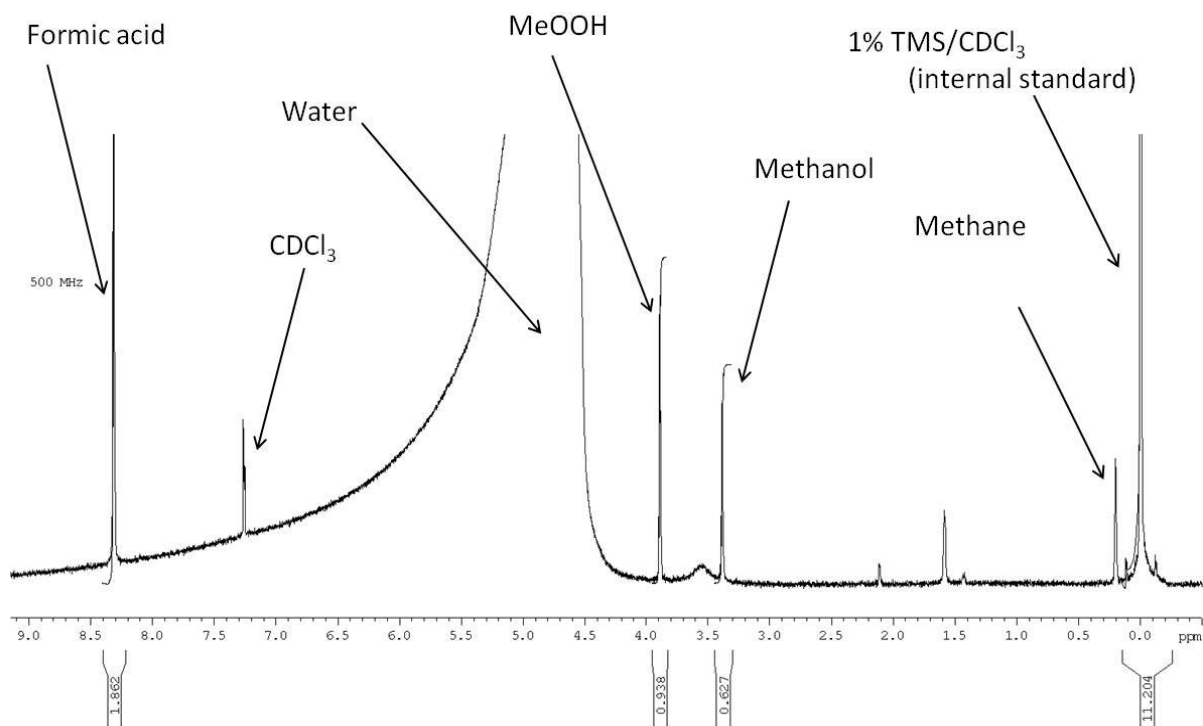
Figure 2.2 1H-NMR spectra of the reaction mixture obtained from the oxidation of methane. The signals at 0, 1.55 and 7.26 are due to the TMS standard and solvent contained in the calibration insert. In this example hydrated CH_2O cannot be observed but it would be observed at δ = 5.1 ppm in the spectrum.

2.5. Characterisation Techniques

2.5.1. Transmission Electron Microscopy (TEM)

This form of microscopy is akin to light microscopy but utilises electrons as the source of incident radiation as opposed to light. The resolution had when a beam of radiation passed through an ultra thin sample and interacts (scattering and interference) depends on the ratio of the photon wavelength to the numerical aperture of the system. Electrons (in beams) can be focussed onto much smaller areas than collimated light beams so this greatly reduces the numerical aperture. Also a property of electrons is their wave-particle duality which results in a finite wavelength characteristic for any electron beam. This wavelength is primarily related to the inverse square root of the energy multiplied by rest mass of the electron. In TEM measurements a beam of electrons is finely focussed on a prepared sample and images collected after the electron beam has passed through the sample. Information on the nature of the atoms present, shape and size of particles, particle orientation and composition can be obtained using this technique with certain modifications. For example to distinguish between to metals of differing atomic mass in a particle/sample bright field imaging can be applied where the heavier atoms appear as darker portions of the collected images allowing contact between atoms of different atomic mass (Z contrast).

Samples for examination by transmission electron microscopy (TEM) and scanning transmission electron microscopy (STEM) were prepared by dispersing the catalyst powder in high purity ethanol, then allowing a drop of the suspension to evaporate on a holey carbon film supported by a 300 mesh copper TEM grid. Samples were then subjected to bright field imaging experiments using a JEOL 2000FX TEM

operating at 200kV. Phase contrast lattice imaging and high-angle annular dark field (HAADF) imaging experiments carried out using a 200kV JEOL 2200FS transmission electron microscope equipped with a CEOS aberration corrector

2.5.2. X-Ray Photoelectron Spectroscopy (XPS)

This technique is based on photoelectric effect. When a material is irradiated with photons of suitable energy the material may absorb energy from the photon and emit electrons (i.e. photoelectrons) which have discrete and characteristic energies. The emitted photoelectrons are characteristic of a material's binding energies for electrons held in particular electron shell- orbitals from which they were ejected. This is also called the work function of a material and the process is an ionisation process. It follows that if the incident energy of the photon is known and the kinetic energy of the photoelectrons can be determined then the work function/ binding energy can be calculated since:

$$E_k = hv - E_b - \varphi \qquad \text{Equation 12}$$

Where E_k- kinetic energy of the ejected photoelectron

hv- Plank's constant x frequency of the incident radiation of excitation

E_b- binding energy of the photoelectron at a particular energy level in the atom/ material (Fermi Level)

φ- work function of the spectrometer

Using this technique one is able to obtain information about the identity of surface species present, oxidation states and physical composition of a material's surface (1-12nm depth).

X-ray photoelectron spectra were recorded on a Kratos Axis Ultra DLD spectrometer employing a monochromatic AlK$_\alpha$ X-ray source (75-150W) and analyser pass energies of 160 eV (for survey scans) or 40 eV (for detailed scans). Samples were mounted using double-sided adhesive tape and binding energies referenced to the C(1s) binding energy of adventitious carbon contamination which was taken to be 284.7eV.

2.5.3. Ultra Violet- Visible Electromagnetic Radiation Spectroscopy (UV-Vis)

The technique of UV-Vis is well known. It is based on the absorption of radiation in the UV and visible light regions of the electromagnetic spectrum by ions/molecules which have discrete energy levels associated with them. This technique can be very sensitive to changes in electronic environment as the absorption of a photon of particular energy is related to a precise excitation of an electron from one discrete level to another. These levels are affected by the charge of the ion, its localised environment or electronic bonding and can provide in many cases a fingerprint of the type of species present in a sample. In this thesis data is reported for solid state UV-Vis which operates under the same principle with the exception that the sample to be analysed is in the powdered state and is referenced to a white background (provided usually by barium sulphate or a white plastic reference) The spectra obtained have unique fingerprints of the states of Fe^{3+} and Cu^{2+} since these transition metal ions have characteristic d-d transitions when isolated in zeolites. Furthermore, when in the form of larger oxides and clustered species different absorption characteristics are obtained which may, by comparison to known standards, allow the identification of many types of iron and copper species/states in ZSM-5. Thus the technique was used to identify isolated species in tetrahedral or

octahedral coordination, oligomeric species, small clusters and larger oxides of varying size.

All spectra were recorded at room temperature in air after manual grinding of samples using a ceramic mortar and pestle. Spectra were recorded on a Varian Cary 4000 spectrometer with range 900-200nm using a white PVC standard for a reference background. Data was recorded at room temperature and atmospheric pressure at a data interval of 1nm.

2.5.4. X-Ray Diffraction Spectroscopy (XRD)

This technique is based on the interaction of atoms in an ordered lattice structure with incident electromagnetic radiation (X-Rays in this case) to produce a diffraction pattern of scattered constructive inference waves through elastic scattering of X-Rays. When order exists in a material its atomic planes diffract radiation according to Bragg's Law:

$$n\lambda = 2d \, Sin \, \theta \qquad Eq. \, 13$$

Where n- whole integer, and is the order of reflection plane

λ- wavelength of the x-rays

d- distance between the atomic /lattice planes

θ- angle between the incident and normal to the reflecting lattice planes

The wavelength of the radiation and the spacing between the lattice plane must be comparable for a successful scatter and interference pattern to be observed. Since the incident radiation can be refracted at different angles by an atomic/lattice plane

an interference pattern is obtained which is characteristic of the order of atoms in that plane or material.

Powder X-ray diffraction (XRPD) was performed using a PANalytical X'Pert PRO X-ray diffractometer, with a CuKα radiation source (40 kV and 40 mA). Diffraction patterns were recorded between 6-55° 2θ at a step size of 0.0167^o (time/step = 150 s, total time = 1 h). Samples were usually mounted onto a silicon wafer for analysis after manual grinding. In general this technique was merely used to identify any loss in structural integrity of zeolite samples after heating (observed though loss of the parent material peaks) and was not to estimate particle size of deposited metals since they were too small to be detected by this technique (i.e. < 5nm in size if present).

2.5.5. Electron Paramagnetic Resonance (EPR)

EPR is a very sensitive technique which is used to study the behaviour of paramagnetic species, i.e. species with unpaired electrons. It is routinely used to study transition metals in certain electronic states and organic radical species. The techniques relies on the ability of an unpaired electron to move between two energy states created when an electron's magnetic moment aligns itself with an externally applied magnetic field. This alignment happens in two states due to electrons having dual magnetic components of $m_s=\pm1/2$. When the unpaired electron moves between the two energy states (parallel and anti-parallel alignments) it may absorb energy and resonate. This condition can be described by the expression

$$h\nu = g_e\ \mu_b B_o \quad \text{Equation 14}$$

Where h= Planck's constant

v= wavelength of the energy absorbed

g_e= g-factor of an electron

μ_b= Bohr magneton

B_o= external magnetic field strength

Thus the resonance condition occurs at a certain magnetic field strength and because local magnetic fields due to nearby atoms and molecules can affect the g factor of a particular electron, information about the chemical state can be obtained by considering the effects of to spin- orbit coupling.

All EPR spectra were recorded at room temperature on an X-band *Bruker EMX* spectrometer operating at 100 kHz field modulation, 10 mW microwave power and fitted with a high sensitivity cavity (ER 4119HS). The g-values were determined using a DPPH standard, and are accurate to 0.001. EPR computer simulations were performed using a Simfonia program. For measurements using solid catalysts, a 5,5'-dimethyl pyrroline-N-oxide (DMPO) solution (5 mL *ca.* 18-25 mg DMPO/mL, Sigma-Aldrich >97%) in distilled water, was added to the catalyst (27mg) and stirred briefly prior to the addition of H_2O_2 solution (5 mL, 1M, Sigma-Aldrich). A sample prior to reaction with methane was removed, filtered and trapped in a sealed glass pipette tip by immersion in liquid N_2. The reaction was subsequently carried out in an autoclave for 5-10 minutes under methane (30 bars) with stirring (1500rpm). The reactor was degassed and a sample quickly withdrawn and frozen after filtering. For the EPR measurements, the samples were thawed and measured at room temperature with a minimum of 20 scans being performed. Where an aqueous source of Fe^{3+}/Cu^{2+} was also used the needed amount was derived from nitrate salt. H_2O_2 (0.285ml, 50% water solution) was added after the Fe^{3+}/Cu^{2+} + DMPO (aq)

was mixed. For calibration experiments using methanol Fe^{3+} (aq.) was mixed with aqueous methanol (0.1M, 10ml) followed by addition of the DMPO solution and then hydrogen peroxide.

2.5.6. Metal Content of Samples

Fe content of zeolite samples was obtained using Inductively Coupled Plasma (ICP) techniques (Warwick Analytical Service). As prepared samples were accurately weighed (50mg usually) and digested in concentrated hydrofluoric acid (HF) followed by digestion in Aqua Regia after evaporation of HF. The solution was then neutralised and infused into an ICP machine for analysis.

2.5.7. EXAFS

X-Ray Absorption spectra and analysed data were provided by The Dow Chemical Company and used as provided in this thesis. The data was analysed by Joo Kang (scientist working in Dow). X-ray absorption spectra were measured at the DND-CAT, at the Advanced Photon Source (APS) of Argonne National Laboratory. The synchrotron X-ray beam was monochromatized with a Si(111) double-crystal and the monochromator was detuned to 70% of the maximum intensity to reject harmonics. All samples were made to self supporting wafers and measured at room temperature. For catalysts, fluorescence spectra were collected using 13-Element Ge detector while for Fe oxide standards, transmission spectra were collected using ionization chambers. Fe foil standard was used to calibrate Fe K-edge (7112 eV) energy. Each represented data for catalysts are the average of 5 to 25 scans.

The XAS data were analyzed using Athena and Artemis [1], which implement the FEFF6 [2] and IFEFFIT [3] codes. Using crystal structure of reference compounds, theoretical phase shifts and amplitude functions were computed by the FEFF code for several different scattering of atom pairs (Fe-O, Fe-Fe, Fe-Si). Fitting the EXAFS part of the data to computed scattering functions were performed in the r-space with multiple k-weight factors. This was also done for Cu using appropriate standards and fitting parameters.

References

1. Sivakumar, P.; Ishak, R.; Tricoli,V. *Electrochimica Acta* 50, 3312-3319 (2005).

2. Dal Santo, V.; *et al. App. Catal. A: General* 346,126-133 (2008).

3. Ravel, B,; Newville, M. J.Synchroton Rad. 12, 537- 541 (2005).

4. Zaninsky, S.I.; Rehr, J.J.; Ankudinov, A.; Ablers, R.C.; Eller, M.J. *Phys. Rev. B* 52, 2995- 3009 (1995).

5. Newville, M.J. *Synchrotron Rad.* 8, 332- 324(2001).

Chapter 3

Low temperature aqueous phase methane oxidation with Fe/ZSM-5 based catalysts.

CH$_4$ + H$_2$O$_2$

Surface CVI catalyst calcined

Multiple Fe sites within zeolite pores and on zeolite external surface

CH$_3$OOH + CH$_3$OH+ CH$_2$O + HCOOH+ CO$_2$

O$_h$ and T$_d$ Fe $^{3+}$ in ZSM-5 pores All catalysts

Fe/ZSM-5

CVI catalyst "reduced"

Fe/ZSM-5(30) is 5 times more active than sMMO for methane oxidation !
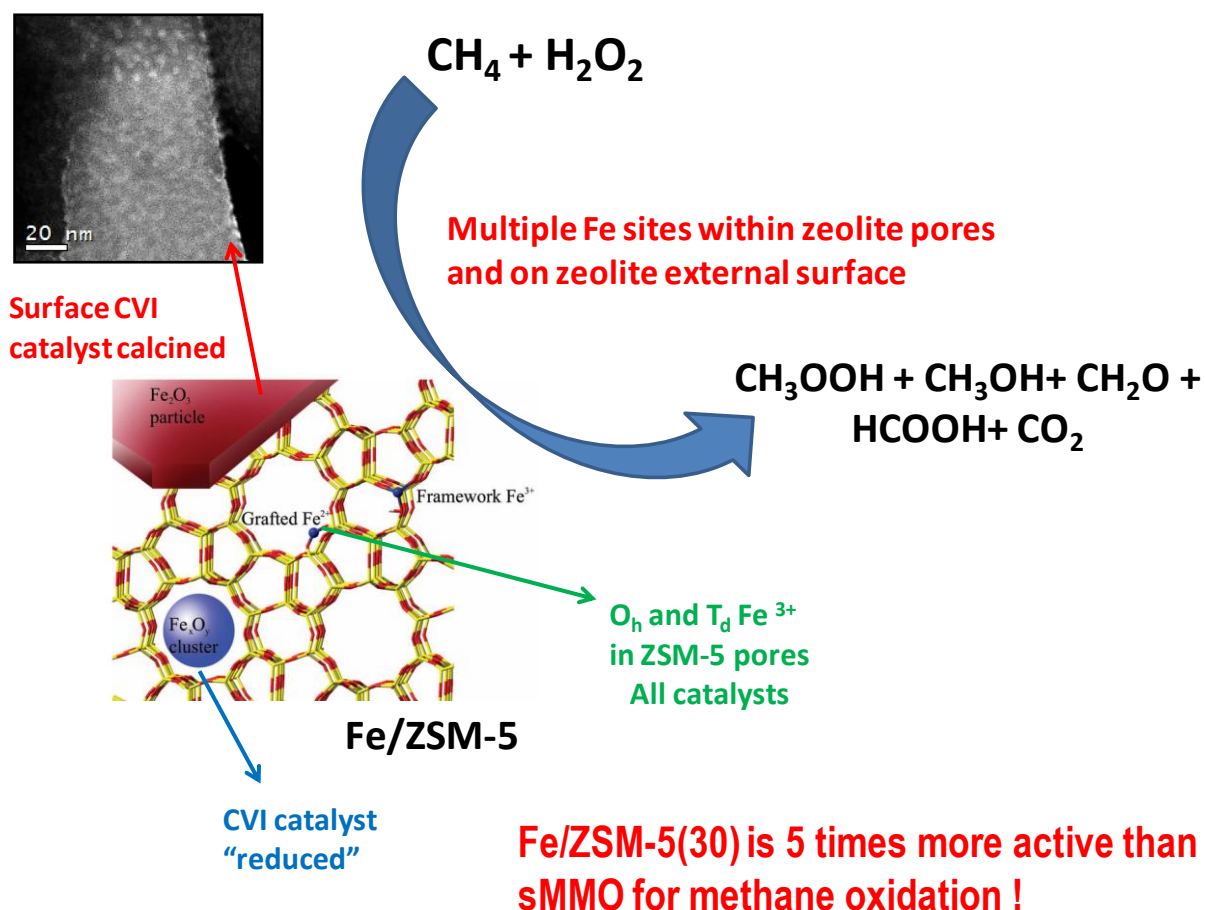
3.1. Targets

Before beginning the discussion, mention must be made about the target catalyst productivity that has driven this work. In terms of the wider DOW Methane Challenge it was agreed that the academic benchmark catalyst would be the sMMO [1] system. This was because it represented a well studied system for methane oxidation which remains an active area of research as most of the recent efforts in the area of methane oxidation have been to mimic the enzyme active site. No other heterogeneous catalyst to date has been reported to achieve 5.05 mol (CH_3OH) kg (catalyst)$^{-1}$ h^{-1}, the *in vivo* activity of sMMO. However, when one replaces the NADH co-factor, necessary for this enzyme to utilise molecular oxygen, with H_2O_2 the productivity drops to 0.067mol (CH_3OH) kg (catalyst)$^{-1}$ h^{-1}. Hence the higher productivity value for the intact enzymatic system was chosen as an academic challenge within our group.

From an industrial perspective, molecular oxygen is the preferred oxidant as H_2O_2 is not economical due to the price similarity between the desired product, methanol, and the oxidant[a]. Even if dilute H_2O_2 could be used to achieve appreciable conversion levels, in aqueous solution the methanol formed has the additional complication of an energy intensive distillation to obtain pure methanol. Moreover, the approach of using hydrogen plus oxygen in the fed gas for *in situ* hydroperoxy generation and capture is also non-viable at this moment due to the price of hydrogen. In reality the ideal system would catalytically turn over molecular O_2 with small amounts of initiator or even cheap H-donor (e.g. sacrificial solvent from

---

[a] A simple price comparison of hydrogen peroxide vs. methanol from Sigma-Aldrich reveals that a 30% solution of hydrogen peroxide costs ca $74/L whilst pure methanol costs $37/L.

biorenewable source, glycerol). This can be seen as a future target and the data which follows is based on using hydrogen peroxide as an oxidant.

It should also be mentioned here that some key parts of the overall challenge to understand the catalysis presented with ZSM-5 based materials was performed by fellow colleagues C.Hammond (ZSM-5 and hydrothermally synthesised materials) [2] and A.Thetford (DFT)[b]. For methane oxidation with Au-Pd systems the primary concern was oxygenate productivity and catalyst stability as the conversion levels are generally low (<0.1%) though HCOOH was not observed. Much higher conversion levels have been achieved with the zeolite based systems. Thus a general testing scheme using "standard conditions" was utilised with some tests performed under "high conversion conditions" for catalyst screening protocol [c] . Total productivity is generally reported (moles product kg(catalyst)$^{-1}$ h^{-1}) as the exact amount of catalytically active metal (Fe) remains unknown and thus reporting turn over frequency in a meaningful way is not possible. Furthermore use of catalyst productivity (or volumetric productivity) allows direct comparison of data available for sMMO. Oxygenate selectivity refers to the amount of liquid phase oxygenates as a percentage of the total products observed. Discussion based on TON has been avoided as many previous workers in this area have reported artificial values of TON by considering each subsequent product as a separate "oxidation" step so that the calculated TON is actually a sum of multiples of each actual product amount based on the number of H's in the product molecule. When the main primary product is methyl hydroperoxide (CH_3OOH), as in the present report, a range of possible reactions of this intermediate may occur in solution without the need of catalyst. For

[b] Thetford, A; Unpublished Thesis, Cardiff University
[c] Standard Conditions: 27mg catalyst, 0.5M H_2O_2, 30.5b CH_4, 50°C, 10ml H_2O
High Conversion Conditions: 54mg catalyst, 1.0M H_2O_2, 5b CH_4, 50°C, 20ml H_2O. This is basically a scaled up reaction.

example, the transformation of methyl hydroperoxide to methanol this is clearly a reduction step whilst the transformation of methyl hydroperoxide to formaldehyde in solution readily occurs in the presence of acid and may not involve a formal oxidation using a catalyst surface. Methyl hydroperoxide may also be thermally decomposed to CO_x.

3.2 Early work with CVI[d] catalysts

The vapour deposition methodology was first used to deposit a range of metals on TiO$_2$ as support. The ability to achieve controlled particle size in the absence of solvents, inorganic resides and in a reproducible manner was the target. For the screening phase it was envisaged that many metals and support materials would be used. CVI allows the deposition of a wide variety of metals (provided they have suitably volatile organometallic precursors) on a wide variety of support materials, with the exception of activated carbon for which it was found that most of the metal was left in the deposition tube and not on the support material. The role of small nanoparticles in oxidation reactions is well established. A recent example can be drawn from the work of Kesavan *et al.* [3] on toluene oxidation with molecular O$_2$ under mild conditions, where sol-immobilisation methods were used to prepare highly active Au-Pd catalysts when simple wet impregnation methodology produced less active catalysts. The differences in activity were attributed to the smaller and controlled particle size distribution afforded by the sol-immobilisation technique.

The ease of preparation and lure of being able to deposit highly dispersed small nanoparticles was the main driving force behind using the chemical vapour deposition technique. A simple procedure of using a Schlenk flask connected to a vacuum line was enough to achieve this, as will be shown further in this chapter. The key to this process was the use of metal acetylacetonate compounds (primarily) because of their high volatility at low temperature and ease of decomposition. These compounds have not been used extensively to prepare supported metal catalysts in the past. The conditions set out in the Chapter 2 Section 2.2.3 were chosen based

---

[d] CVI- chemical vapour infiltration, so called as mainly it was used to load porous materials with an organometallic precursor followed by heat treatments to decompose the supported precursor.

on the observed sublimation temperatures for each organometallic precursor when used in the CVI apparatus without the addition of support material. A temperature at which most of a sample of organometallic precursor was vaporized and sublimed onto the walls of the Schlenk tube was generally used as the deposition temperature. Due to the volume of work performed during the last three years detailed study of the technique was not performed but in general higher temperatures than required for appreciable sublimation, presence of water vapour and long deposition times led to less active catalysts.[e]

Initial studies were merely exploratory work in catalyst screening and preparation. A variety of metals (Ag, Al, Cu, Fe, Ga, Pd, Pt, Ru, Zn) were deposited onto titania using the CVI technique usually at 2.5 nominal wt%. These materials were tested for methane oxidation in the batch reactor under standard conditions alongside testing to analogous materials prepared by other members of our group using "wet" techniques. In general, noble metal CVI catalysts showed a high rate of hydrogen peroxide decomposition whereas base metals gave more promising results. When compared to analogous materials prepared by wet methods, the CVI catalysts had lower productivity and higher hydrogen peroxide decomposition except in the case of Fe and Cu. It was found that Fe, and to a lesser extent Cu, showed the best activity in methane oxidation (see Table 3.1). In the case of Pd, Pt, Ag, Ru, Zn (not shown) and Cu (entries 1, 2 Table 3.1) the low activity could easily be explained by the high H_2O_2 decomposition tendency facilitated by the very small particle size (see example of TEM micrographs in Appendix 1) and so no further work was performed on these systems.

---

[e] Based on unpublished room temperature CO oxidation for Pd/Pt catalysts and methane oxidation data for Fe catalysts.

Interestingly, Fe/TiO$_2$ showed favourable activity (Entries 3, 4 Table 3.1), as compared to other metals tested, and also required less hydrogen peroxide for the oxidation reaction to occur. This result was surprising as Fe is well known for Fenton's type chemistry and it was thought small iron oxide particles would more efficiently decompose hydrogen peroxide, to oxygen and water, as compared to the other materials. Furthermore, when the reaction filtrate was assayed less than 2ppm of leached Fe was found in all cases and thus the issue from leached metals carrying out the oxidation was ruled out, taking into account the data presented in Chapter 4.4.3 on Fenton's chemistry using ppm levels of aqueous iron salts.

This was the first indication that Fe and Cu, presumably as oxides, could be active for methane oxidation and also produce a key intermediate, namely methyl hydroperoxide. Even more interesting in all these cases is the production of CO$_2$, an over-oxidation product, but not formic acid from which it can more easily be produced by consecutive oxidation. It should be here noted that studies on CuO/Cu$_2$O carried out in our group showed that larger particles of copper oxide were more active than Cu/TiO$_2$ prepared by CVI and produced mainly methyl hydroperoxide or methanol depending on the ratio of copper oxidation states in the catalyst.

It can also be proposed that the difference in selectivity to methyl hydroperoxide or methanol for Fe/TiO$_2$, entries 5 & 6 Table 3.1, might be attributed to oxidation state changes due to reduction treatment in 5% H$_2$/Ar. In later discussions data will be presented showing that reduction of the Fe containing catalyst increases the selectivity to methanol for catalysts which have much higher activity than these TiO$_2$ based materials. However, XPS analysis of those samples did not show any change

in Fe oxidation state between calcined and "reduced" samples. This will be discussed in due course.

Table 3.1 Methane oxidation using H_2O_2 and varied TiO_2 supported metal nanoparticle catalysts.

Entry	Catalyst M/TiO₂	Product amount (µmol)				Oxy. Prod.[c]	H₂O₂ Left /µmol [d]
		CH₃OOH[a]	CH₃OH[a]	HCOOH[a]	CO₂ in gas[b]		
1	2.5wt%Cu Reduced	n.d.	0.582	0	0.84	0.06	993
2	2.5wt%Cu Calcined	n.d.	0.877	0	0.75	0.08	<25
3	2.5%Fe Calcined	2.91	0.98	0	1.50	0.38	2506
4	2.5%Fe Reduced	1.32	2.07	0	1.69	0.32	3562
5	2.5%Cu@2.5%Au Hybrid, Calcined	0	1.79	0	0.95	0.18	<25
6	2.5%Cu@2.5%Au Hybrid, Reduced	0	0.45	0	1.54	0.04	170
7	2.5%Fe@2.5%Au Hybrid, reduced	0.69	1.16	0	1.07	0.25	2497

Reaction conditions: Reaction Time: 0.5h; Reaction temp: 50°C, Solvent: H_2O: 10 mL; 0.5M H_2O_2 ; P (CH_4): 30b; All catalysts were calcined at 400°C, 3h in static air or reduced in 5% H_2/Ar at 400°C, 3h.[a] Analysis using ¹HNMR, [b]Analysis using GC-FID, [c] mol of products (CH_3OH+ CH_3OOH+ HCOOH) kg(catalyst)$^{-1}$ h^{-1} , [d] Assayed by titration against acidified $CeSO_4$ with Ferroin indicator.

Additionally, Au was deposited by impregnation onto titania followed by deposition of Fe or Cu by CVI (the so-called "hybrid method") due to the syngeristic effect of Au with Pd for C-H activation in toluene noted by Lokesh *et al.*[3] Under H_2O_2 addition protocol there was no positive effect of Au in conjunction with Fe. However, the

Fe@Au/TiO$_2$ catalyst was active for *in situ* hydroperoxy capture to produce methyl hydroperoxide and methanol (entry 2 Table 3.2, see conditions in the caption). Under similar conditions Au-Pd/TiO$_2$ (a reference catalyst) gave lower productivity as compared to the Fe@Au/TiO$_2$ catalyst even though Au-Pd/TiO$_{2(IMP)}$ is much better than Au/TiO$_{2(IMP)}$ at H$_2$O$_2$ synthesis [4] which was thought to be crucial to the ability of the catalyst to oxidise CH$_4$. As mentioned in Chapter 1 this approach has already been employed for alkane oxidation Fe-Pd catalysts. [5]

These results led to the use of Fe and Cu on ZSM-5(30) to synthesise very active catalysts after it was found that ZSM-5(30) itself was active for methane oxidation.[2]

Table 3.2 Liquid phase CH$_4$ oxidation with various catalysts using H$_2$ and O$_2$

Entry	Catalyst	Product amount (µmol)				Oxygenate Productivity [c]
		CH$_3$OOH[a]	CH$_3$OH [a]	HCOOH[a]	CO$_2$ in gas[b]	
1	2.5%Au-2.5%Pd/TiO$_2$ IMP calcined	0.29	1.31	0	0.24	0.12
2	2.5%Fe@2.5%Au/TiO$_2$ Hybrid, reduced	3.49	0.99	0	0.69	0.43
3	2.5%Cu@Au/TiO$_2$ Hybrid, calcined	0	trace	0	1.53	0

IMP= wet impregnation. Calcination in air or reduction in 5%H$_2$/Ar at 400°C for 3h Reaction conditions: Reaction Time: 30 min, Reaction temp.: 50°C Solvent: H$_2$O, 10 mL. P(CH$_4$) = 352 psi (61.1%), P(O$_2$) =16 psi (2.7%), P(H$_2$) =8 psi (1.3%), and P(N$_2$) =200 psi (34.72%).[a] Analysis using ^{1}HNMR, [b]Analysis using GC-FID, .[c] mol of oxygenates (CH$_3$OOH+CH$_3$OH+ HCOOH) kg(catalyst)$^{-1}$ h^{-1}

3.3. Elucidation of the active site for methane oxidation with ZSM5 (30)[f]

In parallel to the finding reasonably active metals for this reaction, C. Hammond [2] discovered that Au-Pd/ZSM-5(30) prepared by impregnation or deposition precipitation was active for the target transformation or methane to methanol. As my work showed better activity from "hybrid" catalysts containing Au and Fe/TiO$_2$ prepared by CVI, Fe and Pd were deposited by CVI onto Au/ZSM-5(30). Due to the vacuum treatment used for CVI the parent ZSM-5(30) was also vacuum treated and calcined samples of ZSM-5(30) were prepared for comparison as a baseline of catalytic activity. The data are presented in Table 3.3. Entries 1, 2 and 3 for Au/ZSM-5(30)$_{IMP}$, Pd-Au/ZSM-5(30)$_{IMP}$ and Pd@Au/ZSM-5(30) $_{CVI@IMP}$ showed diminished activity as compared to the unmodified ZSM-5(30), entry 4 Table 3.3. The Pd-Au containing catalysts also had greater loss of the oxidant with no increase in detected products. This clearly showed that the zeolite itself was the active component for the selective reaction and the great loss of hydrogen peroxide observed was due to the additional metals (N.B. small Pd particles are active for H$_2$O$_2$ decomposition as evidenced by observed vigorous evolution of gas of the aqueous hydrogen peroxide solution immediately on contact with Pd/TiO$_2$ $_{CVI}$ which had average particle size of 2.3nm).

Furthermore, the improved activity of the calcined vacuum pre-treated sample (Entry 5 Table 3.3) suggested that the zeolite itself could be modified by heat treatment to create a more active catalyst. It is well known that heat treating ZSM-5 materials leads to de-alumination of the material whereby Al^{3+} in framework positions migrate

---

[f] ZSM5- Zeolite Socony Mobil #5, (x) represents the silica to alumina ratio of the material

to extra-framework positions with increase in Lewis acidity of the sample. [6, 7] The role of aluminium is discussed later.

Fe@Au/ZSM-5(30)$_{CVI}$ heat treated in reducing atmosphere had a productivity of 20.7 mol of products kg(catalyst)$^{-1}$ h^{-1}, entry 6 Table 8) which is remarkable. This catalyst shows four (4) times the productivity of the native sMMO system with O$_2$.[1] The calcined Fe@AuZSM-5(30)$_{CVI}$ and Fe/ZSM-5(30)$_{CVI}$ materials had similar productivities (entries 7, 8 Table 3.3) but different product distribution . Since the calcined or reduced Au/ZSM-5(30) could not account for the observed activity, Fe was put forward as the pivotal metal for promoting catalytic activity. An important difference, due to heat treatment conditions, was the product distribution for the "reduced" vs. calcined Fe@Au catalyst (entries 6, 7 Table 3.3). The higher methanol selectivity in the case of heat treatment of the catalyst under H$_2$/Ar showed that the material was very different from its calcined counterpart. This is further discussed in Chapter 4. These observations show that (i) addition of Fe was important for the catalysis, (ii) the zeolite itself also a source of catalytic activity and (iii) different combinations of metals and heat treatments could be used to tune catalytic activity and selectivity.

Also, by comparison to biological and homogeneous methane activation where acidity within the catalytic system is pivotal for methane oxidation activity it was proposed that the acidity of the zeolite (without additional metals) was the source of the observed catalysis. This would not be surprising as solid acid catalysts, and in particular zeolites, are used widely in the petrochemical industry to perform alkylation, esterification, isomerisation, cracking etc. [9] However, addition of acids (nitric acid, sulphuric acid and phosphoric acid) to other catalysts or the ZSM-5 itself and testing of other solid acid catalysts (zeolites, heteropolyacids, acidic resins)

showed that acidity was not the only factor explaining the origin of the high catalytic activity[g]. Thus other properties of ZSM-5 were examined in an attempt to correlate the observed activity to some specific property of the material.

Table 3.3 Catalytic methane oxidation using Fe, Pd@Au/ZSM-5(30) and ZSM- 5(30).

Entry	Catalyst	Product amount (µmol)				Total Productivity [c]	H_2O_2 Left /µmol [d]
		CH_3OOH[a]	CH_3OH [a]	HCOOH[a]	CO_2 in gas[b]		
1	Au/ZSM-5(30)$_{IMP}$ reduced	10.2	3.6	3.2	6.6	1.7	2796
2	Au-Pd/ZSM-5(30)$_{IMP}$ calcined	-	7.0	11.2	4.6	1.7	3650
3	Pd@Au/ZSM-5(30) CVI@IMP Hybrid	1.2	6.9	7.6	0.9	0.6	264
4	ZSM-5(30) uncalcined	15.9	6.7	5.0	0.35	2.0	4820
5	ZSM-5(30) Vacuum treated, calcined	13.9	11.6	32.0	2.1	4.4	3098
6	Fe@Au/ZSM-5(30) Hybrid, reduced	0	114	123	42	20.7	498
7	Fe@Au/ZSM-5(30) Hybrid, calcined	3.2	36.3	168.0	46.7	18.8	1421
8	Fe/ZSM-5(30) calcined	3.1	22.1	167.6	63.3	18.9	1319

Reaction conditions: Reaction Time: 0.5h; Reaction temp: 50°C, Solvent: H_2O: 10 mL; 5000µmoles H_2O_2 ; P (CH_4): 30b; 27mg catalyst. All catalysts were calcined at 400°C, 3h in static air unless otherwise specified.[a] Analysis using ^{1}HNMR, [b]Analysis using GC-FID, [c] mol of products (CH_3OH+CH_3OOH+ HCOOH+CO_2) kg(catalyst)$^{-1}$ h^{-1} , [d] Assayed by titration against acidified $CeSO_4$ with Ferroin indicator.

---

[g] Work on acid conditions performed by C.Hammond and H. Mohamed AbRahim

A systematic study into the effect of varying the supports was performed. Since many of the acidic materials (zeolites, heteropolyacids, acidic resins such as Nafion, etc) tested had low activity as compared to ZSM-5(30), Fe was deposited onto a variety of support materials. As shown in Figure 3.1 the deposition of Fe by CVI onto various support materials resulted in an active catalyst thus the promotion of activity is undoubtedly linked to the Fe content of the samples. In the case of microporous supports containing aluminium the effect was enhanced, for example Zeolite Y or Ferrerite. In the case of amorphous supports it is evident that small iron nanoparticles (<5nm) or even smaller iron clusters have been deposited and are the active species, as observed with Fe/TiO_2. This hypothesis is based on the absence of any peaks characteristic of iron phases when the Fe@ amorphous materials are analysed by powder XRD. Since Fe was actually present in these catalysts this showed that surface Fe species must be smaller than 5nm. STEM imaging on five different materials with metals deposited by CVI (i.e. $Fe/ZSM-5(30)_{CVI}$, $FeSil-1_{CVI}$, Pd/TiO_2, Pt/TiO_2, $Pd-Pt/TiO_2$)[h] all showed highly dispersed fine crystallites of average particle diameter below 4nm which suggests that the technique routinely deposits very small nanoparticles on a variety of support materials.

---

[h] Example micrographs given in Appendix 1.
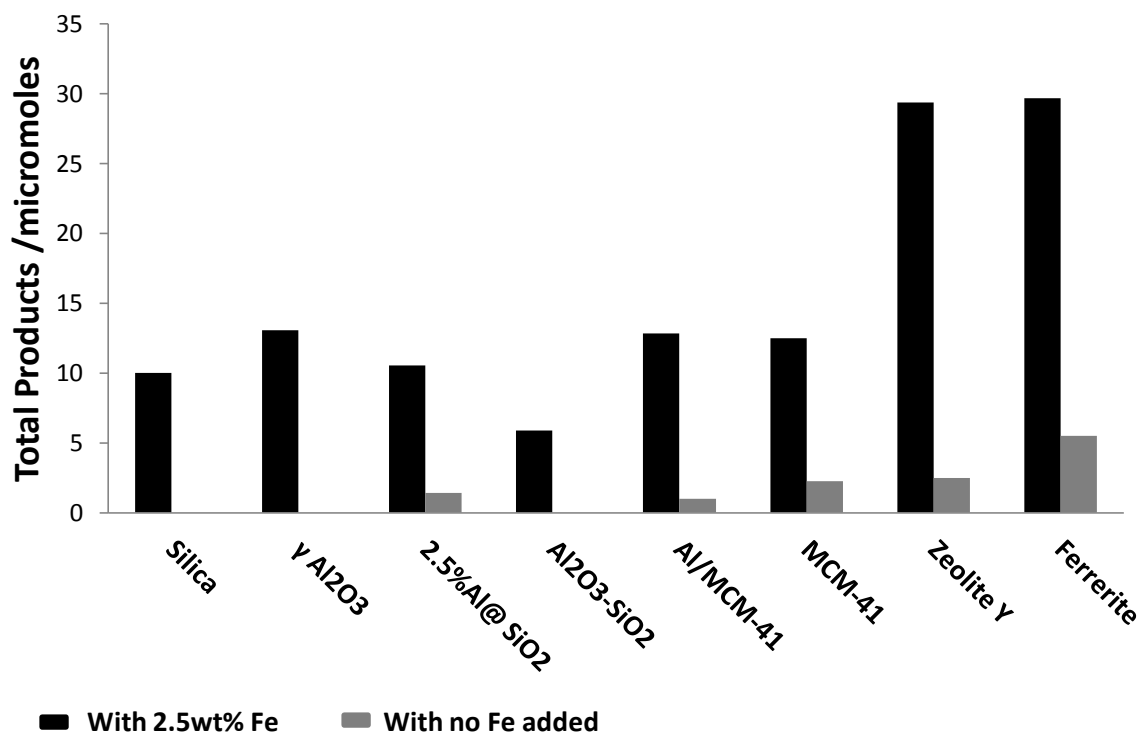
Figure 3.1 The effect of depositing Fe from $Fe(acac)_3$ using the CVI methodology on a variety of supports. All catalysts were calcined at 400 ^{o}C in static air for 3h and a nominal 2.5wt% Fe was deposited. Black bars- catalysts with additional Fe; grey bars- catalysts without additional Fe. In all cases the addition of Fe by CVI promoted methane oxidation. Note that SiO_2 (Degussa) and Al_2O_3 (neutral γ-form from Sigma) showed some activity at long reaction times and using higher mass of catalyst but not under these specific conditions. General reaction conditions are as in Table 3.3

The ability of iron nanoparticles to perform methane oxidation with H_2O_2 was further investigated by depositing varying amounts of Fe on silica and alumina, Figure 3.2. These support materials were chosen since the most active material, ZSM-5, is composed of Si and Al and thus study of the catalytic activity of components of ZSM-5 was warranted. Previous work on gas phase methane oxidation showed that highly dispersed isolated Fe^{3+} and FeO_x clusters on silica could effectively convert methane to formaldehyde and CO_x using molecular O_2.[10,11] Additionally doped silicas with better iron dispersion at higher iron loading (0.35wt%) were shown to have higher

activity for gas phase methane oxidation .[12,13] Since the CVI technique routinely allows deposition of highly dispersed small metal nanoparticles (oxides, sub- nm clusters and isolated metal species) it was thought that studying the effect of metal loading on an amorphous support would shed light on the effect of particle size (related to iron loading) on the oxidation activity of iron nanoparticles. Also, study of metal loading may have resulted in a highly active non-ZSM-5 material and given information on whether or not the high hydrogen peroxide decomposition observed with Fe/ZSM-5(30)$_{CVI}$ was merely due to surface iron oxides

The data in Figure 3.2 supports the hypothesis that the iron oxide nanoparticles or other small iron species on the silica surface can perform the oxidation of methane under these conditions. As mentioned previously, it could be proposed that any support which can increase the dispersion of these species may also be used to prepare a more active catalyst since high metal dispersion is pivotal in many catalytic applications which use metals supported on oxides where the metal itself or its interface with the support is the active site. In fact this idea has been used previously in a number of iron based methane oxidation systems. Undoubtedly, the iron doped silica and alumina materials contain external iron species as these supports are not meso/microporous materials. For Fe/ZSM the iron may be in a number of positions within the zeolite pores or on its external surface. Hence it is probable that the highly dispersed surface iron species observed with Fe/ZSM-5(30) contributes to the catalysis but the question remains as to the contribution of each type of iron species to the overall oxidation.

It should be mentioned that for the oxidation activity observed in Figure 3.2 these catalysts have much lower usage of hydrogen peroxide as compared to the Fe/ZSM-5(30) $_{CVI}$ in Table 3.3. The observation suggests that under these reaction conditions

small surface iron oxide particles do not decompose hydrogen peroxide as efficiently as the zeolite analogue which shows high oxygenate productivity. Thus the oxygenate productivity (i.e. ability of the material to oxidise methane) is actually linked to hydrogen peroxide usage.
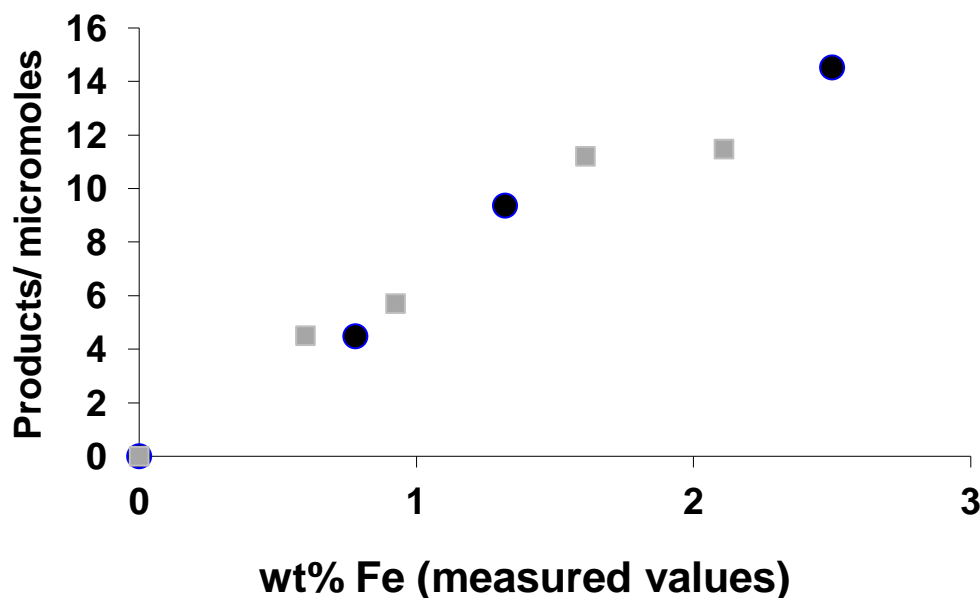
Figure 3.2 Catalytic activity of Fe deposition on SiO_2 and γAl_2O_3 by CVI. Circles- SiO_2; squares- Al_2O_3. Both support materials are inactive with additional Fe for the reaction conditions tested. There is a maximum amount of Fe which can be deposited without modification of the preparation and above *ca.* 2.5wt% the activity of the catalyst drops accompanied by higher decomposition of the oxidant.

A key observation is that the most active materials were zeolites and also contained Al. Other work showed clear trends of the effect of heat or steam treatments on ZSM-5 [2], i.e. formation of extra framework Al and extra framework Fe sites from the trace impurities of Fe present in the catalyst, in promoting the activity of benzene to phenol oxidation by isolated Fe^{3+} ions or oligomeric species. Al^{3+} had a pivotal role in providing stabilisation for Fe^{3+} ions at cation exchange sites. [14-19] This finding was

also supported by the work of Wood and co-workers in the oxidation of methane by a Fe-Al-MFI material using N_2O. [20]

One must also consider that a second effect of the zeolite structure can also be essential to the catalysis observed for a variety of reactions. Zeolites have been used as shape/size selective catalysts for decades due to the confinement effects afforded by their structure. An early work by Herron and Tolman [5] on Fe-Pd-Zeolite 5A using the *in situ* approach (i.e. Pd to produce H_2O_2 and Fe to perform the oxidation simultaneously) was effective for low temperature oxidation of cyclohexane and n-octane. They identified absorption of products as the reason for the observed decreasing activity with increasing conversion and indeed complete dissolution of the zeolite was necessary for accurate product quantification. This hinted at the probability that catalysis was not only occurring on the external surface of Zeolite 5A but within the pores as well. Furthermore it was stated, without supporting evidence, that using ZSM5 avoided the deactivation issue as its pore was larger than in Zeolite A and therefore the product could be desorbed easily from the internal cavities of the material. Knops-Gerrits reported that di-nuclear Fe complexes encapsulated in hexagonal mesoporous solids were active for cyclohexane and butane oxidation with H_2O_2/TBHP [21]. It was suggested that the cages of the support material were important in the catalysis as it controlled the oxidation process by allowing intimate contact of the substrate with an active di-iron species. Moreover, Raja and co-workers [22,23] used this principle to prepare the active zeolite encapsulated Fe/Cu/Co-phthalocyanine catalysts. In this system partial oxidation of methane with selectivity of 15.1, 52.9 and 19.5% to methanol, formic acid and CO_2 respectively when using tertiary butyl hydroperoxide (TBHP) as oxidant and water as solvent was achieved at *ca.* 1.5% conversion in 12h.

Since ZSM-5(30) in this system is essentially the same catalyst as used in previous work on methane activation using N_2O as an oxidant and also showed the trends observed that heat treatment of Fe/ZSM-5 promoted catalytic activity with iron being essential for the catalysis it was proposed that iron, aluminium and the confinement effect have a combined role in producing an active catalyst. To investigate this hypothesis a simple series of catalysts were prepared and tested in the oxidation of methane.

Materials with the same structure as ZSM-5 (i.e. MFI materials) were used in the presence and absence of additional iron. The results are given in Figure 3.3. Also Fe-Silicalite-1 was prepared by hydrothermal synthesis and tested in a similar manner.[i] The data in Figures 3.1, 3.2 and 3.3 show that when iron is deposited by the CVI technique the resulting material is always catalytically active hence the technique of depositing additional metals is important. Using materials with the same structure as ZSM-5 but without Al present in the material resulted in activity at the same levels as observed with iron on amorphous supports showing that Al was necessary for the synthesis of a very active catalyst when iron was added by post deposition methods. However, the observation of catalytic activity for methane oxidation in the absence of Al in Fe-Sil-1(HTS) made by hydrothermal synthesis shows that Al was only necessary to produce an active catalyst when <u>using post deposition methods</u>. This is true even though the metal loading was not the same as in the other samples since in the case of the HTS catalyst the Fe performs the function of Al^{3+} in the framework and also exists as extra-framework species within the pores. Finally, only deposition on a particular MFI material (ZSM-5) produces very high catalytic activity and this observation also shows that the confinement

---

[i] Hydrothermal synthesis (HTS) of these materials and testing was performed by C.Hammond. The metal loading achieved in the HTS method is lower than for post-deposition methods and was found to be 0.5wt%

effect of the porous MFI system was not as important as the composition/properties of the MFI material itself.
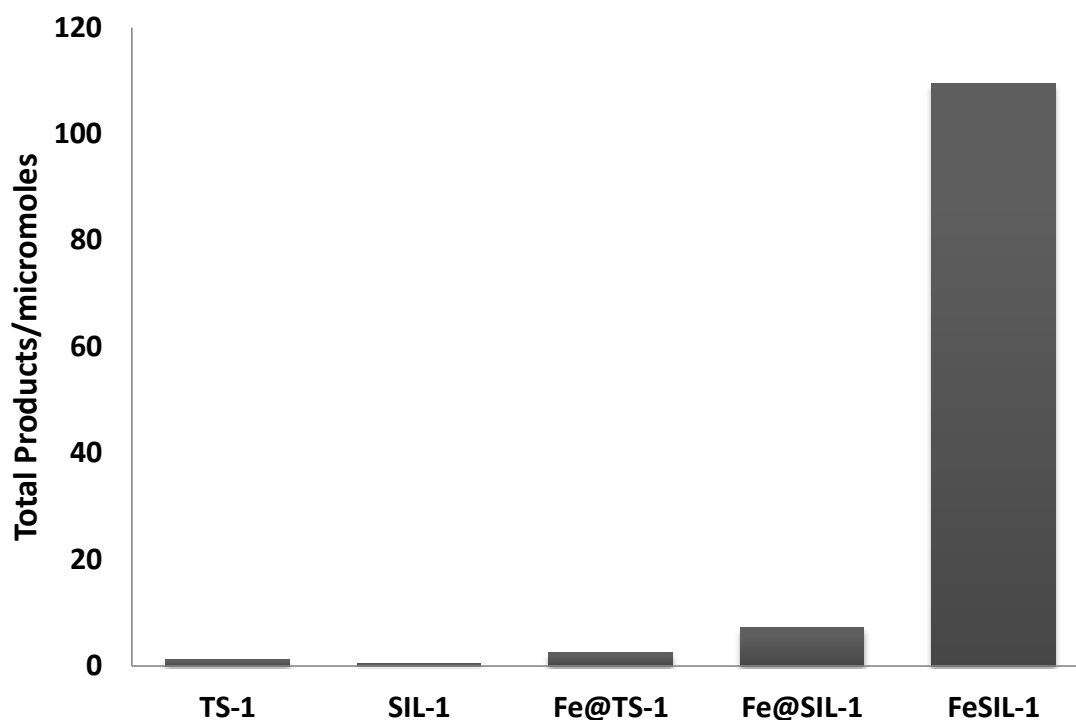
Figure 3.3 Catalytic activity of MFI structured materials with and without the deposition of additional Fe. Fe@TS-1 and Fe@SIL-1 were prepared by the CVI method whilst FeSIL-1 was prepared by hydrothermal synthesis of the material followed by a calcination-steaming treatment (note activity is lower if dry calcination is performed). Metal loadings were 2.5wt%, 2.5wt% and 0.5wt% respectively.

Analysis of ZSM-5 and other zeolites showed that Fe was present in trace amounts and that the catalytic activity for methane oxidation was not correlated to the iron content (see appendices 2, 3). As traces of iron was contained in ZSM-5, it was proposed [2] that similar species to that observed with other reactions catalysed by ZSM5 were proposed, i.e. iron oligomeric species, di-nuclear iron oxo dimers [15,19] may be present in our catalysts. XANES and EXAFS analysis were performed on ZSM-5 samples to obtain additional information about the iron species which were in

trace amounts. Firstly, it is well known that when Fe is in a centro-symmetric environment (octahedral coordination, O_h) the pre-edge intensity of the signal decreases since the Fe K-edge feature observed in XANES spectra is a result of a 1s-3d transition which is forbidden in an octahedral field. [24,25] Thus the decreasing intensity of the pre-edge feature corresponds to a loss of tetrahedral Fe^{3+}. It was observed that for ZSM-5 treated under different conditions the pre-edge intensity decreased as the material was heated to progressively higher temperatures (See appendix 4). This suggested that the Fe^{3+} present in the material was increasingly found in O_h coordination upon heating and this correlated with experimental findings of increasing activity with higher temperature catalyst pre-treatments. Data fitting performed by The Dow Chemical Company gave a model of the iron species in the sample which is similar to previous proposals for this material and resembles the active site of sMMO. [26] This model was used for DFT studies by A.Thetford [27] in our group. Though this is the subject of other work it is instructional to include the catalytic cycle proposed by DFT calculations.

The resting state of the proposed active iron species is labelled (**1**) in Figure 3.4 and one Fe center interacts with H_2O_2 to first produce a species (**2**) in which the hydrogen peroxide is coordinated to the Fe, followed by movement of -H to give a $Fe^{(3+)}$ -OOH moiety (species **3**). Several rearrangements and interaction with a second hydrogen peroxide molecule produces the key species (**4**). As H---(CH$_3$) approaches the Fe(IV)=O group an H atom is abstracted while simultaneously the HOO-CH$_3$ is formed, species (**5**) . The CH$_3$OOH group can be removed by another H_2O_2 molecule to close the loop and re-form species (**2**), or by water to re-form the initial resting state species (**1**). Subsequent solution decomposition of methyl hydroperoxide leads to methanol with sequential oxidation for formaldehyde, formic

acid and CO_x. It has also been postulated that homolytic breaking of the O-O bond in methyl hydroperoxide leads to surface bound methoxy species which can be desorbed by interaction with a water molecule. This process produces two hydroxyl radicals per methanol molecule formed.

This mechanism does not take into account the chemistry of Fe(IV)=O which is well known to abstract a H from CH_4 to give a methyl radical ($\bullet CH_3$) or a bound methoxy species if radical rebound occurs. The key to the newly proposed mechanism for ZSM-5 is the presence of a second iron hydroperoxy species in just the right geometry and proximity to the very reactive ferryl group which allows production of methyl hydroperoxide as the primary product in a concerted manner and regenerates the active site thus closing the catalytic cycle. In the case of N_2O as the oxidant, as used in previous work [15], there is no possibility to form both reactive centres simultaneously to create this active site and high concentration of Fe^{2+} is required for the transformation with N_2O. Thus by using the correct oxidant a closed catalytic cycle is achieved with an excellent match between experimental data on ZSM-5(30) and the mechanism suggest by DFT [j]. This point is important in validating the strength of the modelling approach used for the proposed iron species.

The active site proposed by DFT calculations and EXAFS has been placed into the large intersections of the zeolite for modelling purposes. It follows that only a certain amount of Fe can be incorporated in this way, i.e. Fe: Al= 1:1, for charge balance since 2 (Al^{3+}) are required to anchor one $(FeOH)_2(OH)_2(H_2O)_2$ site. Thus it is proposed that efficient exchange of H^+ (Brønsted protons) for Fe ions in the zeolite will lead to even higher catalytic activity. The work that now follows attempts to

---

[j] E_a, H_2O_2 stiochiometry and the observed primary species match between experiment and theory.

increase the catalytic activity observed, with ZSM-5(30) in particular, by post deposition of Fe onto the zeolite material.
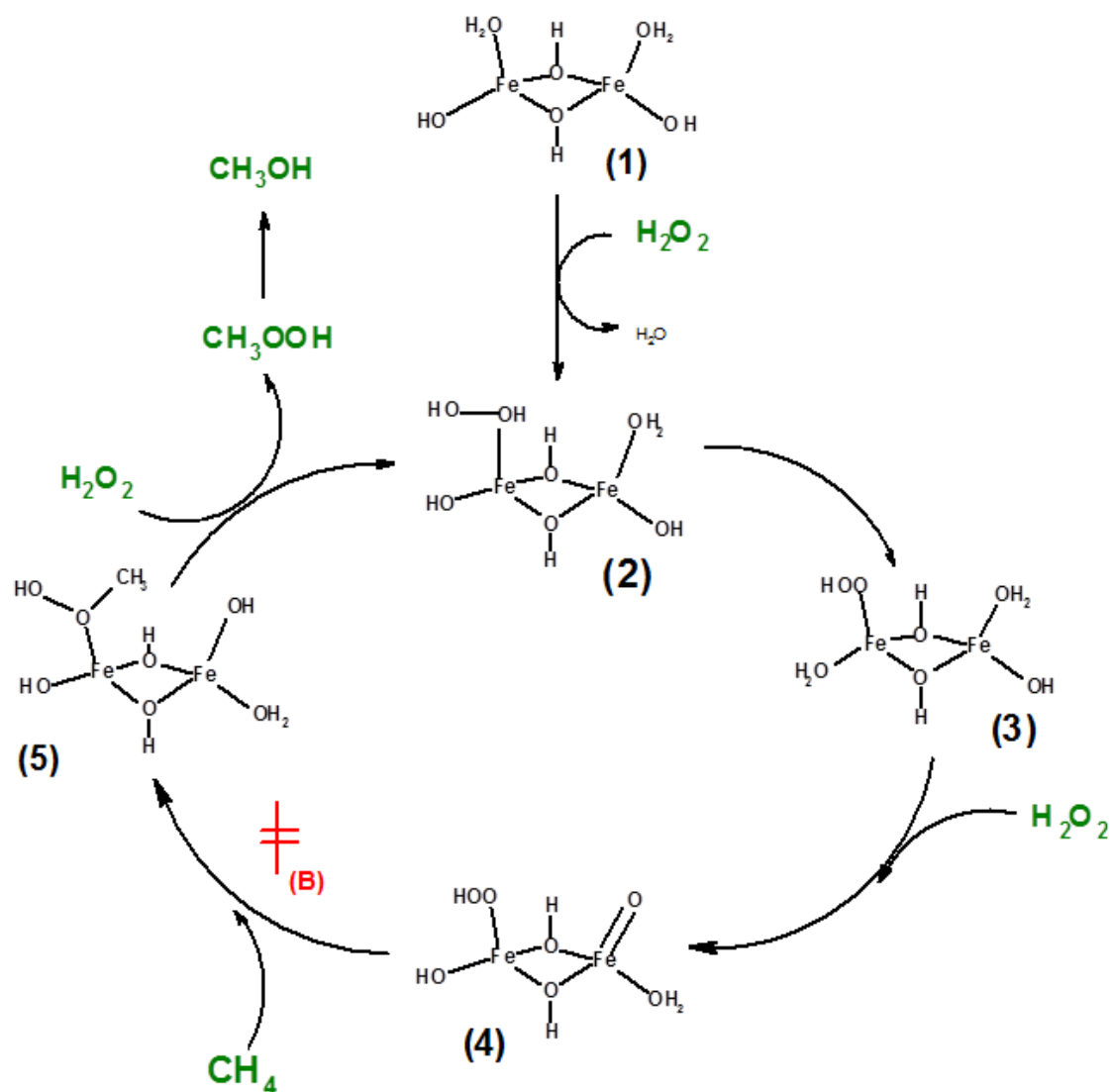
Figure 3.4 Proposed mechanistic cycle for methane oxidation with ZSM-5(30)

It should be noted that the active site as described above is merely one of many iron species in Fe/ZSM-5(30) and it is proposed in this thesis that other iron species also play major roles in the catalytic activity observed. Furthermore, results will be presented that show homogeneous Fe^{3+} under acidic conditions, as well as Cu^{2+} and

Al^{3+}, can produce methyl hydroperoxide selectively. Due to the observed products with other heterogeneous Fe/Cu catalysts, presented earlier, it is certain that other materials without the proposed ZSM-5 active site can also perform CH$_4$ oxidation to give the same products and thus the observed products are not unique to ZSM-5, strictly speaking. However, the specific structure and chemical composition of ZSM-5(30) has aided in the synthesis of catalysts which surpass the oxygenate productivity to sMMO[1] (intact system) and even match the Periana system [28] in terms of volumetric productivity.

3.4. Effect of catalyst preparation and treatment on the catalytic activity of Fe/ZSM-5(30)$_{CVI}$ for methane oxidation

3.4.1. Effect of heat treatment in air (calcination) on catalytic activity

The CVI technique is a two-stage process. The organometallic precursor is deposited onto the "support" at low temperature and pressure followed by heat treatment at high temperature to remove the organic moieties leaving only the metal loaded support. Heat treatment is pivotal for the high activity of the parent ZSM-5 material and also for removing organic species in the post deposition technique. UV-VIS spectroscopy is a useful tool for studying electronic state of metal ions and it has been extensively used to probe the state of Fe in ZSM-5 [29]. Thus this technique was used to study the electronic/ geometric state of Fe in the CVI materials.

Figure 3.5 shows the spectra of a 2.5wt% FeZSM-5(30)$_{CVI}$ the catalyst before (a) and after calcination (b). It is expected that the iron acetylactetonate precursor (Fe(acac)$_3$) when vaporised onto ZSM-5(30) would show Fe^{3+} in octahedral coordination(O$_h$) [k]. This is clearly the case as the intense peak at 278nm and small shoulder peak at 227nm in Figure 3.5(a) is usually attributed to isolated octahedral Fe^{3+} in ZSM-5. [30,31] There is a notable peak at *ca.* 350nm which may be assigned to Fe^{3+} in a mixed T$_d$/O$_h$ state such as in small iron hydroxide clusters. [17,29,30,32] The very broad peak around 450nm is usually assigned to small ion oxides on the ZSM-5 external surface. In the calcined sample (Figure 3.5(b)) the intensity of the Fe^{3+} O$_h$ peak at 278nm has decreased and a new feature at 210nm is observed. This may indicate that there is a change in coordination to T$_d$ since peaks around 218nm have been observed for Fe^{3+} in T$_d$ coordination in Fe-Sil-1. [29] Unfortunately, the entire

---

[k] See Appendix 5 for survey of assignments for Fe in silica based materials.

region below 300nm is not well resolved to pinpoint/ quantify both T_d and O_h Fe^{3+} exactly. The other features around 250nm and 450nm are assigned as in the uncalcined sample. There is a clear change in the iron coordination upon calcination which applies to iron in the ZSM-5 pores since any external iron species such as iron clusters of α-FeOOH would have been observed above 300nm. The presence of small surface iron oxides is supported by TEM data given in 3.4.2.
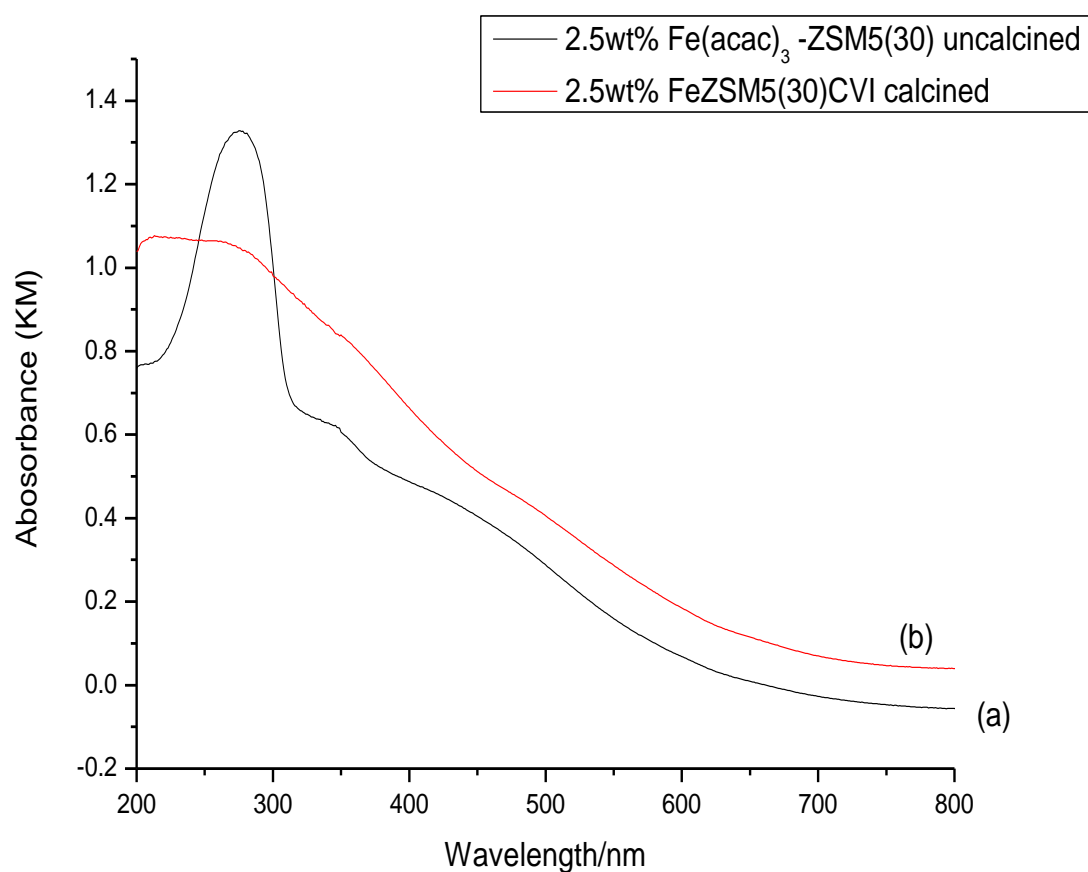
Figure 3.5 UV-VIS spectra of (a) Fe(acac)$_3$ deposited onto ZSM-5(30) before calcination and (b) Fe.ZSM-5(30)$_{CVI}$ after calcination. The nominal metal loading is 2.5wt% and after calcination the measured iron loading (by ICP) is 2.2wt%.

It is interesting that even before calcination surface iron oxides can be found on the material and small iron clusters are also present. This suggests that the heat treatment under vacuum starts the process of decomposition of the organometallic precursor. Thus it can be said that without further treatments these CVI materials always contain very small surface iron oxides as well as other isolated Fe^{3+} species within the zeolite pores. These analyses led to the study of the effect of temperature of the heat treatment used to prepare these materials as it applied to catalytic activity. As with ZSM-5(30) it is envisaged that treating Fe/ZSM-5(30) at different temperatures may affect the catalytic activity. This would be due to (i) migration of Al^{3+} to extra-framework positions thereby increasing the Lewis acidity of the sample and allowing anchoring of isolated Fe^{3+} sites which improves Fe dispersion; (ii) more efficient decomposition of the organometallic precursor at higher temperatures leading to better re-dispersion of iron as precursor decomposition occurs (iii) formation of higher concentration of surface iron species which may affect the catalysis depending on their contribution to the overall reaction.

In Table 3.4 the effect of heat treatment in static air on 1.1wt% Fe/ZSM-5(30)$_{CVI}$ is presented. From comparison of data in entries 1- 4 it is clear that there is an optimal temperature for calcination to produce a highly active catalyst. Total productivity is varying from about 13.6 in entry 4 to *ca.* 28 mol products kg(cat) $^{-1}$ h^{-1} in entry 2 Table 3.4. Partial oxygenate /methanol selectivity only shows slight variation. Steaming is also beneficial for activity as there is a slight increase in total productivity from 28 to 30 mol products kg(cat) $^{-1}$ h^{-1} upon steaming at 550°C (entry 2 vs. 6 Table 3.4). Temperatures higher than 550°C seem to decrease the ability of the catalyst to oxidise methane under these conditions.

A very intriguing result is presented in Entry 5, Table 3.4. When the ZSM-5(30) was pre-calcined and then iron deposited in the usual manner followed by calcination the activity of the catalyst was retained with higher selectivity to oxygenates (91% as opposed to 78% in entry 2 Table 3.4) and more oxidant was left at the end of reaction. Calcination of the parent material (ZSM-5(30)) would have the effect of producing the "active sites" as outlined in Section 3.3 using the trace iron impurities in the material. Also at this high temperature of calcination migration of Al^{3+} to extra-framework positions has undoubtedly occurred thus increasing the Lewis acidity of the parent zeolite prior to addition of iron by CVI.

Deposition of additional Fe onto this material should in principle mean that the formation of the <u>same number</u> of isolated active Fe sites (i.e. the proposed $(FeO)_2$ species in ZSM-5(30)) as with any analogous catalyst containing 1.1% Fe would not be possible since the formation of such sites is linked to the migration of framework Al^{3+} and the ability of the Lewis acid sites to anchor the iron species within the zeolite channels. If however other active Fe species not related to the initial ability of the zeolite to selectively form extra framework $(FeO)_2$ sites are active for methane oxidation then the catalysis would not be greatly perturbed by pre-calcination of the base material.

In fact, vacuum treatment of ZSM-5 (30) at $150^{\circ}C$ prior to introduction of the metal precursor also removes Al^{3+} to octahedral positions hence the increase in activity over the untreated ZSM-5 (Table 3.2 entry 4 vs. 5), as well as removes excess absorbed water. Even pre-treatment at 700 $^{\circ}C$ followed by deposition of Fe does not result in loss of catalytic activity and again these data suggests that there is more <u>than one active Fe^{3+} site present.</u>

Table 3.4 Effect of heat treatments on the catalytic activity of 1.1wt% Fe/ZSM-5 $(30)_{CVI}$ for methane oxidation with H_2O_2(aq). Actual loading is 1.02 wt % after calcination at 550°C.

Entry	Catalyst Treatment	Total Products/µmoles [a],[b]	Oxygenate Selectivity % [c]	Methanol Selectivity % [d]	H_2O_2 Left /µmol [e]
1	Calcined in static air 400°C, 3h	202.9	75.5	7.6	936
2	Calcined in static air 550°C, 3h	382.9	78	5.9	1042
3	Calcined in static air 600°C, 3h	287.1	79	7.4	1000
4	Calcined in static air 750°C, 3h	183.6	79	18.0*	1023
5	Calcined in static air at 550°C, 3h, ZSM5(30) pre-calcined before Fe deposition	335.5	91	7.8	1832
6	Steamed in flowing air 550°C, 3h	404.1	85	10.1	797
7	Steamed in flowing air 600°C, 3h	285.1	84	12.9	1063

Reaction Conditions- Reaction Time: 0.5h; Reaction temp: 50°C, Solvent: H_2O: 10 mL; 5000µmoles H_2O_2; P (CH_4): 30b; 27mg catalyst. [a] ($CH_3OOH+CH_3OH+CH_2O+HCOOH+CO_2$) [b] aqueous phase analysed using ^{1}HNMR and gas phase analysed using GC-FID, [c] ($CH_3OH+CH_3OOH+CH_2O+HCOOH$)/ ($CH_3OH+CH_3OOH+CH_2O+HCOOH+CO_2$) X 100, [d] ($CH_3OH$)/ ($CH_3OH+CH_3OOH+CH_2O+HCOOH +CO_2$) X 100 , [e] Assayed by titration against acidified $CeSO_4$ with Ferroin indicator. These data are for catalysts used immediately after calcinations treatment.

Steaming which is known to cause de-alumination of zeolites has been performed, entries 6, 7 Table 3.4. Increased activity for the 550°C steaming treatment was observed whilst higher temperature steaming had little effect and

in both cases methanol selectivity increased slightly. A pre-steamed ZSM-5 (30) sample with additional Fe deposited in a second step showed the same trend in a similar manner to the pre-calcination treatment. The presence of water, introduced during washing of catalysts, is essential for producing $[Fe(OH)_2]^+$ or $[FeO]^+$ in samples prepared using sublimed $FeCl_3$ as a precursor. [7,33,34] This is because water is necessary to hydrolyse the initially deposited Cl^- containing species prior to calcination. In the case of the CVI technique water is removed from the sample before introduction of the Fe precursor and deposition is carried out under vacuum. The formation of Fe species on the catalyst is related to the decomposition of the precursor and not hydrolysis *per se.* However it may be that the presence of water is necessary for both the efficient de-alumination of the zeolite framework and the formation of hydroxyl containing Fe species.

The above results show that temperature treatment in static air affects the observed catalytic activity of the Fe/ZSM-5(30)$_{CVI}$.

3.4.2. Effect of metal loading

In section 3.3 effect of metal loading on silica and alumina was discussed. Iron was deposited on ZSM-5(x) with different $SiO_2:Al_2O_3$ ratios to explore the effect of Fe : Al ratio assuming that the trend on Fe loading observed with silica and alumina would apply to ZSM-5 samples. This was not strictly the case as ZSM-5(x) materials with higher metal loading (i.e. Fe: Al = 1:1) did not produce more active catalysts. Also the addition of iron to parent zeolites with lower catalytic activity for methane oxidation, as compared to ZSM-5(30), resulted in promotion of the catalytic activity but not to the extent as observed with ZSM-5(30). Thus for ZSM-5(23) which had approximately 3.1wt% Al deposition of 3.1% Fe (i.e. Fe: Al =1:1) resulted in catalytic activity that was four times lower than for the analogous ZSM-5(30) with 2.2wt% Al and 2.2wt% additional Fe (50 vs. 200 µmoles of products) as shown in Figure 3.6.

Interestingly there appears to be an optimal loading of Fe in these experiments which corresponds to an Fe:Al ratio around 1:2. This ratio is close to the maximum experimentally observed exchange capacity for formation of isolated Fe^{3+} sites , i.e. 60% of the Al^{3+} can be replaced with Fe. [7,33] It was initially thought that Fe could replace Al^{3+} and remain in tetrahedral coordination within the zeolite framework followed by migration to extra-framework sites upon calcination. IR measurements (see Appendix 6) on any of these catalysts did not reveal the characteristic Si-O-Fe-stretch observed at 656cm^{-1} [35,36] and thus this idea was ruled out. In all of these samples the more active catalyst had a Fe: Al ratio of 1: 2.

However, it can be postulated that the aluminium content affects the stability and exact form the exchanged Fe species and consequently the metal dispersion within

the pores and upon the external surface of the zeolite. This is supported by previous

reports on Fe deposited by sublimation techniques from $FeCl_3$ onto ZSM-5. Low iron

loadings (Fe/Al<0.5) lead to isolated $[FeCl_2]^+$ species which are decomposed to

$[Fe(OH)_2]^+$ or $[FeO]^+$ upon washing and calcination. [7,30,33,38] The percentage of these

species and any iron oxides formed by their migration during heat treatment affected

the activity of MFI materials for NO_x reduction, N_2O based oxidation of benzene to

phenol and also methane to methanol or CO_x. [6,14,15,38,39]
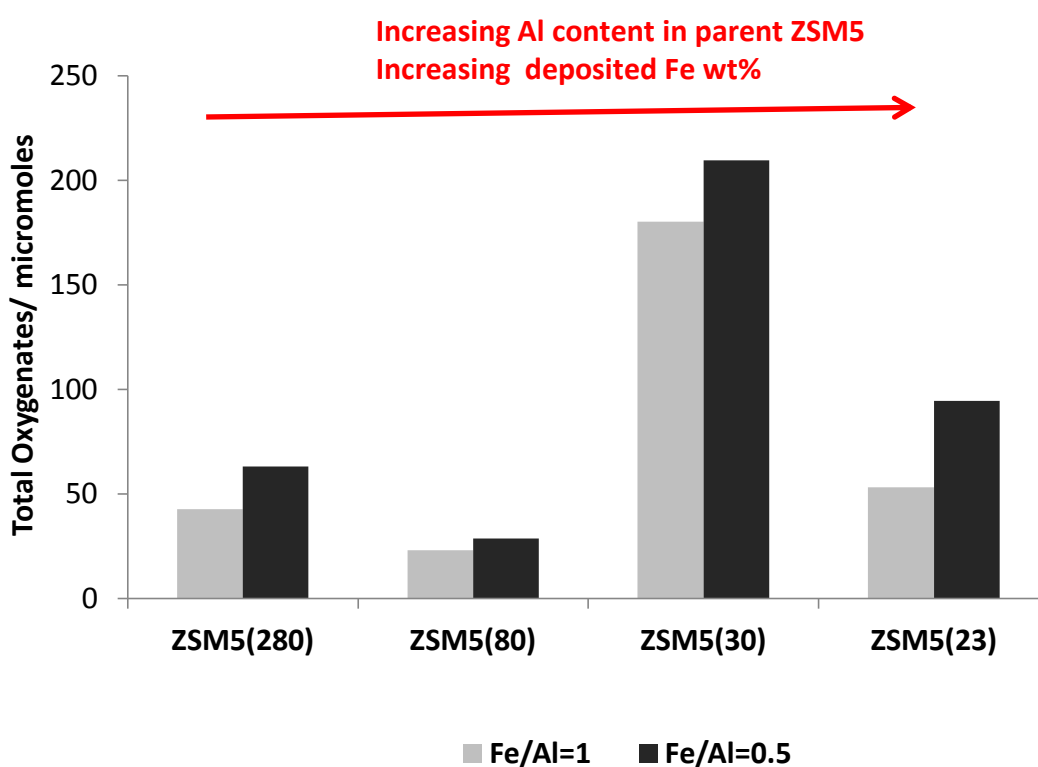
Figure 3.6 Effect of Fe loading on ZSM-5 with different SiO_2:Al_2O_3 ratios. Light grey
bars- Fe/Al=1/1, higher loading; dark grey bars- Fe/Al=1/2, lower loading. It can be
seen that in all cases the lower metal loading leads to better catalytic activity

Unfortunately, similar studies on Fe(acac)$_3$ as a deposition precursor in this process

has not been studied in any detail although the data in Figure 3.6 supports the idea

of optimal Fe loading (Fe:Al ≤0.5) leading to higher oxidation activity in all ZSM-5(X) materials heat treated under the same calcination conditions (550°C , 3h in static air).

Following these studies ZSM-5(30) was chosen as it displayed the highest activity with and without additional iron amongst all the zeolite materials tested. Experimental findings for more extensive study on metal loading are given in Table 3.5. The total productivity of the catalyst increases with increasing metal loading from 0.4wt% to 1.1wt% but not above 2.5wt% Fe. This is related to the drop in oxygenate selectivity from 88% to 71% (i.e. increasing selectivity to CO_2) and the progressively lower amount of oxidant left at the end of the reaction as metal loading increases. The catalytic activity is related to H_2O_2 concentration (1st order, see Chapter 4) and it is evident that high Fe loading leads to higher decomposition of the oxidant without increasing the product amount. An experiment on the decomposition of hydrogen peroxide under reaction conditions at 50°C but in the absence of methane revealed *ca.* 30% loss of oxidant with the formation of molecular oxygen. Thus it can be said that the "effective oxidant level" during the initial phases of the reaction, for catalysts with higher metal loading, is lower due to unproductive oxidant decomposition and thus the overall activity is lowered. However, there is also a fine point to be made concerning 'optimal' metal loading as the amount of isolated Fe sites and clusters within the zeolite pores and the size of surface Fe clusters/nanoparticles varies with the Fe loading. This is supported by TEM analyses in Figure 3.7 a , b which show that the 0.4wt% Fe sample has high dispersion of ~1 nm Fe species (possibly FeO(OH) forming Fe_2O_3 under the beam analysis) whilst the 2.5wt% Fe sample shows ~ 2nm Fe species with high dispersion. In both samples the surface of the

catalyst appears to be coated with a semi-continuous film of Fe, which may be porous.

Table 3.5 Catalytic activity of Fe/ZSM-5(30)$_{CVI}$ calcined at 550°C with varied metal loading.

Entry	Nominal Fe Loading wt%	Total Products/µmoles [a],[b]	Oxygenate Selectivity % [c]	H$_2$O$_2$ Left /µmol [d]
1	0.4	179.9 ± 10.8	88	2390
2	1.1	236.6 ± 6.0	82	1127
3	2.5	237.7 ± 25.2	79	859
4	5.0	224.9 ± 25.8	71	189

Reaction Conditions: Reaction Time: 0.5h; Reaction temp: 50°C, Solvent: H$_2$O: 10 mL; 5000µmoles H$_2$O$_2$; P (CH$_4$): 30b; 27mg catalyst. All catalysts were calcined at 550°C, 3h in static air.[a] (CH$_3$OOH+CH$_3$OH+CH$_2$O+HCOOH+CO$_2$) [b] aqueous phase analysed using ^{1}HNMR and gas phase analysed using GC-FID, [c] (CH$_3$OH+CH$_3$OOH+CH$_2$O+ HCOOH)/ (CH$_3$OH+CH$_3$OOH+CH$_2$O+ HCOOH +CO$_2$) X 100 , [d] Assayed by titration against acidified CeSO$_4$ with Ferroin indicator. ¥ Prepared by doing double deposition of a nominal 2.5wt% Fe(acac)$_3$ onto ZSM5(30) followed by calcination at 550 ^{o}C. ***Note these data are the averages of 6 catalytic tests for each Fe loading examined.***

.

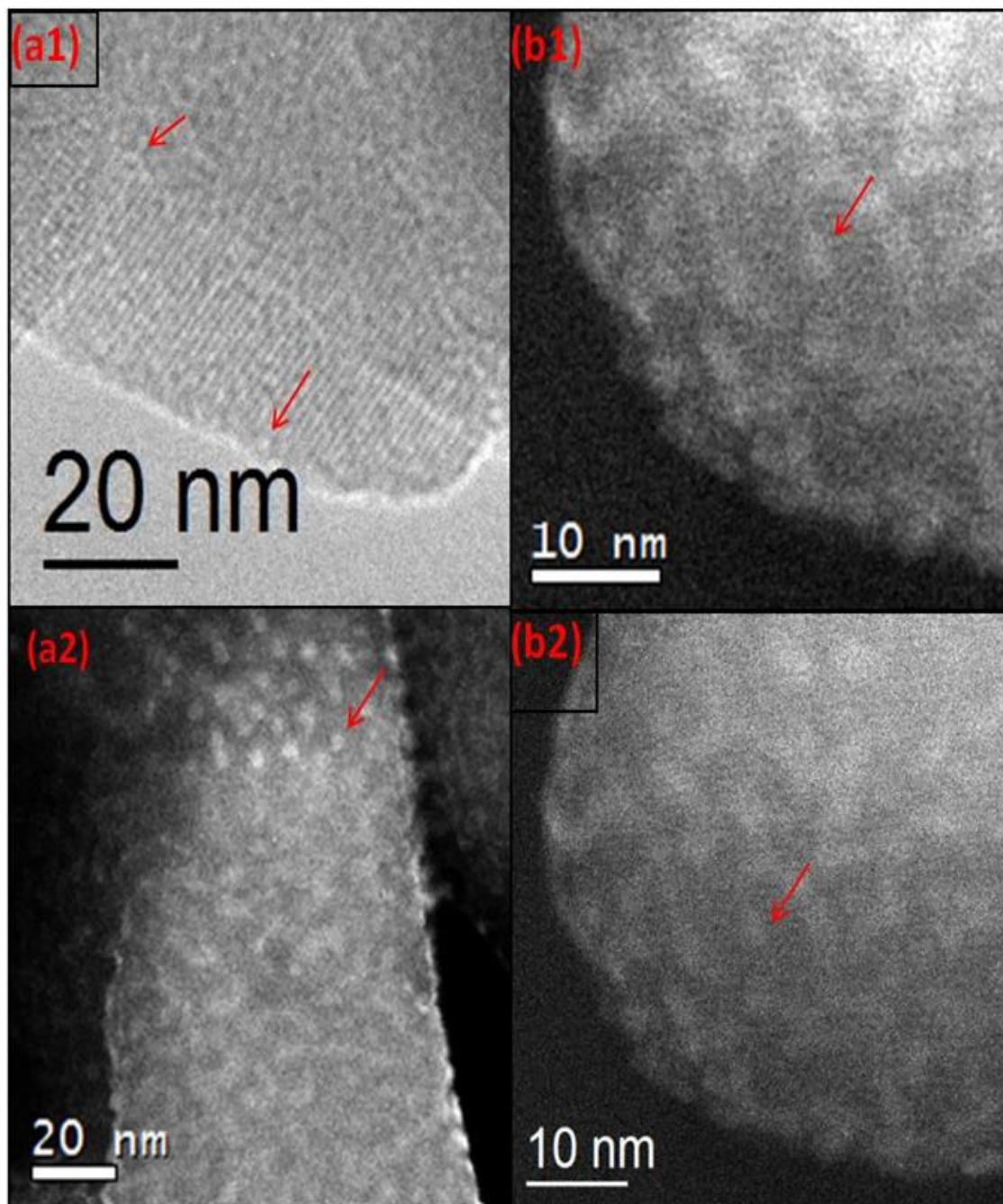**Figure 3.7** STEM-HAADF images of (a) 0.4wt% Fe/ZSM-5(30)$_{CVI}$ and (b) 2.5wt% Fe/ZSM-5(30)$_{CVI}$. Both catalysts were calcined at 550 ^{o}C, 3h in static air. (a1) and (b1) depict a semi-continuous film of Fe species, probably Fe O(OH). (a2) and (b2) depict the formation of small nanoparticles as the red arrow shows under beam time and the transition from film to nanoparticle, ~1nm and 2nm respectively.

The presence of sub nm clusters cannot be ruled out as well. However these species do not account for all the iron in the catalyst. UV-VIS spectroscopy was utilised to study the iron existing as surface species and also within the zeolite channels. UV-Vis spectra of the solid samples, Figure 3.8 shows several peaks which are attributed to various Fe species. An amorphous material, 2.5wt% Fe/SiO_2 prepared by CVI, was first examined. This sample (green curve in Figure 3.7) clearly shows the presence of small surface iron oxides by the peaks *ca.* 460, 575, 660nm.[i] The very prominent peak centred around 250-260nm is assigned as small Fe^{3+} clusters which has been observed by Hensen *et al.* [17] previously. For the zeolite materials (red, blue, black curves) it is clear that small iron oxides (peaks above 450nm) and iron in small oligonuclear clusters (weak shoulder peak *ca* 380nm) are present. [35]

Peaks below 300nm are usually assigned T_d Fe^{3+} (212nm, 240nm) and O_h Fe^{3+} (224nm, 278nm) [17,29,35] but in these samples they cannot be easily de-convoluted. However, one distinguishes that in this region there may possibly be overlapping peaks due to varied coordination state Fe^{3+} species. Notably the intensity of the absorption due to the Fe^{3+} charge transfer (ligand to metal) transitions (i.e. peaks below 300nm) increases with Fe loading suggesting that the level of Fe^{3+} species responsible for these absorptions is increasing. Without information on the extinction coefficients of each the iron species present it is not possible to directly quantify their concentration but a simple peak fitting (i.e. taking the region below 300nm as one peak) would show that more Fe may be found as isolated species as opposed to iron oxides/oligomers due to a smaller relative peak area for the iron oxide species. This type of statistical analysis was not performed since Fe in a Fe O(OH) porous film

---

[i] For review of assignment of Fe species see Appendix 5

may also be observed as isolated O_h species and the assignment of peaks below 300nm exclusively to isolated Fe^{3+} within the zeolite pores may be misleading.
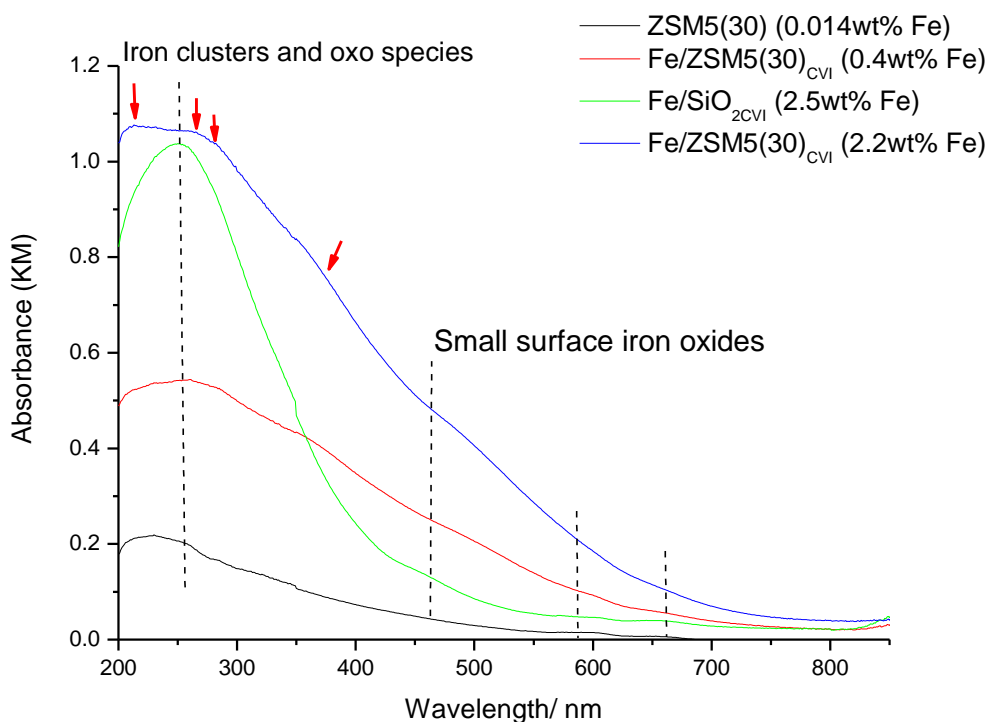
Figure 3.8 UV Vis spectra of calcined CVI samples containing iron. Black line-ZSM-5(30) with 0.014wt% Fe; red line- 0.4wt% Fe/ZSM-5(30)$_{CVI}$; green line-2.5wt% Fe/SiO$_{2CVI}$ and blue 2.2wt% Fe/ZSM-5(30)$_{CVI}$. All catalysts were calcined at 550 ^{o}C, 3h in static air. Red arrows depict isolated Fe^{3+} species of particular interest in ZSM-5 and black dashed lines lineate the position of peaks for clustered Fe^{3+} and small iron oxides particles on silica.

In summary, increasing the iron loading in these samples increases both the concentration of isolated Fe^{3+} (supposedly within the zeolite pores at cation exchange sites) and the size/concentration of very small surface oxidic iron species and clusters. Since the concentration of both types of species is increasing with increasing iron loading but the catalytic activity is similar (for same temperature of calcinations as shown in Table 3.5) within the 1.1-2.5wt%

Fe range it is proposed that the differences in hydrogen peroxide level during reaction accounts for this discrepancy. This may be expected since in the metal: substrate/oxidant ratio is changing whilst the oxidant amount is becoming the limiting factor as the catalysis proceeds.

The spectroscopic data presented thus far does not indicate what level of promotion of the catalytic activity is linked to different iron species. However, by preparing different iron doped materials some information on this aspect of the chemistry was obtained. Firstly, Fe/ZSM-5(30) was prepared by ion exchange techniques and showed similar activity as compared to CVI materials for methane oxidation, but large iron oxide nanoparticles were observed on the catalyst surface by TEM (see Appendix 7). Since it was previously shown that small surface iron oxides (e.g. iron deposited onto silica) were as active as some iron doped zeolite materials (e.g. Fe/ZSM-5(80) or un-doped zeolites with trace iron impurities (e.g. Zeolite Y or ferrerite) one can conclude that only small iron oxides[m] are catalytically active for methane oxidation under the screening conditions used. This was confirmed by testing commercial iron (III) oxide nanopowder (50nm particle size, Sigma Aldrich) which was not catalytically active. Thus the presence of large iron oxides on materials prepared using ion exchange methods is of no consequence as they are not catalytically active.

Secondly, 2.5wt% Fe @ Sil-1 (CVI of Fe onto hydrothermally synthesised Sil-1 as in Figure 3.3) has the same semi-continuous film containing Fe on the Sil-1 external surface as shown in Figure 3.9. It was observed that under the electron beam a transition to Fe_3O_4 occurred as evidenced by a match between the observed spatial pattern and that of Fe_3O_4 (i.e. spinel structure). EXAFS analysis

---

[m] Small iron oxides refers to nanoparticles below 5nm whereas large iron oxides are >15nm

performed by The Dow Chemical Company on this sample also suggests that Fe has similar electronic structure to Fe_3O_4. It is not entirely clear if these observations are merely artefacts due to exposure of the original Fe film to radiation. Since silicalite-1 was inactive for the target reaction and Fe@Sil-1 is active for CH_4 oxidation it can be inferred that the surface Fe is responsible for the observed catalytic activity as Sil-1 has no Fe exchange capacity to allow formation of cation exchanged iron species as an active site within the pores of Sil-1.

There is a clear difference between the Fe deposited by CVI and by other techniques on a variety of support materials. Large Fe oxide particles are not active for the reaction[n] and it is evident from catalytic data that for ion-exchange materials the large iron oxide clusters (~50nm) are not contributing to the reaction whereas it is more than plausible that the small iron particles made by CVI or the semi-continuous film of Fe containing species is catalytically active for methane oxidation in addition to isolated Fe^{3+} species at exchange sites or within the zeolite channels. . The presence of single isolated Fe ions and sub-nm clusters in the CVI materials cannot be ruled out as well.

---

[n] Unreported data on commercially available nano-iron oxides
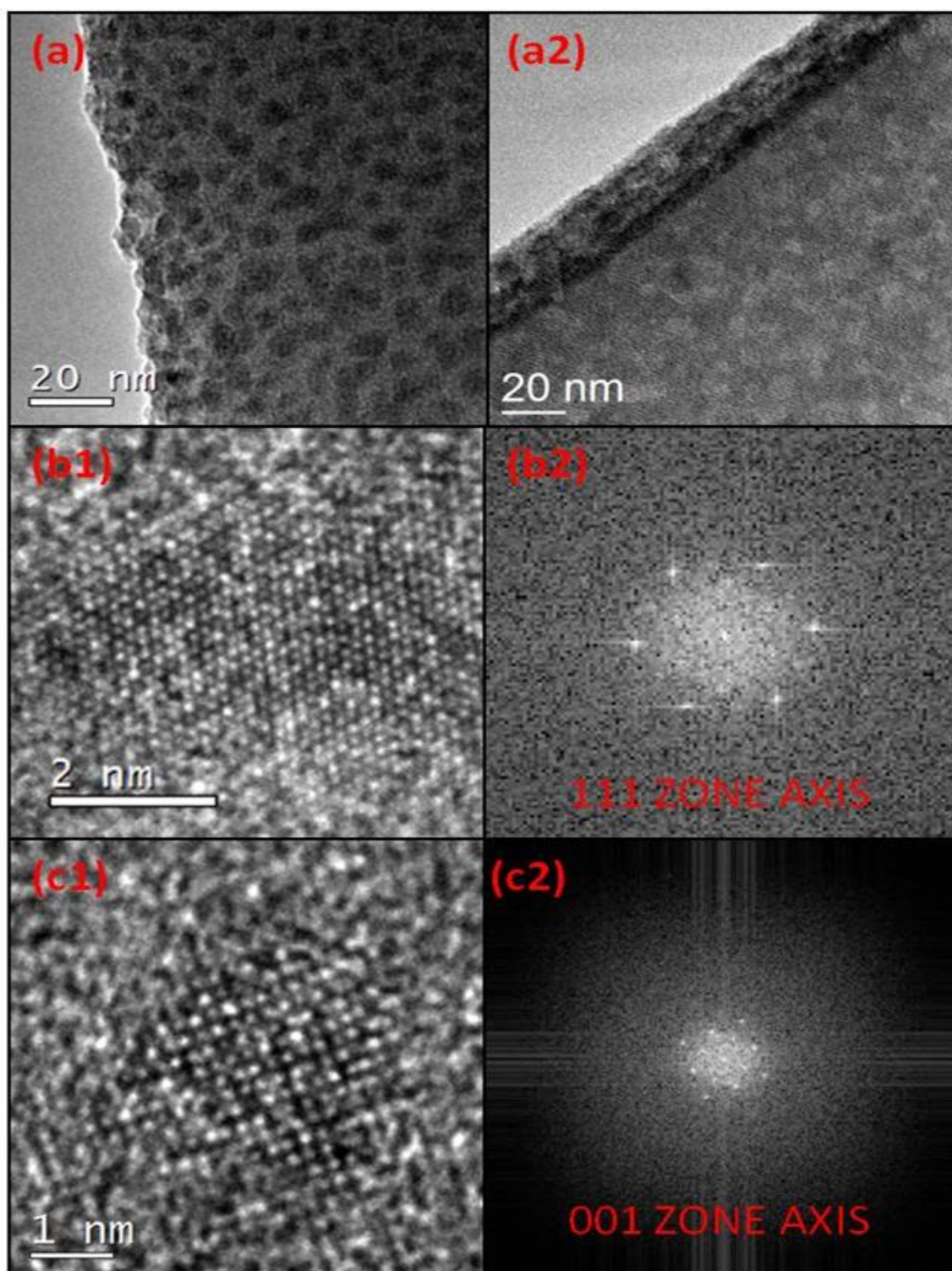
Figure 3.9 STEM-HAADF images of 2.5wt% Fe@Sil-1 calcined at 550°C, 3h in static air. (a1) Semi-continuous film of Fe containing species and (a2) transition to iron oxide particles. (b1, 2)- Analysis of the 111 axis of the observed iron oxide particles showing spinel structure. (c1, 2)- Analysis of the 001 axis of the observed iron oxide particles showing spinel structure.

The data normally reported in these studies are for a reaction time of 0.5 h. Calculation of the initial rates of reaction (5 min reaction) was performed to obtain better understanding of whether or not there are substantial differences between catalysts. The data in Figure 3.10 show clear differences between catalysts with different Fe loading. The differences in activity apply to both initial productivity (rate) and partial oxygenate selectivity as the 2.5 wt%Fe catalyst had approximately 33% lower rate than the 1.1wt% Fe/ZSM-5(30)$_{CVI}$ prepared and calcined under the same conditions. These data validate the differences between a 2.5wt% and 1.1wt% catalyst in terms of initial rate and selectivity reported in Table 3.5 where the catalysts appear to have the same catalytic activity at 0.5h. The washed sample prepared by washing off excess deposited iron acetylacetonate with acetone before calcination is here included for comparison as it has been found to be the best CVI catalyst for methane oxidation under these conditions to date. This material contained 1.5wt% Fe and will be discussed in due course but the reader should bear in mind that modifications of the general CVI protocol can allow synthesis of Fe/ZSM-5 with high metal loading that displays both high activity and partial oxygenate selectivity.
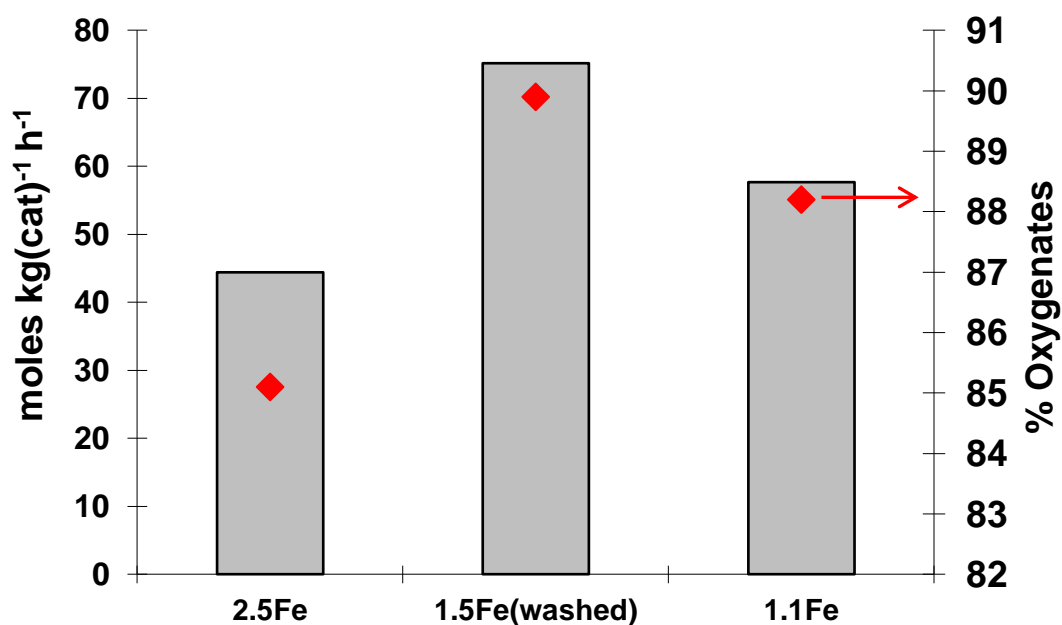
Figure 3.10 Comparison of Fe/ZSM-5(30) catalysts with varying Fe loadings in terms of productivity at 0.083h (5 min) reaction time. Actual metal loading after calcination was 2.2wt%, 1.5wt% and 1.02wt% Fe in decreasing order. All catalysts calcined under the same conditions. Grey bars- total productivity at 0.083h, red diamonds- oxygenate selectivity

3.4.3. Effect of catalyst washing

In an attempt to produce more selective catalysts washing steps were added to the preparation technique used in sections 3.3 and 3.4. It was shown in Figure 3.5 that even before calcination of the CVI catalyst surface iron oxides and iron clusters/ oligomeric species are present in the material. Hence it was conceived that removing any "excess" Fe not anchored to the catalyst (i.e. within the zeolite pores) could be beneficial for methane oxidation. Such benefit could be derived from higher methane oxidation rates due to overall lower hydrogen peroxide decomposition for materials with appreciable levels of iron but low surface iron content (since the reaction is 1st order with hydrogen peroxide). Additionally, the oxygenate selectivity may be increased when surface iron oxides which may participate in methanol over-oxidation are removed.

In traditional sublimation techniques for preparing Fe/ZSM-5, using $FeCl_3$, water washing is performed to remove Cl residues and allow formation of -O or -OH containing Fe species. In the case of Fe $(acac)_3$, the metal precursor used in CVI, it has low solubility in water and thus cannot readily be hydrolysed or removed by water washing . However, this complex is readily soluble in acetone (and other organic solvents). The effect of washing was thus investigated using acetone, water, diluted HNO_3 (aq.) and hydrogen peroxide solution. Organic solvents which could be easily oxidised by the Fe/ZSM-5 catalyst under reaction conditions were avoided as trace impurities of such solvents absorbed/ adsorbed on the catalyst could potentially result in experimental errors due to contamination.
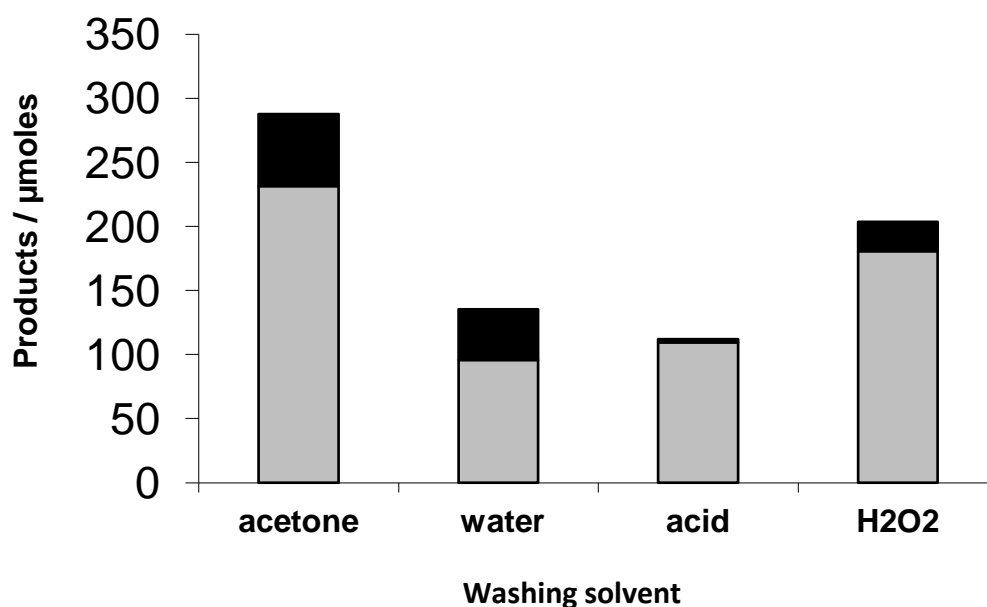
Figure 3.11 Effect of washing the as-prepared nominal 2.5 wt% Fe(acac)$_3$@ZSM-5(30) prior to calcination in static air for 3 h at 400°C. Conditions: reaction time: 0.5h, reaction temperature: 50°C, H$_2$O: 10 mL, H$_2$O$_2$: 0.5M, P (CH$_4$): 30 bars, 1500rpm. Grey bars- total aqueous phase oxygenates, black bars- CO$_2$ in gas phase

Acetone washing was performed by first stirring the catalyst in acetone (4mg/ml) and then filtering and rinsing the residue with three aliquots of acetone (100ml). It was observed that the solvent removed some of the precursor as evidenced by the appearance of an intense orange-red colour to the washing filtrate after the initial filtration. Further washing with acetone (after filtration) did not remove much more of the complex as the filtrate soon ran colourless. At this point the catalyst was air dried followed by drying at 50°C under dynamic vacuum for 3h and then calcined for use and developed a characteristic orange brown colour of Fe/ZSM-5. ICP and EDX analysis of this catalyst showed that 1.5wt% Fe was present in the sample.

The acetone washed catalyst displayed very high catalytic activity and good oxygenate selectivity, Figure 3.11. This data was confirmed by reproducing the test with a second batch of catalyst. Since the catalyst was re-useable and other studies showed that acetone could not be oxidised by Fe/ZSM-5(30) $_{CVI}$ the observed products have been assigned to methane oxidation and not carbon impurities on the catalyst. Unfortunately $^{13}CH_4$ as not available at the time of testing to further validate this hypothesis. However the high activity may be explained by the removal of excess Fe which would have formed iron aggregates upon calcination and lead to unproductive H_2O_2 decomposition during catalysis. Interestingly this catalyst prepared from a nominal 2.5wt% Fe material actually contained 1.5wt% Fe after washing and calcination and had much higher activity than, the unwashed 2.5wt%Fe/ZSM(30)$_{CVI}$ material which contained 2.2wt% Fe after calcination (based on ICP analysis) as shown in Figures 3.10 and 3.11.

Water washing resulted in decreased activity (2nd bar Figure 3.11) though no appreciable loss of the organometallic precursor during washing was observed. The decreased activity may be due to the formation of different iron species in the presence of excess moisture during calcination as the catalyst was only air dried overnight before calcination. Another explanation would simply be that the iron content is higher in this sample and thus activity is lower for reasons outlined previously. H_2O_2^{o} washing did not appear to remove much Fe as evidenced by the lack of orange colour in the filtrate but was good for improving oxygenate selectivity of the catalyst. The oxygenate selectivity of the H_2O_2 washed material is *ca* 89% whilst for similar level of products a 2.5wt% or 1.1wt% Fe material had oxygenate selectivity if 79 and 82% respectively (Figure 3.11, entries 2 and 3 Table 3.5). The

---

^{o} See Chapter 2.2.3.4 for details

reason for the positive effect on oxygenate selectivity is not known but data reported by other members of our group using different Fe/ZSM-5 catalysts showed that in reuse testing the oxygenate selectivity improved with catalyst use suggesting that interaction with hydrogen peroxide tuned the catalyst active sites in some way.

The final washing technique, acid washing[p] , removed most of the Fe from the catalyst as evidenced by a visual observation of orange to cream colour change in this material during washing. After calcination 0.4wt% Fe was detected in the acid washed catalyst by ICP analysis. This material had much lower activity, as expected for the lower iron content, but higher oxygenate selectivity as compared to the other washed materials.

The differences in oxygenate selectivity <u>may</u> be attributed to different iron loading thus further studies were conducted on the acid washed vs. acetone washed catalyst. The former had *ca* 0.4% Fe with lower initial rate and the latter 1.5% Fe with a much higher rate for 0.5h reaction (i.e. 8 vs. 21 moles (products) $kg(cat)^{-1}$ h^{-1}). Comparison at iso-conversion level is useful in analysing the catalytic activity. Under standard reaction conditions iso-conversion can be observed using different reaction times, 0.5h for the acid washed catalyst and 0.083h or 5 min for the acetone washed catalyst. As shown in Figure 3.12 (two light grey bars) the selectivity is very different at iso-conversion under these conditions. This is confirmed by a second set of experiments (dark grey bars in Figure 3.12) done with higher oxidant level and at longer reaction time. Under the modified conditions the acid wash catalyst performs similarly to the acetone washed catalyst in terms of productivity but maintains high oxygenate selectivity above 90%. Also H_2O_2 level at the end of the reaction was greater for the acid washed sample by 30% indicating that this reaction could

---

[p] See Chapter 2.2.3.4 for details

proceed further as sufficient oxidant was present after 2h for continued catalytic activity.

Since the reaction is 1st order with respect to H_2O_2, the increased oxidant level was deliberately chosen to prevent the acetone washed catalyst from being limited by oxidant level as the reaction proceeded since it consumed over 90% of the oxidant under standard conditions . If methane was not limiting one would expect to see up to eight (8) times the amount of product since doubling oxidant would double the activity and increasing reaction time from 0.5 h to 2 h should quadruple the amount of product in a pseudo 1st order reaction. This has not occurred and prompted the time on line analysis presented in Chapter 4.

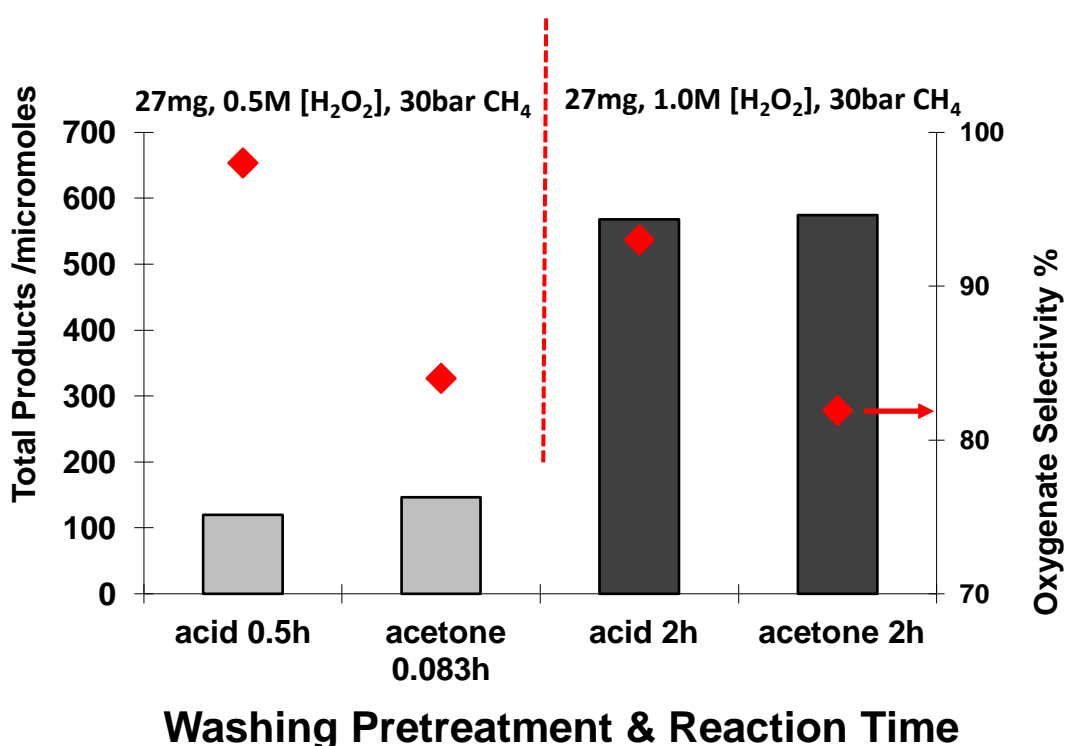**Figure 3.12** Comparison of two Fe/ZSM-5(30) catalysts at iso-conversion. The acid washed catalyst had 0.4wt% Fe whilst the acetone washed catalyst had 1.5wt% Fe and both were prepared by washing 2.5wt% Fe(acac)$_3$@ZSM-5(30) prior to calcination at 400°C, 3h, static air. Light grey bars- standard conditions with 0.5M H_2O_2(aq), 0.5h reaction; dark grey bars- standard conditions with 1.0M H_2O_2(aq), 2h reaction.

As conversion increases the concentration of methane in the aqueous phase to the products decreases and thus is it plausible that competition for the active site, absorption of products blocking the zeolite pores or poisoning of certain active sites accounts for the deviation from ideal behaviour. The reader should note that if comparison at iso-conversion based on using different mass of catalyst the observation of higher selectivity at similar conversion levels for the acid washed material is upheld. This data facilitated the choice of catalyst for flow reactor studies by another researcher in our group which is still ongoing at the time of writing this thesis.

The washing technique allowed the development of active catalysts which could be compared in terms of catalytic activity and oxygenate selectivity but each material had different Fe loading. Another fruitful comparison is possible if catalysts of similar Fe loading synthesised by different methods were available. Fortunately such a comparison can be made by considering the acid washed 0.4wt% Fe/ZSM-5(30), Fe-Sil-1 prepared by hydrothermal synthesis and 0.4wt% Fe/ZSM-5(30)$_{CVI}$ prepared by the CVI technique without any washing steps. The data for these materials were presented previously but is again given in Figure 3.13 for ease of discussion.

For the 0.4wt% Fe prepared by sole deposition of Fe^{3+} by CVI the activity is almost double those of other catalysts with similar iron loading but the partial oxygenate selectivity is lower accompanied by much higher usage of H_2O_2 (about double that of the other two catalysts in Figure 3.13). For the acid washed catalyst (prepared from 2.5% Fe then washed in dilute nitric acid) the selectivity is 98% and *ca.* 90% H_2O_2 is left at the end of the reaction. The hydrothermally synthesised sample, Fe-

Sil-1, showed slightly lower activity than the acid washed Fe/ZSM-5(30) but maintained very good oxygenate selectivity.
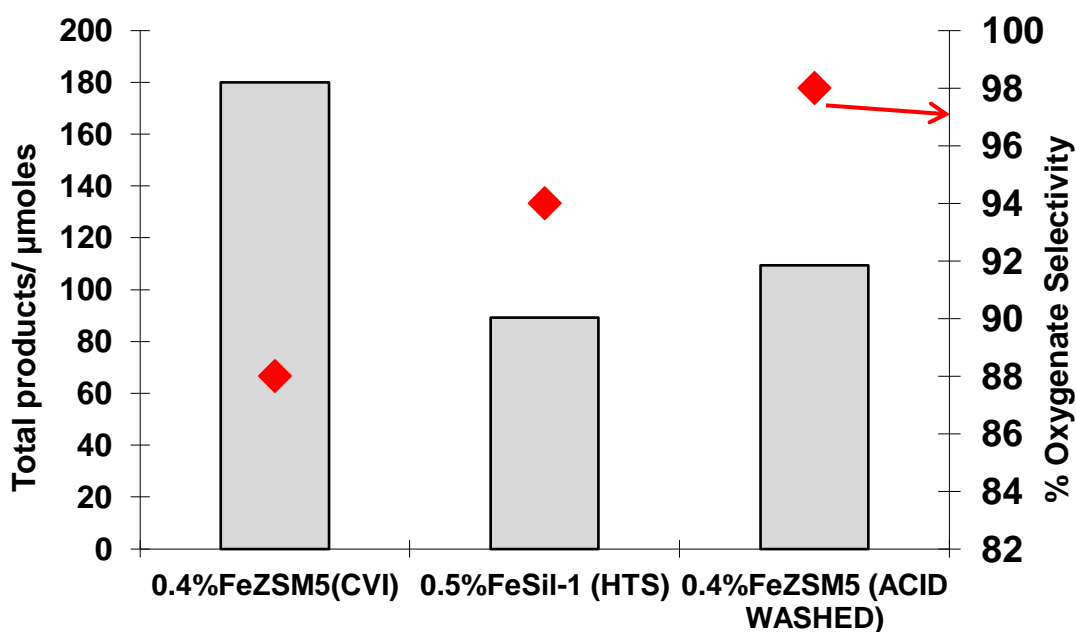
Figure 3.13 Comparison of Fe/MFI catalysts with similar metal loading prepared by different methods. Loading given are actual measured values. Light grey bars- total amounts of products (µmoles), red diamonds- partial oxygenate selectivity.

The first difference between these three catalysts is the presence of aluminium in ZSM-5(30) vs. Sil-1. This relates to the acid strength of the ZSM-5(30) vs. Sil-1 catalysts when calcined under the same conditions. However the two Fe/ZSM-5(30) catalysts presented in Figure 3.13 above both have the same iron content and aluminium content but very different activity and selectivity as described above. Hence the presence of Al in ZSM-5 cannot be the sole reason for the difference in activity. The varying activity and selectivity of these three samples (with similar iron

loading but different preparation techniques can now be ascribed to different forms of iron in the catalyst.

Therefore it is at this point that the form of the Fe species present in the catalysts merits further discussion. It was previously shown that for the CVI materials there is a semi-continuous film of Fe containing species resembling FeO (OH) and for the 0.4wt%Fe/ZSM-5(30) material the iron particles are *ca.*1nm in diameter (Figure 3.7 (a)). The presence of surface Fe, mainly in the +3 oxidation state, is confirmed by UV-VIS and XPS data in Figure 3.14 (red curve) and Figure 3.15 (a). The UV-VIS spectrum the 0.4wt%Fe/ZSM-5(30)$_{CVI}$ material shows features attributed to isolated O_h Fe $^{3+}$ sites (characteristic peaks *ca.* 226 nm and 280 nm), possibly isolated T_d Fe^{3+} (peak at 214nm), oligomeric species (peak at 385 nm) and small iron oxides (broad peaks above 450 nm). [17,29,35] XPS analysis given Figure 3.16(a) shows a major peak with binding energy of 711.5eV and a small satellite peak at ~ 719eV which indicates Fe^{3+} in a similar electronic state to Fe$_2$O$_3$. This corroborates the observation of iron oxides by UV-VIS and TEM analyses.

The 0.5wt% Fe-Sil-1 hydrothermal sample has no surface Fe as shown by XPS (Figure 3.16 (b)) and the majority of the Fe species are present isolated Fe clusters within the zeolite pores and oligomeric Fe^{3+} species (intense peak centred around 235 nm and shoulder at 387nm respectively, green curve Figure 3.15). From the acquired spectrum the tetrahedral framework and octahedral extra framework isolated Fe^{3+} (peaks at 212, 240nm and 224, 278nm respectively) cannot be distinguished. The spectrum resembles that of Fe/SiO$_{2\ CVI}$ presented earlier in Figure 3.8 but without the presence of bulky iron oxides. However, this material has the same XRD pattern as silicalite-1 as reported in the literature (See Appendix 9).

0.4wt% Fe/ZSM-5(30) acid washed has an off-white colour, as is the case with the 0.5wt% Fe-Sil-1, which for this level of Fe is uncharacteristic (i.e. it should be orange as the other 0.4wt% sample detailed previously) and this strongly suggests that the iron is located inside the pores of the zeolite and not covering the surface of the catalyst. XPS analysis shows no surface iron species (Figure 3.15 (c)) and the UV-VIS spectra confirms that there is little iron oxides present in the material[q] due to the noticeable absence of any broad peaks above 450 nm, Figure 3.14(black curve). The isolated Fe^{3+} gives rise to the peaks centred at 215 nm and 260 nm. It could be proposed that these peaks are due to T_d and O_h Fe^{3+} respectively but additional characteristic peaks from these species may be overlapped in the signal observed as usually pairs of peaks at 212 nm, 240 nm and 225 nm, 275 nm are observed for such species. In a detailed study by Bordiga *et al.* [29] it is proposed that for Fe-Sil-1 (calcined) an additional defined peak at 258 nm in the UV-VIS spectrum corresponds to isolated clustered Fe^{3+}. By comparison it is clear that all the species in the parent ZSM-5 are also present in the acid washed sample but there is a major contribution from clustered Fe^{3+}.

---

[q] Note that two minor peaks around 590nm and 650nm are also present for the untreated ZSM-5(30) parent material.
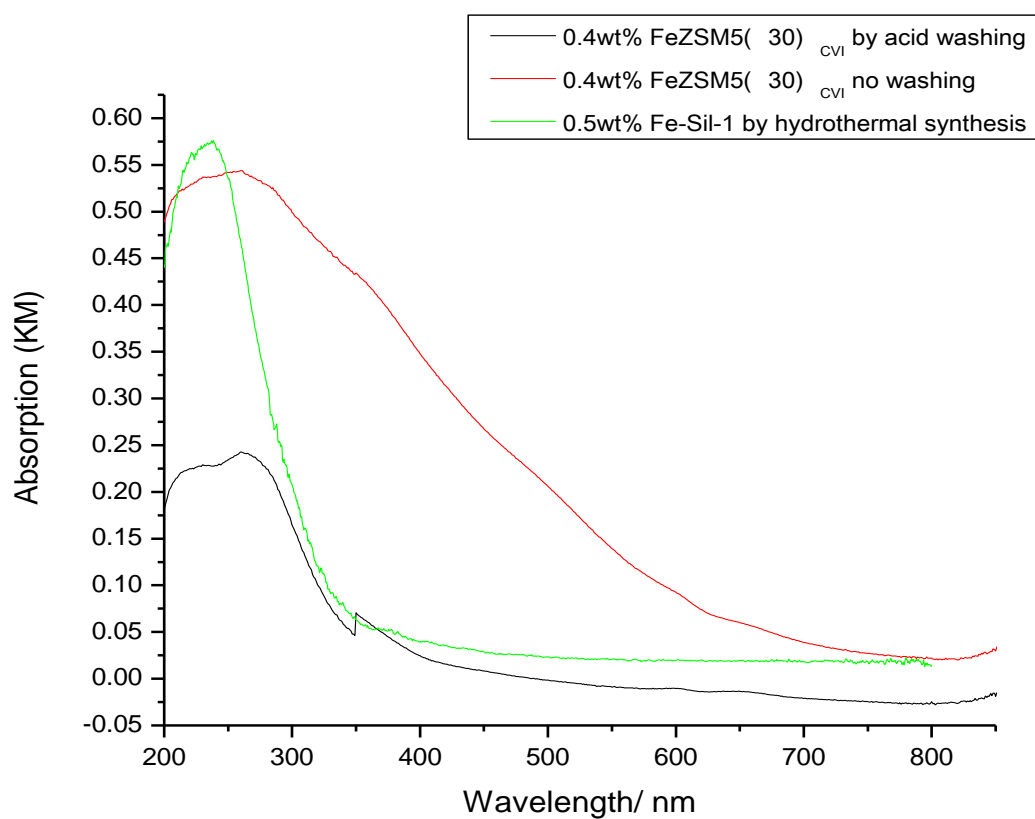
Figure 3.14 UV-VIS analysis of calcined 0.4-0.5wt%Fe loaded MFI materials prepared by different techniques. black curve- iron deposited by CVI and then washed off using an acid wash; red curve- iron deposited by CVI with no washing; green curve- iron in silicalite-1 prepared by hydrothermal synthesis.
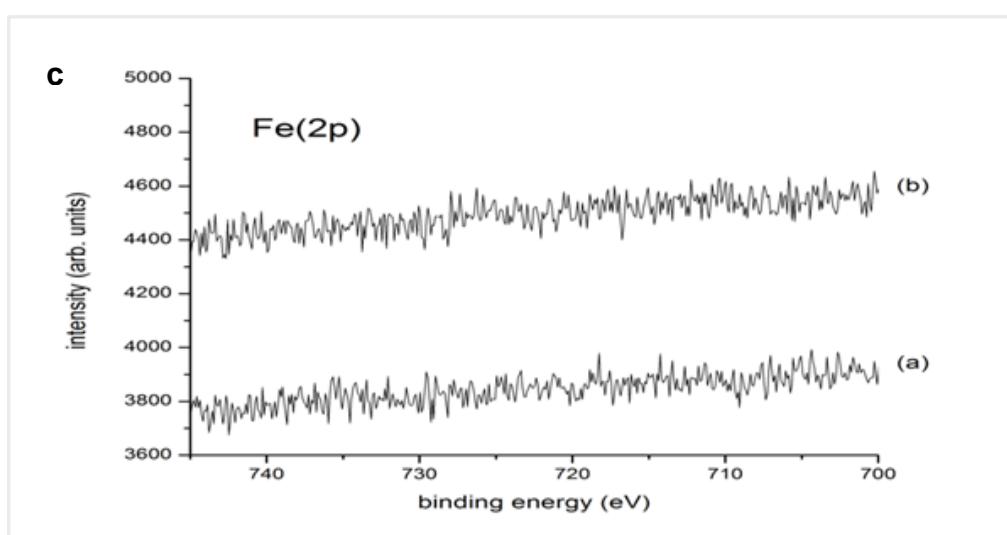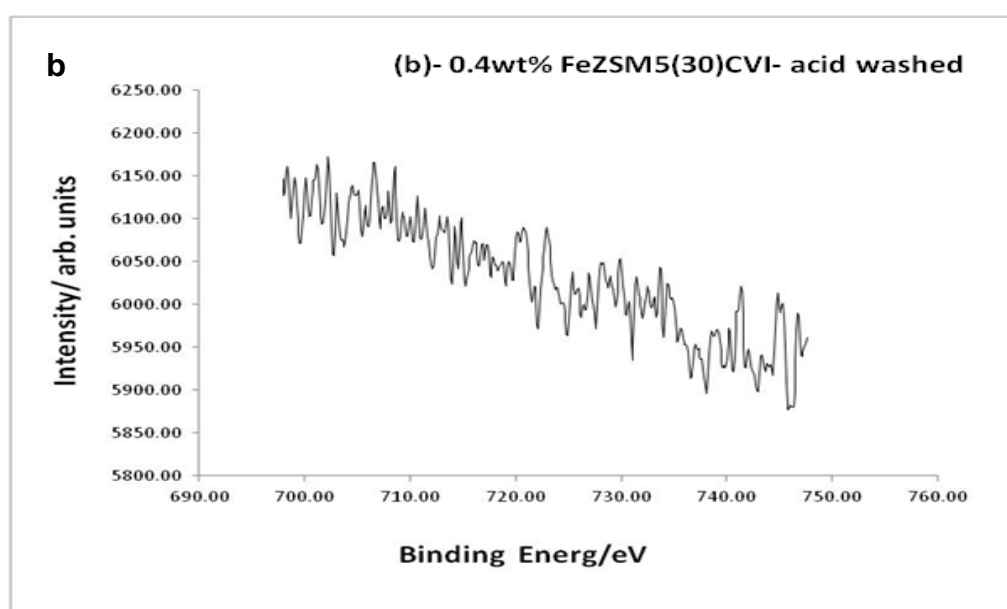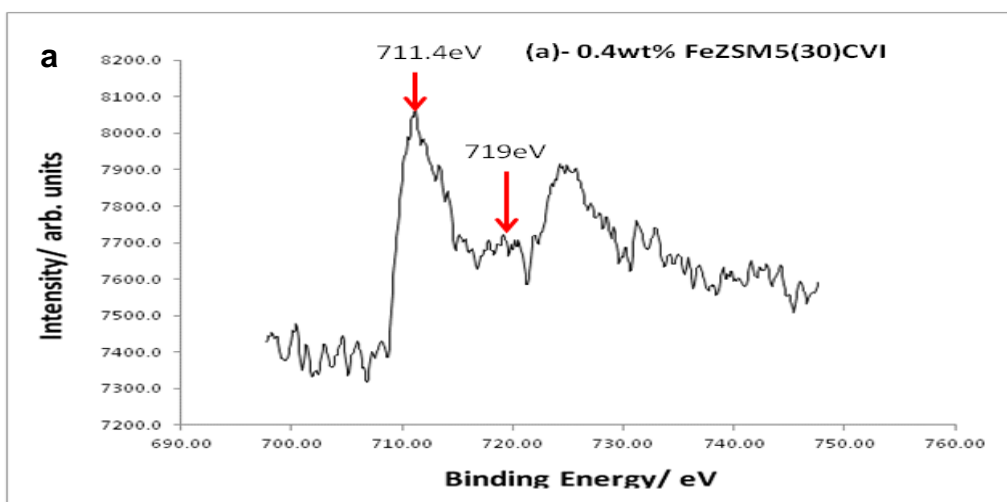
Figure 3.15 XPS analysis of (a) 0.4wt% Fe/ZSM-5(30)$_{CVI}$, (b) 0.4wt% Fe/ZSM-5(30)$_{CVI}$ prepared by acid washing and (c) 0.5wt% Fe-Sil-1 prepared by hydrothermal synthesis. All samples were calcined at 550°C for 3h in static air.

It was not possible to quantify how much of each site is present but it is clear that the sample with surface iron species (0.4wt% $Fe/ZSM-5(30)_{CVI}$) is the most active which strongly implicates the role of surface iron oxides in the catalysis in addition to the other isolated Fe^{3+} species observed in these three materials. It follows that if one considers that for the same iron loading the presence of surface iron species equates with less iron being available for formation of isolated Fe^{3+} sites within the zeolite channels then observation of higher activity should be linked to the action of both types of iron sites. It can also be proposed that the lower oxygenate selectivity (i.e. over-oxidation propensity of the material) is linked to the iron oxides participating in the reaction since the catalyst with significant amount if surface Fe (0.4wt% $Fe/ZSM-5(30)_{CVI}$) showed lower oxygenate selectivity assuming that the over-oxidation pathways occur at the iron oxide surface and not simply through solution phase chemistry.

Finally, it is intriguing that the acid washed catalyst and Fe-Sil-1 both have no surface iron oxides and different isolated Fe^{3+} species but show only slight difference in activity and oxygenate selectivity. Though no further data is available to clarify this observation the available data suggest that different iron sites within the zeolite channels may have similar activity for methane oxidation. All of these observations firmly support the hypothesis that the CVI technique allows preparation of catalysts with different Fe species (clusters, small oxides, oligomers etc) which impact the catalysis. Furthermore, the technique of acid washing as the advantage of being able to prepare active catalysts with appreciable iron loading that still display high oxygenate selectivity using commercially available materials in place of in-house catalyst preparation via time consuming hydrothermal syntheses.

3.4.4. Effect of heat treatment in H_2 (reducing atmosphere) on the catalytic activity of Fe/ZSM-5(30)$_{CVI}$

For data presented in the preceding sections the major reaction product is formic acid and not methanol or methyl hydroperoxide. It is highly desirable to be able to tune the catalyst to produce methanol selectively. In section 3.2 it was shown that treating Fe/TiO$_2$ catalysts in a reducing atmosphere had the effect of increasing selectivity to methanol at the same level of oxygenate productivity and total partial oxygenate selectivity as compared to the calcined material (Table 3.1 entries 5 versus 6). Thus this treatment was employed with Fe/ZSM-5(30)$_{CVI}$ materials in an attempt to increase methanol selectivity. It was found that heat treatment in a reducing atmosphere had a positive effect on methanol selectivity and this will now be discussed.

Comparison of a 1.1wt% Fe/ZSM-5(30)$_{CVI}$ material calcined or heat treated in a reducing atmosphere shows similar catalytic activity and total oxygenate selectivity but an increase in methanol selectivity for the "reduced" sample. This is shown in Table 3.6 entries 1 vs. 2. There is also a higher usage of hydrogen peroxide for the catalyst treated under a reducing atmosphere (about 10% of the oxidant is left after reaction in entry 2 Table 3.6). The first interpretation of this data would be to assign the changes in catalytic behaviour to reduction of Fe^{3+} to Fe^{2+} during the catalyst pre-treatment.

To investigate this XPS analysis of "reduced" Fe/ZSM-5(30) material was performed. Only Fe^{3+} is detected (Figure 3.16) as in the case of the calcined sample (Figure 3.14(a)) but the actual binding energies of the Fe^{3+} (2p) is 712eV with a small satellite peak at 720eV. In the calcined Fe/ZSM-5(30) (Figure 3.15 (a)) the peak at

Table 3.6 Catalytic activity of ZSM-5(30) and Fe/ZSM-5(30) materials heat pre-treated under reducing atmospheres prior to use.

Entry	Catalyst	Total Products/ μmoles [a],[b]	Oxygenate Selectivity % [c]	Methanol Selectivity % [d]	H_2O_2 Left /μmol [e]
1	1.1 wt%Fe/ZSM-5(30) calcined in static air 550°C, 3h	212.6	82	12	1354
2	1.1 wt%Fe/ZSM-5(30) H_2/Ar treated 550°C, 3h	205.5	80	30	406
3	1.1wt%Fe/ZSM-5(30) He treated 550°C, 3h	216.0	80	32	379
4	ZSM-5(30) calcined in static air 550°C, 3h	54.9	96	20	3098
5	ZSM-5(30) He treated 550°C, 3h	48.6	96	31	3698
6	ZSM-5(30) Calcined in static air then H_2/Ar treated 550°C, 3h	51.9	97	21	3292
7	1.1wt%Fe/ZSM-5(30) calcined in static air 550°C, 3h then H_2/Ar treated at 550oc , 3h	209.0	76	16	505
8	1.1 wt%Fe/ZSM-5(30) H_2/Ar treated 550°C, 3h (pre-calcined ZSM5 for deposition)	226	84	36	392

Reaction Conditions: Reaction time 0.5h; Reaction temp: 50°C, Solvent: H_2O: 10 mL; 5000μmoles H_2O_2 ; P (CH_4): 30b; 27mg catalyst. [a] ($CH_3OOH+CH_3OH+CH_2O+HCOOH+CO_2$) [b] aqueous phase analysed using ^{1}HNMR and gas phase analysed using GC-FID, [c] ($CH_3OH+CH_3OOH+CH_2O+HCOOH$)/($CH_3OH+CH_3OOH+CH_2O+ HCOOH +CO_2$) X 100, [d] ($CH_3OH$)/ ($CH_3OH+CH_3OOH+CH_2O+HCOOH +CO_2$) X 100 , [e] Assayed by titration against acidified $CeSO_4$ with Ferroin indicator.

711.4eV with a small satellite at 719eV is indicative of Fe^{3+} possibly as an oxide, Fe_2O_3. This has been discussed previously. For the Fe/ZSM-5(30) heat treated in 5% H_2/Ar neither Fe^{2+} nor Fe^0 is observed and the peak at 712eV is indicative of small Fe^{3+} clusters/oxides or an FeO (OH) type structure (Fe 2p $_{3/2}$) . From XPS analysis further information about the effect of the treatment on the catalysis cannot be gained since there is no reduction of the iron sites on the catalyst surface. It is interesting however that the "reduced" materials are grey in colour whilst the calcined samples are orange-brown.

To investigate the state of the iron within the sample, and in particular within the zeolite pores since XPS is a surface/near surface technique, UV-VIS spectroscopy was utilised. Three samples were initially analysed, 2.5 wt% Fe/ZSM-5(30) calcined or "reduced" and 1.1wt% Fe/ZSM-5(30) "reduced", and the spectra obtained are given in Figure 3.17 (a). The spectra of the "reduced" materials are strikingly different to the calcined sample. There are distinct peaks observed for the "reduced" materials below 300nm which is unlike any of the other calcined samples analysed by UV-VIS spectroscopy, except the acid washed Fe/ZSM-5(30) studied in the previous section. For both "reduced" materials, i.e. 1.1wt% and 2.5wt% Fe/ZSM-5(30), three peaks are clearly visible in the ligand to metal charge transfer region of the spectrum. The peak *ca.* 212nm is clearly visible and this has been assigned to Fe^{3+} T_d in Fe-Sil-1 and also in uncalcined Fe/ZSM-5 prepared by hydrothermal synthesis by other researchers. [17, 29] There is also a second distinct band *ca.* 259nm which is assigned to small extra framework Fe^{3+} oxo clusters. This has been observed in H/ZSM-5 by Hensen *et al.* [17] and was reported to have occurred as Fe^{3+} T_d from the zeolite framework became dislodged upon heating. These small oxide clusters were also present in Fe/SiO_2 reported in that work and in Figure 3.8 (CVI

113

material). A third feature is also observed *ca.* 230nm and this is shown by the expanded spectrum in Figure 3.17 (b). A similar feature was observed in the spectrum of 0.5wt% Fe-Sil-1 in Figure 3.14 but it was much more intense and was the prominent feature of that spectrum. This is tentatively assigned to small isolated iron clusters within the zeolite pores.
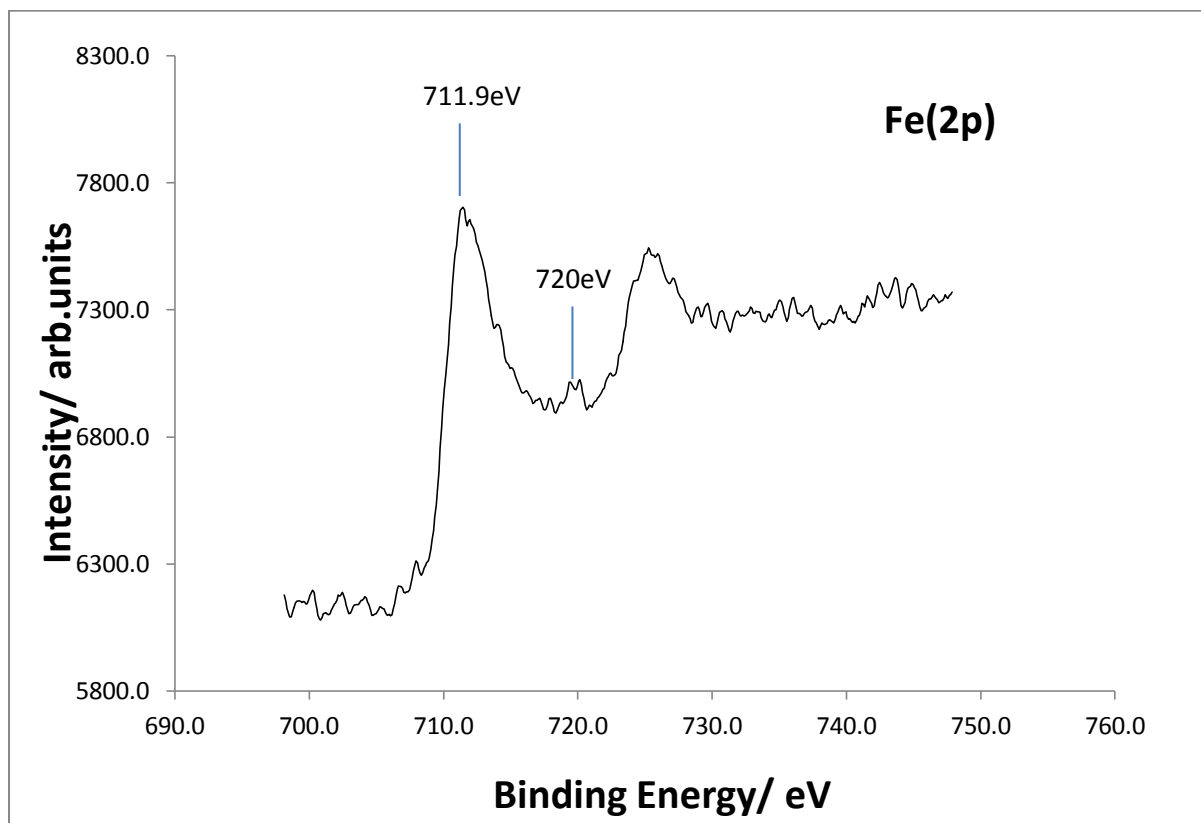
Figure 3.16 XPS of Fe 2p region of Fe/ZSM-5(30) subjected to heat treatment in a reducing atmosphere.

Notably the intensity of isolated Fe^{3+} species within the zeolite pores is higher for the "reduced" versus calcined material (Figure 3.17) clearly indicating higher contributions from these species in the spectrum. There are no clear features in the spectra of the "reduced" FeZSM5(30) samples to suggest Fe^{3+} O_h as observed in the analogous calcined material (i.e. peak around 278nm) but it may be overlapping

with the feature at 259 nm. Furthermore, there is no indication of bulk iron oxide particles on the zeolite surface due to an absence of the characteristic broad peaks above 450 nm for such species.
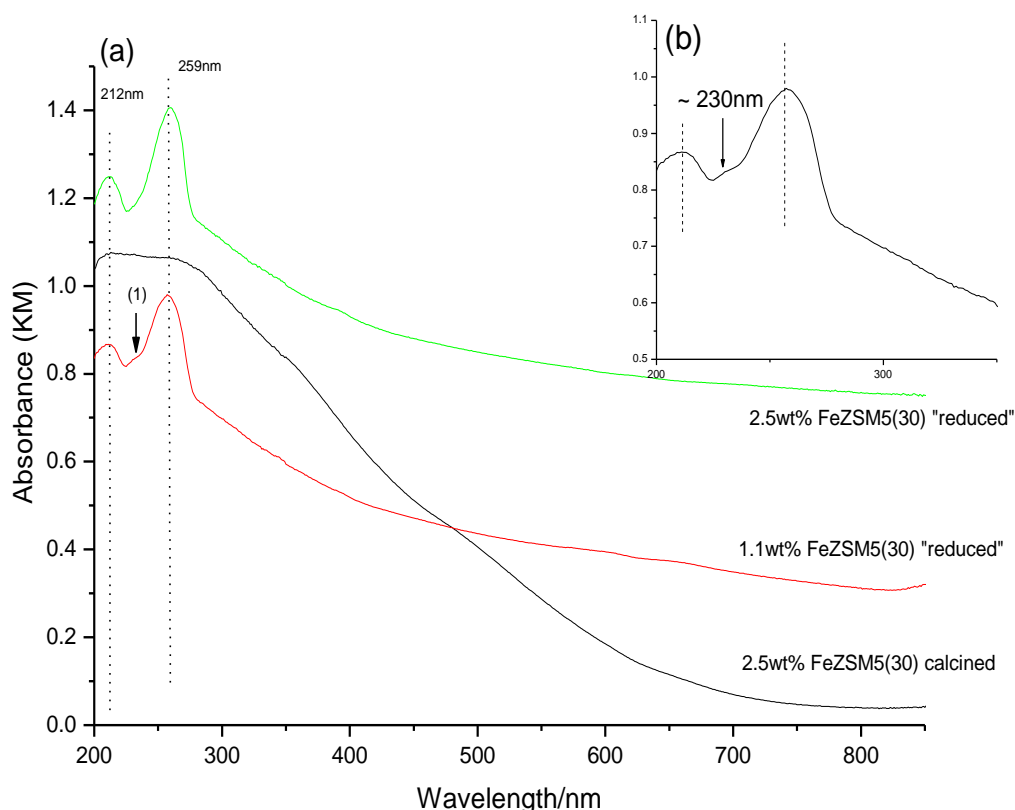
Figure 3.17 UV-VIS analysis of the Fe/ZSM-5(30) subjected to calcination and reduction treatments.

However, the fact that the intensity of the spectra beyond 300nm is significantly high (i.e. not tapering off as quickly as for the calcined material) and this suggest that the surface may be covered with iron species. This hypothesis is supported by the observation of surface Fe^{3+} with similar binding energy to FeO (OH) from XPS analysis. These data give us an explanation for the higher methanol selectivity observed when using the "reduced" 1.1wt% Fe/ZSM-5(30)$_{CVI}$ catalyst. There are

different iron species in this material, as compared to the analogous calcined catalyst, which are responsible for direct methane oxidation or controlling methanol over oxidation.

According to the literature [31-40], the use of reductive treatment on Fe/ZSM-5(30) , H_2-TPR experiments, is a standard way of estimating the concentration of isolated Fe^{3+} and iron oxides in ZSM-5. This information is obtained by considering the amount of H_2 consumed for reduction events occurring during a TPR experiment which correspond to different isolated Fe^{3+} and iron oxides. In the reduction process it is postulated that –O from isolated iron oxo species can be removed at lower temperature (400-500°C). This causes an oxidation state change from +3 to +2 for isolated iron-oxo species. Processes above 500°C correspond to reduction of the Fe^{3+} in iron oxides to the +2 oxidation state and then metallic state. These events occur in a 5% H_2/Ar atmosphere. Thus the reduction of Fe^{3+} to Fe^{2+} and Fe^{3+} to Fe^0 can be followed in TPR experiments. In theory reduction of isolated Fe^{3+} in iron-oxo species should alter the structure and properties of these sites. In the treatment used at 550°C for the 1.1wt% or 2.5wt% Fe/ZSM-5(30) the temperature is below that necessary for reduction of bulky surface iron oxides and so only major effect should be on the isolated iron-oxo species.

It is therefore intriguing that for the CVI materials there seems to be no real "reduction" occurring on the basis of UV-VIS and XPS measurements though these materials display different catalytic behaviour. The reader should note that for TPR studies the zeolite is normally calcined in O_2 at high temperature before studying reduction processes. The technique of reduction without a prior calcination is markedly different from the techniques used in the literature. There is however one account of using an auto-reducing atmosphere to pre-treat Fe/ZSM-5(25) by Lobree

et al. [33] They found that the He pre-treatment (or oxygen calcination) left iron as Fe^{3+} in the material which could be reduced by H_2 around 540°C. Thus in the data presented here there should be some reduction of Fe^{3+} to Fe^0 at this temperature depending on the form of iron in the sample. To further investigate this observed effect of reducing atmosphere a series of experiments were performed (Table 3.6 entries 3-8).

Firstly, high temperature treatment in helium was performed as this is well known to cause auto-reduction of Fe^{3+} to Fe^{2+} in zeolites [33, 40] and we observe a beneficial effect on CH_3OH selectivity at the same level of methane conversion as with the calcined sample (32% vs. 12% for the calcined sample, entries 3 versus 1 Table 3.6). Achieving higher selectivity to methanol merely by this heat treatment was remarkable. The parent ZSM-5(30) was heat treated in a reducing atmosphere to probe whether or not higher methanol selectivity could also be achieved in this way using the material with 0.014wt% Fe. By comparing the data in entries 4 vs. 5 in Table 3.6 it is clear that helium treatment also has a beneficial effect on methanol selectivity. However, treatment in 5% H_2/Ar was not sufficient to increase methanol selectivity for ZSM-5(30) (data not shown). This hypothesis is supported by the visual observation of a cream/white to light grey when helium treatment is performed unlike the H_2/Ar treatment. Calcination followed by reduction has no effect on the methanol selectivity, entry 6 Table 3.6. The proposed active site in ZSM-5, $[Fe_2(\mu_2\text{-}OH)_2(OH)_2(H_2O)_2]^{2+}$, contains two Fe^{3+} Oh centres and would be severely altered by treatment in 5%H_2/Ar or He at 550°C since Fe-O bonds would be broken and Fe^{2+} sites would result. Other iron species (iron oxides, small iron clusters/ oligomers) should not be affected as the temperature of treatment is too low for full reduction of these species. Examination of the He treated material by UV-VIS spectroscopy (

Figure 3.18 red curve) shows that whilst the sample has the same 0.014wt% Fe as the calcined material (Figure 3.18 black curve) the intensity of the signal is increased and features are now clearly visible which possibly correspond to both T_d and O_h Fe^{3+} (as shown by black arrows in Figure 3.18). There also appears to be a greater contribution from iron oligomeric species as the broad shoulder peak *ca.* 380 nm is more pronounced. Thus the increase in methanol selectivity when ZSM-5 is heat treated in a helium atmosphere must relate to changes in iron species within the zeolite pores.
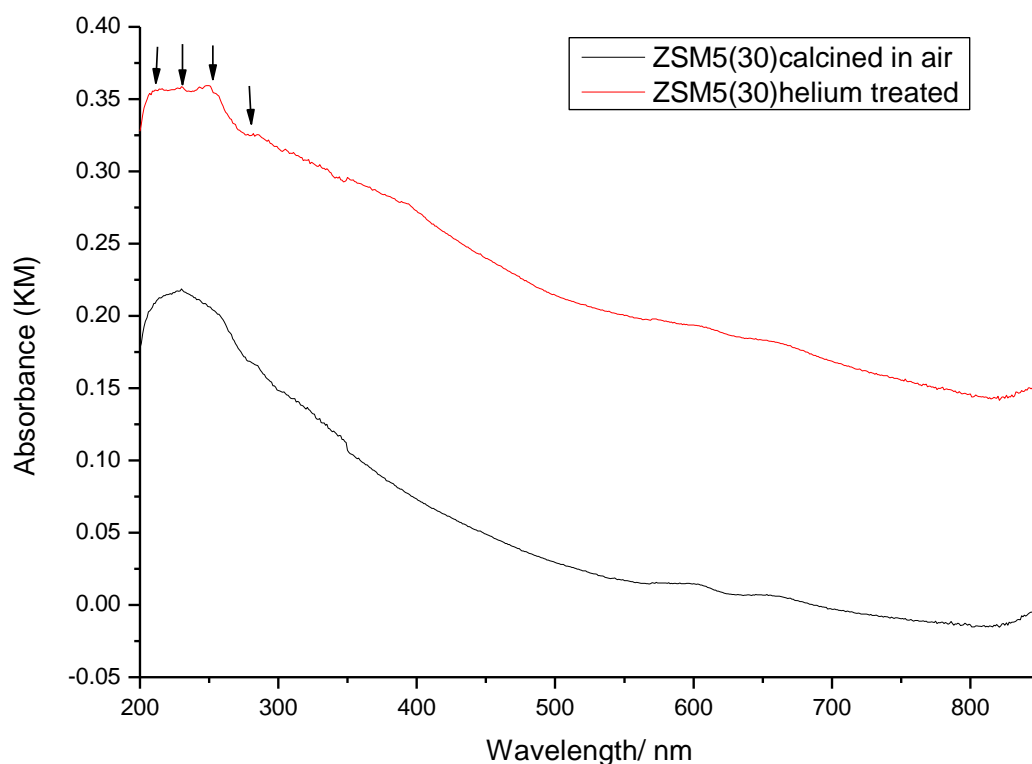
Figure 3.18 UV-VIS spectra of ZSM-5(30) treated in flowing air (black curve) and helium (red curve) at 550°C for 3 h. The black arrows mark the position of Fe^{3+} T_d peaks (212nm), small isolated Fe^{3+} oxides within the zeolite channels (230nm), isolated Fe^{3+} clusters (254nm) and Fe^{3+} O_h at 280nm.

Reduction, as performed in literature studies with prior calcination was also performed on 1.1wt% Fe/ZSM-5(30), entry 7 Table 3.6. This technique does not have a significant effect on methanol selectivity. Thus it can be said that forming active iron species in the material and then changing the oxidation state is ineffective while forming active iron sites under a reducing atmosphere leads to higher methanol production.

Finally, ZSM-5(30) was calcined in air and then iron deposited using the CVI technique followed by heat treatment in a reducing atmosphere, entry 9 Table 3.6. In this sample it is known that the first calcination should form specific Fe sites in ZSM-5(30) which cannot be reduced to produce the selectivity effect (as shown in entries 5, 6 Table 3.6). Thus any other effect of reduction after the deposition of Fe can only be explained by the presence of other Fe species on the catalyst as in the purely reduced material, entry 2, 3 Table 3.6. The enhanced methanol selectivity is here assigned to the effect of H_2 on the formation of different Fe species during heat treatment.

These findings show that the catalyst behaviour can be modified by heat treatment in a reducing atmosphere and the observed changes in selectivity is linked to the increased formation of well defined isolated iron sites (as small oxides in the channels and O_h/T_d Fe^{3+} species). To give further explanation for the catalytic data would require detailed study of the surface species by TEM and the electronic state of the iron by XANES/EXAFS. At the time of writing this thesis further studies on the "reduction" treatment have been arranged as part of a collaborative project.

The "reduced "catalysts will be used again in catalysts employed of ethane oxidation (Chapter 5) where a beneficial effect on increasing ethanol selectivity over the calcined materials is observed.

3.4.5. Validation of catalytic activity and catalyst stability

For any catalytic system the observed activity should be validated as originating from the action of the catalyst on the proposed substrate. This is particularly important for systems in which the catalyst or solvent may also provide a source of the observed reaction products. For example when acetonitrile (CH_3CN) is used as a solvent in the oxidation of methane C1 oxygenates derived from methyl groups in the solvent may be observed and assigned as originating from methane. A case in point would be the system of Sorokin and co-workers where it was found that a bio-mimetic catalyst was actually being oxidised during methane oxidation testing and the observed products were derived from carbon in organometallic catalyst and methane itself. [41] A series of experiments were performed to validate that the data presented in this thesis is based on products of methane oxidation and not carbon contamination in the system; from the reactor or residual carbon on the Fe/ZSM-5(30) since an organometallic precursor was used in the preparation of the material.

$^{13}CH_4$ and $^{12}CH_4$ tests were performed under the same conditions. One would expect that ^{13}C products have a split signal in ^{1}H-NMR experiments while ^{12}C products only give one resonance which falls in the centre of the two resonances due to ^{13}C products. Isotopic labelling, shown in Figure 3.19, unequivocally shows that $^{13}CH_4$ results in $^{13}CH_3OOH$, $^{13}CH_3OH$, $^{13}CHOOH$. The minor contribution from 12C products is due to the 1% $^{12}CH_4$ in the $^{13}CH_4$ feed (i.e. as supplied by BOC Gases).

Reuse testing and the "filtrate" test was performed on one sample of Fe/ZSM-5(30). For the filtrate test, the reaction was performed as usual and then catalyst removed by filtration and the reaction was continued using only the filtrate. Additional water
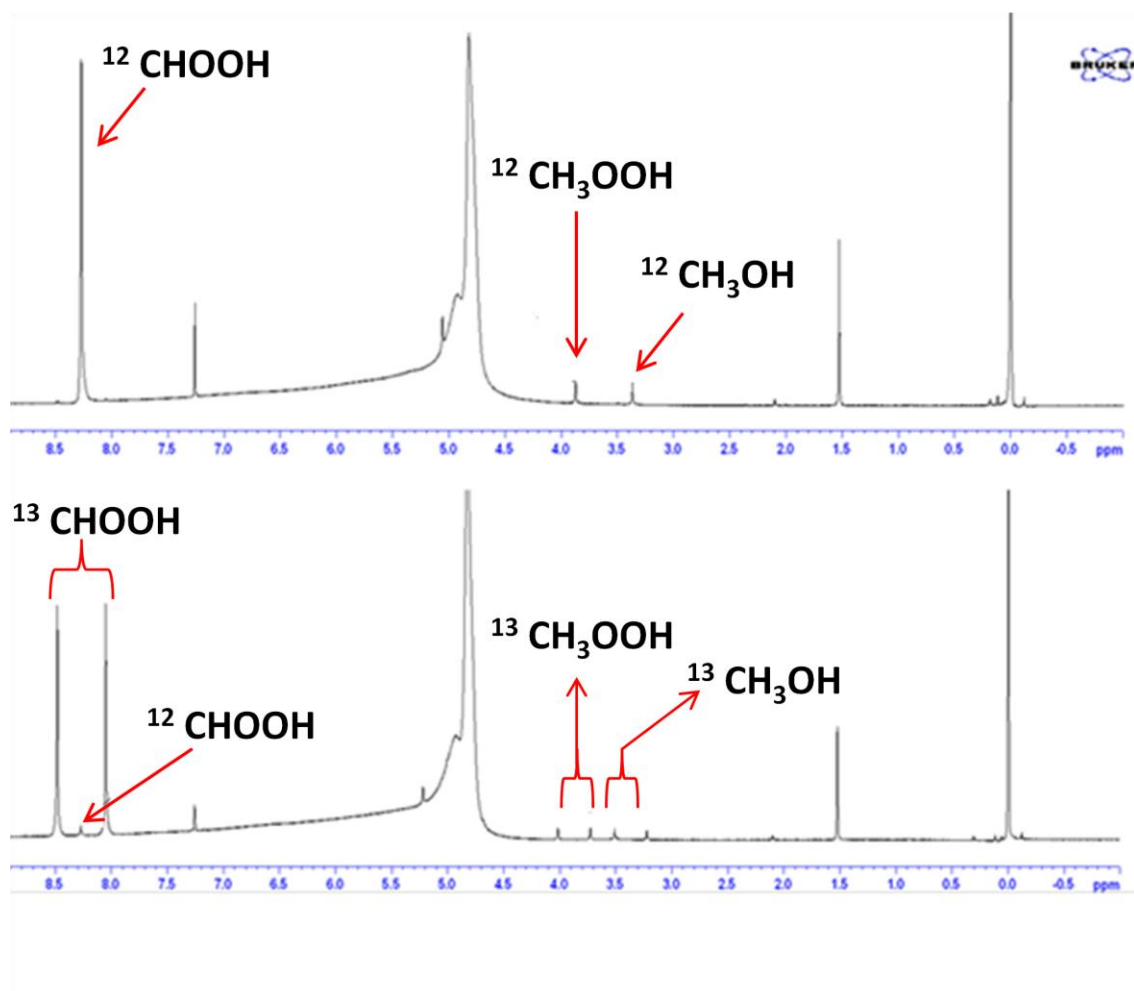
Figure 3.19 1H-NMR spectra of $^{12}CH_4$ tests (upper spectrum) and $^{13}CH_4$ tests (lower spectrum) performed using 1.1wt% Fe/ZSM-5(30) calcined at 550°C, 3h, static air. Reaction conditions: 54mg catalyst, 20ml water, 1M [H_2O_2] , 5bar methane, 0.5h, 1500rpm, 50°C. Chemical shifts for each product is given in Chapter 2.

and hydrogen peroxide were added to the filtrate to ensure the volume and oxidant level matched the initial experimental conditions. The assayed filtrate only displayed *ca.* 7% of the activity of the intact system with solid catalyst, Figure 3.20 (a). It should be noted that the very fine particulate nature of the catalyst eludes perfect removal of the solid catalyst by filtration. Furthermore, the catalyst showed no loss of activity or selectivity when re-used twice under the same conditions. These data support the

hypothesis that the catalytic reaction is truly catalysed by the solid catalyst, Fe/ZSM-5(30).
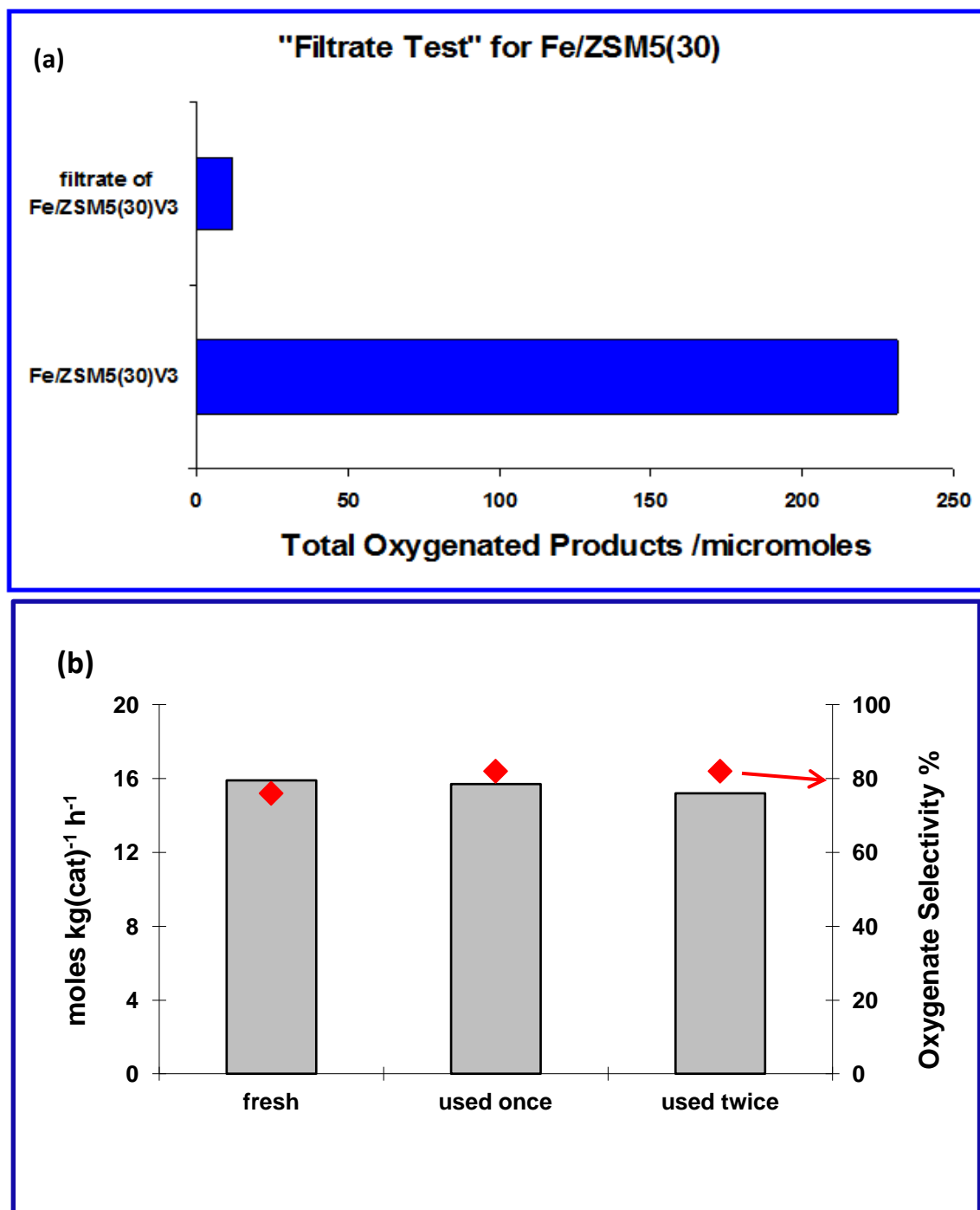
Figure 3.20 (a) Activity of the reaction filtrate and (b) re-use testing of an Fe/ZSM-5(30)$_{CVI}$ catalyst. In (b) grey bars- total productivity, red diamonds- partial oxygenate selectivity (HCOOH is the major product).

As will be shown in Chapter 4 aqueous Fe can perform selective methane oxidation under appropriate conditions but the level of leached Fe in this system (below 6ppm, see appendix 8 for details) is too low to account for any appreciable activity in the reaction timeframe of 0.5 h. Finally it has been confirmed that these catalyst can be used for long reaction times (24) under flow reaction conditions with no loss of activity upon reuse under those conditions.[r]

During the course of studies on Fe/ZSM-5(30) catalysts prepared by different methods it was found that the activity of the material decreased with time. This was termed catalyst deactivation. Stability of a heterogeneous catalyst is crucial to its use in industrial setting and reproducibility of data obtaining during initial academic studies on the material. A catalyst which is quickly deactivated under reaction conditions and cannot be easily regenerated may only have a very limited application. Catalyst deactivation due to ambient ageing in air at room temperature (catalyst held in a dark drawer) was studied, Table 3.7.

It was observed that a freshly prepared and calcined 1.1wt% Fe/ZSM-5(30) catalyst had the best catalytic activity but its productivity decreased with age, entries 1-3 Table 3. This was even more drastic for some catalysts, e.g. ZSM-5(30) itself or Cu/ZSM-5(30). Interestingly 1.1wt% Fe/ZSM-5(30) treated in a reducing atmosphere had better stability, entry 4 and 5 Table 3.7. The deactivation was thought to be due to the effect of atmospheric water and storage in air. It is possible that slow oxidation of isolated iron species to iron oxides or hydroxides is occurring with time stored in air.

---

[r] Unreported data gathered by Dr. Nick Dummer at Cardiff Catalysis Institute

To probe this, catalysts were re-calcined before use or treated under vacuum. In most cases the original activity was not restored though some level of re-activation was observed for high temperature treatment. Furthermore, it was observed that the as-prepared CVI samples when calcined many months after preparation did not show the same activity as the freshly prepared and freshly calcined materials. Thus in general data for 'fresh' catalysts is normally presented in this thesis.

Table 3.7 Catalyst stability with ageing in air at room temperature. 'Age' refers to time between calcination and use in a methane oxidation reaction.

Entry	Catalyst	Age	Total Productivity [b]	% Oxygenate Selectivity [c]
1	1.1%Fe/ZSM-5(30) $_{CVI}$ calcined	fresh	22.0	79
2	1.1%Fe/ZSM-5(30) $_{CVI}$ calcined	5 days	15.4	85
3	1.1%Fe/ZSM-5(30) $_{CVI}$ calcined	1 year	8.4	91
4	1.1%Fe/ZSM-5(30) $_{CVI}$ reduced	fresh	19.1	86
5	1.1%Fe/ZSM-5(30) $_{CVI}$ reduced	5 days	18.1	87

Reaction Conditions: Reaction time 0.5h; Reaction temp: 50°C, Solvent: H_2O: 10 mL; 5000µmoles H_2O_2 ; P (CH_4): 30b; 27mg catalyst All catalysts tested under standard conditions and were heat treated at the 550°C ; [b] mol of products ($CH_3OH+CH_3OOH+ HCOOH+CO_2$) kg(catalyst)$^{-1}$ h^{-1} ; [c] ($CH_3OH+CH_3OOH+CH_2O+ HCOOH$)/ ($CH_3OH+CH_3OOH+CH_2O+ HCOOH +CO_2$) X 100

3.6. Summary

Fe is a very active metal for methane oxidation when in the form of small iron oxidic species (<5nm), iron clusters and oligomeric and dinuclear iron –oxo species. The preparation of these iron species can be achieved reproducibly using the CVI methodology without the formation of large iron oxides (>15nm) which are inactive for the reaction. The oxidation of methane using iron based materials with hydrogen peroxide is linked to both the level of oxidant and the state of the iron species present on the catalyst. Different catalysts with similar metal loading can produce very different results in terms of productivity and selectivity of the material. This is due to the location of the iron species in the zeolite (i.e. within the pores and on the external surface). The presented catalysts show up to 5 times the activity of sMMO, our chosen benchmark enzyme, for methane oxidation under mild conditions.

Treatment of the catalysts under a reducing atmosphere is beneficial for achieving higher methanol selectivity, but this is not due to the oxidation state of the Fe as XPS analysis shows no change versus the calcined materials. However, it is highlighted that the formation of new active iron sites upon reductive heat treatment accounts for the changes in selectivity towards methanol. It was shown that the catalysis is heterogeneous in nature and that the catalyst deactivation is lined to the age of the material.

References

1. Colby, J.; Stirling, D. I.; Dalton, H. *Biochem. J.* 165, 395-402 (1977).

2. Hammond, C.; Submitted thesis, Cardiff University (2011).

3. Kesavan, L.; *et al. Science* 331, 195-199 (2011).

4. Edwards, J.K.; *et al. J. Catal.* 236, 69-79 (2005).

5. Herron, N.; Tolman, C. *J. Am. Chem. Soc* 109, 2837-2839 (1987).

6. Chen, H. A.; Sachtler, W. M. H. *Catal. Today* 42, 73-83 (1998).

7. El-Malki, E. M.; Santen, R. A. v.; Sachtler, W. M. H. *J. Phys. Chem. B* 103, 4611-4622 (1999).

8. Auerback, S.M.; Carrado, K.A; Dutla, P.R. (edts.) <u>Handbook of Zeolite Science and Technology</u> Marcel-Dekker, New York, pgs 217, 234 (2003).

9. Auerback, S.M.; Carrado, K.A; Dutla, P.R. (edts.) <u>Handbook of Zeolite Science and Technology</u> Marcel-Dekker, New York, pgs 26, 82-86, 866 (2003).

10. Kobayashi, T.; Nakagawa, K.; Katsuki, T.; Haruta, M. *Chem. Commun.* 1609-1610 (1994).

11. Kobayashi, T.; Guilhaume, N.; Miki, J.; Kitamura, N.; Haruta, M. *Catal. Today* 32, 171-175 (1996).

12. Arena, F.; Gatti, G.; Coluccia, S.; Martra, G.; Parmaliana, A. *Catal. Today* 91-92, 305-309 (2004).

13. Arena, F.; Parmaliana, A. *Acc. Chem. Res.* 36, 867-875 (2003).

14. Panov, G.; Sheveleva, G. A.; Kharitonov, A. S.; Rommikov, V. N.; Vostrikova, L. A. *App. Catal. A: General* 82, 31 (1992).

15. Panov, G.; Sobolev, V. I.; Kharitonov, A. S. *J. Mol. Catal A: Chemical* 61, 85-97 (1990).

16. Jia, J. F.; Pillai, K. S.; Sachtler, W. H. M. *J. Catal.* 221, 119-126 (2004).

17. Hensen, E. J. M.; *et al. J. Catal.* 221, 560-574 (2004).

18. Wang, Y. *Res. Chem. Intermed.* 32, 235-251 (2006).

19. Kubánek, P.; Wichterlová, B.; Sobalik, Z. *J. Catal.* 211, 109-118 (2002).

20. Wood, B. R.; Reimer, J. A.; Bell, A. T.; Janicke, M. T.; Ott, K. C. *J. Catal.* 225, 300-306 (2004).

21. Knops-Gerrits, P. P.; Verberckmoes, A.; Schoonheydt, R.; Ichikawa, M.; Jacobs, P. A.; *Microporous and Mesoporous Mater.* 21, 475-486 (1998).

22. Raja, R.; Ratnasamy, P. *App. Catal. A: General* 158, L7-L15 (1997).

23. Ratnasamy, P.; Srinivas, D. *Catalysis Today* 141, 3-11 (2009).

24. Battiston,A.A; Bitter, J.H.; Heikboer, W.M; Groot de, F.M.F.; Koningsberger, D.C. *J. Catal.* 215, 279-293 (2003).

25. Battiston, A. A.; Bitter, J. H.; Koningsberger, D. C. *J. Catal.* 218, 163-177 (2003).

26. Merkx, M.; et al. Angew. Chem. Int. Ed. 40, 2782-2807 (2001).

27. Thetford, A. Unpublished communications within the DOW Methane Challenge, Cardiff University (2011).

28. Periana, R. A.; *et al. Science* 280, 560-564 (1998).

29. Bordiga, S.; *et al. J. Catal.* 158, 486-501 (1996).

30. Marturano, P.; Drozdova, L.; Pirngruber, G. D.; Kogelbauer, A.; Prine, R. *Phys. Chem. Chem. Phys* 3, 5585-5595 (2001).

31. Lehmann, G. *Z. Phys. Chem. Neue Folge* 72, 279-297 (1970).

32. Bongiovanni, R.; Pellizzetti, E.; Borgarello, E.; Meisel, D. *Chim. l'Indust.* 4, 261-266 (1994).

33. Lobree, L. J.; Hwang, I.; Reimer, J. A.; Bell, A. T. *J. Catal.* 186, 242-253 (1999).

34. Kucherov, A. V.; Shelef, M. *J. Catal.* 95, 106-112 (2000).

35. Ali, I. O.; Ali, A. M.; Shabaan, S. M.; El-Nasser, K. S. *J. Photochem. Photobio. A: Chemistry* 204, 25-31 (2009).

36. Inui, T.; *et al. J. Catal.* 139,482- 489 (1993).

37. El-Malki, E. M.; Santen, R. A. v.; Sachtler, W. M. H. *J. Catal.* 196, 212-223 (2000).

38. Yuranov, I.; Bulushev, D. A.; Renken, A.; Kiwi-Minsker, L. *App. Catal. A*: *General* 319, 128-136 (2007).

39. Sobolev, V. I.; Kharitonov, A. S.; Paukshtis, Y. A.; Panov, G. I. *J. Mol. Catal.* 84, 117-24 (1993).

40. Chen, H.; Sachtler, W.M.H. *Catal. Today* 42, 73-83 (1998).

41. Forde, M.M.; *et al. J. Catal.* 290, 177-185 (2012).

Chapter 4

Use of ZSM-5(30) doped with other metals for aqueous phase methane oxidation and mechanistic studies
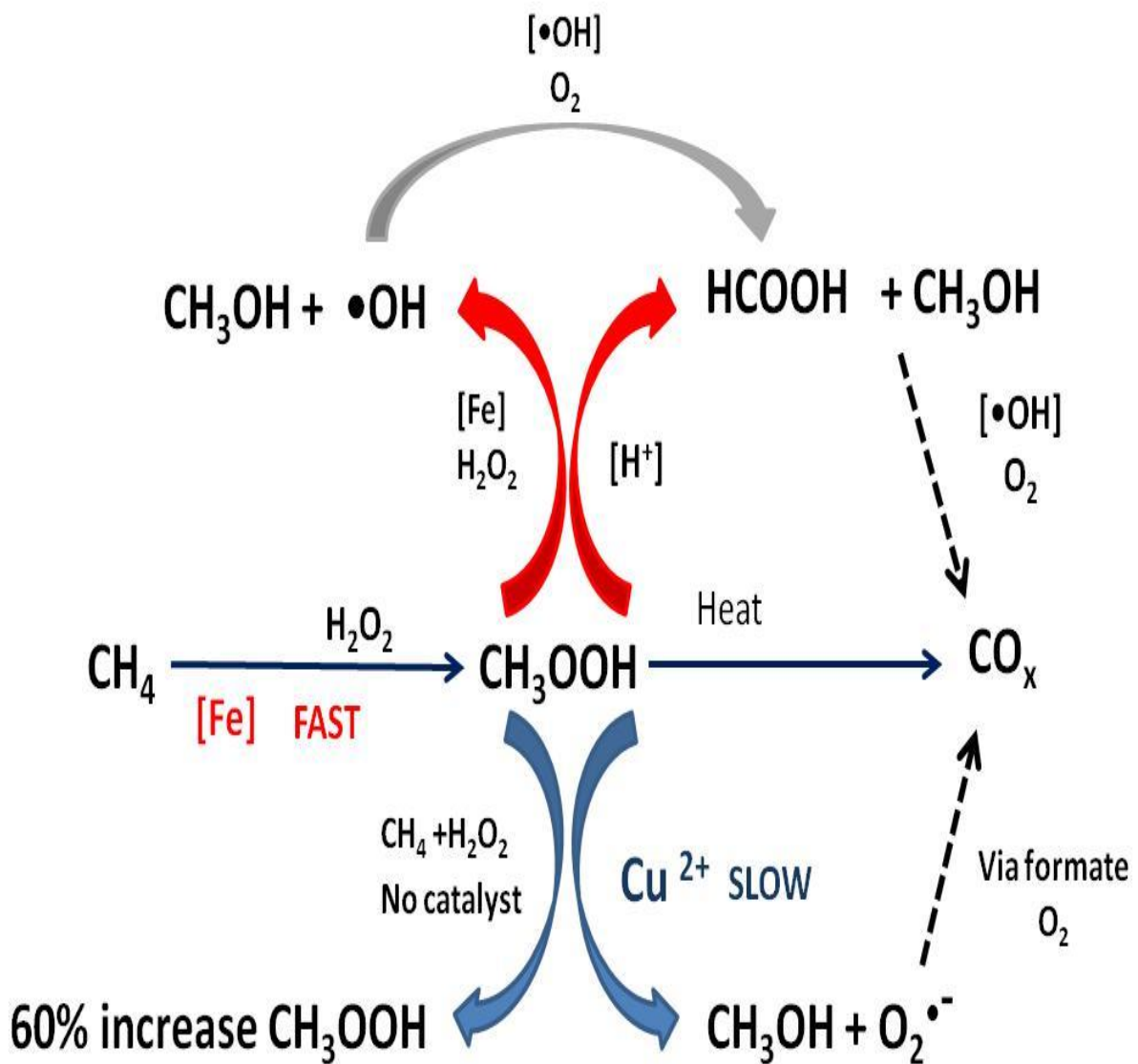
4.1. Investigation into the effect doping ZSM-5(30) with other metals (Ga, Zn, Cu, Ru) for methane oxidation

After studying the Fe/ZSM-5 catalysts (Chapter 3) other metals were introduced by post-deposition methods into ZSM-5(30) and assayed for methane oxidation activity. The aim of these experiments was to determine whether other metals could promote ZSM-5's activity in methane oxidation or increase the selectivity to methanol. It is known that removal of framework Al in ZSM-5 results in the creation of extra-framework Al sites which are Lewis acids. Anchoring of isolated iron species Fe at exchange sites in HZSM-5 also creates Lewis acid sites (i.e. Fe^{3+} is a Lewis acid). Work by El-Malki [1] *et al* confirms that other metals such as Al, Ga, Zn can also have this effect and the strength/number of the Lewis acid sites increases in the order Al> Ga> Zn> Fe. To probe whether the reaction was affected by the Lewis acid strength of the added transition metal several catalysts were synthesised utilizing the CVI technique to deposit Ga, Zn and Cu from the corresponding acetylacetonate sources. In theory, if the Lewis acid strength of the isolated metal species was a factor then the catalytic activity should be affected. As presented in Table 4.1 no promotion of the activity of ZSM-5 was observed with the introduction of Ga or Zn (Table 4.1, entries 1, 2). It may be that the preparation technique used deposited the metal oxides which are inactive for the reaction and not exchanged H^+ sites effectively to produce isolated metal ions as in the case of FeZSM-5(30) prepared by CVI.

However, Cu had a beneficial effect on both promoting the activity of ZSM-5 and changing the selectivity of the system to produce methanol as the major oxygenate product with high selectivity, ca. 89% selectivity to methanol Table 4.1 entry 3. This material will be discussed in the following section.

Table 4.1 Activity for ZSM-5 based catalysts doped with 2.5wt/% of various metal by CVI for methane oxidation

Entry	Catalyst	Products (µmol)				Total Productivity [c]	H_2O_2 Left /µmol [d]
		CH_3OOH[a]	CH_3OH [a]	HCOOH[a]	CO_2 in gas[b]		
1	Ga/ZSM-5(30)	18.4	16.1	33.2	10.1	5.8	4042
2	Zn/ZSM-5 (30)	11.8	5.4	9.7	2.6	2.2	4556
3	Cu/ZSM-5 (30)	2.9	103.6	0	10.4	8.7	4300
4	Ru/ZSM-5(30)	13.5	12.5	11.2	2.9	3.0	4398

Reaction Time: 0.5h; Reaction temp: 50°C, Solvent: H_2O: 10 mL; 5000µmoles H_2O_2 ; P (CH_4): 30b; 27mg catalyst. All catalysts were calcined at 400°C, 3h in static air unless otherwise specified.[a] Analysis using ^{1}HNMR, [b]Analysis using GC-FID, [c] mol of products (CH_3OH+CH_3OOH+ HCOOH+CO_2) kg(catalyst)$^{-1}$ h^{-1} , [d] Assayed by titration against acidified $CeSO_4$ with Ferroin indicator.

Ru was also tested since it is a group 8 element, like Fe, and showed good results for methane oxidation when supported on TiO_2 as compared to other supported metals on TiO_2.[a] In general it was observed that metals supported on TiO_2 which showed good activity for methane oxidation also showed good activity when doped into ZSM-5 materials. In the case of Ru this observation in not substantiated by the data in entry 4 Table 4.1 since the total productivity is lower than for calcined ZSM-5(30) (3.0 versus 4.4 in Table 3.3 Entry 5). Though there is no significant effect on productivity it is apparent that the methyl hydroperoxide and methanol selectivity is much higher in the Ru doped catalyst (40.1% and 31.2% versus 23.3% and 19.4% respectively for entry 4 Table 4.1 versus entry 5 Table 3.3). In spite of these

[a] Unreported data- subject of future work in the DOW Methane Challenge

selectivity advantages the low productivity excluded this material from further investigations. This was also the case for Cr, V, Mn and Co.

4.2. The effect of Cu- the case of bimetallic Cu-Fe catalysts

Significant scientific work has been focused in recent years on the utilisation of Cu catalysts for methane oxidation. In 1997 Raja and Ratnasamy [2-5] described Cu and Fe phthalocyanines encapsulated in zeolites for methane oxidation. Some of the data presented is similar to this current report (under like conditions) but firm evidence of the lack of homogeneous chemistry was not given in their work. In that study $CuCl_{16}Pc$ was encapsulated into Na-X and Na-Y zeolites and used for methane oxidation with $TBHP/O_2$ in acetonitrile solvent. Conversion was *ca.* 4% and selectivity to methanol was at least 50% of all products. The analogous Fe based catalyst showed similar selectivity and slightly higher conversion (5%). This work was extended by Yafang *et al* [6] with the "in situ" H_2O_2 approach first demonstrated by Sen[7] adopted. Cu phthalocyanine was the lead complex in that study and showed that CuPc catalysed the conversion of methane to oxygenates only when hydrogen peroxide was formed *in situ* from O_2 and H_2/CO using a Pd catalyst.

The Schoonheydt group recently presented compelling evidence for the formation of $[Cu_2O]^{2+}$ cores in ZSM-5 and mordenite after O_2 treatment of the catalysts [8-11]. This active site could oxidise methane selectively to methanol (yield was 8.2 μmol methanol per gram of catalyst). Like the Fe/ZSM-5 with N_2O work [12-14], Cu/ZSM-5 or Cu/MOR system is not catalytic and the presence of water decomposes the active site. However, their work is also supported by a report of measurable and specific interaction of CH_4 with Cu/MFI catalysts even at room temperature [8-11] following high temperature O_2 activation. It was observed that one particular feature in the UV-VIS spectra of O_2 activated Cu/ZSM-5(12) disappeared within 25 minutes upon interaction with methane at 125°C coinciding with the production of methanol in the

system. Furthermore, the work of Itadani [15] *et al.* supports the hypothesis that specific copper sites can oxidise methane since they report a significant interaction between Cu^+ ions in Cu/ZSM-5(12) at 27^oC as shown by IR and XANES/EXAFS data. This interaction is weaker and less populated than the interaction of O_2 with Cu sites in the same sample and is purported to occur though the –H atoms in methane.

In nature Cu is the active metal in pMMO for selective methane oxidation and though the actual mechanism remains elusive there is new consensus that a tri copper cluster is responsible for the oxidation of methane. As discussed in Chapter 1 pMMO is not as versatile as sMMO in its ability to oxidise a wide variety of substrates. Work in our group indicated that small copper oxide particles are effective for methanol production since Cu/TiO_2 made by CVI or commercially available copper oxides [16] carried out the target transformation in low yield though methanol and methyl hydroperoxide were the main products. This prompted use of Cu as a transition metal in ZSM-5 since it was proposed that Cu would be more selective considering all the heterogeneous and homogeneous catalysis data available at the time.

Cu can also act as a Lewis acid and be exchanged into in ZSM-5. The data in Table 4.2 entry 1 shows a difference in terms of activity and selectivity for the Cu catalyst. Unlike other metals tested in Section 4.1 Cu was an effective metal additive. The data in entry 1 was the first report of very high methanol selectivity, without the need for the presence of additional Fe in a calcined zeolite based catalyst, i.e. 88% selectivity to methanol. The high methanol selectivity reported here was reproduced for a number of different batches of catalyst though total productivity as compared to ZSM-5(30) varied[b] . The deviation in data observed for Cu catalysts may be

---

[b] This is thought to be due to differences in the ZSM-5 itself as samples of the material from different sources or batches have been shown to have varying catalytic activity.

explained by difference in the parent zeolite or the inferred instability of Cu species in this material. Also it is highly probable that only a minor fraction of the added Cu species are actually active for methane oxidation when doped into ZSM-5 since in the previously mentioned gas phase Cu/ZSM-5(12) catalysed reaction only a very minor fraction of the Cu sites are responsible for the reaction.[c]Unlike the case with Fe on ZSM-5, Cu on ZSM-5 was also effective if prepared by wet impregnation methods. This hinted at the possibility that Cu oxides may be the reason behind the changes in selectivity since it is known that wet impregnation leads to the formation and deposition of bulky oxides after calcination but that hypothesis was not supported by UV-VIS studies on samples prepared by wet impregnation in which bulky copper oxides were not detected in the catalyst materials.

Preparation of bimetallic Cu-Fe/ZSM-5(30) catalyst (entry 2, Table 4.2) was also performed in an effort to stabilise the Cu species formed and possibly achieve high catalyst productivity with high methanol selectivity. This led to an active catalyst with the same selectivity trends as the Cu/ZSM-5. In the case of the bimetallic Cu-Fe catalyst the hydrogen peroxide usage is higher by a factor of 2 and the total productivity is lower than for Fe/ZSM-5(30) with similar metal loading (i.e. 16-20 moles products kg(cat)$^{-1}$ h^{-1}). These findings are easily explained by the fact the metal content in the case of the bimetallic catalyst is doubled versus the monometallic Cu catalyst resulting in higher usage of hydrogen peroxide (mainly due to Fe) which is linked to lower catalyst productivity. Thus using a total of 2.5wt% metal in place of 5wt% metal in entry 2 Table 4.2 resulted in increased catalyst productivity while maintaining high methanol selectivity.

---

[c] Personal communication with a member of the Schoonheydt group at the ACS 242ND Meeting in Denver, USA.

Table 4.2 Oxidation of methane using bimetallic Fe & Cu CVI catalysts

Entry	Catalyst	Product amount (µmol)				Total Prod. [c]	CH_3OH Select. %	H_2O_2 Left /µmol [d]
		CH_3OOH [a]	CH_3OH [a]	HCOOH [a]	CO_2 in gas[b]			
1	2.5wt% Cu/ ZSM-5(30)	2.9	103.6	0	10.4	8.7	91	4300
2	Cu-Fe/ZSM-5(30) 5wt% total loading	1.2	125.2	0	28	11.4	82	1830
3*	1.1wt%Fe/ZSM-5(30) 1.25wt %Cu/ZSM-5(30) 1:1 Physical mixture	1.4	81.0	0	71.5	5.7	52	1340
4**	0.4wt% Fe/ZSM-5(30) (acid washed)	17.3	24.4	365.4	135.5	10.0	4.5	3000
5***	0.4wt% Fe/ZSM-5(30) (acid washed) 2.5wt% Cu/ZSM-5(30)	10.7	32	300.7	326.4	9.9	4.8	1600

Reaction Time: 0.5h; Reaction temp: 50°C, Solvent: H_2O: 10 mL; 5000µmoles H_2O_2 ; P (CH_4): 30b; 27mg catalyst. All catalysts were heat treated at 550°C, 3h in static air . %. * 27mg of 1.1wt% Fe and 27mg 1.25wt% CuZSM-5 , ** 108mg catalyst, 10000µmoles H_2O_2; *** 108mg Fe catalyst and 27mg Cu catalyst, 10000µmoles H_2O_2.[a] Analysis using ^{1}HNMR, [b]Analysis using GC-FID, [c] mol of products ($CH_3OH+CH_3OOH+ HCOOH+CO_2$) kg(catalyst)$^{-1}$ h^{-1}, [d] Assayed by titration against acidified $CeSO_4$ with Ferroin indicator

It was also observed that in reproducing these results that in some case formic acid (or methyl formate under different reaction conditions) was a reaction product and this prompted investigation of how the ratio of Fe: Cu affected the catalysis and particularly the selectivity to methanol. To investigate further a physical mixture of Fe/ZSM-5 and Cu/ZSM-5 was used to catalyse methane oxidation, entry 3, Table 4.2. The metal loading ratio was approximately 1:1[d] and a 1.1wt% Fe/ZSM-5(30) catalyst was chosen since it shows very high oxygenate productivity without utilising all the neat hydrogen peroxide. Formic acid was not produced by the physical

---

[d] Note that the nominal loading is 1.1wt% Fe and 1.25wt% Cu.

mixture but the total productivity decreased severely as compared to 1.1wt% Fe/ZSM-5(30) alone (5.7 for the physical mixture versus 16- 20mol products kg (cat)$^{-1}$ h^{-1}). Additionally the overall oxygenate selectivity is very poor (54%) indicating that Cu in the reaction results in increased production of CO_2. Another set of experiments were performed to validate these results. 0.4wt% Fe/ZSM-5(30) prepared by acid washing (see Chapter 3.4.3) was in conjunction with Cu/ZSM-5(30) due to its low iron loading (iron is within the pores of the zeolite thereby mimicking ZSM-5(30) itself) and high oxygenate selectivity. This material displays very high selectivity under standard conditions with low hydrogen peroxide usage. In entry 4 Table 4.2 the catalyst mass and oxidation level is increased resulting in high catalyst productivity at 75% oxygenate selectivity. As with all calcined Fe based catalysts the methanol selectivity is low. Addition of Cu at similar wt% as Fe was done using a physical mixture of Cu and Fe/ZSM-5(30). The amount of hydrogen peroxide left after reaction of the Fe based catalyst is above the level used by Cu/ZSM-5(30) (entry 4 versus 1 Table 4.2). The addition of Cu to this system resulted in severe decrease in oxygenate selectivity (75% to 51%, entries 4 and 5 Table 4.2) whilst maintaining the oxygenate productivity without any increase in methanol selectivity. Thus it is clear that in this case Cu increases the production of CO_2 and usage of hydrogen peroxide. These findings were reproduced during the writing of this thesis with the bimetallic catalyst used in entry 3 Table 4.2 and it was observed that though formic acid was shut off in those cases, the favoured product was CO_2.
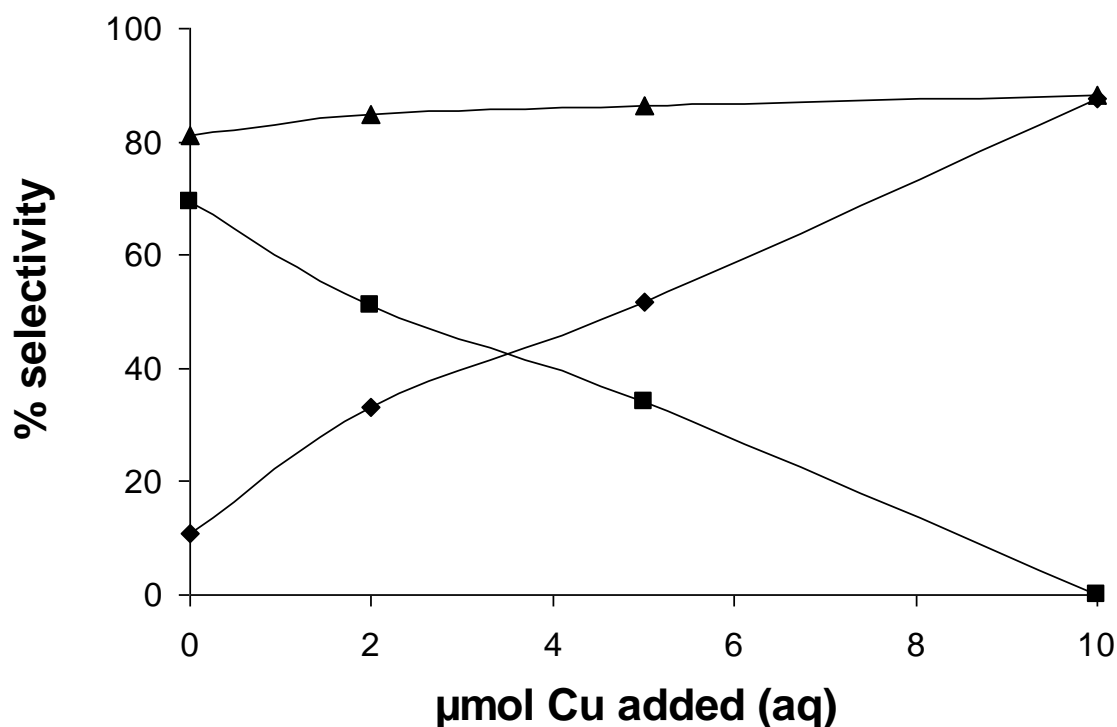
Figure 4.1 Controlling oxygenate selectivity with Fe/ZSM-5(30) as a catalyst by the addition of Cu^{2+} (aq) to the reaction mixture. Triangles- CO_2 selectivity, squares- HCOOH selectivity, diamonds- CH_3OH selectivity. The addition of Cu^{2+} alters the reaction pathway to produce the desired product, methanol.

To further investigate this, C. Hammond performed experiments where homogeneous copper (as the nitrate or chloride salts) was added to the reaction mixture. The results in Figure 4.1 show that if the loading with Cu was lower than Fe then HCOOH was observed in the products and thus only a 1:1 molar ratio of Cu to Fe could alter the product distribution so that only methanol is produced. This supported the previous data for the physical mixture and bimetallic Cu-Fe/ZSM-5(30) presented in Table 4.2 where a 1:1 ratio of Fe: Cu is necessary to obtain methanol as the major reaction product. All of these results demonstrate that (i) CO_2 was still produced without HCOOH being observed indicating that consecutive oxidation of HCOOH to CO_2 is only one pathway to produce CO_2 in this system since shutting off

over-oxidation does not result in 100% oxygenate selectivity; (ii) if Fe in Fe/ZSM-5 was performing methane oxidation by the same mechanism as suggested in Chapter 3.3 then in the case of the physical mixtures of Fe and Cu catalysts the increased methanol selectivity must be due to solution phase chemistry since the active sites (Fe and Cu) cannot interact when on two separate solid catalysts.

The data reported when a second heterogeneous Cu catalyst is added to Fe/ZSM-5 cannot be explained by diffusion of aqueous phase Cu^{2+} ions into the zeolite pores where they alter the reaction mechanism, as can be invoked for the mixture of Fe/ZSM-5 with homogeneous Cu^{2+}. It is possible to hypothesise that the primary product (methyl hydroperoxide) can desorb from the iron sites in ZSM-5 and diffuse into the reaction solution where there are selectively decomposed on other Cu sites (on the external surface in the case of the physical mixture system or Cu-Fe/ZSM-5). For Cu/ZSM-5 the presence of Cu may participate in the selective decomposition of methyl hydroperoxide to methanol which means that Fe in ZSM-5 may remain the active metal for methane activation.

These hypotheses are plausible, however it is necessary to investigate the form of the transition metal ions in these materials to further understand the role of Cu in this system, i.e. are the same Fe species present in all cases or does Cu change the form of the iron present? To obtain more information on the state of Fe and Cu in these materials XANES/EXAFS and UV-VIS studies were performed. Firstly, examination of the electronic structure of Cu in 2.5wt% Cu/ZSM-5(30) calcined at 500 ^{o}C in air showed that Cu was in the form of Cu^{2+} and had a very similar spectrum to copper (II) sulphate. Notably a peak at 8977 eV is present (Figure 4.2 a) which is a fingerprint of Cu^{2+} 1s→3d transition. [10] This was the first indication that Cu was in the +2 oxidation state. In Figure 4.2(a) it can also be observed that the Cu in

Cu/ZSM-5 does not match either copper (II) oxide or copper (I) oxide. An absence of any features at 8985 eV, which are characteristic of T_d Cu^{2+} $1s \rightarrow 4p_z$ transition [17], indicates an octahedral environment which is supported by the spectrum of the copper (II) sulphate standard.

Note copper (II) hydroxide was also used as a standard but the spectrum obtained was markedly different from Cu/ZSM-5 herein presented which is incidentally also different to a well studied reference Cu/ZSM-5(12) reported by Groothaert and co-workers[10] that performs methane oxidation after oxygen activation. Furthermore examination of the R-space data also suggests that the Cu in Cu/ZSM-5 resembles copper (II) sulphate (Figure 4.2(b)) and thus it is assigned to a distorted O_h environment. Preliminary fitting (reported by Joo Kang[e]) [18] showed a mean Cu-O coordination number of 3.7±0.1 and Cu-O distance of 1.946 ± 0.004Å respectively. These values suggest that the Cu species are in a highly distorted geometry with the other two coordinating O atoms in a different configuration. The fitted Cu•••Cu separation is 2.95 Å. All these results are similar to results reported by Groothaert and co-workers[10] for Cu/ZSM-5 prepared by ion exchange from copper acetate except that the feature in the XANES spectra indicating tetragonal Cu^{2+} is absent. It is therefore suggested that in the CVI samples the Cu^{2+} is isolated in a distorted O_h environment. These findings are unlike the reported Cu/MFI for methane activation where Cu^{1+} was observed to be the active component for CH_4 interaction in the work of Itadani *et al.* [15] The Cu^{1+} was fitted to a mean coordination number of 2.57 ± 0.18 and Cu-O distance of 1.95± 0.01Å after high temperature vacuum treatment.

---

[e] Of The DOW Chemical Company, internal presentation.
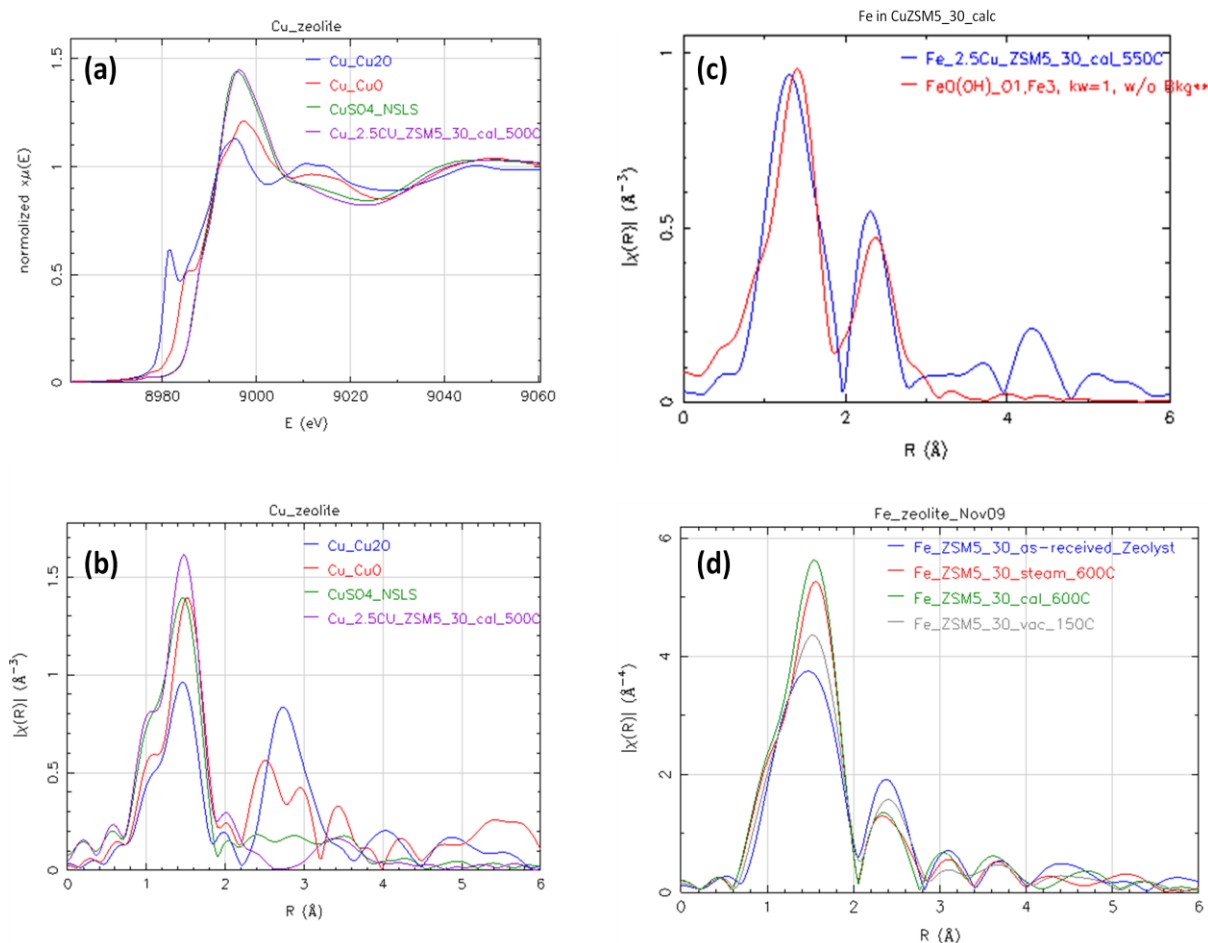
Figure 4.2 (a) XANES spectra and (b) EXAFS functions for Cu/ZSM-5(30) calcined and Cu standards showing that the Cu in ZSM-5(30)$_{CVI}$ is in the +2 oxidation state and resembles the electronic structure of Cu(II) sulphate. (c) EXAFS functions for the Fe (trace levels ~ 200pm) in CuZSM-5(30) calcined and a fitted FeO(OH) showing dissimilarity between O_h Fe in the fitted model and the Fe observed in the actual catalyst. (d)EXAFS functions for Fe (trace levels ~ 200pm) in ZSM-5(30)treated under different conditions.

One must also consider that 0.014wt% Fe is present in the parent ZSM-5(30) which may still be the active site for methane activation when the material is calcined. The EXAFS data analysis (<u>preliminary</u>) of the Fe in 2.5wt% Cu/ZSM-5(30) gave a Fe-O coordination number of 3.3 ± 1.0 and Fe-O distance of 1.92 ± 0.3 Å and Fe-Fe distance of 2.91± 0.04 Å. These values are different from the fitting results for Fe in

ZSM-5(30), calcined at similar temperature (i.e. 6 ± 0.4, 2.04Å, 2.97 Å respectively) upon which the DFT studies by Adam Thetford was based. The data suggest that the trace Fe in Cu/ZSM-5 is actually in T_d coordination with a shorter Fe-O distance than for trace Fe impurities in calcined ZSM-5(30). Figure 4.2 c, d shows the dissimilarity between the Fe in the Cu/ZSM-5 and its parent ZSM-5 heat treated under similar conditions and the attempted fitting to O_h Fe in FeO(OH) in which the R space data resembles the as-received zeolite which has minimal catalytic activity in comparison to calcined ZSM-5(30). T_d Fe could correspond to framework Fe hence there is an issue in assigning the activity of CuZSM-5(30) $_{CVI}$ to the trace impurities of Fe alone[f].

Since the EXAFS fitting was not fully refined at the time of preparing this thesis the Cu/ZSM-5(30) catalyst was studied using UV-VIS, as a complementary technique, due to the fact that different forms of Fe^{3+} and Cu^{2+} species should be easily distinguished by this technique. In Figure 4.3 comparison of the parent to the Cu^{2+} loaded material is presented. The first observation is that the Fe in both samples appeared to be different in nature. A very prominent feature for the Cu/ZSM-5(30) at 208 nm and weak should peak at 247-252 nm suggests T_d Fe^{3+} as opposed to the very broad a less intense features in this region for ZSM-5(30) which were assigned to isolated T_d/O_h/clustered Fe^{3+} in Chapter 3. One would expect that if there is a mixture of Fe^{3+} species as opposed to one iron species at the same trace levels of iron (i.e. 0.014wt%) then the spectrum of the ZSM-5(30) material would show an overall lower intensity absorbance in this region due to distribution of the iron amongst all the species present (i.e. lower individual concentrations and contributions of each form). When ZSM-5(30) is loaded with Cu by CVI the trace impurities of iron exists as tetrahedral species even after high temperature

---

[f] It may also be the case the trace Fe is not within the zeolite framework but exists as some new iron species with tetrahedral coordination.

calcination which usually has the effect of forming octahedral iron species in unmodified ZSM-5(30). This is supported by the difference spectrum in the insert (upper right Figure 4.3).
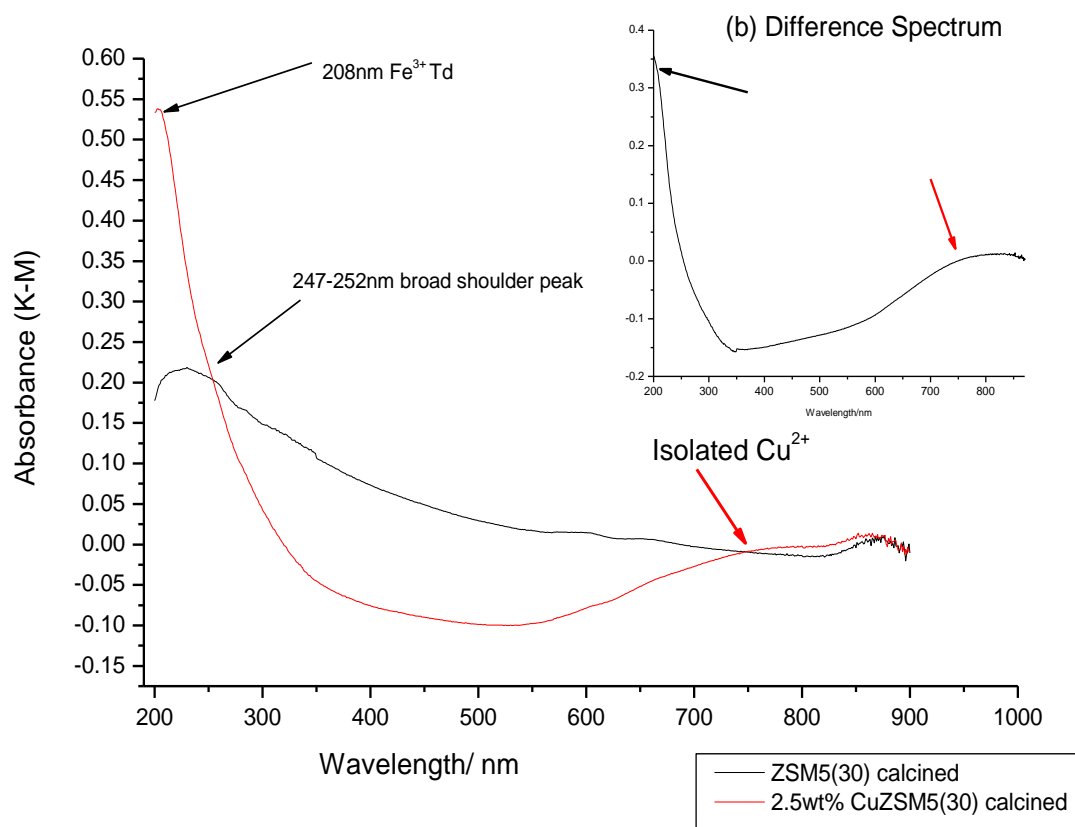
Figure 4.3[g] UV-VIS spectra of calcined 2.5wt% Cu/ZSM-5(30)$_{CVI}$ – red curve and calcined ZSM-5(30)- black curve. The difference spectrum between the Cu loaded and parent ZSM-5(30) is given in the insert (upper right) to show the identification of the new species on Cu/ZSM-5(30)

---

[g] This experiment was repeated but issues with our spectrometer did not improve the spectra obtained however the same peaks as in the one herein presented were clearly identified.

The second prominent feature is a very broad peak between 700-800 nm for Cu/ZSM-5(30). There is consensus in the literature that in Cu/ZSM-5 isolated distorted octahedral field Cu^{2+} ions are responsible for peaks between 714-800 nm in UV-VIS spectra. Also dimeric copper species (370nm feature), copper oxides (312-370nm) and linear CuO clusters (434-555nm) can also be readily distinguished. [19-23] Yashnik and co-workers have shown that isolated Cu^{2+} ions are present in all calcined samples of Cu/ZSM-5 they prepared and studied, irrespective of the preparation method and copper concentration. [19,21] In the CVI materials only the isolated Cu^{2+} can be detected by UV-VIS spectroscopy even for the high metal loading of 2.5wt%. No copper oxides were observed in these materials according to this analysis. This finding is supported by the difference spectrum in Figure 4.3 and these findings corroborate the data gathered in XANES/EXAFS studies. In summary the iron species in Cu/ZSM-5(30) are different from the iron species in ZSM-5(30) and other Fe/ZSM-5 materials discussed in Chapter 3. The Cu in Cu/ZSM-5 is in the +2 oxidation state and occurs as isolated ions with a distorted octahedral environment based on the pre-edge feature at 8977eV in the XANES analysis and broad peak form 714-800nm in the UV-VIS spectrum. It has been postulated that such ions are easily removed from the material by exchange reactions in aqueous solutions. Thus if this were happening in the reaction mixture a source of homogeneous Cu^{2+} would be present in the "heterogeneous" reaction and could account for the observed increased selectivity to methanol when using a physical mixture of Fe and Cu/ZSM-5. Analysis of the reaction filtrate did not show significant amounts of copper in solution (<6ppm). Also the catalyst develops and keeps a yellow colour when hydrogen peroxide interact with it suggesting that copper hydro-peroxy species or superoxide species are present on the catalyst surface.[24,25] These

observations rule out the probability of leached copper as the source of the observed changes in product distribution.

Furthermore, reduction of a Cu/ZSM-5(30)$_{CVI}$ catalyst (Cu^{2+} to Cu^{1+} transformation facilitated by heat treating in 5% H$_2$/Ar) causes severe reduction in catalytic activity whereas reduction of the parent ZSM-5 in H$_2$/Ar does not affect the catalytic activity(entry 6 Table 3.6). If the Fe impurities in the ZSM-5 were still performing the oxidation, in the manner describes in Chapter 3, with the Cu only controlling the decomposition of the primary product of the Fe catalysed reaction there should be little effect on the catalytic activity for a reduced Cu/ZSM-5 sample, though the product distribution may be altered. Notably Cu^{1+} can promote Fenton's type chemistry with the generation of •OH accompanied by increased decomposition of H$_2$O$_2$, and this species has been put forward as critical to N$_2$O decomposition and CH$_4$ activation in other studies.[15] Interestingly, using the Cu/ZSM-5(30) catalyst under long reaction times does not result in increased conversion levels as with ZSM-5 or Fe/ZSM-5 but rather similar amounts of products as displayed in 0.5h reaction time but with higher CO$_2$ selectivity.

From homogeneous reaction data (Table 4.5) one would predict isolated Cu sites to be less active than Fe since the redox potential and ability to perform Fenton's reactions is lower for Cu^{2+} than it is for Fe^{3+}. Exposure of the Cu/ZSM-5 to H$_2$O$_2$ results in an immediate blue to yellow colour change. This can easily be ascribed to the formation of Cu-OOH in a similar manner to TS-1 where a white to yellow colour change is due to the formation of Ti-OOH which is the active oxygen species for many reactions. [24] The formation of a special active Cu species similar to the proposed active iron species in ZSM-5(30), as outlined in Chapter 3.3, cannot occur in the event of isolated Cu sites but M-OOH species are well known to carry out a

variety of oxidation reactions leading to the formation of hydroperoxy intermediates, alcohols and ketones/aldehydes. Thus it is highly plausible that Cu is an active component for this reaction since Cu-OOH is observed and this species may have the ability to oxidise alkanes in the same way as TS-1 or vanadium complexes [25], though the activity of TS-1 for methane oxidation in particular is appreciably low. Further evidence for the role of Cu in Cu/ZSM-5(30) will be discussed in Section 4.4.5 on EPR studies .To investigate the location and form of the metal species in bimetallic Cu-Fe/ZSM-5(30) catalyst UV-VIS spectroscopy was utilised. In Figure 4.4 it is observed that the region below 300 nm has two prominent peak *ca.* 212 and 259 nm. These peaks have been observed before in Fe containing samples and correspond to T_d Fe^{3+} and isolated clustered Fe. A broad peak around 500nm is also visible and this can assigned to small surface iron oxide species though there is literature to support an assignment to small copper oxide clusters (435-555nm). [19-23] In the bimetallic sample one cannot differentiate isolated Cu^{2+} species nor O_h extra-framework Fe^{3+} species which is probably due to overlapping signals from other ions. Interestingly the isolated Cu species in Cu/ZSM-5(30) identified by a characteristic broad absorbance around 714-800nm is absent in the case of the bimetallic sample. No further insight can be had from the UV-VIS analysis to answer the questions surrounding the form and location of the 2.5wt% Cu in the sample studied.
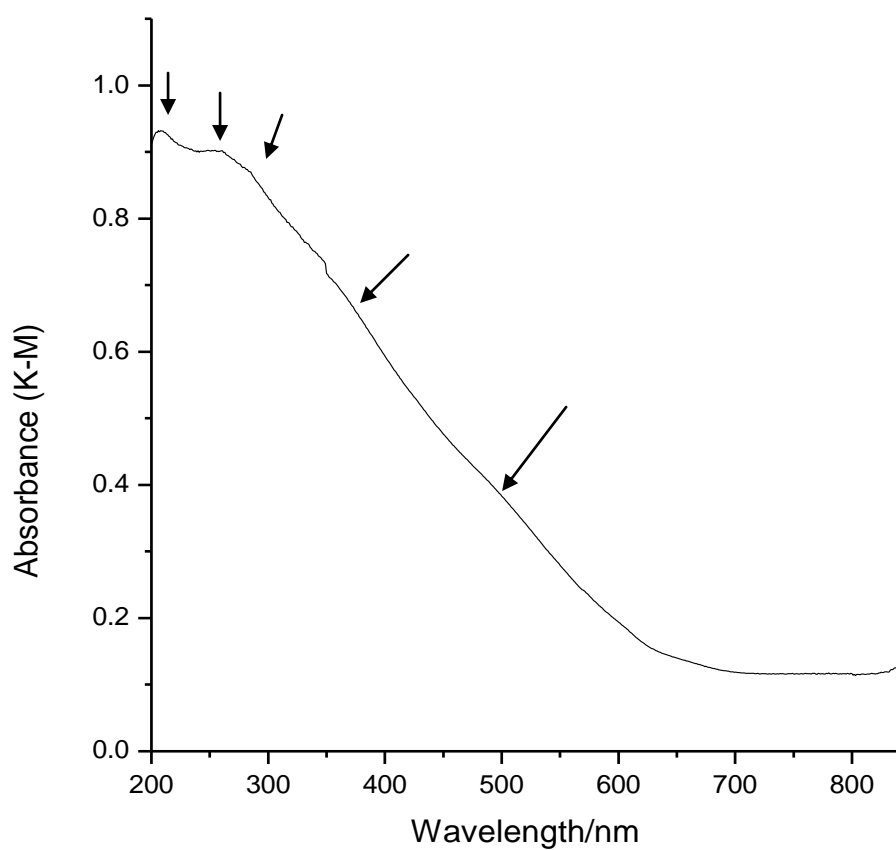
Figure 4.4 UV-VIS spectrum of 1.25wt% Fe-1.25wt% Cu/ZSM-5(30) calcined in air at 550°C , 3h. Arrows indicate areas of interest corresponding to Fe species in the material.

4.3 The effect of Au- the case of bimetallic Fe@Au catalysts

In Chapter 3.2 data was presented which demonstrated the beneficial effect of Au-Fe/TiO$_2$ when used in the "*in situ*" approach for methane oxidation. From the work of H.Ab Rahim[16] it was reported that Au-Pd/TiO$_2$ prepared by wet impregnation was not a highly efficient catalysts for methane oxidation due to the high hydrogen peroxide decomposition rate. When Au-Pd/ZSM-5 was tested for methane oxidation it proved to be less active than ZSM-5 which is explained by the unproductive decomposition of hydrogen peroxide to oxygen and water (see Chapter 3.3). However, the Fe and Au combination was further investigated since Fe was very active for the reaction and its associated hydrogen peroxide decomposition rate could be controlled based on earlier work. Thus it was thought that a similar *in situ* approach may work in the case of the bimetallic Au-Fe catalyst using ZSM-5 as a support. This goal was not achieved due to the mismatch between the hydrogen peroxide production rate by Au and usage rate by Fe. Earlier work by Herron and Tolman[26] showed that a Fe-Pd-Zeolite 5A combination was effective for methane oxidation using the *in situ* approach when used with cyclohexane/octane and it was reported that this was also possible with ZSM-5 as a support. This approach was not further investigated.

However, the ability of Au as an additional metal to tune selectivity of the reaction to produce high yields of methanol under H$_2$O$_2$ addition protocol was observed. Entry 1 Table 4.3 shows that the addition of Au to ZSM-5(30) before heat pre-treatment in H$_2$/Ar does not affect the activity of the catalyst. This was discussed in Chapter 3.3. It was also shown in Chapter 3 that heat treatment of 1.1wt% Fe/ZSM-5(30) in H$_2$/Ar resulted in increased selectivity to methanol in the catalytic reaction and that the iron species in that material corresponded to small extra-framework iron oxide and iron

clusters and T_d Fe^{3+} in the zeolite pores. The metal loading is critical for the actual productivity of the catalyst though a "reductive" heat treatment always increases methanol selectivity , as can be observed for the 2.5wt% FeZSM-5(30) shown in entry 2 Table 4.3 for which higher metal loading has lower productivity but similar methanol selectivity (vs. the "reduced" 1.1wt% Fe material, entries 2 and 3 Table 3.6).

Table 4.3 Activity of Fe@Au/ZSM-5(30) materials for CH_4 oxidation.

Entry	Catalyst	Product amount (µmol)				Total Productivity [c]	H_2O_2 Left /µmol [d]
		CH_3OOH[a]	CH_3OH [a]	HCOOH[a]	CO_2 in gas[b]		
1	Au/ZSM5(30)$_{IMP}$ reduced	10.2	3.6	3.2	6.6	1.7	2796
2	2.5wt%Fe/ZSM5(30) reduced	0	42.3	58.2	33.9	10.0	<50
3	2.5wt%Fe@2.5wt%Au/ ZSM5(30) Hybrid, reduced	0	114	123	42	20.7	498
4	2.5wt%Fe@2.5wt%Au/ ZSM5(30) Hybrid, calcined	3.2	36.3	168.0	46.7	18.8	1421

Reaction Conditions- Reaction Time: 0.5h; Reaction temp: 50°C, Solvent: H_2O: 10 mL; 5000µmoles H_2O_2 ; P (CH_4): 30b; 27mg catalyst. All catalysts were heat treated at 550°C, 3h in static air or 5%H_2/Ar. Nominal loading of each metal was 2.5wt%. [a] Analysis using ^{1}HNMR, [b]Analysis using GC-FID, [c] mol of products $(CH_3OH+CH_3OOH+ HCOOH+CO_2)$ kg(catalyst)$^{-1}$ h^{-1}, [d] Assayed by titration against acidified $CeSO_4$ with Ferroin indicator

What is remarkable is that the addition of 2.5wt% Au to ZSM-5(30) by wet impregnation before the introduction of 2.5wt% Fe by CVI followed by heat treatment under H_2/Ar , entry 3, Table 4.3, results in a catalyst with similar activity to a calcined

2.5wt% Fe or "reduced" 1.1wt% Fe loaded ZSM-5(30) catalysts (entries 2, 3 in Table 3.5 and entries 2, 3 in Table 3.6 respectively) but *ca.* 41% selectivity to methanol. Calcination of this material does not produce the effect of increased methanol selectivity (14% in entry 4 Table 4.3) though the catalyst productivity is similar to its "reduced" analogue or calcined monometallic Fe/ZSM-5(30).

 Thus it is clear that even at higher iron loadings the presence of Au in combination with reductive treatments leads to excellent productivity while maintaining high CH_3OH selectivity. Additionally the "reduced" bimetallic catalyst has ca. 10% of the hydrogen peroxide left after reaction whilst for the "reduced" monometallic sample less than 1% of the hydrogen peroxide is left after reaction. The higher amount of un-reacted oxidant is also observed if one compares the 29% hydrogen peroxide left after reaction in entry 4 Table 4.3 versus 18% in entry 3 Table 3.5 for the calcined materials. In both cases the amount of un-reacted oxidant is about 10% higher in the presence of Au. This may hint at the role of Au in allowing more efficient utilisation of the oxidant or by producing hydrogen peroxide/hydroperoxy species during the reaction as the *in situ* production of hydrogen peroxide from oxygen and H donors in the presence of small Au particles is well known.

Though the precise structure of the Fe and Au in the catalyst is not known some information was obtained by UV-VIS and XPS analysis. The UV-VIS spectrum in Figure 4.5 shows well resolved features at 215, 230, 247 and 259 nm with indications of possible additional shoulder features to these peaks. As is the case with the "reduced" 1.1wt% Fe/ZSM-5 material these peaks are well defined and correspond probably to T_d Fe^{3+} and small iron clusters (259 nm peak which dominates the spectrum) or iron oxides within the zeolite channels (230nm peak). There is a broad peak from 300-320 nm which may be due to oligonuclear Fe^{3+} oxo

clusters[27] and this is notably absent from the spectrum of the calcined material (Figure 4.5 (b)). The additional minor shoulder features on the 259nm peak may indicate O_h Fe^{3+}. There is no significant peak characteristic of Au clusters/nanoparticles (Au Plasmon peak) in the region 500-700 nm for the "reduced" material.
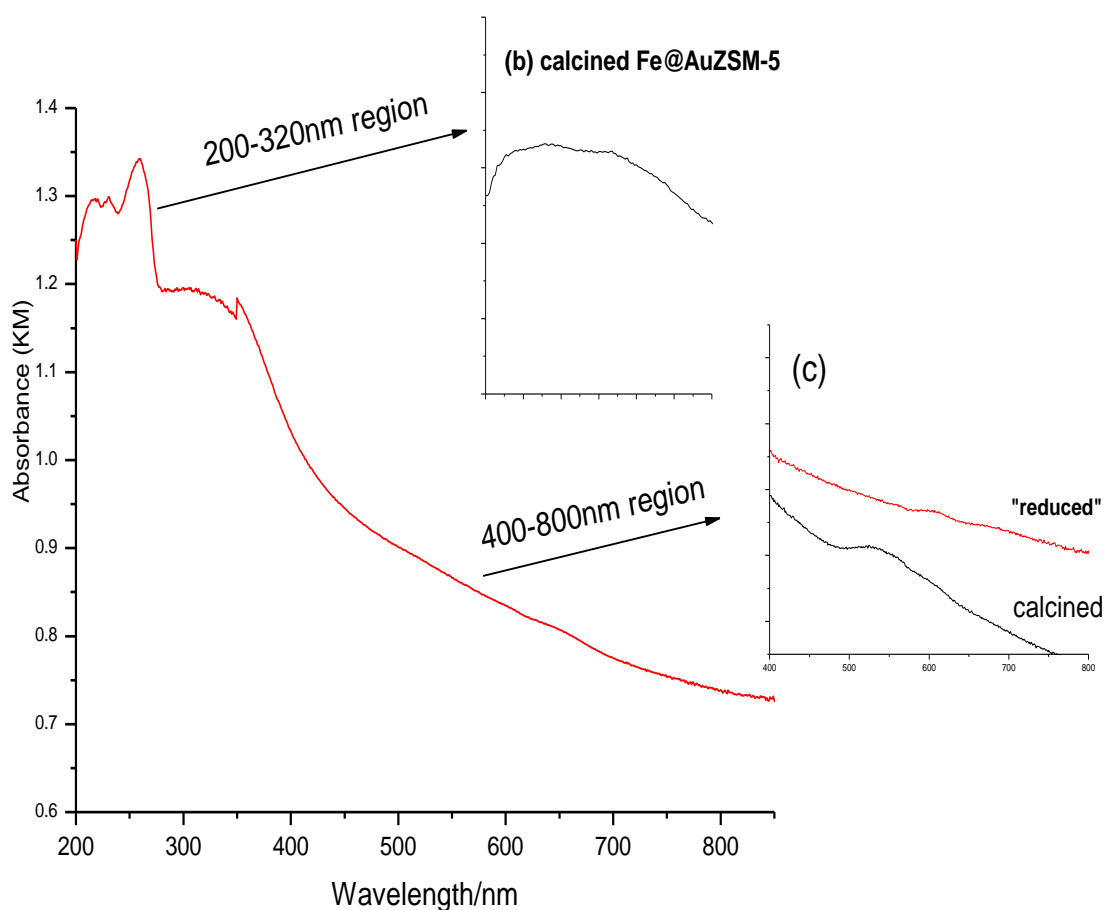
Figure 4.5 UV-VIS spectra of the "reduced" 2.5wt% Fe@2.5wt% Au/ZSM-5(30)$_{CVI@IMP}$ catalyst and (b) 200-230nm region for the analogous calcined material showing very unresolved peaks from Fe^{3+} and (c) the 400-800nm region for both calcined and "reduced" versions of the catalyst showing a distinct Au Plasmon peak in the calcined catalyst.

The small features at 610 and 681nm as are present in all calcined or reduced ZSM-5 materials. In the case of the calcined bimetallic Fe@Au catalyst there is a

prominent peak *ca.* 527nm which may tentatively be assigned to metallic gold species due to the presence of surface Plasmon peak (500-600 nm) and after the work of Zhao[28] and Sobczak. [27] Since both samples contain 2.53wt% Au, as determined by ICP analysis, one can propose that the Au is not predominantly on the zeolite surface as small nanoparticles when the material is heat treated in H_2/Ar. It is also possible that an alloyed Fe-Au nanoparticle structure exists on the catalyst surface or within the zeolite channels.

XPS analysis of these samples was also useful in that differences in the Fe signals were observed for the calcined and reduced materials. The Fe 2p shell in the reduced Fe@Au material has a markedly different binding energy as opposed to the Fe 2p shell in the calcined sample. As is the case with the monometallic calcined Fe/ZSM-5(30) the binding energy of the latter is *ca.* 711.4eV with the usual satellite at 719eV indicating Fe $^{3+}$ as iron oxides (Figure 4.6 b).

For the reduced material (Figure 4.6 a) , however, the Fe 2p peak at 712.4eV is similar to Fe^{3+} in minerals such as andradite ($Ca_3Fe_2(SiO_4)_3$) or possibly as very small Fe^{3+} clusters. The latter was indicated by UV-VIS and since there is no calcium in these samples it is improbable that such a mineral has been formed. However, Al has also been known to form similar sorts of mineral structures to andradite in combination with Fe and Si. There is also the strong possibility of surface Fe-Au alloy particles[h]. It should also be noted that the very broad feature in Figure 4.6(b) between 730-735 eV and the inflection point on main peak at 711.4eV (slightly visible) may indicate that some Fe^{2+} is present at the surface or near surface regions of this material.

---

[h] Work on other CVI@IMP/SI hybrid bimetallic samples using TiO_2 support showed that the metal deposited by CVI forms a shell over small Au particles to produce a core shell structure.
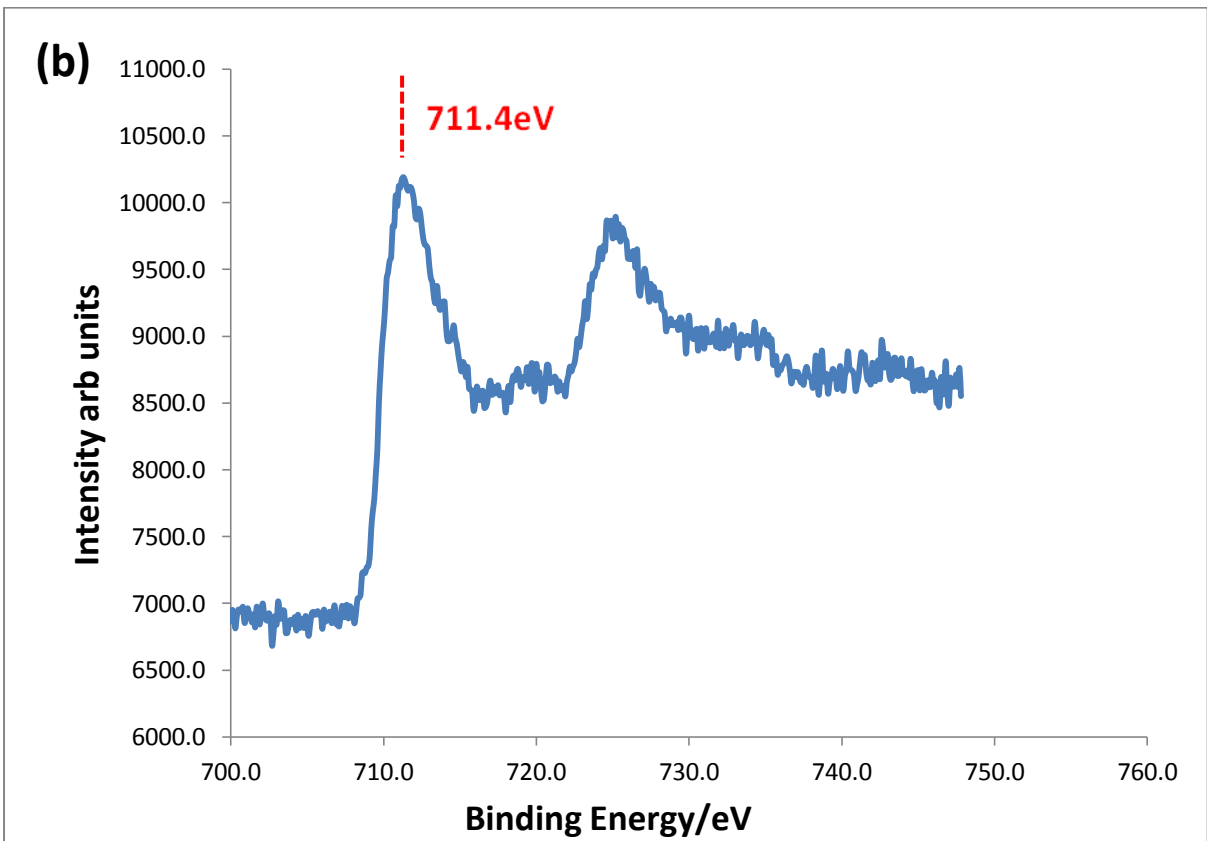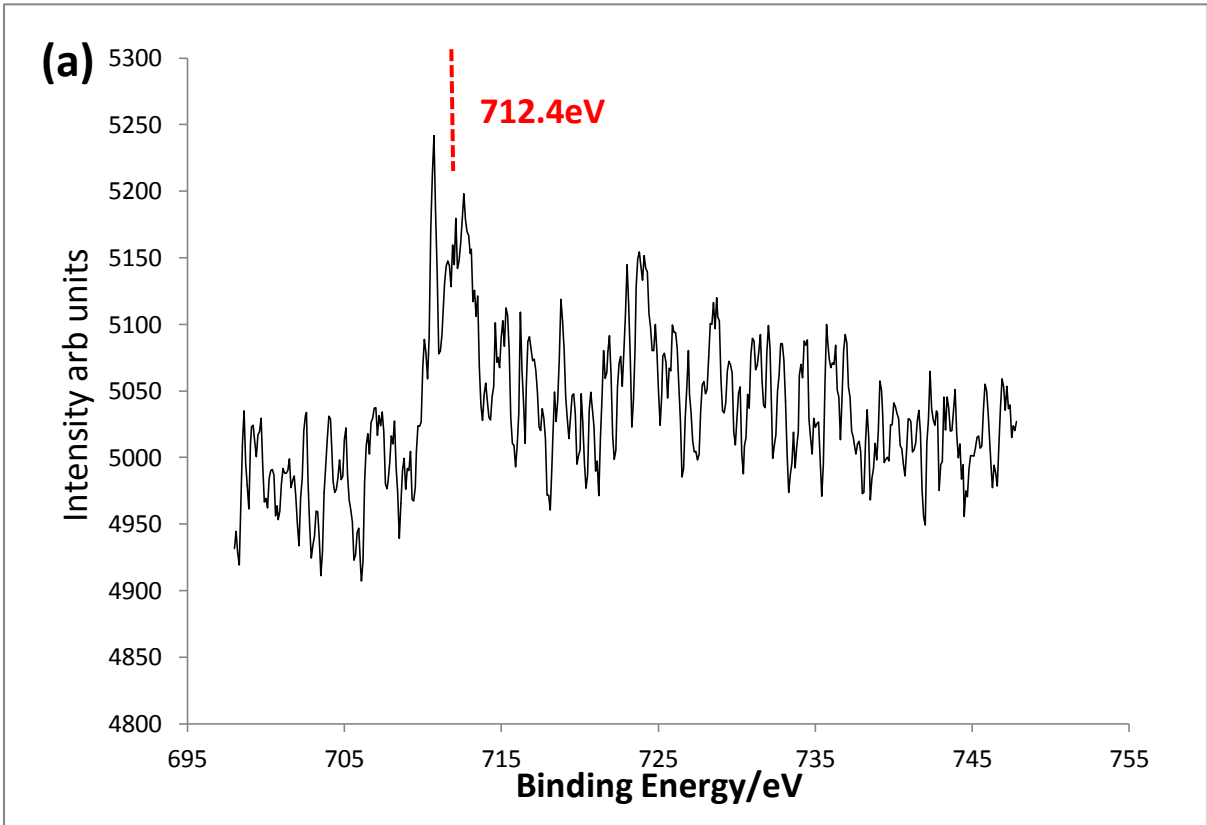
Figure 4.6 XPS spectra of (a) Fe (2p) in reduced 2.5wt% Fe@Au/ZSM-5 (30) and (b) Fe (2p) in calcined 2.5wt% Fe@Au/ZSM-5 (30).

Importantly, the signal intensity for the reduced material is very much lower than for the calcined material indicating a lower concentration of surface Fe. This corroborates the UV-VIS data for the reduced Fe@Au catalyst which did not show any pronounced peaks associated with bulky surface iron oxides. In this entire sample set XPS revealed that Au was mostly metallic in nature (peak with binding energy 84.5 eV) with some contribution from Au^+.

These data suggest that the presence of Au does not have a profound effect <u>on its own</u> in the reaction mechanism as both calcined and reduced Fe@Au/ZSM-5(30) catalyst have presence of mostly metallic gold but showed a different product distributions. It is however clear that the iron in the reduced bimetallic catalyst has different structure to the calcined catalyst but bears similarity to the iron in the monometallic "reduced" Fe/ZSM-5(30) presented in Chapter 3. One cannot rule out that when Au is present a higher concentration of iron is found within the zeolite channels when treated in a reducing atmosphere, and so the concentration of the isolated iron clusters and small oxidic species may have simply increased leading to better productivity as compared to the "reduced" monometallic 2.5wt% Fe/ZSM-5 catalyst but similar methanol selectivity. This is a very plausible argument if we especially consider the UV-VIS results. There may also be a third explanation for the increased activity and maintenance of high methanol selectivity for the reduced bimetallic sample which invokes the presence of new hetero-nuclear mineral-like forms of iron or alloyed particles in this sample. Further studies are needed to evaluate this idea and detailed EXAFS/XANES studies may be very useful in this aspect.

4.4. Mechanistic Studies

4.4.1. Basic study of reaction parameters

Thorough assay of the activity of a number of mono and bimetallic iron containing ZSM-5 catalyst for methane oxidation using neat hydrogen peroxide has been presented in the preceding sections and Chapter 3. In order to gain deeper understanding into how the catalytic system worked (outside of idealised DFT calculations) further studies were carried out to investigate the effect of reaction parameters for Fe/ZSM-5 which shows the highest catalytic activity.

Firstly, time on line analysis was performed. In Figure 4.7 the plot is not a linear one due to the decreasing oxidant level as time proceeds, *i.e.* the initial rate cannot be maintained due to decreased hydrogen peroxide level. After 15 minutes of reaction about 50% of the initial hydrogen peroxide has been consumed and prolonging the reaction to 0.5 h results in a 80% use of hydrogen peroxide. It is interesting that a plateau region from 5-15 minutes exists which is unusual. The data was reproduced for different catalysts to be certain it was not an analytical issue or experimental error resulting in unexpected results and this prompted a test of the catalytic activity at the T= 0 min point, the time when stirring begins after heating to the required reaction temperature. The T=0 min test revealed that at the start of the reaction conversion was ~0.2% with selectivity to HCOOH and CO_2 being 68.4% and 20.8% respectively. The data for 2 min reaction is the same for T= 0 min point thus it is proposed that the reaction occurring with the diffusion of dissolved CH_4 into the zeolite pores or across the Fe/ZSM-5 surface is facile and it appears that desorption of the products is an issue. The time on line can be explained due to the following reasoning: the reaction occurs instantly in the presence of H_2O_2 , Fe/ZSM-5 and CH_4 and the

products initially formed need a specific time to desorb which is facilitated by stirring the reaction at T=0 min. As the reaction proceeds the active species need to be re-formed again (requiring interaction of Fe and H_2O_2), products are formed and do not desorb fast enough to maintain the reaction rate across 5-15 minutes. At this point the catalyst active sites are either functioning optimally (and allowing efficient desorption of products due to some other reactive species interacting with the active sites) or a second mechanism (in solution) is occurring which accounts for the constant gradual increase in observed products without any plateau. After 2h the amount of oxidant is very low and the catalyst "shuts down" for lack of oxidant.
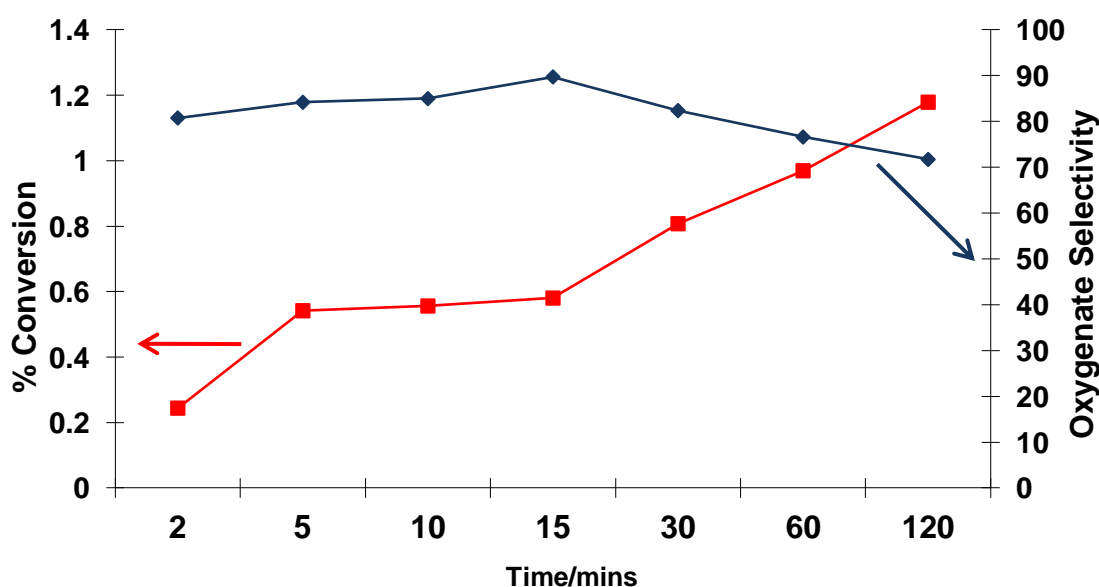

Figure 4.7 Time on line analysis for methane oxidation using 1.5wt% Fe/ZSM-5 (30) calcined at 400°C from an acetone washed sample.

Even at very low reaction time there is measurable conversion with the major product always being HCOOH and CO_2 selectivity increases with time. Within the 2h

156

reaction the H_2O_2 is consumed almost completely. It is interesting to note that after 6 h, 12h and 20 h, there is still oxidant left (at very similar levels) and the product amount continues to increase slowly with decreasing oxygenate selectivity to *ca.* 50% after 20 h. This may suggest that hydroperoxy (Fe-OOH) and –O species (Fe^{4+}=O, surface bound oxygen containing radicals) remain on the catalyst and are not utilised hence in long reaction times the catalysis continues with no real decrease in oxidant level or that some other reactive oxygen species is involved, namely O_2 made from decomposition of H_2O_2 on the Fe surface. It is important to note that at no point in this reaction is methyl hydroperoxide a major reaction product, even for catalyst with very low loading of Fe deposited by CVI, which is in contrast to the parent ZSM-5(30) catalyst.

Following this study the kinetic parameters for the reaction of Fe/ZSM-5(30)$_{CVI}$ and CH_4 in the presence of H_2O_2 is shown in Figure 4.8. The reaction depends on temperature, concentration of substrates and oxidant. In Figure 4.8 (a) we observe the increasing productivity with coincident decrease in selectivity at higher reaction temperatures. Above 50 ^{o}C the catalyst is much more active but there is a drastic drop in oxygenate selectivity (oxygenate productivity is increased by a factor of 50% at 70°C but selectivity to oxygenates is below 50%). This may be due to the faster decomposition of hydrogen peroxide at higher temperatures leading to unselective radical reactions.
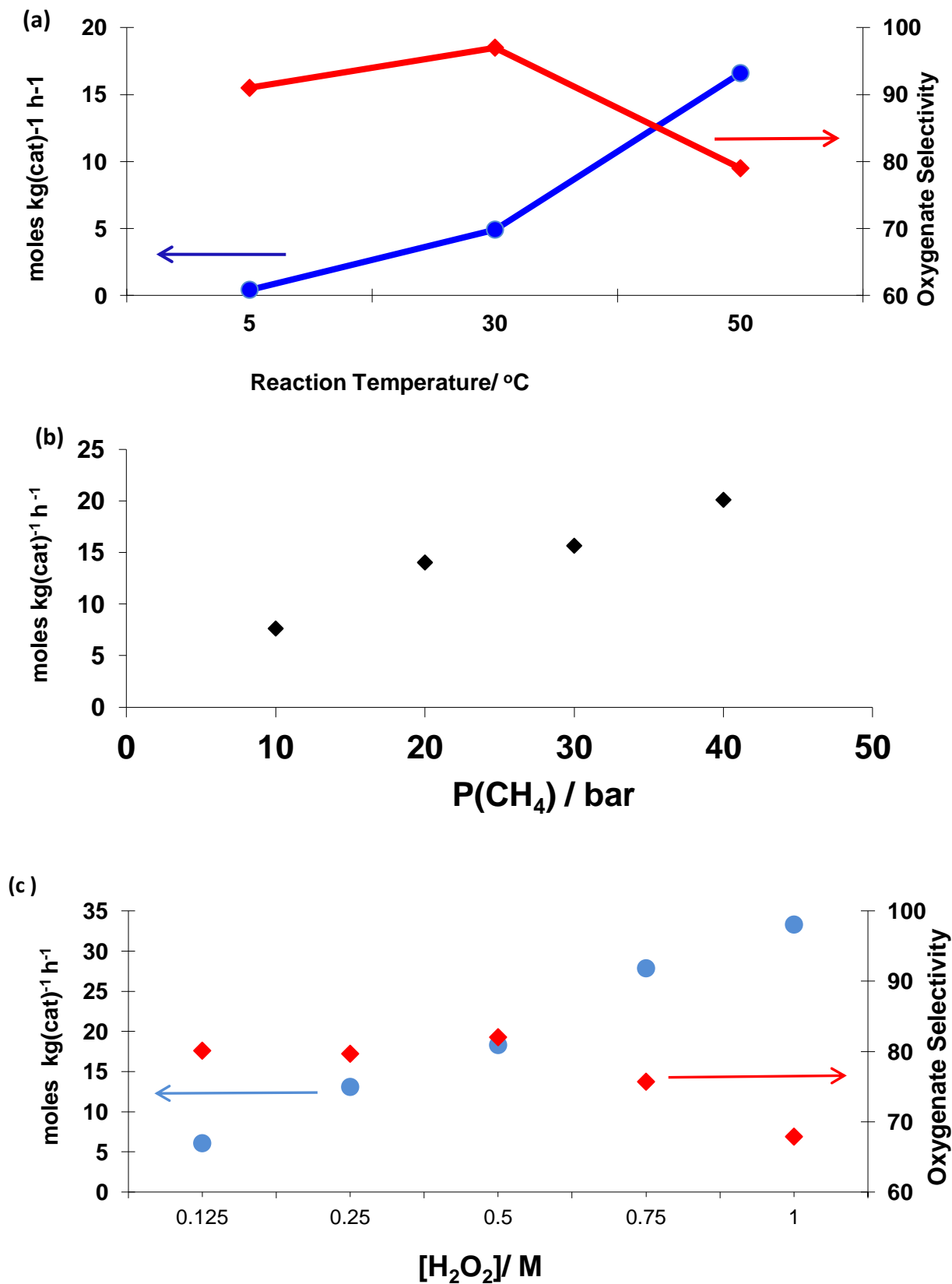
Figure 4.8 a) Effect of temperature, (b) effect of initial methane pressure, (c) effect of oxidant concentration for methane oxidation with Fe/ZSM-5(30)$_{CVI}$ under standard conditions

The reaction is first order with respect to CH_4 as shown in the characteristic first order plot obtained in Figure 4.8 (b) when the initial pressure of methane was varied in the reaction supporting the hypothesis that methane is involved in the rate determining step (s) of the reaction. It should be noted that this data applies only to methane pressure above 5 bar and H_2O_2 above 0.0625 M. If the hydrogen peroxide level is below this value no dependence on methane pressure is observed as the catalysis overall rate is very slow. Below 5 bars of methane there is not enough dissolved methane to give a meaningful rate under standard conditions for catalysts with high iron loading though under "high conversion conditions" this is not the case due to the higher solvent amount (20ml vs. 10ml) and higher oxidant level (1.0M versus 0.5M).

The reaction also appears to be first order with respect to hydrogen peroxide concentration within the range evaluated as shown by the characteristic linear plot in Figure 4.8 (c). This is to be expected as the activity of the catalyst must be related to the amount of oxidant present to interact and produce the active oxygen species. As the oxidant level is increasing the selectivity to oxygenates is decreasing indicating that the propensity for over-oxidation of the products to CO_x is linked to the concentration of hydrogen peroxide. It will be shown that the Fe/ZSM-5 catalyst produce hydroxyl radicals from hydrogen peroxide which are implicated in the oxidation of methanol to formic acid and CO_x.

4.4.2. Stability of products

In an effort to shed light on the reaction pathway the stability of the reaction products were studied using Fe and Cu/ZSM-5 samples. The CVI catalysts were studied using similar amounts of substrate (250 μmoles of methanol/ formaldehyde/formic cid in 10ml water) added to the reaction media in the absence of CH_4. Each substrate in aqueous solution was added to 27 mg of catalyst and then hydrogen peroxide introduced (0.5 M). The reaction was performed under nitrogen atmosphere at 50 ^{o}C for 0.5 h and analysed in the usual way.

$^{13}CH_3OH$ stability was used in the methanol stability study shown in Figure 4.9(a). $^{13}CH_3OH$ was oxidised to $^{13}CHOOH$ and CO_2 in all cases. Comparison of the Fe and Cu catalyst confirmed that methanol stability was improved over the Cu catalyst but notably the carbon balance was poor. The "unaccounted product" is thought to be absorbed on the catalyst. Note that in the presence of CH_4, high amounts of CH_3OH (> 600 μmoles in 10 ml) in the starting reaction medium deactivates the Fe catalyst completely. This may be due to strong adsorption of methoxy species blocking the active sites.

The same trend of oxidation and significant absorption occurs with CH_2O and HCOOH, Figure 4.9 (b) and (c). It appears that the stability follows the trend HCOOH<CH_3OH<CH_2O for both Fe and Cu catalysts. The absorbed/undetected substrate is similar for each substrate on a particular catalyst with the Cu/ZSM-5 showing higher absorption of products. The question arises as to whether or not the lower productivity and lack of HCOOH for the Cu/ZSM-5 data (when used to oxidise methane) is due to absorption of products. It is also interesting that the Cu/ZSM-5
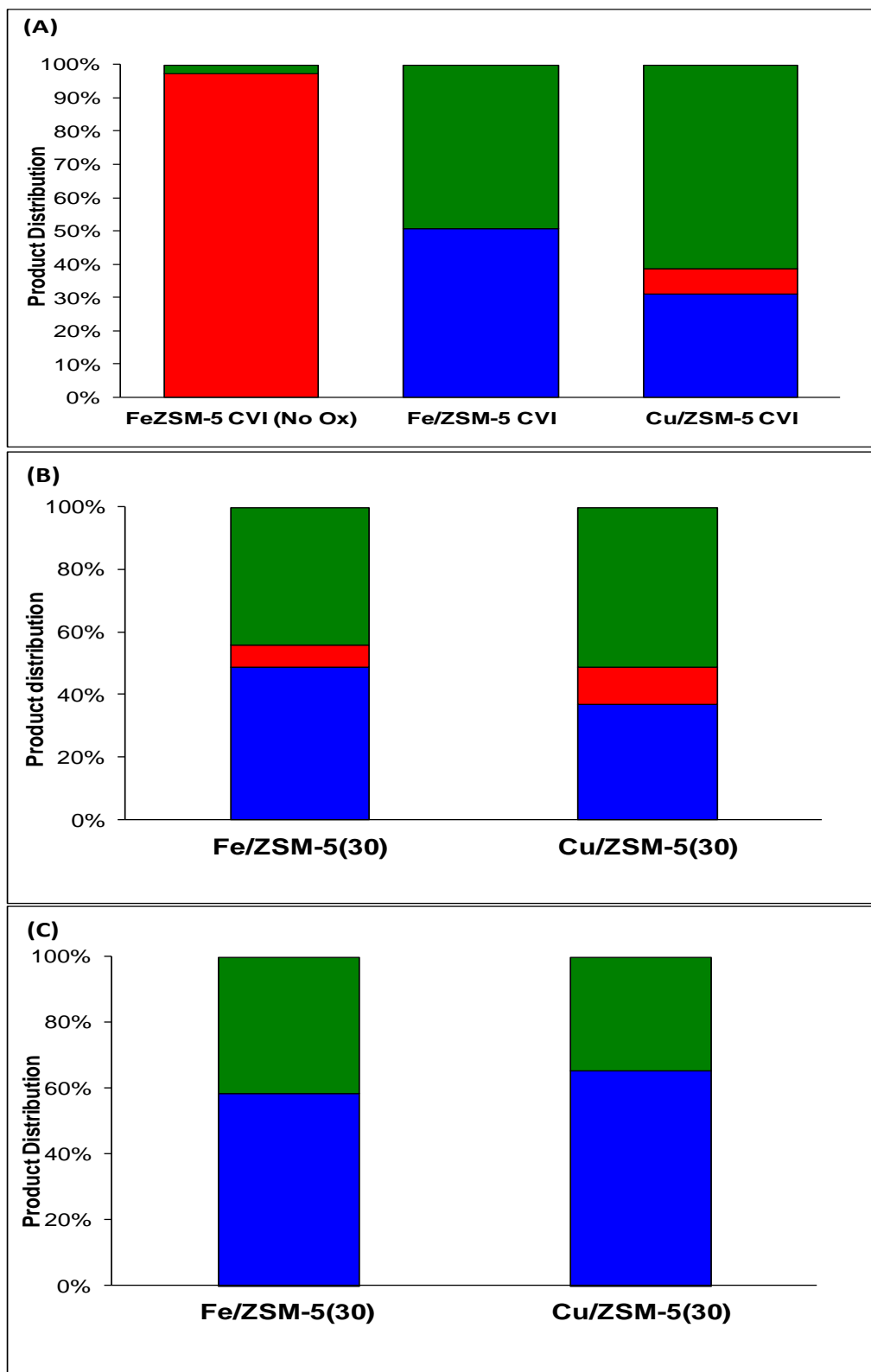
Figure 4.9 Stability of (A) $^{13}CH_3OH(aq)$, (B) $CH_2O(aq)$, (C) HCOOH (aq) under general reaction conditions with the addition of Fe and Cu catalysts. Red- unconverted substrate, green- substrate unaccounted for, blue- converted substrate. In (A) the first data set was generated without the addition of oxidant and labelled Fe/ZSM-5(30) (No Ox.) All catalysts were calcined and tested under the same conditions.

catalyst decomposed CH_3OH or CH_2O to HCOOH and CO_2 but HCOOH is not observed when an actual reaction is performed with this catalyst. Based on stability studies the following can be proposed:

$$CH_3OH \rightarrow CH_2O \rightarrow HCOOH + CO_2$$
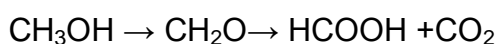
and we will discuss in the following data that second pathway (not involving H_2O_2 directly) to the deeper oxidation products may be in operation.

At this point one must also consider the stability of CH_3OOH. Its stability could not be studied in the same manner as the other products as it can only be produced in relatively low amount (< 60μmole per 10ml using either a nanoparticulate copper oxide catalyst of high temperature auto-oxidation of methane with hydrogen peroxide in the absence of catalyst) and when the stability reaction was attempted (*i.e.* reaction of CH_3OOH in the presence of an Fe doped catalyst and hydrogen peroxide under N_2 atmosphere at 50 ^{o}C , 0.5h) neither substrate nor products were observed. This is thought to be due to the absorption of CH_3OOH on the Fe/ZSM-5 catalyst surface. However in the case of Cu supported on other oxides such as TiO_2 and not ZSM-5 it was observed that CH_3OOH was selectively decomposed to methanol under reaction conditions along with the formation of CO_2. Fe on amorphous supports decomposed CH_3OOH primarily to HCOOH and CO_2. Also, solutions containing CH_3OOH when left in an NMR tube without catalyst at room temperature decomposition afforded CO_2 /O_2 as evidenced by pressure build up in the tube and lack of liquid phase products after 3-4 days. This is due to thermal decomposition. These data suggest that only Cu leads to the selective reduction of CH_3OOH to

CH$_3$OH under reaction conditions[i] and thermal decomposition of CH$_3$OOH is **mainly responsible** for CO$_2$ formation. In the absence of a catalyst, CH$_3$OOH can 'turn over' methane to increase the concentration of CH$_3$OOH as shown in entry 1 Table 4.4. The reaction is thought to be a radical process involving the remaining H$_2$O$_2$ in the reaction mixture. This also clearly demonstrates that the presence of a catalyst is necessary for the selective decomposition of CH$_3$OOH to CH$_3$OH (a reduction process) and importantly in the oxidation of methane with hydrogen peroxide the initially formed product, CH$_3$OOH, may catalyse further oxidation of methane to CH$_3$OOH without participation of the catalyst in solution, a possible radical process.

Table 4.4 Reaction of CH$_3$OOH in the presence of HNO$_3$, CH$_4$ and H$_2$O$_2$ but in the absence of a catalyst. CH$_3$OOH was synthesised using CuO or by autooxidation[j] of CH$_4$ with H$_2$O$_2$ prior to use for these tests.

Entry	Additive		Products/ μmoles					Increment (%)
			CH$_3$OH[a]	CH$_3$OOH [a]	HCOOH [a]	CO$_2$ in gas[b]	Total	
1		Initial	0.76	16.42	0	-	17.18	
	-	After	0.94	33.83	0	8.76	43.53	60
2	0.24 M	Initial	0.48	11.65	0	-	12.13	
	HNO$_3$	After	10.74	23.05	15.1	0.37	49.26	75

Reaction conditions- P$_{CH4}$:30 bar. [H$_2$O$_2$]: 0.5M, 1500rpm, Reaction temperature: 50°C, Reaction Time: 20 min, [a] Analysis using ^{1}H-NMR, [b] Analysis using GC-FID.

---

[i] Au has also been reported to have this effect by H. Moh'd Ab Rahim.
[j] At 90°C CH$_4$+ H$_2$O$_2$ under the typical reaction conditions produces CO$_2$+ CH$_3$OOH and very low amounts of CH$_3$OH. Cu$_2$O/CuO can also be used to obtain CH$_3$OOH in good yield and without significant Cu leaching.

In the presence of acid (pH 3-4) however CH_3OH and $HCOOH$ can be formed from this reaction (without catalyst) and even higher increases in products than for the less acidic reaction is observed (note commercial H_2O_2 solutions are acidic themselves pH~5). This is a well known process according to the following pathway[29]

$$ROOH + H^+ \rightarrow ROH + R=O \quad Eq. \ 4.1$$
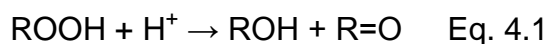
These data were confirmed using $^{13}CH_4$ and shows the remarkably ability of the alkyl hydroperoxy species to catalyse methane oxidation and be transformed into other products. Therefore under strongly acid aqueous conditions the primary product can be decomposed to CH_3OH and CH_2O and in the case of ZSM-5 which is an acid catalyst this applies. Under acid conditions (Table 4.4 entry 2) formic acid is formed as an additional product. In the absence of a solid or metal based homogeneous catalyst this finding is unexpected since methanol is <u>not oxidised</u> to formic acid at these temperatures in the presence of H_2O_2 but absence of catalyst. Hence it is proposed that CH_3OOH itself is participating in a radical process for both the oxidation of methane and decomposition to formic acid in low pH aqueous media (N.B. final pH of usual reaction mixtures is pH 3-4).

4.4.3. Fenton's Chemistry and the effect of additives

One of the main challenges in using the Fe/ZSM-5 catalyst is the ability to demonstrate that the mechanism is substantially different from other previously studied systems and indeed novel. It was proposed early on in the project that leaching may be occurring and the activity observed is due to homogeneous chemistry. This hypothesis was explored in Chapter 3, where it was shown that the catalyst was reusable and the reaction filtrate had very little activity for methane oxidation. This is not surprising considering the report of excellent stability of Fe/ZSM-5 in a H_2O_2 decomposition study (i.e. Fe/ZSM-5 as a Fenton's agent). [30] In that work it was reported that Fe was stable under the reaction conditions, had relatively low H_2O_2 decomposition ability and ethanol was stable over the catalyst. This was due to the low reaction temperature used (35 ^{o}C).

Methane oxidation by the aqueous nitrates of Al^{3+}, Cu^{2+} and Fe^{3+} was studied (Table 4.5) to probe the potential for Fenton's like chemistry in our reaction. As shown, all metals had activity for CH_4 oxidation. Al^{3+} and Cu^{2+} were selective in forming CH_3OOH and CH_3OH respectively (entry 1, 2, Table 4.5). Considering the data presented in the previous sections this is in line with the observation of selectivity differences due to Cu^{2+} in ZSM-5 and shows that in general Cu^{2+} operates by a modified route to produce methanol selectively from methane Al^{3+}, as a Lewis acid , can also perform the oxidation albeit low levels of products were detected.

The ability of a variety of metal chlorides to oxidise methane using hydrogen peroxide has been extensively studied. [31,32] Depending on the solvent and actual conditions used methyl hydroperoxide, methanol, formaldehyde or formic acid is observed. In general it was observed that Fe^{3+} as a catalyst results in poor oxygenate selectivity but other metals may have much better activity and selectivity to oxygenates and especially methanol (See Table 1.3 in Chapter 1 for examples). This is supported by the data in Table 4.5 since in entry 3 for Fe^{3+} (aq) the overall TOF is much higher (11.3 h^{-1} versus 1.5 h^{-1} for Cu^{2+} in entry 2) but the oxygenate selectivity is only 53%.

Table 4.5 Homogenous catalysed methane oxidation with various metal nitrates.

Entry	Catalyst	Product amount (µmol)				TOF [c] / h^{-1}	Oxygenate Selectivity [d]
		CH_3OOH[a]	CH_3OH [a]	HCOOH[a]	CO_2 in gas[b]		
1	Al^{3+} (aq) 20µmol	**3.6**	**1.4**	**0**	**0.35**	0.5	92
2	Cu^{2+} (aq) 20µmol	1.4	12.6	0	0.79	1.5	95
3	Fe^{3+} (aq) 11µmol	11.4	4.2	17.4	29.3	11.3	53
4*	Fe^{3+} (aq) 5.2µmol, acidified	10.0	4.4 (7.3)¥	40.3	18.5	31	77

Reaction conditions- Reaction Time: 0.5h; Reaction temp: 50^oC, Solvent: H_2O: 10 mL; 5000µmoles H_2O_2; P (CH_4): 30b; 27mg catalyst. [a] aqueous phase analysed using ^{1}HNMR; [b] gas phase analysed using GC-FID, [c] Total moles of products/ mol Fe x time(h); [d] (CH_3OH +CH_3OOH+CH_2O+ HCOOH)/ (CH_3OH+CH_3OOH+CH_2O+ HCOOH +CO_2) X 100 . * Reaction mixture acidified with HNO_3 (aq) to pH 3 and Fe loading is equivalent to that in 27mg of a 1.1% FeZSM-5(30) catalyst. ¥ CH_2O was detected for this reaction only in the value amount given in ( ).

It is reported that the Fenton's system is positively affected by lowering pH. [34,35] In the Fe/ZSM-5 catalysed reaction the final pH of the reaction mixture is pH 3-4 and thus the homogeneous reaction of Fe^{3+} was studied under acidified conditions. The

choice of acid was nitric acid as the metal salt used was a nitrate. In entry 4 Table 4.5, lowering the pH resulted in higher activity (*ca.* 33% increase in total products) and better oxygenate selectivity (77% versus 53% for the non-acidified reaction). This is not related to the effect of metal concentration on hydrogen peroxide usage as in both cases about 50-60% of the hydrogen peroxide is used in the reaction. It is important that the reader understands that in general Fenton's type chemistry does not solely operate by the formation of •OH radicals (which cause –H abstraction from CH_4) and is very dependant on the ratio of Fe/H_2O_2, oxidation state of the Fe, presence of dissolved O_2 and pH of the media. [29,33-37]

In most cases, homogeneous Fenton's type reactions result in the alkyl hydroperoxide, alcohol and ketone/ aldehyde as the main product especially under oxygenated conditions and at low pH. This is supported by the data in Table 4.5 entry 4 and Figure 4.10 a, b. In the former there is moderate overall oxygenate selectivity with HCOOH as the main product. Under these conditions CH_3OOH is also observed which is in agreement with a vast amount of literature suggesting Fe^{3+} (and others) can oxidise alkanes to the corresponding alkyl hydroperoxides. The level of Fe is important and its oxidation state. To investigate this homogeneous Fe solutions (from chloride and nitrate sources) of varying concentration were used for methane oxidation with hydrogen peroxide. In both cases (Figure 4.10 a, b) using high amounts of Fe is ineffective as H_2O_2 is decomposed unselectively to water and oxygen. Fe^{2+} (aqueous $FeSO_4$) as the metal catalyst gives very high productivity but mostly CO_2. One can easily see that a simple system of very small amounts of Fe^{3+} (10-20ppm) under acidic conditions is highly effective for methane oxidation. TOF values of over 150 h^{-1} were achieved with 10 ppm $FeNO_3$ at pH 3-4 but the issue

with using this system is the eventual mineralisation of the metal which deactivates the catalyst.
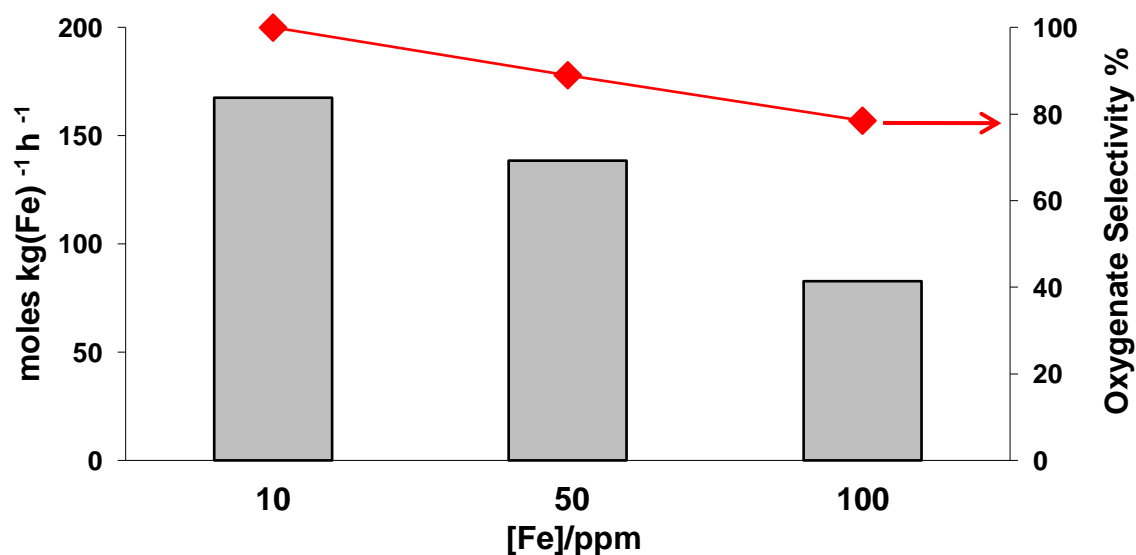
(a)
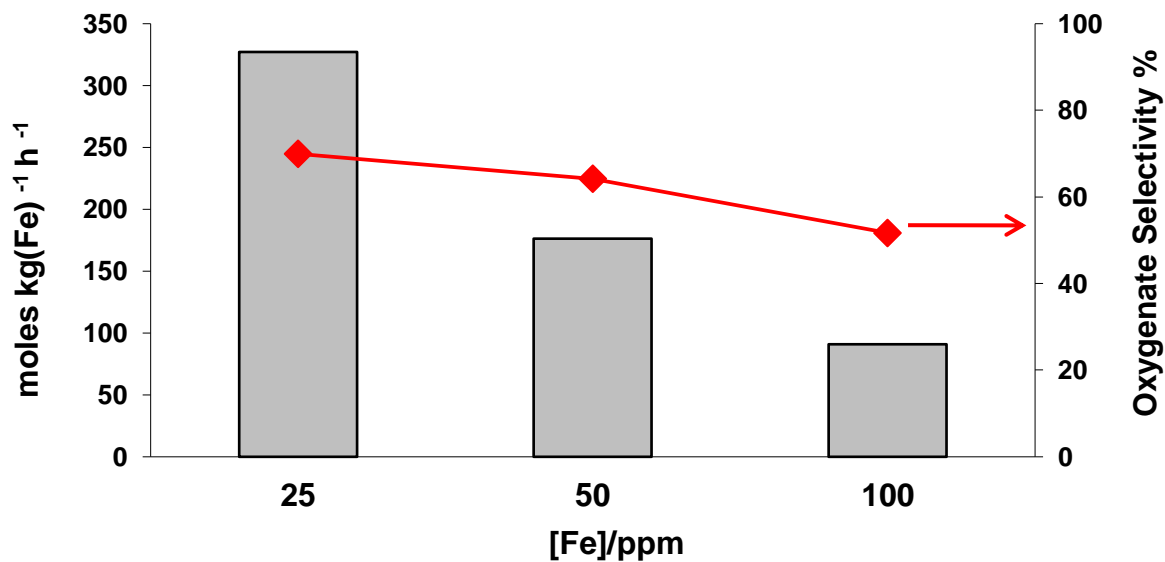
(b)

Figure 4.10 Effect of [Fe] for homogeneous methane oxidation with simple iron salts. (a) $FeCl_3$ (aq) and (b) $FeNO_3$ (aq). All tests conducted under standard conditions in acidic media (pH 3-4 adjusted with HNO_3). The H_2O_2 amount left after reaction decreases with the increasing Fe content.

It is also clear by comparison of the activity of the 10 ppm $FeNO_3$ solution (Figure 4.10b) with ZSM-5(30) containing trace impurities of Fe (150-200ppm) the latter is orders of magnitude more productive in terms of TOF defined as moles (product) mole $(Fe)^{-1}$ h^{-1} (~150 versus >2200 respectively) though both have very high oxygenate selectivity. Increasing the iron level in the ZSM-5 system results in grossly lower TOF as compared to the parent zeolite (~189 h^{-1} for a 0.4wt% Fe catalyst tested under standard conditions). The parent ZSM-5 material with trace impurities cannot achieve the high amounts of products in short reaction time under similar conditions and thus it is important to deposit additional Fe onto ZSM-5 to increase the productivity based on mass of catalyst for a more viable reaction.

The main point of this work was to probe the Fenton's system so as to obtain some information on its potential for methane oxidation before studying the effect of radical scavengers by adding inorganic additives to the reaction mixture. The role of •OH in over-oxidation was proposed but not proven for the ZSM-5 system. Sodium sulphite was chosen as an inorganic •OH scavenger (sulphite anion to sulphite radical to sulphate transformation) for this study. [38-40] Benzoic acid was also used in a similar manner and produced the same results in the following discussion[k].

The results of introducing radical scavengers into the reaction mixture are given in Table 4.6. Firstly the classical acidified Fenton's system with the same level of Fe as in the 1.1wt% Fe/ZSM-5(30) catalyst was affected by the presence of sulphite. Entries 1, 2 in Table 4.6 shows a four-fold decrease in the total products, two-fold increase in H_2O_2 left after reaction and much higher selectivity to oxygenates in the presence of a hydroxyl radical scavenger. In Fenton- type chemistry the following sequence of reactions is possible: When starting with an Fe^{3+} centre the initial

---

[k] Data not shown

interaction with H_2O_2 produces $[Fe-OOH]^{2+}$ (K = 0.002). This species reacts with the alkane directly or through another intermediate to give alkyl hydroperoxy species. Decomposition of $[Fe-OOH]^{2+}$ produces Fe^{2+} and $\cdot OOH$ ($0.0016s^{-1}$) . Fe^{2+} interacts with H_2O_2 to produce $\cdot OH$ ($68\ M^{-1}s^{-1}$) which then mediates the Fe^{2+} to Fe^{3+} reaction (slow) and also produces $\cdot OOH$ by interaction with H_2O_2 (very fast). In aqueous solution, $\cdot OOH$ is in equilibrium with $O_2^{\cdot -}$ and mediates the formation of O_2. Removal of $\cdot OH$ decreases the production of O_2 (using $\cdot OOH$) and the efficiency of the redox couple and may remove the –H abstraction from alkane step [25]. O_2 is pivotal to the propagation of alkyl radicals and the catalyst is "shut down". This results in lower amounts of products but higher selectivity as radical reactions leading to HCOOH and CO_2 is diminished. In the Fenton's type reaction data (entries 1, 2 Table 4.6) this is exactly what is observed.

With the Fe/ZSM-5(30) it is observed that the activity is decreased in the same manner as for the homogeneous system (entries 3 and 4 Table 4.6). It could be hypothesised that the sodium sulphite is merely reacting with H_2O_2 and decreasing the concentration of oxidant hence the reaction rate is retarded or that the sodium/sulphur species are poisoning the catalyst. The data in entry 4, Table 4.6 shows that in the absence of catalyst sodium sulphite does react with hydrogen peroxide and potentially utilises 30% of the oxidant in this way. If this is accounted for by comparison based on the probable level of hydrogen peroxide (*ca.* 0.35M) then there is still a decrease in the productivity (review of the data on effect of hydrogen peroxide concentration for this catalyst (Figure 4.8 c) shows productivity of around 15 whilst the entry 4 Table 4.6 has a productivity of around 10 moles oxygenates kg $(cat)^{-1}$ h^{-1}). Hence it is more than merely the effect of potentially lower

oxidant level. Furthermore, entry 6 Table 4.6 shows that Na^+ and SO_4^{2-} do not affect the reaction.

Table 4.6. Effect of additives (radical scavengers) on the oxidation of methane by Fe/ZSM-5(30) and Fe (aq)

Entry	Catalyst	Additive	Products				Total product (μmol)	H_2O_2 left (μmol) [c]
			CH_3OH[a]	CH_3OOH[a]	HCOOH[a]	CO_2 in gas[b]		
1	5.42 μmol FeNO$_3$ pH3-4	-	10.0	11.7	40.3	18.5	80.5	1875
2	5.42 μmol FeNO$_3$ pH3-4	Na$_2$SO$_3$ 0.1M	7.8	7.4	4.8	2.1	22.1	3142
3	1.1%Fe/ZSM-5	-	20.6 (25.4)	4.4 (0.5)	160.1 (176.0)	45.7 (40.5)	230.8 (242.40)	1207 (1048)
4	1.1%Fe/ZSM-5	Na$_2$SO$_3$ 0.1M	19.3	2.2	44.9	68.5	134.9	1780
5	-	Na$_2$SO$_3$ 0.1M	-	-	-	-	-	3390
6	1.1%Fe/ZSM-5	Na$_2$SO$_4$ 0.1M	23.4	0	144.6	64	232.0	1608
7	1.1%Fe/ZSM-5	Na$_2$SO$_3$ 0.05M	25.3	2.3	131.0	35.8	194.4	996

Reaction conditions- Reaction Time: 0.5h; Reaction temp: 50°C, Solvent: H_2O: 10 mL; 0.5M H_2O_2 ; P (CH$_4$): 30b; Solid catalyst: 27mg catalyst, Fe (aq) catalyst: 30ppm [a] aqueous phase analysed using ^{1}HNMR; [b] gas phase analysed using GC-FID. ( ) represents a second test of the same material in a different reactor.

At 0.1M sodium sulphite concentration the activity of the catalyst is halved and there is still a 16% decrease at low additive amounts (i.e. 0.05M entry 5 Table 4.6). Even more important than the decreasing activity is that only the production of HCOOH is affected significantly. One would expect that if this were merely a case of consecutive oxidation reactions mediated by •OH then removing this ROS[l] will result in similar productivity but higher selectivity to the primary products and not lower productivity. The reader should also bear in mind that (i)1/5th of the total reaction products for Fe/ZSM-5(30) are observed at T= 0 min , unlike ZSM-5(30), with HCOOH and CO_2 as the major products; (ii) for the Cu system in which selectivity to primary products is very high (i.e. no HCOOH is formed) the CO_2 selectivity cannot be tuned; (iii) for Fe^{3+} (aq) the CO_2 selectivity decreases greatly as •OH is removed.

Taking into account the above observations, it can be proposed that an alternate pathway (using Fe centres) to produce the deeper oxidation products exists and this pathway is responsible for a significant portion of the reaction products. The reader should take into account with the following information in support of this hypothesis, namely[m]: (i) in the CH_3OOH turn over experiment, Table 4.4, under non-acidic conditions no HCOOH is observed and EPR studies on this system showed high levels of •OH radicals during and at the end of the reaction; (ii) for the Au-Pd/TiO_2 system which does not produce HCOOH the major spin trapped radical observed is •OH by EPR with minor contributions from C based radicals and superoxide ($O_2^{.-}$).

These additional findings suggest that HCOOH is not necessarily a deep oxidation product linked solely to the production of •OH. A brief summary of work carried out

---

[l] ROS- Reactive Oxygen Species
[m] Work done my myself and not reported in this thesis

using EPR techniques will now be presented as the study of radicals *via* trapping techniques has afforded further insight into the reaction mechanism.

4.5. EPR studies and ^{18}O activation

The mechanistic data obtained by study of the reaction parameters, Fenton's chemistry and the effect of hydroxyl radical scavengers suggests that the Fe catalysed methane oxidation reaction involves radical species. Spectroscopic studies on Cu/ZSM-5(30) and "reduced" Fe containing systems also suggested that differences observed in product distribution, particularly higher methanol selectivity, was due to changes in the iron structures within the zeolite channels. Radical trapping and detection by EPR spectroscopy has been a valuable tool in identification and study of radicals in oxidation processes. This tool has been employed using the well known radical trap N,N'-dimethylpyrrolidine oxide (DMPO) which has distinguishable radical trap signals for methyl, hydroxyl, hydroperoxy and superoxo radicals.[41] As a "calibration" of the method used in these studies, the oxidation of methanol using an iron catalyst was studied after the work of Bosnjakovic & Schlick. [41] This was done to be certain that any radicals which may present in the Fe/ZSM-5(30) catalysed oxidation of methane could be observed with the available technique. In this classic system at low reaction times one observes all the expected radicals, *i.e.* •OH, •CH$_3$, •OOH/O$_2$•- , and at longer reaction times •OCH$_3$ was also observed by their spin trapped adducts with DMPO (Figure 4.11). Thus there is confidence that all the possible radical species may be detected in the trapping experiment under actual reaction conditions, bearing in mind that the DMPO-radical adduct may be trapped within the zeolite pores as well. The efficiency of trapping the proposed radicals depends on their concentration and lifetime but it is known that methyl radicals and hydroxyl radicals have similar probability of being trapped in aqueous solution. [42]
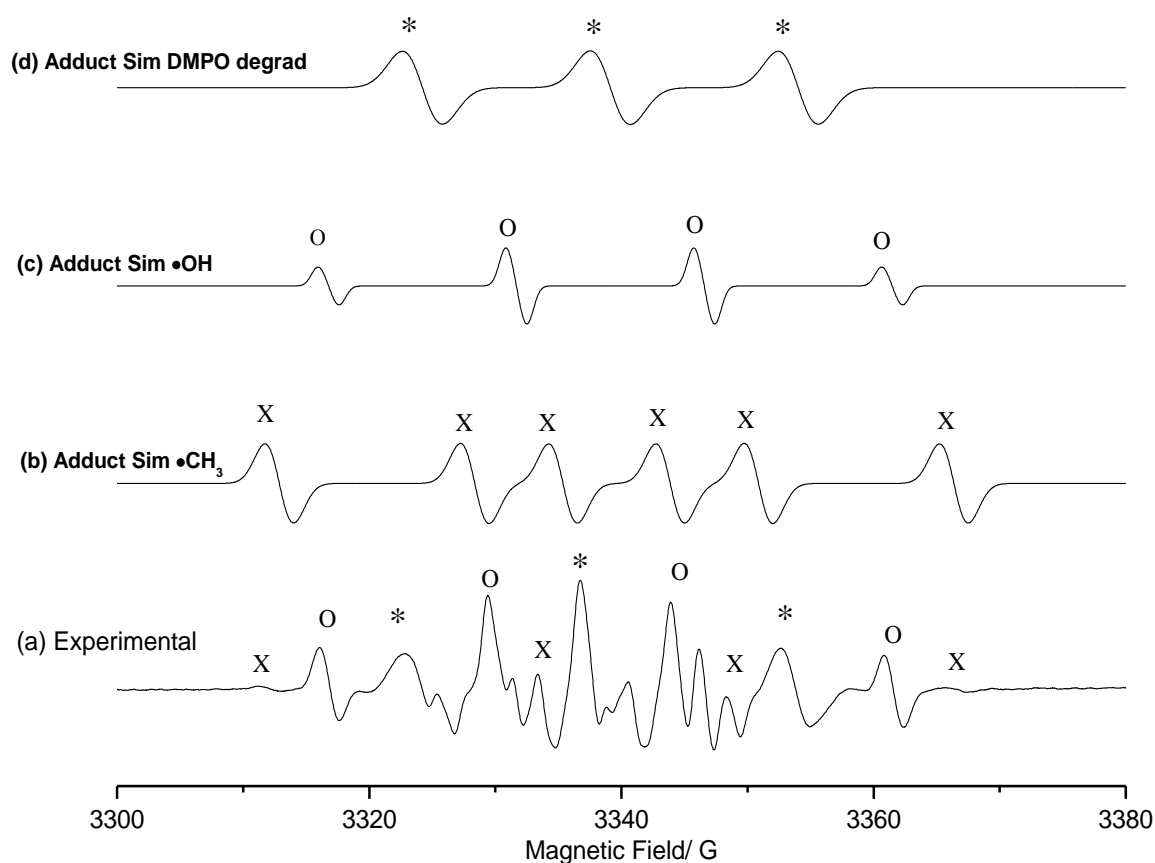
Figure 4.11 EPR spectrum of a homogeneous Fenton's oxidation of <u>**methanol**</u>. (a) The spectra obtained after 5 min reaction of $CH_3OH + H_2O_2 + Fe^{3+}$ (aq); (b) simulated spectrum of $\cdot CH_3$ adduct with DMPO; (c) simulated spectrum of $\cdot OH$ adduct with DMPO; (d) simulated spectrum of DMPO-O_x decomposition adducts. Contributions from $\cdot CH_3$, $\cdot OH$ are dominant and there is a minor contribution from $\cdot OOH/ O_2^{\cdot -}$ which is masked by the contribution of the degradation of DMPO. The appearance of DMPO-$CH_3O_x\cdot$ adduct is observed with longer reaction times (not shown). The only reaction products were HCOOH and CO_2 as observed by ^{1}H-NMR and GC-FID analysis.

Interestingly, when the same procedure was applied to the oxidation of CH_4 by Fe^{3+} (aq) in the presence of H_2O_2 there was a notable absence of $\cdot CH_3$ adduct but this is also the case with many biological systems where the methyl radical remains elusive due to very facile reactions with ROS or its low concentration in solution. Since

175

attempts to deconvolute the spectrum obtained in this experiment were unsuccessful this data is not herein presented.
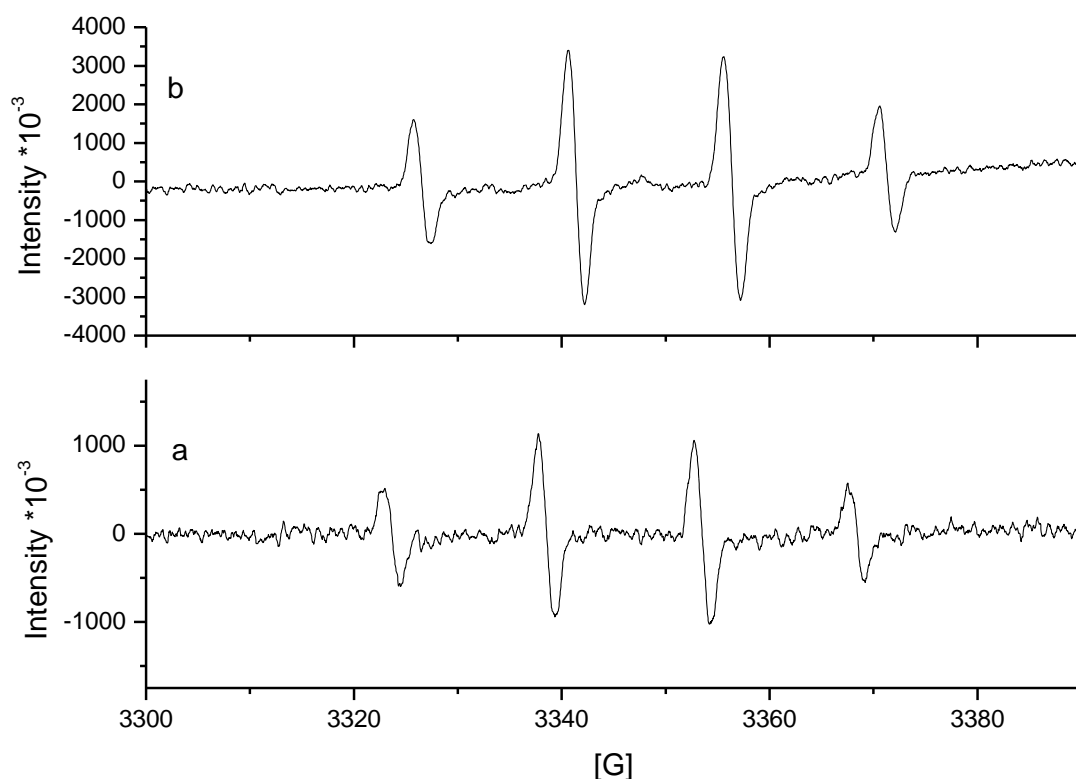

Figure 4.12 EPR spectrum of methane oxidation reaction catalysed by ZSM-5(30) (calcined; 550°C, 3h, static air) with H_2O_2. (a) spectrum obtained before the introduction of CH_4 in which only •OH adduct with DMPO is observed; (b) spectrum obtained after the addition on CH_4 in which •OH adduct with DMPO is observed and also some DMPO-Ox degradation adducts(minor). The reaction products were CH_3OOH, CH_3OH, $HCOOH$ (major) and CO_2. Reaction time was 5 minutes.

Both ZSM-5(30) and Fe/ZSM-5(30)$_{CVI}$ gave EPR spectra with only •OH observed at short or longer reaction times (Figure 4.12). This data suggested that the •CH_3 radical was not present in the reaction; however it has to be noted that in the classical Fe^{3+} (aq) catalysed reaction the methyl radical was not observed and in the case of a zeolite with small pores such as ZSM-5 it is possible that the spin trap

(DMPO) cannot diffuse into and out of the pores successfully. Also methyl radicals may be transiently present in very low concentration. Thus if we assume most of the catalysis is occurring inside the pores then absence of methyl radicals is not conclusive evidence of this species not being present during the reaction. However, qualitatively the intensity of the adduct signal for Fe/ZSM-5 is more intense than for ZSM-5. Also the intensity of the adduct signal increases when methane is present (Figure 4.12 (a) vs. (b)) indicating that [•OH] , the interaction of Fe with hydrogen peroxide and the onset of reaction with methane are linked to each other.
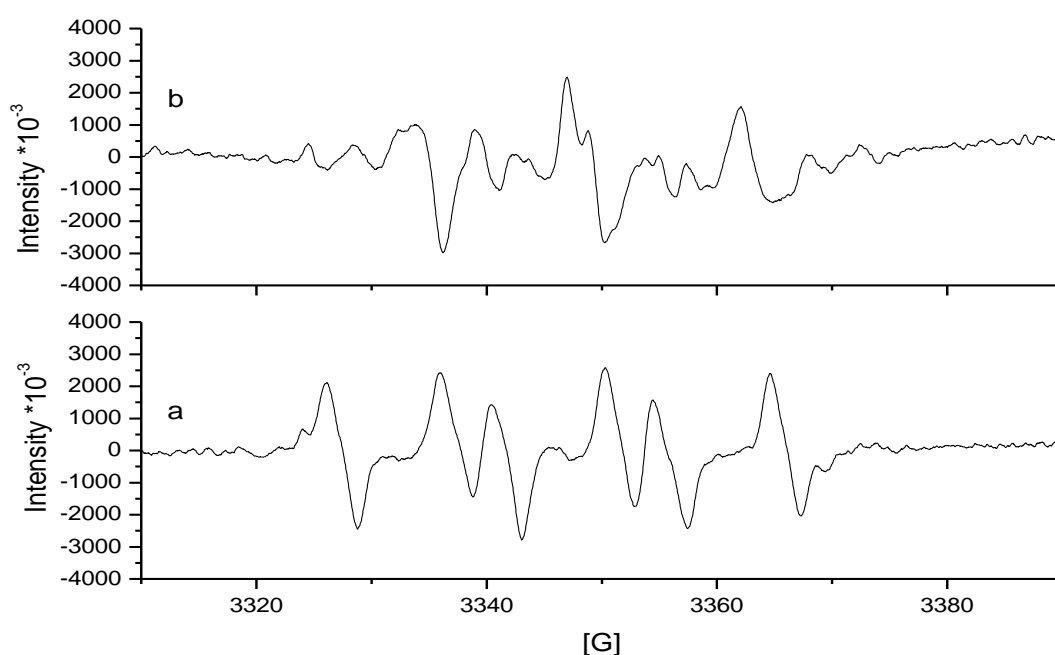
Figure 4.13 EPR spectrum of the methane oxidation reaction catalysed by Cu/ZSM-5(30) prepared by CVI (calcined; 550°C, 3h, static air) with H_2O_2. (a) spectrum obtained before the introduction of CH_4 in which $O_2^{\bullet-}$ adduct with DMPO is observed; (b) spectrum obtained after the addition on CH_4 in which O_2^- adduct with DMPO and also DMPO-Ox degradation adducts are observed. $O_2^{\bullet-}$ is the equilibrium product of •OOH. The reaction products were CH_3OH (major), CH_3OOH and CO_2. Reaction time was 5 minutes.

Furthermore, EPR radical trapping experiments using Cu/ZSM-5(30) in the presence of methane and hydrogen peroxide were performed. The spectra in Figure 4.13 a, b is very different from the case of ZSM-5(30) previously presented. For the Cu/ZSM-5(30)$_{CVI}$ the main species observed was $O_2^{\bullet-}$ and not $\bullet OH$ at the start of the experiment (Figure 4.13). This adduct is still present after 5 min reaction of the catalyst with methane in the presence of H_2O_2 (reaction product is CH_3OH and not HCOOH). At a first glance this can be used as good evidence that the production of HCOOH is linked to the production of $\bullet OH$ by the catalyst and provides a plausible explanation for the role of Cu. However Cu/ZSM-5 still has Fe as trace impurities (0.014wt %) in the parent zeolite channels/framework which gave an appreciable signal for $\bullet OH$ adducts in Figure 4.12.

 Where have the hydroxyl radicals gone if Fe in CuZSM-5(30) was responsible for the reaction?

It was proposed in discussion with colleagues that Cu ions may act as hydroxyl radical scavengers. To the best of my knowledge there is no literature to support this proposal. Explaining the effect of Cu in this way also does not account for the presence of superoxide species) $O_2^{\bullet-}$ in the reaction mixture for CuZSM-5(30)$_{CVI}$. It is known that Cu^{2+} does not efficiently react with H_2O_2 to perform Fenton's type chemistry and produce $\bullet OH$ but instead Cu-hydroperoxy complexes are formed. Degradation of $[Cu-OOH]^+$ could produce $\bullet OOH$ which is the hydrated from of $O_2^{\bullet-}$ ($K = 1.3 \times 10^{-5}$). $O_2^{\bullet-}$ is known to be a precursor to $\bullet OH$ in photochemical systems involving porphyrins and can result in generation of $\bullet OH$ by interaction with H_2O_2. The observation of a yellow colour to the usually blue Cu/ZSM-5 suggests that Cu-OOH species are being formed and this assumption is supported by the observation of superoxide ions in solution as shown in Figure 4.13. In the case of alkane

oxidation this system would have low rates due to the low concentration of ROS and the low reactivity of the ROS ($\cdot$OOH or $O_2^{\cdot-}$) formed. The observation of superoxide adducts suggests appreciable concentration of $\cdot$OOH since the equilibrium constant is very low). Also one must recall that the UV-VIS and EXAFS/XANES analyses of the Fe in Cu/ZSM-5(30)$_{CVI}$ revealed that the Fe^{3+} was in tetrahedral form (possibly as framework Fe or another species). If these iron species are not involved in the oxidation then one would expect that the $\cdot$OH would not be produced during the catalysis. An EPR study on homogeneous Cu^{2+} methane oxidation is merited here.

Discussion of the case of the addition of aqueous Cu^{2+} to the Fe/ZSM-5 catalysed reaction is also necessary since this system also "shut off" formic acid when a 1:1 ratio of Fe: Cu was used. Moreover, the combination of Fe and Cu metal in a heterogeneous catalyst also had this effect though UV-VIS analysis showed that iron was in the same forms as in calcined Fe/ZSM-5(30) and ZSM-5(30), unlike the case of Fe in Cu/ZSM-5(30).   The homogeneous Cu system was investigated so that correlation between the data in Figure 4.1 could be carried out but it should be noted that the calcined Fe-Cu/ZSM-5(30) heterogeneous catalyst gave the same EPR spectra as shown in Figure 4.14.

Interestingly the major radical species observed is $\cdot$OH with possible contribution from superoxide, though it is too low in intensity to be observed clearly in the experiment where homogeneous Cu^{2+} is added to the reaction mixture containing the heterogeneous Fe catalyst. Thus, in the system which is selective to CH_3OH hydroxyl radicals are still produced. This supports the previously mentioned hypothesis that "over-oxidation" of the primary product is not solely linked to hydroxyl radicals. However it was also observed that the intensity of the signal due to $\cdot$OH adducts did not increase as the reaction proceeded in contrast to ZSM-5(30). This

result may be explained by the competition of both metals for the oxidant rendering iron species incapable of producing more •OH as they perform the transformation of CH_3OOH (i.e. switching off the onward reaction of CH_3OOH at the iron site). Also in the selective reduction of CH_3OOH to CH_3OH by Cu^{2+}, •OH is not produced in contrast to the process mediated by iron sites.
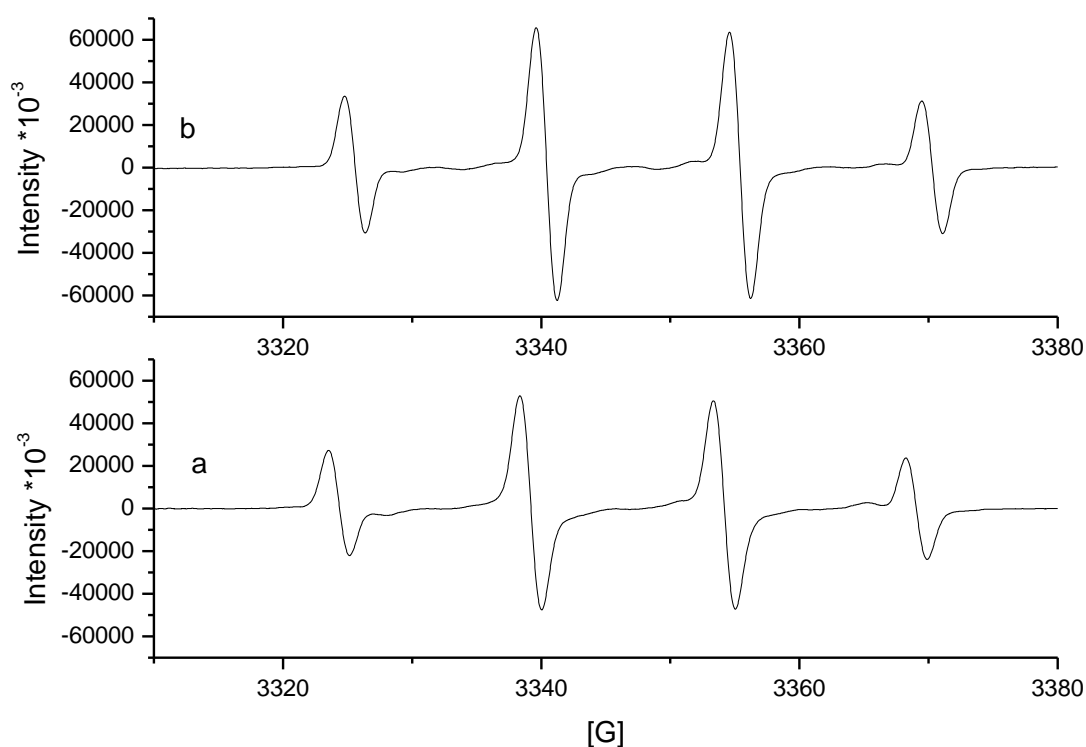
.

Figure 4.14 EPR spectrum of methane oxidation reaction catalysed by Fe/ZSM-5 (30) prepared by CVI (calcined; 550°C, 3h, static air) <u>**with addition**</u> of homogeneous $Cu(NO_3)_2$ (aq) and H_2O_2. (a) spectrum obtained before the introduction of CH_4 in which •OH adduct with DMPO ; (b) spectrum obtained after the addition on CH_4 in which •OH adduct with DMPO . The Cu^{2+} (aq): $Fe_{(catalyst)}$ ratio was 1:1. The reaction products were CH_3OOH, CH_3OH (major) and CO_2.

Summarising, one can only speculate further about the real role of Cu in the bimetallic catalyst at this stage. In the monometallic Cu/ZSM-5 system it is probable

that the Cu is active for oxidation showing lower activity than Fe, whilst in the bimetallic system both Fe and Cu may be working synergistically to produce CH_3OH. It is also highly possible that Cu merely absorbs HCOOH as a formate species on the catalyst surface based on the stability studies. This hypothesis cannot be verified by any spectroscopic data as formate species could not be detected on the surface of used Cu loaded catalysts when extraction methods were employed. This may be due to the very low concentration (µmoles in 27mg catalyst).

Finally towards the end of these studies using Fe and Cu zeolites experiments were performed using $^{18}O_2$ in an attempt to incorporate oxygen into the products. It is desirable to utilize molecular oxygen as the terminal oxidation in place of H_2O_2 due to its lower cost. This work was prompted by the observation of a promotion in the catalytic activity of an aged catalyst when O_2 (3-5%) was present in the gas mixture with CH_4 (95-97%). The data obtained in these oxygen activation studies were not reproducible and the effect was only observed with CVI catalysts under very specific conditions (5%-10% O_2/90%-955% CH_4, 50^oC, 0.5M H_2O_2). The lack of reproducibility may be explained by the fact that radical reactions can be very difficult to control. Moreover, the Fe doped zeolite catalyst produces O_2 though hydrogen peroxide decomposition during the reaction and this is linked to the iron loading as higher iron loading leads to higher peroxide decomposition rate. Thus it is proposed that more oxygen is available from the decomposition of hydrogen peroxide than is available from dissolution of gas phase oxygen into then aqueous solution, which results in a lack of reproducibility. This is also the case with Cu since superoxide radicals have facile reaction with Fe^{3+} to produce O_2. Another challenge is the higher solubility of oxygen to methane in water possibly resulting in lower levels of methane when oxygen was present.

However, very useful information was obtained by the analysis of products for the $^{18}O_2$ label experiments. Firstly Fe/ZSM-5(30) was used under standard conditions with a 96.5%:3.5% CH_4 : O_2 mixture at 30 bars. The reaction products were assayed using ^{1}H-NMR and also LC-MS. The products were methyl hydroperoxide, methanol and formic acid (major) and CO_2 (by GC-FID analysis). The reaction solution was infused into the LC-MS system and spectra were obtained in the EI$^-$ mode (electrospray ionisation negative mode). Formic acid could be observed as dimeric and trimeric species using this protocol. Dimers of formic acid were observed with incorporation of one ^{18}O per dimer, i.e. one labelled O out of 4 O per dimer in total. 6% incorporation of $^{18}O_2$ was estimated by integration of the peaks obtained from this analysis (Figure 4.15). In this reaction promotion of the catalytic activity was not observed but indications of incorporation of ^{18}O into the reaction products are observed. Unfortunately this method did not allow the analysis of methanol, a primary reaction product, and due to the low level of incorporation into HCOOH it was postulated that oxygen exchange reactions under these acidic conditions may account for the ^{18}O in formic acid. Furthermore, we could not analyse ^{18}O in CO_x (gas phase) which may arise from the oxidation of labelled HCOOH.

Incorporation of 18O into formic acid could be due to radical based Fenton's type chemistry thus it is important to evaluate if any incorporation into methanol or methyl hydroperoxide can occur. Such incorporation is envisaged by the oxidation of methanol by ^{18}O radical species which are formed by the interaction of alkyl and alkyl hydroperoxy radicals with dissolved oxygen in solution. To investigate further, the Fe-Cu/ZSM-5(30) bimetallic catalyst was used since it has high catalytic productivity and high selectivity to methanol. A modified extraction method was employed whereby the reaction mixture was mixed with toluene (10ml) following reaction and

the toluene phase removed and analysed by GC-MS. This method had the advantage of extracting significant amounts of both methanol and formic acid from water rendering a solution which could be analysed reproducibly using GC-MS.
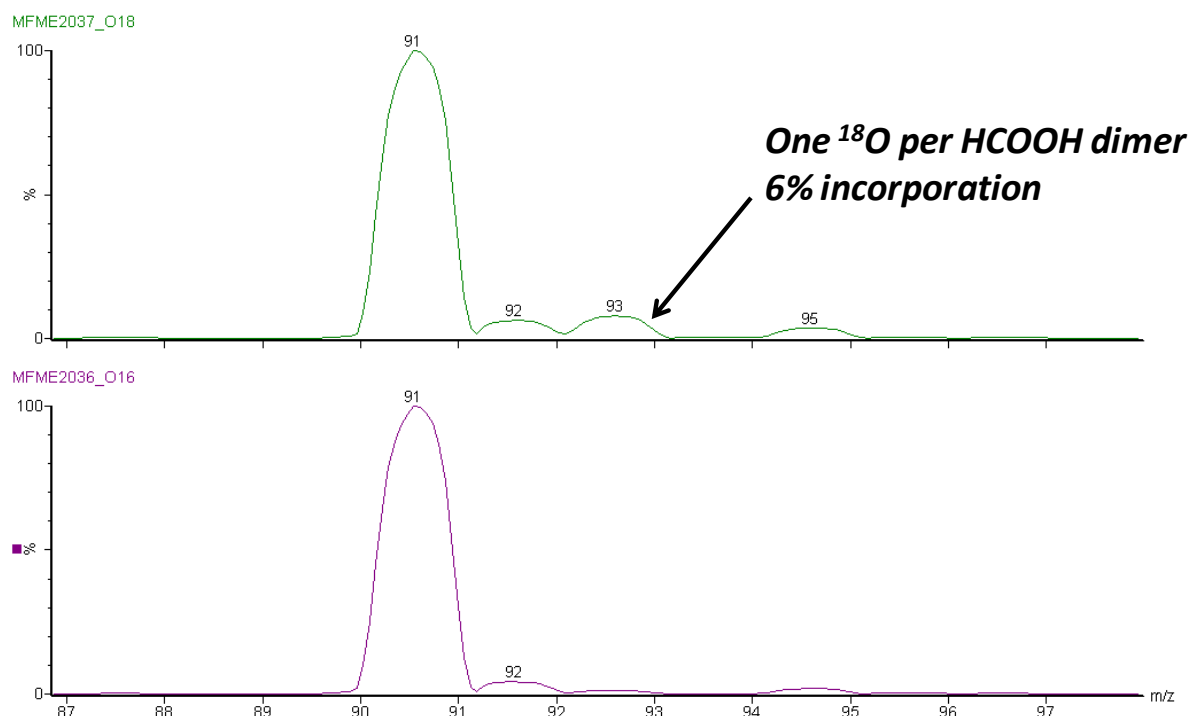

Figure 4.15 LC-MS spectra of a reaction mixture following the reaction of methane and hydrogen peroxide using a Fe/ZSM-5 catalyst and with $^{16}O_2$ (bottom) or $^{18}O_2$ in the gas phase mixture (top). 6% incorporation into formic acid is observed in the peak at 93 m/z in the top spectrum.

It was observed that ^{18}O was not incorporated into methanol (>150µmoles produced in the reaction (Figure 4.16(a)). Interestingly 50% ^{18}O incorporation into methyl formate was observed. In the ^{1}H-NMR analysis methyl formate is not detected in the aqueous reaction filtrate. Thus the level of methyl formate in the toluene- extracted solution is very low (i.e. below 0.5 µmoles in 10ml which is the reasonable detection limit of the 1H-NMR analyses for HCOOH) This data however suggests that formate

species were on the catalyst surface and were selectively desorbed during the toluene extraction process which then allowed esterification with the highly available methanol or that methyl formate species are present on the bimetallic catalyst in low quantity. Furthermore incorporation of ^{18}O into this product suggests that $^{18}O_2$ in solution reacts at the catalyst surface/active site to participate in the oxidation of methanol to formate which may then contribute to CO_2. Unfortunately, ^{18}O label in CO_2 could not be analysed with the existing technical equipment which could have clarified the point of consecutive oxidation involving molecular oxygen. One should bear in mind that formic acid is not observed as a reaction product with bimetallic Cu-Fe catalysts and thus the data indicates that ^{18}O is incorporated in formate species which are being transformed to CO_x. Hence it is probable that the presence of Cu merely increases the rate of oxidation of any surface formate to CO_2 which accounts for the absence of formic acid in the reaction filtrate. One should bear in mind that Cu surfaces are known for selectivity to formaldehyde or surface formate when methanol is in the presence of O_2 at the surface at low temperatures. [43] In Table 4.2 entry 3, 5 it was shown that the addition of a second heterogeneous Cu catalyst drastically increased selectivity to CO_2 which supports this theory.

The hypothesis is corroborated by experiments performed using Cu/ZSM-5 for long reaction times (12-20h) where the total product amount does not increase greatly but the oxygenate selectivity decays drastically with time suggesting that Cu merely catalyses the initial oxidation of methane to methanol and then oxidises methanol to CO_2 and not formic acid. This is unlike the case of ZSM-5(30) in which conversion increases with time on line while maintaining good selectivity to oxygenates.

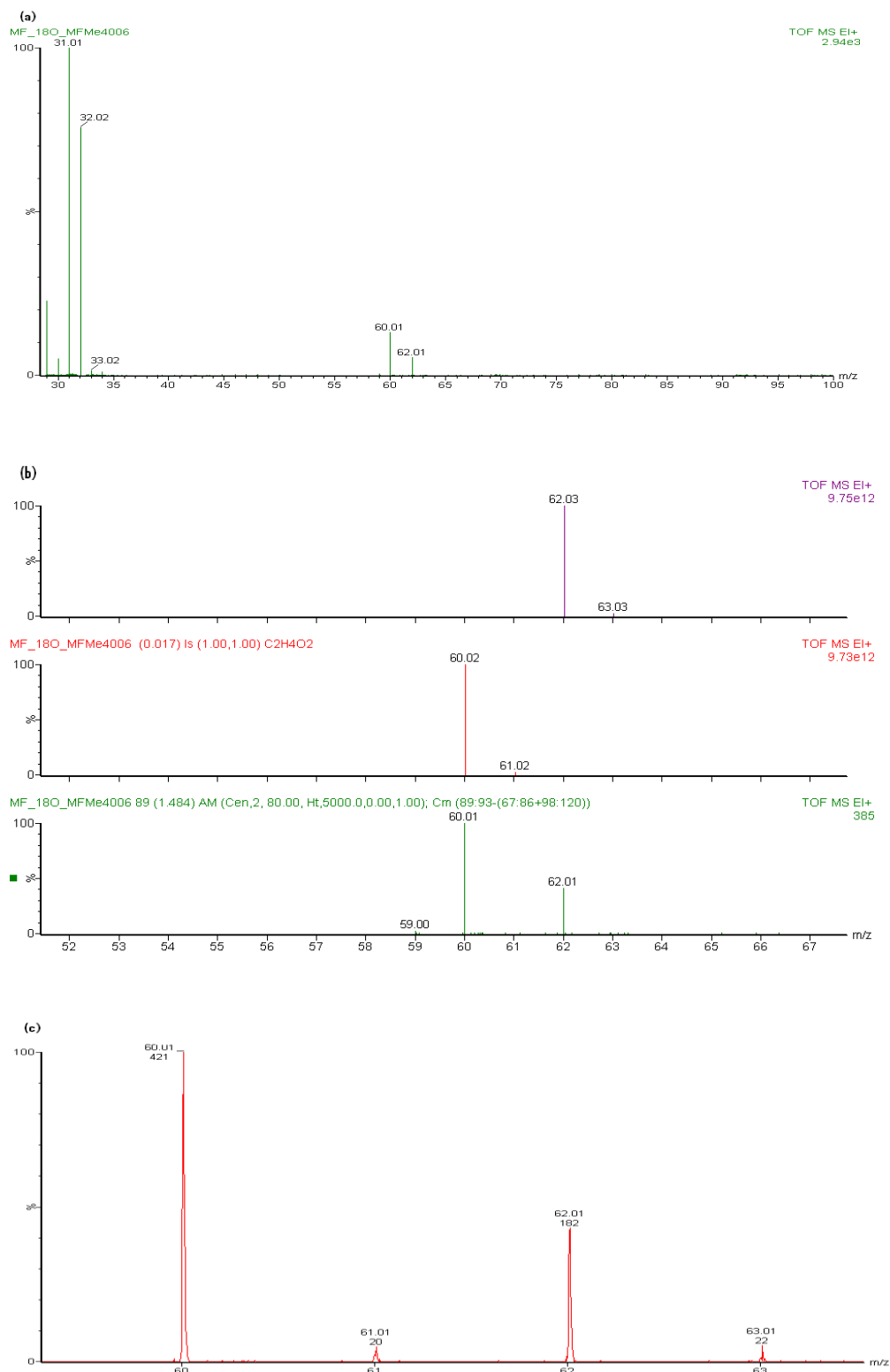**Figure 4.16** (a) Whole GC-MS spectrum of toluene extraction reaction mixture for a reaction where $^{18}O_2$ was present in the gas phase; (b)Isotope patterns for methyl formate indicating incorporation of one ^{18}O per methyl formate molecule formed; (c) integrated peaks corresponding to methyl formation show in 50% incorporation of ^{18}O into the product peak at m/z = 62.

The conclusions from this work are that:

a) Molecular oxygen may be involved in the over-oxidation of methanol and since molecular oxygen is readily produced from hydrogen peroxide during the catalytic reaction it is a component of the reaction mixture even when oxygen is not added as part of the gas phase reaction mixture.

b) The effect of Cu may be to increase the rate of oxidation of formate species to CO_2 at the surface of the catalyst , as compared to Fe, and thus formic acid is not released in solution but CO_2 is still produced.

c) For the bimetallic Fe-Cu catalyst the Fe component performs methane oxidation to produce methyl hydroperoxide, the primary product. Methyl hydroperoxide is selectively decomposed to methanol preferably on Cu sites after being released into solution. Because the Fe species do not decompose methyl hydroperoxide at the same rate as in the absence of Cu this results in low production of •OH, which is linked to the decomposition of methyl hydroperoxide at Fe sites. Finally, Cu also interacts with hydrogen peroxide to produce superoxo species which removes the oxidant from solution and lowers the overall rate of the Fe species (1st order with H_2O_2) and hence the overall catalyst productivity is lower but selectivity to methanol remains is high. It is also probable that for this material absorption of products plays a role in the observed low formic acid selectivity

d) Though Cu on ZSM-5 or as a homogeneous additive to the reaction does not produce formic acid, it is also increased the selectivity to CO_x in long reaction times (>2h) or at high catalyst : oxidant ratios (e.g. 58mg catalyst: 1M H_2O_2) which suggests that the usefulness of this method for catalyst tuning in the bimetallic system may be limited

186

e) For the Fe@Au combination the beneficial effect of Au is only observed upon heat treatment in a "reducing" atmosphere and high methanol selectivity is observed. Further study on the form and location of both metals in this catalyst is warranted

f) Methyl hydroperoxide can react with methane in the presence of H_2O_2 in solution to produce more methyl hydroperoxide and this may represent a background reaction for all catalysts.

g) The production of •OH is not solely responsible for over-oxidation reactions.

References

1. El-Malki, E. M.; Santen, R. A.; Sachtler, W. M. H. *J. Phys. Chem. B* 103, 4611-4622 (1999).

2. Raja, R.; Ratnasamy, P. *App. Catal. A: General* 143, 145-158 (1996).

3. Raja, R; Ratnasamy, P. *App. Catal. A: General* 158, L7-L15 (1997).

4. Raja, R.; Ratnasamy, P. *Catal. Letters* 48, 1-10 (1997).

5. Ratnasamy, P.; Srinivas, D. *Catal. Today* 141, 3-11 (2009).

6. Fan,Y.; Wang,C.; Ding, M.A.; Bao, X. *Chinese J. Catal.* 31, 302-306 (2010).

7. Lin, M.; Sen, A. *J. Am. Chem. Soc.* 114, 7308-7310 (1992)

8. Woertink, J. S. *et al. PNAS* 106, 18908-18913 (2009).

9. Smeets, P. J.; Woertink, J. S.; Sels, B. R.; Solomon, E. I.; Schoonheydt, R. A. *Inorg. Chem.* 49, 3573-3583 (2010).

10. Groothaert, M. H.; Bokhonev, J. A. V.; Battiston, A. A.; Weckhuysen, B. M.; Schoonheydt, R. A. *J. Am. Chem. Soc.* 125, 7629-7640 (2003).

11. Groothaert, M. H.; Smeets, P. J.; Sels, B. F.; Jacobs, P. A.; Schoonheydt, R. A. *J. Am. Chem. Soc.* 127, 1394-1395 (2005).

12. Wood, B. R.; Reimer, J. A.; Bell, A. T.; Janicke, M. T.; Ott, K. C. *J. Catal.* 225, 300-306 (2004).

13. Panov, G.; Sheveleva, G. A.; Kharitonov, A. S.; Rommikov, V. N.; Vostrikova, L. A. *App. Catal. A: General* 82, 31 (1992).

14. Panov, G.; Sobolev, V. I.; Kharitonov, A. S. *J. Mol. Catal A: Chemical* 61, 85-97 (1990).

15. Itadani, A. *et al. J. Phys. Chem. C* 113, 7213-7222 (2009).

16. Mohd Hasbi Ab Rahim; Submitted thesis , Cardiff University 2010.

17. Kau, S.L.; Hodgson, K.O.; Solomon, E.I. *J. Am. Chem. Soc .* 118(18), 7103-7109 (1989)

18. Kang, J. "EXAFS Data", The Dow Chemical Company, February 2010, internal presentation.

19. Anufreinko, V.F.; *et al. Dokl. Akad. Nauk.* 386, 770 -774 (2002)

20. Yashnik, S. A.; Ismagilov, Z. R.; Anufrienko, V. F. *Catal. Today* 110, 310-322 (2005).

21. Ismagilov, Z. R.; *et al. App. Surf. Sci* 226, 88-93 (2004).

22. Lever, A.B.P. <u>Inorganic Electron Spectroscopy</u> Elsevier (1984).

23. Schoonheydt, A. *Catal. Rev. Sci. Eng.* 35, 129 (1993).

24. Shul'pin, G. B.; Sooknoi, T.; Romakh, V.; Suss-Fink, G.; Shul'pina, L. S. *Tetrahedron Letters* 47, 3071-3075 (2006).

25. Shul'Pin, G. B. *J. Mol. Catal A: Chem*. 189, 39-66 (2002).

26. Herron, N.; Tolman, C. *J. Am. Chem. Soc.* 109, 2837-2839 (1987)

27. Sobczak, I.; Pawlowski, H.; Chmielewski, J.; Ziolek, M. *J. Hazard. Mater*. 179, 444-452 (2010).

28. Zhao, R. *et al. Chem. Commun.* 904-905 (2004).

29. Navalon, S.; Alvaro, M.; Garcia, H. *App. Catal. B: Environmental* 99, 1-26 (2010).

30. Kuznetsova, E. V.; Savinov, E. N.; Vostrikova, L. A.; Parmon, V. N. *App. Catal. B: Environmental* 51, 165-170 (2004).

31. Shul'pin, G. B.; Nizova, G. V.; Kozlov, Y. N.; Cuervo, L. G.; Suss-Fink, G. *Adv. Synth. Catal.* 246, 317-332 (2004).

32. Yuan, Q.; Deng, W.; Zhang, Q.; Wang, Y. *Adv. Synth. Catal.* 349, 1199-1209 (2007).

33. Gonzalez-Olmos, R.; Holzer, F.; Kopinke, F.; Georgi, A. *App. Catal. A: General* 389, 44-53 (2011).

34. Sawyer, D. T., Sobkowiak, A. & Matsushita, T. *Acc. Chem. Res.* 29, 409-416 (1996).

35. Sawyer, D.T.; Kang, C., Llobet, A.; Redman, C. *J. Am. Chem. Soc.* 115, 5817-5818 (1993).

36. Barton, D.H.R.; Csuhai,E.; DolLer, D.; Ozbalik,N.; Senglet, N. *Tetrahedron Letters*. 31, 3097-3100, (1990).

37. Yamazaki, I.; Piette, L.H*. J. Am. Chem. Soc* 113, 7588-7593 (1991).

38. Ozawa, T.; Hanaki, A. *Biochem.Biophys. Res. Commun*. 142, 410-416, 1987.

39. Norman, R.O.C.; Storey, P.M. *J. Chem. Soc. B* 1009-1013 (1971).

40. Satoh, A.Y.; Masten, S.J.; Trosch,J. US Patent 7939340 (2011).

41. Bosnjakovic, A.; Schlick, S.   *J. Phys. Chem. B* 108, 4332-4337 (2004).

42. Deighton, N.; Podmore, I. D.; Symons, M. C. R.; Wilkins, P. C.; Dalton, H.
Chem. Commun. 1086-1088 (1991).

43. Roberts, M.W. Catal. Lett. 141, 365-369 (2011).

Chapter 5

Ethane oxidation using Fe/ZSM-5(30) and Cu/Au modified Fe/ZSM-5(30) based catalysts
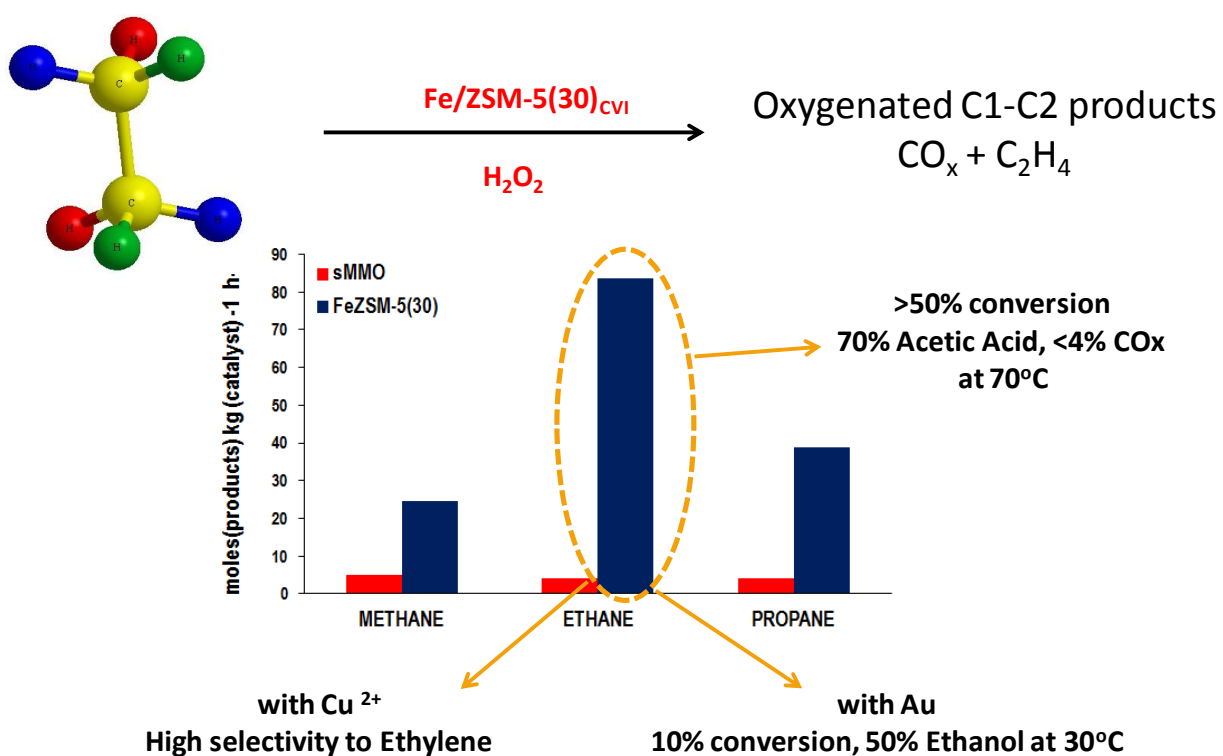
**Functional Tuneable ZSM-5 based Catalysts**

5.1. Introduction

In nature sMMO selectively oxidises methane with high productivity as described in Chapters 1 and 3. Interestingly when ethane is used as a substrate the productivity of the enzyme does not increase as is the case with the oxidation of propane and butane using sMMO. [1] The higher solubility and greater number of C-H bonds for the C2-C4 alkanes should translate into increased catalytic activity unless there the maximum enzymatic velocity is always achieved in the case of sMMO independent of the lower alkane substrate. There are not many studies on heterogeneous liquid phase ethane oxidation, although methane to acetic acid (rhodium chloride catalyst with potassium iodide promoter, 0.27M solution prepared) has been reported. [2] To my knowledge only Shul'pin[3] and Sen[4] have reported low temperature liquid phase ethane to ethanol conversion using heterogeneous catalysts. TS-1 was the catalyst in the former work but very low productivity was achieved (29 mM ethanol and acetylaldehyde solution based on 1 ml reaction in 12 h) and in the latter an *in situ* hydroperoxy capture approach was used as discussed in Chapter 1 (0.55M acetic acid solution based on 5ml reaction in 24h).

The major production of ethanol for human consumption comes from bio-catalysis (fermentation) of sugars. Bio-catalysis of carbon found in plant products also accounts for the major production of ethanol for direct use as a fuel by blending with gasoline. This approach is reported to be renewable and environmentally friendly though the use of agricultural land for food products which do not enter the human food consumption chain has been debated fiercely in recent times, especially as populations struggle to feed themselves. Newer technologies have offered opportunities to use non-food crops, e.g. algae and non-edible grasses, to produce

ethanol via first forming syn-gas as a substrate for enzymatic catalysis of syn-gas to ethanol. This type of technology is based on the ability of *Clostridium ljunjdahlii*, a bacterium [5], to convert CO/CO_2 to ethanol. The obvious advantage is that syn-gas can also be derived from other sources which make the approach very flexible. Currently BRI Energy in the USA has developed technology which is at the commercialisation validation stage and incorporates *C. ljunjdahlii* for its enzymatic catalysis step [6]. It is claimed that any carbon source with less than 30% water content can be thermally gasified and then fed into the enzymatic process to produce ethanol. A key part of this technology is the co-production of electricity through recycling heat lost when cooling the synthesis gas prior to bacterial catalysis. This energy-chemical production system is truly innovative and has significant environmental benefits as part of the required energy is provided by a self-feed back loop into the system

Industrially, ethylene can be transformed into ethanol using an acid catalyst and water according to equation 5.1:

$$C_2H_4 + H_2O \rightarrow CH_3CH_2OH \qquad \text{Eq. 5.1}$$
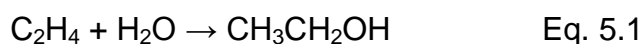
The process is operated at 300 ^{o}C, 60-70 atm using silica supported phosphoric (V) acid catalyst. [7] Ethylene, usually produced from ethane oxidative dehydration or steam cracking of petroleum, is the preferred chemical from ethane as it can be converted to a variety of products, most importantly vinyl chloride. These processes (ethane oxidative dehydration and ethylene hydroxylation) are well understood but still represent an energy intensive option.

Another valuable chemical derived from ethane transformation, is acetic acid, which is usually produced by methanol carbonylation in the Monsanto or Cativa Process. [8]

The catalytic systems are primarily based on Rh and Ir homogeneous catalysts as outlined schematically in Figure 4.1. In both cases the first step is the oxidative addition of methyl iodide to the metal centre (**1** to **2**) followed by ligand exchange and CO migratory insertion into the M-CH$_3$ bond (**2** to **3** to **4**). The M-acetyl species undergoes reductive elimination to produce the halide and regenerate the catalyst. Hydrolysis of the halide fully closes the cycle. Though this is an efficient process, the necessity of methanol as a starting raw material means this is an indirect process and use of hydrogen iodide is undesirable since the latter is corrosive and not considered environmentally benign material

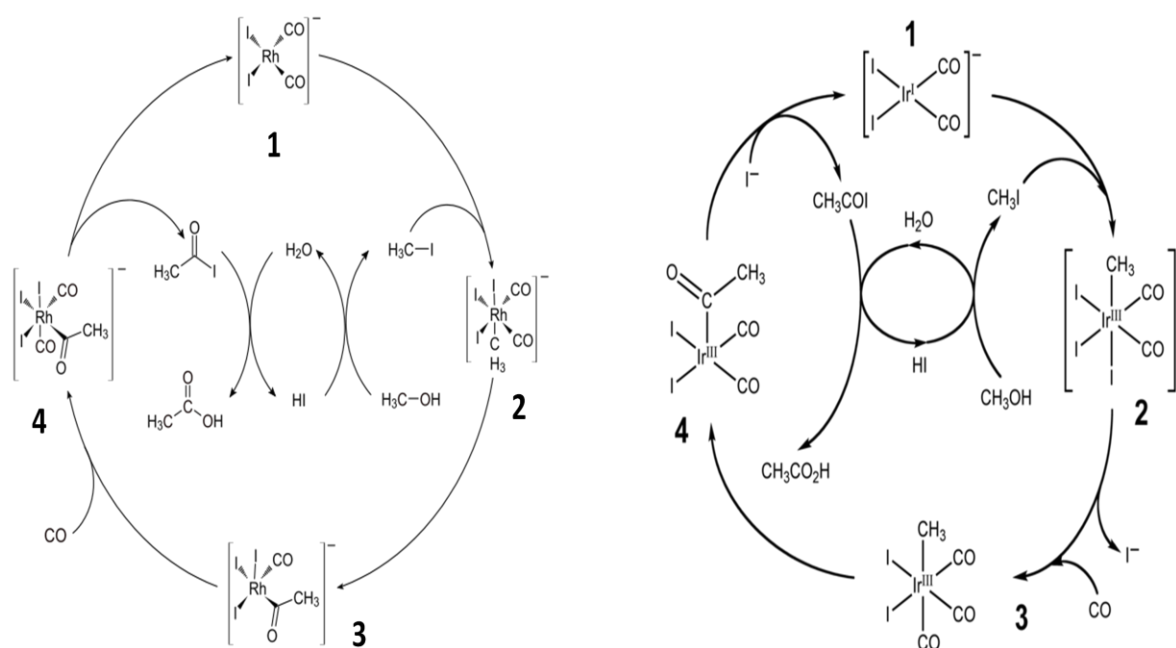**Figure 5.1** Proposed catalytic cycles for the Monsanto and Cativa Processes for methanol carbonylation using aqueous Rh and Ir based catalysts respectively. Figure taken from ref. 8 and is reposted on Wikipedia on the world wide web.

In the preceding chapters a thorough study of methane oxidation using Fe/Cu/zeolite based catalysts synthesised by CVI methodology was presented. It was considered

towards the end of those studies that lack of a favourable price difference between hydrogen peroxide (raw material) and methanol (desired product) meant that application of the zeolite based catalysts in an industrial setting would not be feasible if hydrogen peroxide was used as the terminal oxidant. Thus catalytic use of molecular O_2 or a combination of hydrogen peroxide and molecular oxygen are the only feasible systems for low temperature methane to methanol oxidation. However for the ethane to ethanol transformation hydrogen peroxide as a terminal oxidant is feasible due to the higher price value of ethanol in the marketplace. Also the higher price value of acetic acid means that an ethane to acetic acid process using hydrogen peroxide as the oxidant is also economical. This would of course be based on a process with appreciable conversion and high selectivity to useful oxygenates. With this in mind the Cu and FeZSM-5(30) catalysts were tested for their ethane oxidation ability, and also for propane oxidation.

A direct low temperature and highly selective process for converting ethane to ethanol or acetic acid or ethylene would circumvent all of the indirect energy intensive/ environmentally harmful processes traditionally used. If such a process could show industrially relevant conversion levels then it may have the basis to replace current technologies with significant cost benefit. As will be shown in this chapter the same catalysts used in methane oxidation display truly remarkable activity for ethane oxidation, and in some cases upwards of 50% conversion with 98% oxygenate selectivity or stoichiometric use of the oxidant can be achieved. It is envisaged that this system can form the basis of a new industrial approach to direct ethane oxidation.

5.2. Catalyst screening for ethane oxidation

Initially the activity of catalysts used in Chapters 3, 4 were investigated for ethane oxidation using standard conditions (0.5 h, 50 ^{o}C, 27 mg catalyst, 0.5M [H_2O_2]) at 20 bars of ethane pressure. Firstly, the 2.5wt% Fe/SiO$_2$ $_{CVI}$ material was tested (Entry 1 Table 5.1). This catalyst showed low conversion of ethane but high selectivity towards oxygenates and thus represents the activity of supported iron oxides/ iron clusters for ethane oxidation, since it has been shown in Chapter 3 that these iron species are present on the catalyst surface. The activity of ZSM-5(30) calcined in static air at 550 ^{o}C, (entry 2 Table 5.1), is similar to the 2.5 wt% FeSiO$_2$ $_{CVI}$ catalyst which is unexpected as for methane oxidation there are clear differences in activity between these materials. In fact the productivity of ZSM-5(30) for ethane oxidation (entry 2 Table 5.1) is not higher than observed in methane oxidation even though solubility of ethane in water is double that of methane translating into more substrate being available for the reaction. sMMO also shows this as it productivity does not increase with as carbon chain length increases. It is also important to note the presence of C1 oxygenates in the reaction mixture and ethylene as a gas phase product with appreciable selectivity (7.6% for ZSM-5(30) in entry 2 Table 5.1). This suggests additional reaction pathways are in operation and will be discussed in Section 4.3. Since the C-C bond in ethane is weaker than the C-H bond by about 67-76 kJ/mole ethylene formation from ethane via C-C cracking into radicals after H abstraction from ethane, followed by radical recombination/termination reactions is plausible. This hypothesis can also be invoked to explain the production of methane from ethane as well.

Addition of 0.4-2.5wt% Fe onto the ZSM-5 (30) (Fe/ZSM-5(30)) by CVI resulted in an increased activity as compared to the parent ZSM-5(30), *ca.* 2-4 % conversion as

shown in Entries 3-5 Table 5.1. These values are 3-4 times greater than the conversions obtained in methane oxidation under similar experimental conditions and can be explained by the increased availability of substrate in the aqueous phase as ethane is more soluble than methane in water (0.06g/kg versus 0.024g/kg at 20°C) , and the greater number of C-H bonds translating into an increased probability of reaction. The observation of higher levels of hydrogen peroxide after reaction combined with the higher conversion levels may be due to an oxidant stabilisation effect in the presence of a reactive substrate. The key point for the calcined Fe/ZSM-5(30) is that different or a higher concentration of active sites are present in the material as opposed to ZSM-5(30) and the increased Fe loading has a positive effect on both conversion (productivity) whilst maintaining high oxygenate selectivity. In a similar manner to methane oxidation the 2.5 wt% Fe/ZSM-5(30) catalyst showed higher hydrogen peroxide utilisation as compared to the 1.1wt% Fe/ZSM-5(30) catalyst and the oxygenate productivity is related to the oxidant usage (entries 3 versus 5 Table 5.1).

Additionally, as observed for methane oxidation the reduced Fe/ZSM-5 catalyst shows higher selectivity to the alcohols (10% and 3% higher for ethanol and methanol respectively) with ethane as the substrate. The activity of the reduced catalyst is also higher than its calcined counterpart as shown in entries 3 versus 4 and 5 versus 6 in Table 5.1. The form of the Fe in the catalyst is also important and this is highlighted by the differences in selectivity between the calcined and reduced samples.

Comparison of the data in entries 6 versus 7 Table 5.1 for two catalysts with similar Fe loading again implicates the different forms of iron species in these materials as being responsible for variable activity and selectivity. These materials were

discussed in depth in Chapter 3.4 for methane oxidation. The conversion for the 0.4 wt% Fe/ZSM-5(30) material which has iron on the catalyst surface as well as isolated Fe^{3+} within the zeolite pores (as discussed in Chapter 3) is twice as active as 0.5wt% FeSil-1 sample prepared by hydrothermal synthesis, which has mostly isolated Fe^{3+} clusters within the zeolite pores and no surface iron oxides, for methane oxidation. Also, the product distribution varies for the hydrothermal sample (i.e. 0.5wt% FeSil-1). Indeed it does not match the profile for 0.4 wt% Fe/ZSM-5(30) (or ZSM-5(30) which in theory should share similar active Fe structures with it) as it displays much higher ethanol selectivity, the presence of high amounts of acetylaldehyde ('others' column in Table 5.1) and lower C1 selectivity.

Thus it can be emphasised that for ethane oxidation the different iron morphologies in ZSM-5 catalysts has a more pronounced effect on the catalysis due to multiple reaction pathways operating. This is further supported by the activity of Cu/ZSM-5(30) for ethane oxidation as shown in entry 8 Table 5.1 which shows 7-fold increase in conversion as compared to ZSM-5(30) whereas with methane oxidation this catalyst shows very similar productivity (but with high methanol selectivity) as compared to ZSM-5(30). Cu is proposed as an active metal for ethane oxidation in support of the hypothesis presented towards the end of Chapter 3 that Cu in ZSM-5(30) is also active for alkane oxidation but with lower rate than Fe. The beneficial effect of Cu is shown due the fact that CuZSM-5(30) shows better hydrogen peroxide utilisation (15%) than ZSM-5(30) which is again opposite to the case for methane oxidation. In terms of selectivity, the product distribution for this catalyst is similar to the FeZSM-5(30) in entries 3/5 Table 5.1 though more ethylene is formed at the expense of ethanol. A plausible reason for this will be discussed with data on ethylene oxidation over this catalyst.

Further investigation of the effect of other metals deposited onto ZSM-5(30) for ethane oxidation was conducted. Both Ga and Zn/ZSM-5(30), entries 9, 10 in Table 5.1, show similar conversion to ZSM-5(30) but the product distribution is different. Ga shows a dramatic increase in ethanol selectivity (55% selectivity) whilst Zn favours acetic acid (51% selectivity) and both consume low amounts of hydrogen peroxide for reaction. Both these metals may be active in altering the reaction mechanism or reaction pathway of the Fe component of ZSM-5. These materials may be appropriate for flow reactor studies and further optimisation, especially the synthesis of Ga/ZSM-5 by hydrothermal synthesis. In Chapter 3 it was shown that remarkably Fe-Cu/ZSM-5(30) achieved high methanol selectivity by blocking the pathway to formic acid production. This catalyst was prepared by specific design once it was discovered that Cu/ZSM-5(30) only produced methanol whilst Fe/ZSM-5(30) mainly produced formic acid. Thus this material was studied in an attempt to obtain high ethanol selectivity. However high ethylene selectivity was observed with Fe-Cu/ZSM-5(30)$_{CVI}$ at significant conversion levels. The material remarkably displays 34% ethylene selectivity at 1.6% conversion as shown in entry 11 Table 5.1. This catalyst has a high ethylene oxidation rate as will be shown in section 5.3.3 and thus the high selectivity to ethylene under these conditions is difficult to explain. However it is also possible that absorption of products on the surface of the bimetallic catalyst is the source of this discrepancy. Support for this explanation is given by the non-completion of stability studies on reaction products (ethanol and acetic acid) for this catalyst specifically due to the high absorption rate observed under oxidising conditions.

Following these studies selected catalysts were used in ethane oxidation under optimised conditions (1M H_2O_2, 5bar ethane, 58mg catalyst, 50-7°C, 20ml water) to

obtain higher conversion levels. This was merely for comparison with methane oxidation data and also to obtain information on the activity under scaled-up conditions at low ethane pressure since it was observed that under standard conditions (as used in Chapter 3) the difference in products between 5 bars and 20 bars of ethane was not pronounced. For comparison with methane oxidation the data for 1.1 wt% Fe/ZSM-5(30) under these conditions is presented in entry 1 Table 5.2. High conversion values were achieved for all catalysts with ethane expect ZSM-5(30) in entry 2 Table 5.2. By comparing the methane and ethane conversion levels (8.9% versus 41.8% , entries 1 versus 4 Table 5.2) for 1.1 wt% Fe/ZSM-5(30) higher values than expected for ethane oxidation is observed based on the increased solubility and number of C-H bonds which can be oxidised.

In all cases acetic acid is the major product (40-70% selectivity) followed by formic acid (produced via C2 cracking) and it is apparent that higher metal loading leads to higher conversion, entries 3 versus 4 in Table 5.2, with similar product distribution to each other. This is opposite to what is observed under standard conditions in entries 3 versus 5 in Table 5.1 and for methane oxidation. This is due to the fact that higher metal loading leads to more surface iron species (2nm oxides mentioned in Chapter 3) and thus it is proposed that the surface iron is important in the conversion of the primary product (ethanol) to acetic acid. This hypothesis is supported by the observation of higher selectivity to ethanol and acetylaldehyde for the FeSil-1 hydrothermal sample which has no surface oxides as discussed previously.

The bimetallic sample and the reduced Fe/ZSM-5(30), entries 4 and 5 Table 5.2 respectively, showed no advantage in increased selectivity to alcohols under these conditions. Fe-Cu/ZSM-5(30) however shows higher selectivity to ethylene and lower formic acid selectivity as was observed for ethane oxidation under standard

conditions at 50°C. This catalyst is apparently operating differently to its monometallic analogues. In order to enhance conversion and selectivity we utilised high conversion conditions at lower temperature (30 $^{\circ}$C). The bimetallic Fe-Cu catalyst has a conversion of *ca.* 10% with selectivity of 58% to ethylene, 15% to ethanol and 11% to acetic acid when used at 30°C. This shows that Fe-CuZSM-5(30) has potential for the selective low temperature production of ethylene whilst producing other valuable oxygenated products.

The lower conversion level of the "reduced" 2.5wt% Fe/ZSM-5(30) material as compared to the calcined analogue under high conversion conditions may be linked to the higher hydrogen peroxide decomposition rate (81% in entry 5 versus 50% in entry 2 Table 5.2). This "reduced" catalyst however shows high ethanol selectivity when used at lower temperature and this is discussed in the section of tuning the reaction.

The primary reason for testing the "reduced" Fe/ZSM-5 and calcined Fe-Cu/ZSM-5(30) catalysts under high conversion conditions was to achieve high alcohol selectivity at appreciable conversion level. This was not realised in the experimental findings and prompted testing of bimetallic 2.5wt% Fe@2.5wt%Au/ZSM-5 (30)$_{CVI@IMP}$ heat treated in a reducing atmosphere since this material also displayed high methanol selectivity for methane oxidation. The Fe@Au[a] bimetallic catalyst also gives high conversion (*ca.* 38%) but is the only catalyst to have high ethanol selectivity at 50 $^{\circ}$C, (entry 6 Table 5.2). Notably, the consumption of hydrogen peroxide is higher than the monometallic Fe sample (78% in entry 6 versus 50% in entry 2 Table 5.2). These data show similar trends to the activity of this catalyst in

---

[a] Fe@Au- Fe deposited onto Au/ZSM-5(30) . Au was deposited by wet impregnation and then the material dried before deposition of Fe by CVI in a second step.

methane oxidation. Indeed in later discussions the Fe-Au combination will be presented as a lead catalyst for high ethanol selectivity.

Table 5.1 Liquid phase ethane oxidation using Fe and Cu catalysts

Entry	Catalyst	% Conv. [a]	Aqueous phase products' Selectivity[b]						Gas Phase products Selectivity[c]			%H_2O_2 consumed[d]
			CH_3OOH	CH_3OH	HCOOH	C_2H_5OH	CH_3COOH	Others	COx	CH_4	C_2H_4	
1	2.5%Fe/SiO$_2$	0.3	0	1.2	1.7	8.5	13.1	67.1	4.9	0.0	3.5	55
2	ZSM-5(30)	0.2	2.4	5.7	16.7	26.2	36.6	0.0	1.9	0.0	7.6	23
3	2.5%Fe/ZSM-5(30)	2.2	0.3	3.8	14.9	24.3	53.7	0.3	2.2	0.1	0.6	50
4	2.5%Fe/ZSM-5(30) R(H$_2$)	3.5	0.0	6.1	11.2	36.1	41.5	1.0	3.3	0.4	0.4	95
5	1.1%Fe/ZSM-5(30)	3.3	0.4	3.8	15.7	22.6	54.6	0.0	2.5	0.0	0.4	67
6	1.1%Fe/ZSM-5(30) R(He)	3.6	0.0	6.2	13.4	32.9	44.3	1.2	1.8	0.0	0.1	83
7	0.4wt% Fe/ZSM5(30)	1.1	1.0	5.0	13.8	18.9	49.2	6.0	1.4	0.0	4.7	35
8	0.5%FeSil- 1 HTS	0.4	1.3	3.2	6.8	40.0	30.4	14.4	2.4	0	1.5	34
9	2.5%Cu/ZSM-5(30)	1.4	0.3	3.9	15.7	14.4	59.9	0	0.3	0.1	5.3	15
10	1.1%Ga/ZSM-5(30)	0.3	3.1	0.2	7.9	55.4	31.5	0	1.3	0.2	0.4	29
11	1.1%Zn/ZSM-5(30)	0.4	5.5	3.5	9.8	19.2	50.8	5.5	2.0	0.5	3.1	15
12	1.25%Cu-1.25%Fe/ ZSM-5(30)	1.6	0.1	7.3	0	25.9	30.9	0	1.6	0	34.2	40

Reaction Conditions : 28mg catalyst , 10ml reaction volume, [H$_2$O$_2$] 0.5M, Reaction time 0.5h, P(C$_2$H$_6$)= 20bar, T$_{rxn}$= 50°C, Stirring 1500rpm. All catalysts calcined at 550°C in static air for 3h except in the case of entries 4, 6 and 7 which were reduced in 5%H$_2$/Ar and He respectively. [a] Based on moles C in product/initial moles C in ethane; [b] based on C using product amounts detected by 1H-NMR; [c] based on C using products detected by GC-FID; [d] determined by titration against Ce^{+4} (acidified) using Ferroin indicator.

Table 5.2 Liquid phase ethane oxidation using ZSM-5(30) based catalysts under 'high conversion' conditions

Entry	Catalyst	% Conv.	Aqueous phase products' Selectivity[b]						Gas Phase products Selectivity[c]			%H$_2$O$_2$ consumed
			CH$_3$OOH	CH$_3$OH	HCOOH	C$_2$H$_5$OH	CH$_3$COOH	Others	CO$_x$	CH$_4$	C$_2$H$_4$	[d]
1	ZSM-5(30)	1.5	2.8	1.0	2.5	14.2	40.1	36.1	1.3	0	2.0	15
2	2.5%Fe/ZSM-5(30)	56.4	1.1	2.6	21.1	4.7	69.3	0	1.1	0	0.2	50
3	1.1%Fe/ZSM-5(30)	41.8	1.4	3.0	20.4	6.6	63.4	3.9	1.0	0.1	0.3	45
4	1.25%Cu-1.25%Fe/ ZSM-5(30)	33.8	0.5	8.7	6.2	8.5	49.8	12.6	0.7	0	12.8	70
5	2.5%/FeZSM-5(30)] reduced	47.1	0.1	4.4	21.4	5.9	62.6	2.3	2.8	0.4	0.1	81
6	2.5%Fe@ 2.5Au/ZSM-5(30)reduced	38.5	0.1	5.1	20.3	12.9	58.9	1.1	1.4	0.2	0	78

Reaction Conditions : 54mg catalyst , reaction volume 20ml, [H$_2$O$_2$] 1.0M, Reaction time 0.5h, P(C$_2$H$_6$)= 5.0bar, T$_{rxn}$= 50°C, Stirring 1500rpm. All catalysts calcined at 550°C in static air for 3h except in the case of entries 5 and 6 which were reduced in 5%H$_2$/Ar . [a] Based on moles C in product/initial moles C in ethane; [b] based on C using product amounts detected by 1H-NMR; [c] based on C using products detected by GC-FID; [d] determined by titration against Ce^{+4} (acidified) using Ferroin indicator.

Before discussing mechanistic aspects of ethane oxidation using the zeolite based catalysts mention must be made of the results of a modified reaction protocol. This modification is based on the idea that if the catalyst activity is very high initially (i.e. significant amounts of products are detected before stirring begins) and decreases as the oxidant level drops off then introducing the reactants to the catalyst while changing the temperature to the desired reaction temperature may improve both selectivity and activity of the catalyst. To probe the idea the reaction mixture was stirred while heating to the desired temperature of 50 ^{o}C as opposed to only stirring when at 50 ^{o}C. The data in Table 5.3 shows that a significant amount of products are observed using this modified protocol as compared to the amount of product detected in a 0.5 h reaction under these conditions, i.e. for methane 2.2% versus 4.6% conversion and for ethane 5.6% versus 12% conversion. Furthermore, the selectivity to CO_x is very low in both cases and ethanol selectivity is very high (*ca.* 52% in entry 2 Table 5.3) in the case of ethane oxidation. This is the first demonstration of stoichiometric use of hydrogen peroxide as shown in entry 2 Table 5.3. It was previously thought that this was not possible based on the theoretical mechanism based on DFT studies for methane oxidation as discussed in Chapter 3 in which two (2) moles of hydrogen peroxide is requires to produce one (1) mole of methyl hydroperoxide.

Table 5.3 Catalytic activity of 2.5wt% Fe/ZSM-5(30)$_{CVI}$ calcined at 550 ^{o}C for alkane oxidation using a modified protocol of stirring the reaction mixture while heating to 50°C under "high conversion" conditions. Stirring/heating time is approximately 11min.

| Entry | Substrate | Conv.%[a] | Selectivity | | | H$_2$O$_2$:Products[d] |
			Alcohols[b]	Acids[b]	CO+CO$_2$[c]	
1	CH$_4$	2.2	27.1	68.9	4	12:1
2	C$_2$H$_6$	5.6	51.7	46.7	1.6	1:1

Reaction Conditions : 27mg catalyst , 10ml reaction volume, [H$_2$O$_2$] 0.5M, Reaction time 0.2h, P(C$_2$H$_6$)= 5.0bar, T$_{rxn}$ = 20 to 50°C, Stirring 1500rpm. All catalysts calcined at 550°C in static air. [a] Based on moles C in product/initial moles C in ethane; [b] based on C using product amounts detected by 1H-NMR; [c] based on C using products detected by GC-FID; [d] determined by titration against Ce^{+4} (acidified) using Ferroin indicator

This data supports the hypothesis that multiple reaction pathways are present in the ethane system and that these catalysts should be more useful when tested under flow conditions with short contact times.

5.3. Mechanistic studies on ethane oxidation using zeolite based catalysts

5.3.1. Effect of reaction parameters on ethane oxidation

5.3.1.1. Time on line analysis

In a similar manner to the work described in Chapter 4 mechanistic studies of ethane oxidation over various zeolite based catalysts were performed. The first such experiment was a time on line analysis of the catalytic activity under our standard testing conditions as in Table 5.1. The data is shown in Figure 5.2 below.
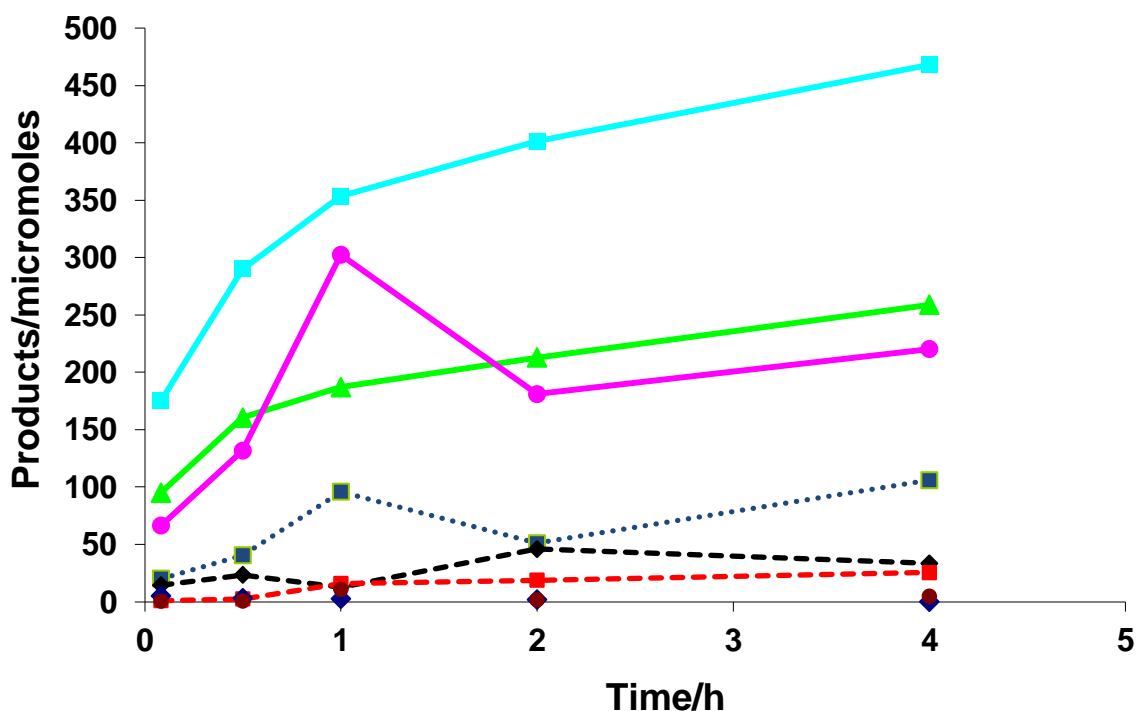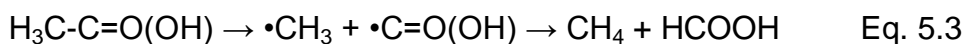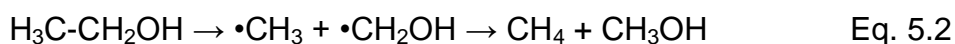

Figure 5.2 Time on Line analysis for ethane oxidation using 2.5wt% Fe/ZSM-5(30)$_{CVI}$ calcined under standard conditions at 30bars ethane pressure. Blue diamonds- CH_3OOH; brown circles- CO; Red squares with dashed line- C_2H_4; Black diamonds with dashed line- CO_2; bark bludesquares with dotted line- CH_3OH; Pink circles with solid line- CH_3CH_2OH; Green triangles with solid line- HCOOH; Light blue squares with solid line- CH_3COOH.

In the case of ethane oxidation a number of aqueous phase products are observed; namely ethanol, acetaldehyde hydrate, acetic acid, methanol, methyl hydroperoxide, formaldehyde and formic acid. The generally accepted reaction pathway for methane oxidation with this catalyst (Fe/ZSM-5(30)$_{CVI}$) is the consecutive oxidation of the primary product, methyl hydroxperoxide, to methanol and then formic acid and carbon dioxide. This simple pathway cannot be applied to ethane oxidation as both C1 and C2 oxygenates as well as carbon monoxide, carbon dioxide and ethylene are observed. Additionally, taking into account that higher selectivity to CO_x (*ca.* 5-10%) was observed in methane oxidation and this increased dramatically when high levels of formic acid were produced (20-40% CO_x for long reaction times) it is surprising that in the ethane oxidation reaction low levels of CO_x are observed even when much higher amounts of formic acid and methanol are produced during the reaction than in the analogous methane oxidation reaction. Furthermore the presence of significant amounts of ethylene as a gas phase product in some cases suggests that a secondary mechanism and multiple reaction pathways are in operation.

It is also interesting that in Figure 5.2 the profiles of the formic and acetic acid mirror each other while the profiles of methanol and ethanol also reflect each other suggesting that cracking of the C2 oxygenates to the corresponding C1 oxygenate is occurring. Thus it is proposed that formic acid is being derived from acetic acid and methanol from ethanol. This hypothesis is supported by work on ethane oxidation using Pd/C or Al$_2$O$_3$ and Pt/C catalysts by Lin & Sen[4] in which formic acid was derived from the oxidation to ethane to acetic acid in aqueous media. Such cracking means that the usual pathway to CO_x through surface bound formate species is avoided and this maybe an explanation for the low levels of CO_x observed. In methane oxidation it was observed that oxygenate selectivity and hydrogen peroxide

usage was better at higher initial methane pressure (60bars versus 30bar) suggesting that the increased availability of substrate suppressed over-oxidation pathways. Since ethane is about twice as soluble as methane this suppression effect can also be evoked to explain the low CO_x observed due to competition for the active sites.

Low levels of methyl hydroperoxide are observed in the time on line analysis which cannot be explained by the cracking of acetic acid into formic acid nor ethanol into methanol (since it formic acid or methanol cannot be transformed into methyl hydroperoxide). It is possible that C2 cracking provides a source of methyl radicals of methane according to:

$$H_3C\text{-}CH_2OH \rightarrow \bullet CH_3 + \bullet CH_2OH \rightarrow CH_4 + CH_3OH \qquad \text{Eq. 5.2}$$

$$H_3C\text{-}C\text{=}O(OH) \rightarrow \bullet CH_3 + \bullet C\text{=}O(OH) \rightarrow CH_4 + HCOOH \qquad \text{Eq. 5.3}$$

Methane or methyl radicals can be transformed to methyl hydroperoxide as discussed in Chapter 3. Indeed it was confirmed that the low level of methane (<15 micromoles) in the gas phase after reaction was not due to contamination of the initial gas feed with methane. Any methane or methyl radicals produced from C2 cracking can also be a source of methanol and formic acid in the detected products. It is not clear what level of contribution to the overall products is from oxidation of methane produced from C2 ethane oxidation products.

Finally the detection of ethylene as a reaction product was unexpected. Ethylene can be produced by oxidative dehydration of ethane in the gas phase at temperatures above 900 ^{o}C[9] and thus it seems unlikely that ethylene can be produced in this low temperature aqueous phase system in this manner. Ethanol can also be dehydrated

to ethylene (i.e. reverse of the acid catalysed ethylene hydroxylation reaction which is used industrially to produce ethanol) but this is unlikely under aqueous conditions though the zeolite is itself quite acidic and may provide a convenient source of H^+ to catalyse the reaction. If this were the case then an increase in ethanol productivity should be accompanied by an increase in the ethylene amount observed. From the data in Figure 5.2 this is not clearly observed. Later in the discussion ethanol stability over this catalyst was studied and no ethylene is produced with ethanol as a substrate. This suggests another pathway to ethylene formation in the overall reaction which may be radical based, such as a possible recombination of two methylene radicals.
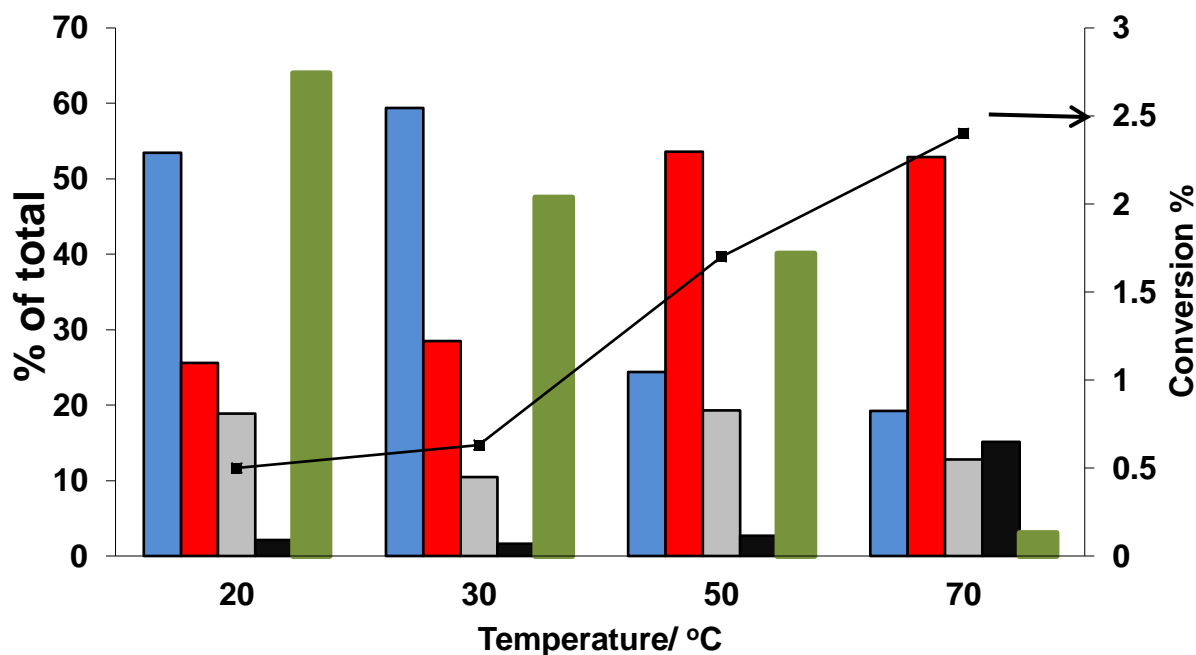
Figure 5.3 Effect of temperature on ethane oxidation using 2.5wt% Fe/ZSM-5(30)$_{CVI}$ calcined under standard conditions at 30 bar ethane pressure. Blue- ethanol; red- acetic acid; light grey- other oxygenates (CH$_3$OOH +CH$_3$OH+HCOOH); black- gas phase products (CO+CO$_2$+C$_2$H$_4$); green-H$_2$O$_2$ left after reaction; black squares – conversion % based on C.

The effect of temperature was then studied within the range of 20°C (room temperature) to 70°C. For higher temperatures auto-oxidation of methane with hydrogen peroxide was observed by other members of our group and so higher temperatures were avoided as with the study of the effect of temperature in methane oxidation. Under the conditions studied for calcined 2.5 wt% Fe/ZSM-5(30)$_{CVI}$ there is significant conversion even at room temperature, *ca.* 0.5%. Under high conversion conditions this number is much higher (*ca.* 3% conversions, data not shown). The conversion increases with temperature with an accompanied drop in ethanol selectivity at temperatures above 30 ^{o}C (almost three-fold decrease) and corresponding increase in acetic acid selectivity of about a two fold increase. At 70

^{o}C the major product is acetic acid followed by ethanol and formic acid. One would expect consecutive oxidation of ethanol to acetic acid to be more facile at higher temperatures. There is also a significant amount of ethylene produced at higher temperatures as about 8% selectivity to ethylene is observed at around 2.5 % conversion based on carbon which accounts for the major portion of gas phase products.

In order to obtain high acetic acid selectivity with appreciable conversion, the temperature needs to be increased whilst for high ethanol selectivity a low reaction temperature is necessary to minimise the over oxidation pathways as could be expected. Another consideration is the effect of temperature is the hydrogen peroxide utilisation. In Figure 5.3 it is apparent that lower temperature reactions favours lower usage of hydrogen peroxide with good selectivity as compared to higher temperature and thus prolonging reaction time at low temperature may result in much high yield with ethanol as the major product. Thus at 20 ^{o}C or 30 ^{o}C after 4h reaction time the selectivity to ethanol is still around 48-55% with ethane conversion of 2-3% and more than 30% of the initial H_2O_2 is detected after reaction under these standard conditions.

The effect of temperature was also studied under "high conversion conditions" and the data is presented in Figure 5.4. As will be shown in Section 5.4 under high conversion conditions acetic acid is the main product, *ca.* 70% selectivity with 48% conversion, at 70 ^{o}C in a 0.5 h reaction. At lower reaction temperature of 30 ^{o}C the conversion is around 14% and the selectivity to acetic acid is still very high *ca.* 60%. Unlike the reaction under standard conditions the calcined Fe/ZSM-5(30) catalyst does not show high ethanol selectivity under high conversion conditions. This is undoubtedly due the high initial oxidant concentration which results in a much higher

rate of oxidation of ethanol to acetic acid even at low temperature. Interestingly about 75% of the oxidant is left after the 0.5 h reaction at 30 ^{o}C and prolonging the reaction under these conditions increases the conversion but has no positive effect on ethanol selectivity. To increase ethanol selectivity under these high conversion conditions a different catalyst is necessary as shown in Section 5.4, Figure 5.12. Strictly speaking calcined Fe/ZSM-5(30)$_{CVI}$ catalysts can achieve high conversion of ethane to useful oxygenates and acetic acid is the major product.
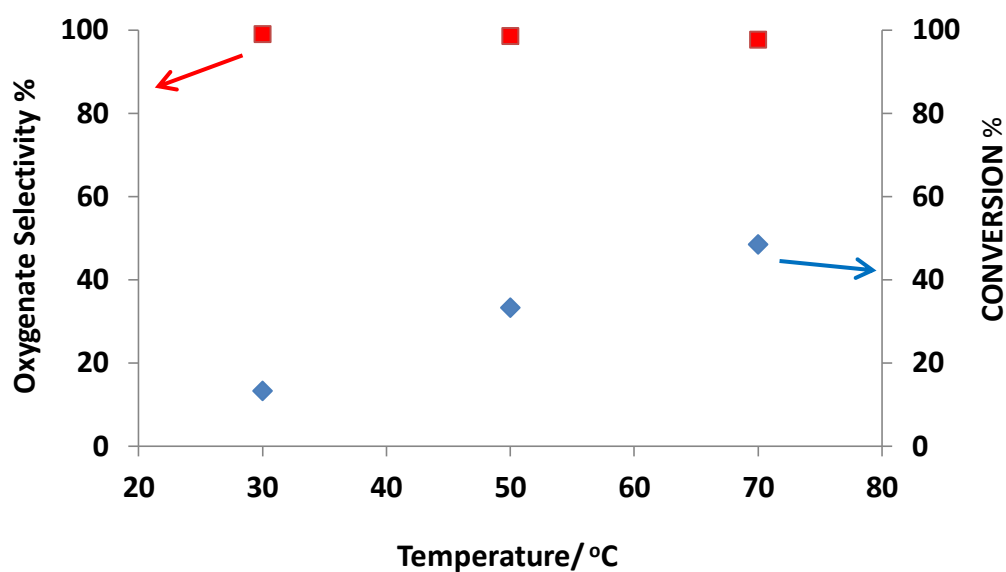
Figure 5.4 Effect of temperature on ethane oxidation using 1.1wt% Fe/ZSM-5(30)$_{CVI}$ under high conversion conditions at 5 bar ethane pressure. Blue diamonds- conversion based on C ; red squares- total oxygenate selectivity based on C.

The effect of oxidant concentration was also studied. The data in Figure 5.5 below shows a linear dependence on oxidant concentration in the ethane oxidation reaction at lower oxidant levels (*i.e.* <0.5M). Under these conditions the conversion begins to plateau off at higher oxidant levels with a corresponding slight decrease in selectivity. It is possible that products are being absorbed on the catalyst at higher conversion levels hence the apparent slowing of the rate at high oxidant levels.
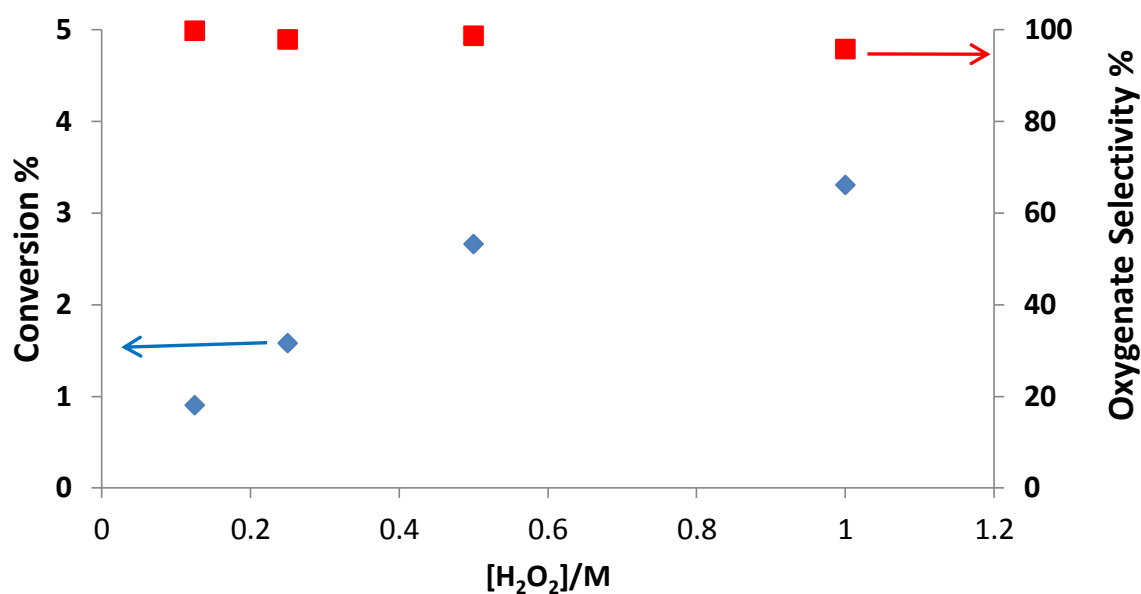

Figure 5.5 Effect of [H_2O_2] for ethane oxidation under standards conditions (30 bar) using 2.5wt% Fe/ZSM-5(30)$_{CVI}$ calcined catalyst. Blue diamonds- conversion based on C; red squares- total oxygenate selectivity based on C.

The percentage of H_2O_2 after reaction does not vary very much across the range tested (*ca.* 50-60% left after reaction) which shows that the rate of oxidant usage as a function of products made is increasing (more oxidant is being used per molecule

of product made as the initial oxidant concentration increases). This may be explained by the unproductive decomposition of H_2O_2 into water and oxygen sparked by high initial oxidant level since the level of substrate is not increased to stabilise the hydrogen peroxide by competitive interaction with the active sites in a similar manner to that observed for methane oxidation. It is also possible that the rates of cracking and other consecutive oxidation reactions increases as oxidant level increases and so the competition between these pathways and the primary oxidation pathway decreases the overall rate as the primary products are not being produced at the same rate.

Figure 5.6 Effect of ethane pressure on ethane oxidation under standard conditions using 2.5wt% Fe/ZSM-5(30)$_{CVI}$ calcined catalyst. Blue squares- total products; red diamonds- conversion based on C.

For the study of methane oxidation a first order dependence on methane pressure was observed in line with the hypothesis that the activation of methane is the rate determining step in the oxidation process. There is also a dependence on the initial pressure of ethane. The data presented in Figure 5.6 shows an interesting "volcano plot" where an initial pressure of 20 bars of ethane results in highest catalyst productivity. This data set was reproduced for three different catalysts which gave the same plot. With methane as a substrate 30 bars initial pressure was chosen but with ethane 20 bars is used for general testing of catalytic activity. The reason for the higher productivity at 20 bars of ethane is unknown though there are suggestions of

possible selective formation of ethane hydrates at this pressure but due to the temperature this is less than likely. It should be noted here that purging the reactor with ethane prior to reaction causes a drop in temperature if performed too quickly (due expansion of the gas requiring energy) and if the initial temperature of filling the reactor with ethane is below 15 ^{o}C the catalytic activity is greatly increased. It was also observed that at some reaction pressures (10-20 bar) cooling the reactor to 8-12 ^{o}C after reaction results in the formation of "ice" within the reactor depending on the reaction composition which is undoubtedly the formation of ethane hydrates. This was not further investigated but should be as it is a possible path to even higher conversions and selectivity to ethanol. Conversion drops as ethane pressure is increased and this prompted testing catalysts at 5 bars of ethane for comparison with proposed flow reaction data, though yet incomplete at the time of writing this thesis.

5.3.2. Product stability studies

The stability of the reaction products, ethanol and acetic acid, towards the catalysts and H_2O_2 were studied with the aim of elucidating the reaction pathway. Firstly the stability of these molecules in the absence of oxidant, Figure 5.7, at similar levels to that reported for the actual ethane oxidation reaction is reported. It was observed that the substrate could be retained on the catalyst as evidenced by the difference between the starting amount of substrate and the final amount in solution as analysed by ^{1}H-NMR labelled as " % absorption" or " unaccounted substrate". No CO_x was observed in these experiments in the absence of oxidant.
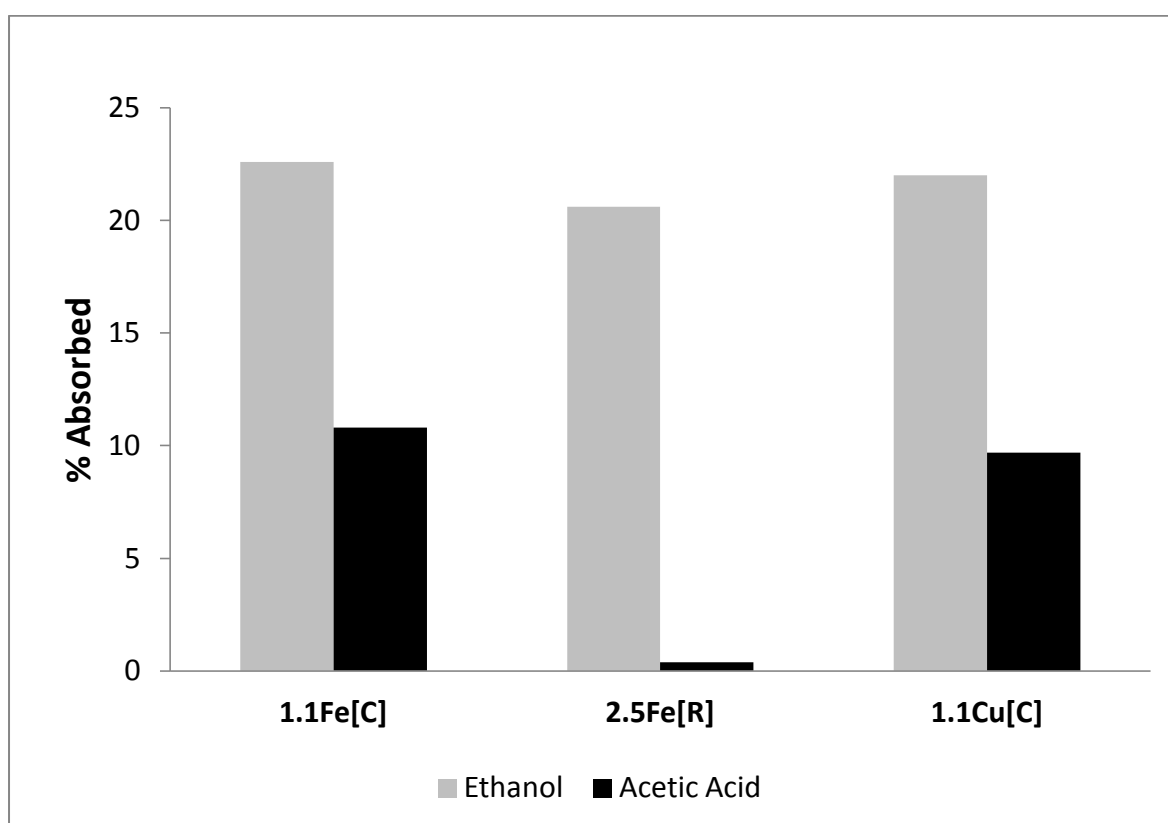
Figure 5.7 Potential absorption of ethane oxidation products by M@ZSM-5(30)$_{CVI}$ catalysts in the absence of H_2O_2. Conditions: 0.05 M [C_2H_5OH] or 0.05M [CH_3COOH] at start, 27 mg catalyst, 0.5 h, 50 ^{o}C, 1500rpm. [C]- calcined in static air, 550 ^{o}C, 3h; [R] - reduced in 5%H_2/Ar, 550 ^{o}C, 3 h. Grey bars- ethanol substrate; black bars- acetic acid substrate.

In the case of ethanol (grey bars Figure 5.7) there is high absorption for all catalysts tested (20-23%) but for acetic acid the reduced Fe/ZSM-5(30)$_{CVI}$ had low absorption whilst the calcined Fe or Cu analogues showed *ca.* 10% absorption rate. These profiles match the "unaccounted for" substrate amounts in Figure 5.8 which suggests that under oxidising conditions some of the product/substrate is also absorbed by the catalyst.
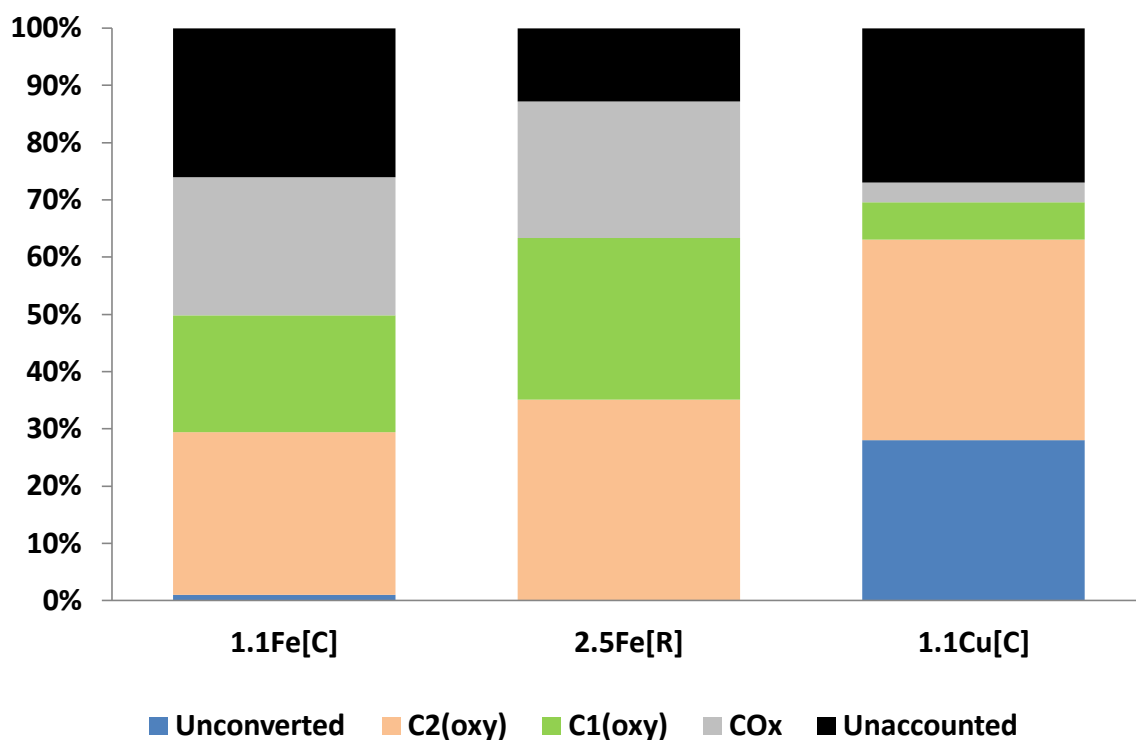

Figure 5.8 Stability of ethanol under oxidising conditions using M@ZSM-5(30)$_{CVI}$ catalysts. Conditions: 0.05 M [C$_2$H$_5$OH] at start, 0.5 M, [H$_2$O$_2$], 27 mg catalyst, 0.5 h, 50 ^{o}C, 1500rpm. [C]- calcined in static air, 550°C, 3h; [R] - reduced in 5%H$_2$/Ar, 550 ^{o}C,3 h. Blue- unconverted substrate; peach- C2 oxygenates (acetic acid); bright green- C1 oxygenates (formic acid, methanol, and formaldehyde); light grey- CO$_x$ in gas phase, Black- substrate unaccounted in total analysis.

In the presence of H$_2$O$_2$ ethanol is transformed to acetic acid with the formation of C1 oxygenates observed which may be explained by cracking of ethanol or acetic

acid. Ethanol was most stable over the Cu/ZSM-5(30) catalyst (*ca* 30% unconverted) and showed similar levels of acetic acid as the Fe/ZSM-5(30) catalyst but lower relative levels of C1 oxygenates and CO_x. Cu/ZSM-5(30) has lower ability to crack C2 products and also produce CO_x as compared to Fe/ZSM-5(30) which is supported by the work presented in Chapter 3 on methane oxidation using Cu/ZSM-5(30). This also suggests that CO_x is linked to the level of C1 oxygenates in the reaction media.
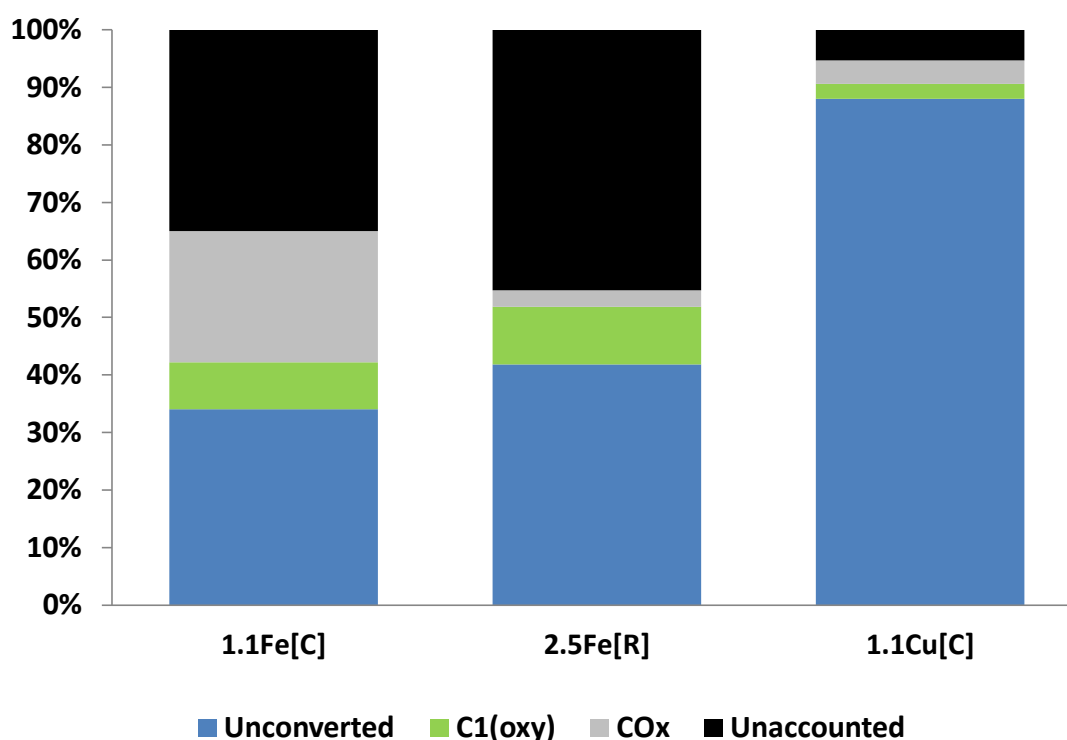

Figure 5.9 Stability of acetic acid under oxidising conditions using M@ZSM-5(30)$_{CVI}$ catalysts. Conditions: 0.05 M [CH$_3$CHOOH] at start, 0.5 M, [H$_2$O$_2$], 27 mg catalyst, 0.5 h, 50 °C, 1500rpm. [C]- calcined in static air, 550°C, 3h; [R] - reduced in 5%H$_2$/Ar, 550 °C,3 h. Blue- unconverted substrate; bright green- C1 oxygenates (formic acid, methanol, and formaldehyde); light grey- CO$_x$ in gas phase, Black- substrate unaccounted in total analysis.

For acetic acid there are some interesting observations. In Figure 5.9 it is clear that acetic acid is most stable over the Cu/ZSM-5(30) catalyst but the reduced Fe/ZSM-

5(30) catalyst showed better acetic acid stability and lower CO_x selectivity than the calcined analogue. This is intriguing as the rate of reaction is apparently faster for the reduced Fe/ZSM-5(30) catalyst (i.e. higher conversion in 0.5 h reaction entry 3 versus 4 or 5 versus 6 Table 5.1) and the acetic acid selectivity is lower in the actual reaction with ethane as a substrate. Unlike the case of acetic acid stability under non-oxidising conditions the "reduced" Fe/ZSM-5(30) has a higher "absorption" propensity under oxidising conditions since the unaccounted for product is 45% in Figure 5.9 versus 1% in Figure 5.7 for this catalyst. This may explain the lower acetic acid selectivity under actual reaction conditions in that the product is merely absorbed on the catalyst when subjected to a heat treatment in H_2/Ar. The reason behind this is not clear at this point.

Furthermore, in the case of the calcined Fe/ZSM-5(30) material the amount of CO_x formed is very much higher than that formed during an actual reaction with similar levels of acetic acid detected to that used in the stability experiments. This suggests that although acetic acid can be oxidised to CO_x this is probably not the major pathway to CO_x in the reaction. To verify this assumption a reaction was performed where acetic acid was added to the starting reaction mixture and ethane oxidation carried out under standard testing conditions. It was observed that oxygenate selectivity was similar to data obtained when acetic acid was not present at the start of the reaction and that the product amounts matched exactly, with a mere summation of the expected plus added acetic acid amounts. The results support the hypothesis that direct oxidation of the acetic acid is not primarily responsible for the presence of CO_x but the formation of C1 oxygenates (methanol and formic acid) is linked to the formation of deeper oxidation products.

One point in the stability studies is that ethylene was not observed in any of these experiments and this rules out the pathway of ethanol dehydration in the formation of ethylene. Since considerable amounts of C1 oxygenates (cracked products) are also observed in these stability studies the probability of radical recombination reactions of radicals derived from C2 cracking in providing the major pathway to ethylene/methane formation is less likely. Thus the hypothesis is that ethylene is formed directly from 'ethane dehydration' at an active site in the catalyst. It was proposed that the mechanism of methane oxidation involved abstraction of H from methane to produce a bound methyl radical-like species and so it is probable that the hydrogen peroxide activated di-meric Fe-O site can abstract 2H from ethane to produce ethylene if two ferryl groups are in the correct proximity to each other. Another probability is the mediation of very reactive species such as hydroxyl radicals with ethane to produce radical species and eventually methane and ethylene. This pathway may be linked to iron clusters and small oxidic surface Fe species or solution phase chemistry since catalysts with significant iron content but no surface Fe species have lower ethylene selectivity than material with surface Fe (e.g. entry 1 or 7 versus 8 in Table 5.1). To the best of my knowledge, there have been no studies on the liquid phase oxidation of ethane using iron oxide catalysts of Fenton's reagents to produce ethylene.

5.3.3. Ethylene oxidation studies

Due to the findings in the preceding section further study of ethylene oxidation at levels observed in the ethane oxidation experiments was performed with the aim of characterising the ability of each catalyst to oxidise ethylene to useful oxygenates. The data in Table 5.4 shows that different catalysts oxidise ethylene with varying rate and display significantly different product distributions. The Fe/ZSM-5(30) materials (entries 1, 2 in Table 5.4) have the highest rate and primarily produce formic acid and CO_2 whereas the Cu/ZSM-5(30), entry 3 Table 5.4, produces mainly methyl hydroperoxide and acetic acid with lower overall rate. It has been shown previously that formic acid is not produced and acetic acid is more stable over the Cu containing catalyst hence it is not surprising that for ethylene oxidation no formic acid is observed. Additionally the detection of methyl hydroperoxide as a product of ethylene oxidation provides evidence for the role of ethylene oxidation in the production of this species (and its subsequent oxidation products) in other ethane reactions. Fe containing catalysts have also been shown to be effective at deeper oxidation of C1 products and C2 cracking and this is also true in the case of ethylene oxidation over Fe/ZSM-5(30).

The product distribution with the Fe-Cu bimetallic catalyst, entry 4 in Table 5.4, is again very different from the monometallic samples. The major product observed is CO_2 and this suggests that the bimetallic catalyst is very efficient deeper oxidation in the case of ethylene oxidation. Formic acid was not produced in this reaction which may be explained by a facile oxidation of formic acid (formed *via* acetic acid cracking or oxidation of methyl hydroperoxide) to CO_2. The possibility of product absorption here cannot be ignored and since there is a much higher difference between the theoretical conversion based solely on gas phase analysis (*i.e.* disappearance of

ethylene) versus the analysis of products. No further rationalisation of the product distribution can be gained by referring to stability data, as done for the Fe or Cu ZSM-5(30) catalysts, as the stability of C2 oxygenates was not studied using the bimetallic catalyst. This was primarily due to issues surrounding product absorption as little or no liquid phase products were detected after an oxidation reaction starting with ethanol or acetic acid as the substrate and minimal amounts of gas phase CO_x products were formed.

Table 5.4 Ethylene oxidation using Fe and Cu based catalysts.

Entry	Catalyst¥	Conversion %		Product selectivity % [a]					
		(gas) §	(prod.)*	HCOOH	CH_3OOH	CH_3OH	C_2H_5OH	$CH_3C=O(OH)$	CO_x
1	1.1Fe/ZSM-5(30) calcined	61	52	49.1	0.0	0.0	0.0	0.6	50
2	2.5Fe/ZSM-5(30) reduced	50.4	41.2	55.2	5.6	0.0	0.0	2.6	37
3	1.1Cu/ ZSM-5(30) calcined	16.2	14.6	0.0	56.6	7.8	0.0	16.6	19
4	2.5Fe 2.5Cu/ZSM-5(30) calcined	45.3	28.4	0.0	2.4	0.0	0.0	5.7	92
5	1.25Fe/SiO₂ Calcined**	<1	0.4	0.0	0.0	0.0	0.0	0.0	100

Conditions: 27 mg catalyst, 50 °C, 0.5 h, 1500 rpm, 0.5 M H_2O_2, 10bar 1%C_2H_4/N_2 ¥ - Number refers to wt% loading of metal, calcination at 550°C in static air, reduction at 550 °C in 5% H_2/Ar, support is ZSM5 (30) unless otherwise stated. § % conversion based on analysis of ethene in the gas phase before and after reaction. * % conversion based on carbon in the sum total of products detected by liquid phase analysis using 1H-NMR and gas phase analysis using GC-FID.** made by impregnation and not CVI [a] Based on actual products detected

The final entry for Fe/SiO₂ (wet impregnation catalyst) is included for comparison to show the poor ability of larger supported surface iron oxides to carry out ethylene oxidation. In this case only CO_2 was detected as a reaction product.
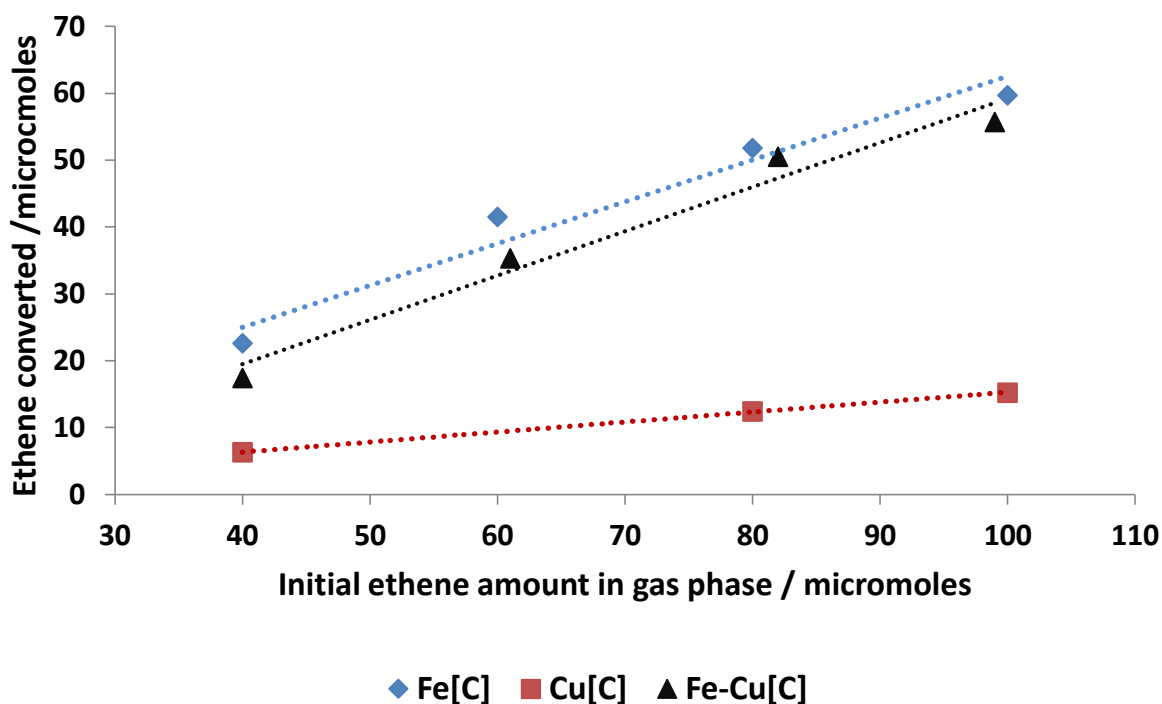
Figure 5.10 Ethylene oxidation using various calcined M@ZSM-5(30)$_{CVI}$ catalysts using standard conditions (27 mg catalyst, 50°C, 0.5h, 1500rpm, 0.5 M H$_2$O$_2$, 4-10bar 1%C$_2$H$_4$/N$_2$). Blue diamonds- 2.5wt% Fe/ZSM-5(30)$_{CVI}$, black triangles- 2.5wt%Fe-2.5wt% Cu/ZSM5(30)$_{CVI}$, red squares- 2.5wt%Cu/ZSM-5(30)$_{CVI}$

In Figure 5.10 data on the effect of ethylene pressure (substrate amount) is presented. In all cases a linear relationship is observed in the range of ethylene amounts studied. The transformation of ethylene into oxygenates is first order with respect to ethylene pressure and one would expect a first order relationship with respect to hydrogen peroxide concentration as is the case with methane and ethane oxidation. From this data set is may be proposed that the Cu/ZSM-5(30) catalyst should have higher ethylene production as compared to a Fe/ZSM-5(30) catalyst since it does not oxidise ethylene as quickly and that the Fe-Cu/ZSM-5(30) material should show similar levels of ethylene as Fe/ZSM-5(30). Fe/ZSM-5(30) (entry 3, Table 5.1 and entry 2/3 Table 5.2) shows very low ethylene selectivity and this is in

keeping with the higher level of oxidation observed in ethylene studies. Cu/ZSM-5(30) (entry 8, Table 5.1) shows higher ethylene selectivity at appreciable conversion (*i.e.* 5.3% selectivity at 1.4% conversion) and this also fits the profile of ethylene oxidation in that more ethylene is observed for catalysts which have low rates of ethylene oxidation. However Fe-Cu/ZSM-5(30) displays very high ethylene selectivity (entry 9, Table 5.1) even though its rate of ethylene oxidation is as high as Fe/ZSM-5(30) which suggests that the catalytic behaviour of the bimetallic catalyst is different to its monometallic counterparts.

All these data point to the possibility of ethylene being an intermediate in the reaction mechanism after its production from ethane. This hypothesis may help explain why the catalytic activity of these materials for ethane oxidation is higher than expected (under high conversion conditions) based on the solubility of ethane and increased probability of H-abstraction which is the rate determining step. In fact stoichometric use of the oxidant is possible with ethane as a substrate but with methane 2:1 usage is theoretically the best usage allowed by the proposed reaction mechanism in Chapter 3.3. This is very clear evidence of the involvement of different reaction pathways. Taking into account that methane and ethylene is formed from ethane the presence of carbon based radicals was checked using EPR radical trapping in a similar manner to work presented in Chapter 4. A DMPO-methyl radical adduct was observed (See Appendix 10) lending support to the hypothesis that radical reactions are in fact occurring during ethane oxidation. Since a percentage of active sites are isolated Fe and Cu species it is also probable that molecular O_2 is involved in the oxidation as these catalysts decompose hydrogen peroxide to O_2 as the reaction proceeds, especially at higher reaction temperatures. As shown for methane oxidation, the hydroxyl radical is also present in these systems and this species can

react with other carbon based radicals to give the termination products. In this way hydrogen peroxide is used more efficiently as all its decomposition products (i.e. M-OOH, •OH, O_2) may be part of the reaction mechanism. Hence it is proposed that for ethane oxidation several pathways exist as outlined in Figure 5.11 below (N.B. involvement of O_2 and •OH or •H not shown).
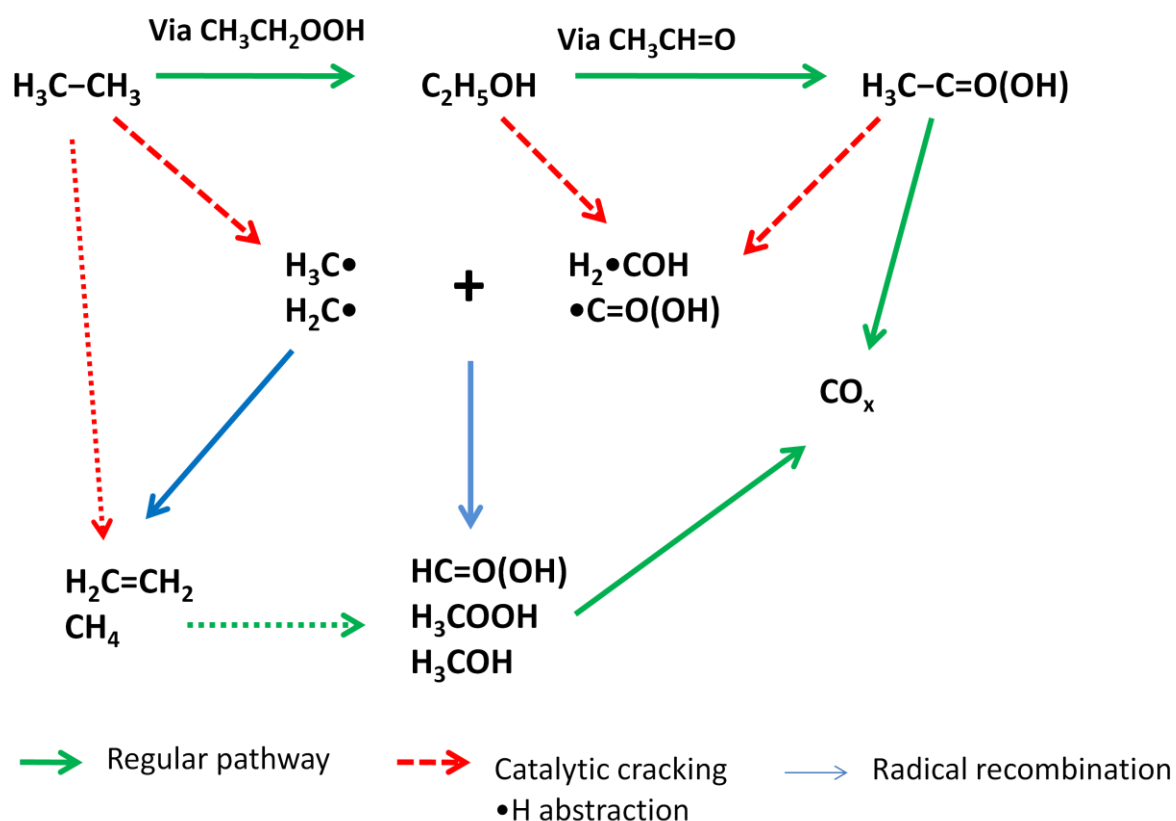

Figure 5.11 Proposed pathways involved in ethane oxidation using Fe and Cu /ZSM-5 based catalysts. Green arrows show the normally proposed non-radical pathway; red arrows show catalytic cracking of ethane or C2 oxygenates and –H abstraction to give ethylene; blue arrows show possibly radical recombination (termination) pathways. Path from ethylene to acetic acid as shown experimentally omitted for clarity.

The oxidation of ethane to ethyl hydroperoxide proceeds through –H abstraction while forming the HOO-CH_2CH_3 bond as for methane. This species is then reduced to ethanol in solution, transforms to ethanol and acetaldehyde at an acid site or transforms to ethanol then acetaldehyde and acetic acid at an Fe site in the catalyst. Ethanol and acetic acid can then be cracked to give methyl radicals and methanol or formic acid respectively (with addition of –H). The C1 oxygenates are oxidised to CO_x but its production is at a low level due to the active sites being involved in many other oxidation processes and the high availability of ethane in the aqueous phase. Also a third pathway may be in operation where abstraction of 2H from ethane (by closely space ferryl groups) in the zeolite cavity occurs thereby producing ethylene ($CH_2=CH_2$). Ethylene is oxidised to methanol, formic acid (preferably) or acetic acid in a facile manner with the products obtained being dependant on the metal cation in the zeolite. Methyl or methylene radicals may be generated in the system and these are also oxidised to C1 oxygenates or recombine to produce methane and ethylene selectively. Methane produced at the active Fe sites is oxidised to methyl hydroperoxide and its subsequent products. Hydroxyl radicals mediate the hydroxylation of methyl radicals to methanol and over oxidation processes. Molecular oxygen may also be involved in the oxygenation of carbon based radical species.

5.4. Tuning the catalysis-Achievements with ethane oxidation

It is highly desirable to be able to tune the catalysis to produce a desired product. In the case of methane oxidation the desired product is methanol and high selectivity to methanol with achieved with Fe-Cu/ZSM-5(30). For ethane oxidation ethanol, acetic acid and ethylene are all valuable products. It has been shown in Section 5.2 that Fe-Cu/ZSM-5(30) is highly selective for ethylene production and merits further studies using variable reaction conditions for evaluation of its low temperature ethylene production activity.
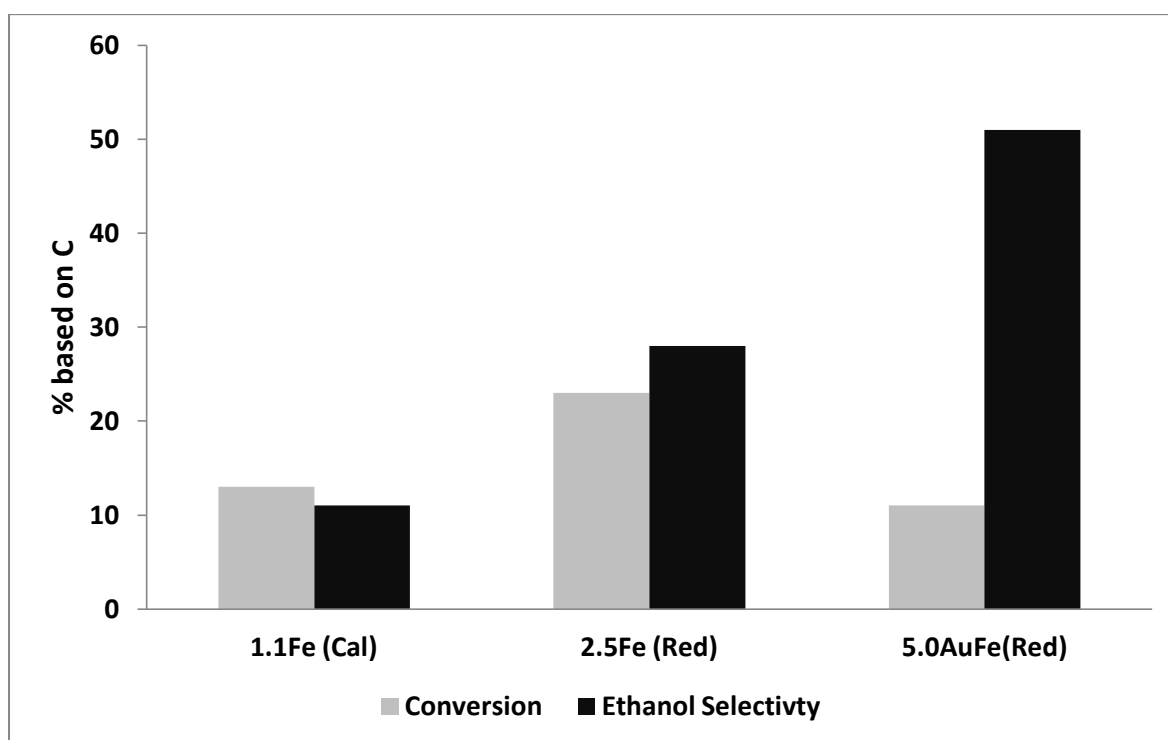
Figure 5.12 Ethanol selectivity for reactions performed at 30 $^{\circ}$C under high conversion conditions. Grey bars- total conversion based on carbon; black bars- partial selectivity to ethanol based on carbon. (Cal) = calcined at 550 $^{\circ}$C, (Red) = reduced in 5% H_2/Ar at 550 $^{\circ}$C.

For ethanol production the reaction temperature is an important factor. Reactions performed at 30 $^{\circ}$C resulted in a 2-fold improvement in ethanol selectivity drastically

for a calcined Fe/ZSM-5(30) catalyst (about 10% in Figure 5.12 versus 4-6% as shown in entries 2 and 3 Table 4.2). Interestingly the reduced catalyst which showed similar product distribution to the calcined sample (as shown in Table 5.2 previously) under high conversion conditions at 50 ^{o}C shows *ca.* 30% ethanol selectivity at 22% conversion at 30 ^{o}C in Figure 5.12. The hydrogen peroxide amount left after reaction is also very high (above 50%) and so this reaction can be prolonged to 12 h to give conversion of *ca.* 40% with 24% ethanol selectivity. The increased stability of ethanol at lower temperature has been reported previously by Kuznetsova and co-workers using Fe/ZSM-5(30) for ethanol oxidation with hydrogen peroxide. [10]

Furthermore, the Fe-Au catalyst has even higher ethanol selectivity though the conversion is only about 10%. Due to the low hydrogen peroxide consumption the reaction can be prolonged in a similar manner to the reduced Fe catalyst. In fact the bimetallic Fe@Au/ZSM-5(30) material may be the lead catalyst for ethane to ethanol conversion as low temperature. Removal of the products, e.g. using a flow reactor or a two phase solvent system for selective extraction, should also allow for high selectivity to ethanol at good conversion without over-oxidation to acetic acid

 Tuning the reaction to produce acetic acid in high yields is also desirable since there are numerous high-value industrial applications of acetic acid[b]. In this case high temperature reactions or high metal loading increases selectivity to acetic acid as shown in Figure 5.13. For a high temperature reaction low iron loading is required as higher iron loading with high temperature leads to unproductive decomposition of hydrogen peroxide to oxygen and water. To promote acetic acid production ethanol must be oxidised efficiently and cracking or oxidation reactions minimised. When lower temperatures are used (i.e. 50°C versus 70°C) the higher metal loading leads

---

[b] Internal communication with DOW Chemical Company

to a faster rate of oxidation and the hydrogen peroxide level is sufficient to maintain the reaction, Figure 5.13.
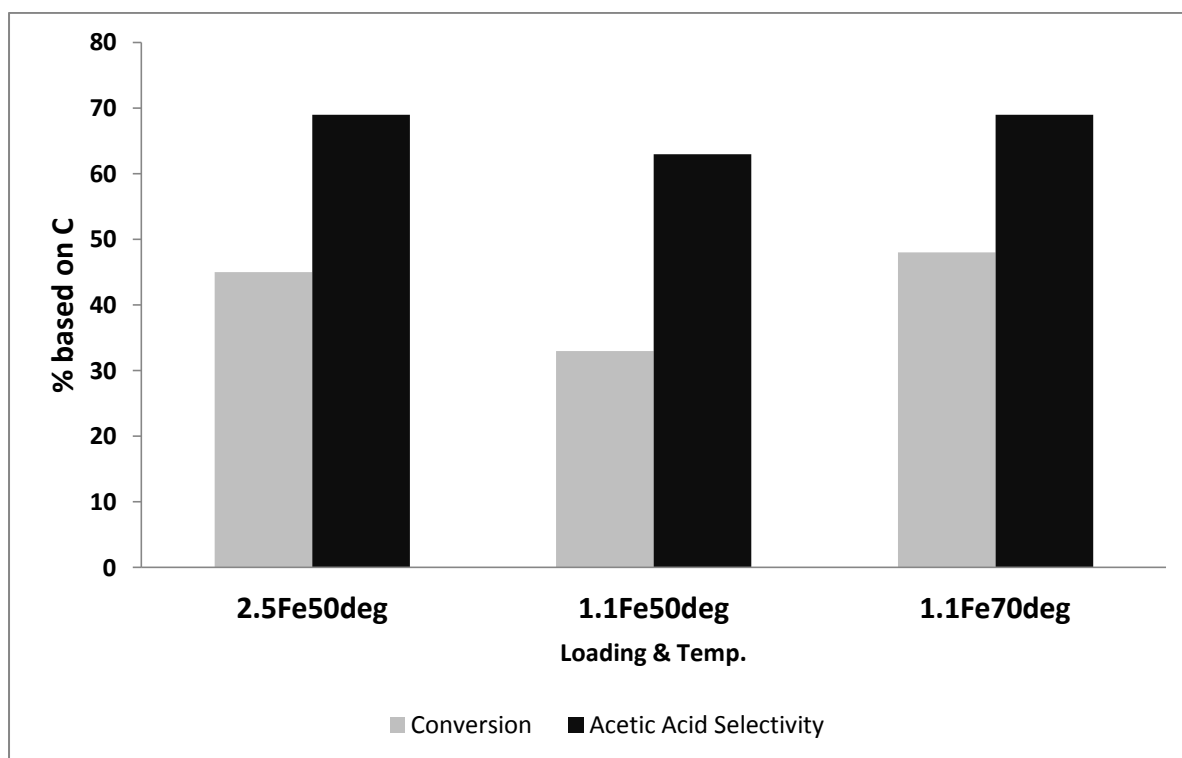

Figure 5.13 Acetic acid selectivity for reactions performed under high conversion conditions (20ml reaction volume, 1M H_2O_2, 0.5 h). Grey bars- total conversion based on carbon; black bars- partial selectivity to ethanol based on carbon. All catalysts calcined at 550 ^{o}C, temperature refers to the reaction temperature employed.

Fe-Cu/ZSM-5(30) was also tested at 70 ^{o}C under high conversion conditions with the aim to obtain high conversion with high selectivity to acetic acid without the presence of large amounts of formic acid or methanol from cracking reactions. High conversion was achieved but there was a large formation of methyl formate. The presence of methyl formate can be explained by the reaction of surface bound formate species and methanol since the methanol amount was quite high under these conditions. Only with the bimetallic Fe-Cu material is methyl formate observed (for methane and ethane oxidation) and this supports the hypothesis that the reason for the lack of

formic acid with this catalyst is that the formate species are bound to the catalyst and undergo facile oxidation to COx with high rate, i.e. higher than with Fe or Cu/ZSM-5(30). As shown in Chapter 4 formate bound to the catalyst can be selectivity desorbed by the addition of toluene to the reaction mixture and shaking.

5.5. Propane oxidation

To investigate the wider applicability of the CVI materials for alkane oxidation reaction propane was used as a substrate. The potential products of propane oxidation (propyl alcohols, propane diols, acetone, propanoic acid) are valuable in the food, chemical synthesis and personal care industries. It was expected that a variety of C1-C3 products would be produced in a similar manner to that observed with ethane as a substrate. As shown in Table 5.5 propan-1-ol, propan-2-ol, propanoic acid, acetone, acetic acid, acetylaldehyde, methanol and formic acid were observed in the reaction mixture. Additionally there were unknown products which were assigned to propane-1/2-diols and other esters. In the gas phase CO, CO_2, methane, ethane, ethylene and propylene were observed.

The first striking observation was that for Fe/SiO$_{2CVI}$ (entry 1 Table 5.5) propyl hydroperoxide species (-OOH at position 1 and 2) were observed. This assignment was made based on the ^{1}H-NMR splitting pattern (which is identical to the corresponding alcohols) but with a shift in the proton resonances for protons attached to the carbon bearing the –OOH moiety. No ethylene and propylene was observed in this case. This data supports the hypothesis that isolated iron clusters and oxides (as discussed in Chapter 3) can perform propane oxidation to yield hydro-peroxy species. Also the observation of propane diols in other cases suggests that oxidation proceeds at more than one position in the same propane molecule simultaneously.

In all other cases (entries 2-8 Table 5.5) the hydro-peroxy intermediates could not be identified clearly in the reaction mixture. The second unexpected observation was that under the conditions used in entries 2-6 Table 5.5 the maximum conversion

(based on C) was 7.8% for the 1.1wt%Fe/ZSM-5(30) "reduced" material. Under these conditions this material (or its calcined form) attains *ca.* 4-5% and 12-14% conversion for methane and ethane respectively. Hence it was expected that the conversion levels with propane would be higher due to the trend. Scaling up the reaction to "high conversion conditions" in entries 7, 8 merely doubled the conversion due to lower initial amount of substrate (4200 versus 2440 μmoles for entries 1-6 versus 7, 8 Table 5.5). The reason for the discrepancy in the conversion levels can be explained when one considers that under these conditions propane may be liquefying in the reactor and not mixing well with the aqueous phase. Furthermore, the chemistry is now more complex as oxidation is competing with a host of cracking and radical recombination reactions of C3 to C2 and C1 oxygenates. More importantly, it was observed by myself with work on applying different solvents (to increase substrate solubility) that acetone and methanol in low levels (1-2% in water) actually poisoned the catalysts (for methane oxidation) and turned off the oxidation reaction under standard conditions. These levels are above those made by the catalysts in methane reactions. This was also the case when propan-2-ol was introduced into the reaction mixture. These very important experiments showed that water was essential for this reaction mechanism but that preparing concentrated solutions of methanol (from methane) was not possible unless another liquid phase was used to selectively extract the methanol from the aqueous phase as it was formed.

Though the conversion levels are not as high as desired there is a fine point to be had from entries 6 and 8 for the bimetallic Fe-Cu/ZSM-5(30) catalyst. This catalyst produced very high selectivity to propylene (*ca.* 50% of total products based on C) which is similar to that observed with ethane as a substrate. Propylene oxidation was

not studied separately but it is again likely that propylene is being oxidised by these catalysts and contributing to the reaction products. It was discussed previously that ethylene was oxidised very efficiently by the bimetallic Fe-Cu/ZSM-5(30) but in ethane reactions high selectivity to ethylene was observed indicating that ethylene was actually being produced from ethane directly and being released into the reaction mixture. This assumption is also applied here but the presence of methane and ethane in the gas phase can also be explained by radical recombination reactions between methyl or ethyl radicals and •H. Further evidence of this lies in the presence of higher alkanes/alkenes in the gas phase which were not present in the original propane feed, i.e. butane and butene. These were in trace amounts (below 0.5μmoles).

Further study on propane oxidation was not undertaken but the data in Table 5.5 also suggests that the C2 position (methylene) of propane is oxidised faster than the C1/C3 (methyl) positions. The total ratio of products from oxidation of the C2 to C1/C3 position or propane could not be determined exactly due to the propensity of cracking reactions (*i.e.* the same cracked products can originate from both 1-ol and 2-ol species etc) but taking into account the total propan-1-ol and propanoic acid versus propan-2-ol and acetone it is clear that the C2 position is preferentially oxidised. However, with these catalysts acetone is very stable and so the hypothesis cannot be proven at this stage without further study on the ability of these catalysts to crack propanoic acid which will determine the level of contribution to the C2 and C1 oxygenates from propan-1-ol or propanoic acid.

Table 5.5 Liquid phase Propane oxidation screening using zeolite based catalysts.

Entry	Catalyst	Liquid phase Products/ µmoles[a]**								Gas Phase Products/ µmoles [b]			H_2O_2 consumed % [c]
		C3 [d]				C2		C1		CO_X [f]	CH_4 C_2H_6 [g]	C_2H_4 C_3H_8 [h]	
		1-OH	2-OH	=O(OH)	$_2$(=O) [e]	=O(OH)	=O	-OH	=O(OH)				
1	1.25%Fe/SiO$_2$	3.6‡	8.6§	0	2.1	0.0	0	trace	trace	3.0	4.5	0.1	30
2	2.5%Fe/ZSM5(30)	56.7	79.0	24.4	41.2	46.4	7.6	10.7	76.6	10.6	6.3	15.0	40
3	1.1%Fe/ZSM5(30)	36.4	36.0	28.4	35.7	66.4	2.9	16.9	112.4	16.3	36.3	17.2	64
4*	1.1%Fe/ZSM5(30)	60.1	44.3	49.2	54.2	80.4	3.1	18.1	144.2	5.7	1.45	6.2	90
5	2.5%Cu/ZSM5(30)	4.4	21.8	0	7.4	0.9	4.1	trace	0.0	23.2	3.7	0.4	33
6	1.25%Cu-1.25%Fe/ ZSM5(30)	3.6	15.6	11.2	35.6	24.2	0.5	7.4	0.0	8.1	40.0	111.4	52
7	2.5%Fe/ZSM5(30)	22.5	35.1	42.9	46.6	82.6	11.1	11.2	138.4	10.5	11.7	10.4	46
8	1.25%Cu-1.25%Fe/ ZSM5(30)	21.5	39.7	13.3	26.1	13.7	3.1	3.4	0.0	4.1	3.8	111.6	31

Reaction Conditions Entries 1-6 : 27mg catalyst , reaction volume 10ml, [H_2O_2] 0.5M, Reaction time 0.5h, P(C_3H_8)= 4.1bar, T_{rxn}= 50°C, Stirring 1500rpm.
Reaction Conditions Entries 7 and 8 : 54mg catalyst , reaction volume 20ml, [H_2O_2] 1.0M, Reaction time 0.5h, P(C_3H_8)= 4.1bar, T_{rxn}= 50°C, Stirring 1500rpm. All catalysts calcined at 550°C in static air for 3h except in the case of entry 4 which was reduced in 5%H_2/Ar .
[a] based on product amounts detected by 1H-NMR; [b] based on products detected by GC-FID; [c] determined by titration against Ce^{+4} (acidified) using Ferroin indicator; [d] ethanol peaks overlap with propan-2-ol, ethanol confirmed by GC analysis, propanediols (< 5µmoles) are present but could not be quantified individually; [e] acetone; [f] CO_2 is the major product except in entry 5 where CO is *ca.* 90% of value quoted, [g] ethane is the major product; [h] propylene is the major product (>90% of value quoted) ‡$CH_3CH_2CH_2O$-OH (1-propyl hydroperoxide) due to slightly higher shift in ^{1}H-NMR as compared to 1-propanol; § $CH_3CH(O$-OH)CH_3 (2-propyl hydroperoxide) due to slightly higher shift in ^{1}H-NMR as compared to 2-propanol.
** Aqueous phase oxygenated products are propanol, isopropanol, propanoic aicd, acetone, Ethanoic acid, acetylaldehyde, methanol, formic acid going from left to right

Furthermore, no epoxides were observed with ethane, ethylene or propane oxidation. It would be expected that a selective reactive species such as Fe(IV)=O (proposed in Chapter 3 as being part of the active site) would result in the formation of epoxides from ethylene or propylene (both present in the reaction products) in a similar manner to $FeCl_3$ reported by Shul'pin and co-workers [11]. Hydroxyl radical based reactions would lead to acids, cracked products and CO_x [12]. Thus it is also highly probable that there is contribution from hydroxyl radical chemistry as implicated in Chapter 4 for methane oxidation and thus high rates and propensity for cracked products. To clarify this study of the hydroxyl radical based oxidation of propane and exploring the reaction selectivity for branched alkanes is also merited. Improvement in the product selectivity may be obtained by using short reaction time (low contact time) since the ability of these catalysts to perform cracking and over-oxidation reaction is indeed linked to the hydrogen peroxide levels. Liquid phase propane oxidation (as opposed to the tri phasic solid-aqueous-gas system) may also result in higher yields.

Finally, it should be noted that aqueous phase oxidation of cyclohexane with hydrogen peroxide over Fe/ZSM-5(30) was briefly attempted (3 phase solid-water-cyclohexane reaction in a glass round bottom flask) and cyclohexanol/ cyclohexanone was the main product as shown by GC-MS analysis. In this rudimentary test the low level of products could only be analysed by GC-MS and there was no detection of cracked products which may be due to the low productivity and inadequate mixing of the catalyst and substrate.

5.6. Summary

This Chapter explores the ability of Fe and Cu doped zeolite materials to perform the oxidation of ethane and propane at low temperature using neat hydrogen peroxide. Both substrates are oxidised with very high oxygenate selectivity (above 95%). The catalysis can be tuned to produce ethanol, acetic acid, ethylene in addition to C1 oxygenates which were found to be produced in cracking reactions in the case of ethane oxidation. For propane oxidation a variety of C1-C3 oxygenates were observed including propylene in the gas phase. The low COx formation and observation of cracked products and alkenes from alkane sources point to multiple reaction mechanisms occurring at the active metal sites in the doped zeolites. Notably a plausible reaction pathway for ethane oxidation is put forward and industrially relevant conversion levels have been achieved. Experiments done with copper present in the catalyst supports work in Chapter 4 on the effect of Cu and the beneficial effect of Au on ethanol selectivity was observed.

Propane oxidation is hindered by the formation of acetone and iso-propanol which selectively poison the catalyst and it is noted that the C2 position of propane is preferentially oxidised which is similar to findings in other systems operating by reactive ferryl species which are anchored to supports. Bimetallic Fe-Cu catalysts have high selectivity for propylene and may be a lead catalyst for low temperature propane to propylene production and this merits further study. Finally the lack of formation of any epoxides in these reactions suggests that facile hydroxyl radical mediated chemistry is also occurring.

References

1. Colby, J.; Stirling, D. I.; Dalton, H. *Biochem. J.* 165, 395-402 (1977).

2. Lin, M.; Sen, A. *Nature* 368, 613-615 (1994).

3. Shul'pin, G. B.; Sooknoi, T.; Romakh, V.; Suss-Fink, G.; Shul'pina, L. S. Tetrahedron Letters 47, 3071-3075 (2006).

4. Lin, M.; Sen, A. J. Am. Chem. Soc. 114, 7308-7310 (1992).

5. Kopke, M; *et al PNAS* 107, 13087-10932 (2010).

6. www.brienergy.com; BRI Energy Inc. (2008)

7. Roberts, J.D.; Caserio, M.C.; Basic Principles of organic chemistry 2nd edt., Menlo Park, California (1981)

8. Jones, H. *Platinum Metals Rev.* 44, 94-105 (2000).

9. Bodke, A. S.; Olschki, D.A.; Schmidt,D.L.; Ranzi,E. *Science* 285, 712-715 (1999*).*

10. Kuznetsova, E. V.; Savinov, E. N.; Vostrikova, L. A.; Parmon, V. N. App. Catal. B: Environmental 51, 165-170 (2004)

11.   Yuan, Q.; Deng, W.; Zhang, Q.; Wang, Y. Adv. Synth. Catal. 349, 1199-1209 (2007).

12. Sawyer, D. T., Sobkowiak, A. & Matsushita, T. *Acc. Chem. Res.* 29, 409-416 (1996).

Conclusions and Future Work

Significant progress has been made in understanding alkane oxidation reactions using ZSM-5 based materials under the experimental conditions used in this work. The efforts of a large team was necessary to perform the studies (and that of three other post-graduate students) presented in this thesis. Considering the number of different zeolite materials, their widespread application and multi-variant chemistry there is obvious difficultly in being able to study all these materials for methane oxidation in depth. The generalised picture however lays the basis for catalyst design for future work

The proposed reaction mechanism occurring in ZSM-5(30) is the facile conversion of methane to methyl hydroperoxide catalysed by an iron-oxo-hydroxo dimeric species existing in ZSM-5 due to trace impurities of iron in commercial zeolites. This species, suggested by the DFT and XANES/EXAFS studies of co-workers, is not the only iron centre in the material which has the potential to be involved in methane oxidation as shown by the successful use of iron deposited on amorphous materials by a variety of techniques. Certainly the catalysis is complex due the ability of many different types of metal centres to be involved in the reaction and the additional reactions required to transform methyl hydroperoxide into methanol, formaldehyde and formic acid. This is a dominant feature of ZSM-5 doped with metals prior to heat treatment since methyl hydroperoxide is not observed as a primary reaction product with these metal loaded materials. The question of whether or not other reaction mechanisms which produce methanol selectively instead of methyl hydroperoxide exists remains unanswered, but it has been shown that methyl hydroperoxide can react with methane in the presence of hydrogen peroxide to produce even more methyl

hydroperoxide (possibly an auto-oxidation reaction). This chemistry requires further investigation since it implicates solution phase chemistry of methyl hydroperoxide in the catalysis.

The involvement of hydroxyl radicals, observed with Fe/ZSM-5(30), has also been probed. Interestingly the methyl radical has not been detected in EPR studies though the ability of acidic zeolites to produce radical and radical cation species from a variety of hydrocarbons is well documented and in many systems which operate by hydroxyl radicals, alkyl radicals are also involved in the reaction. It is proposed that the lack of detection of alkyl radicals is not substantial proof of its absence especially as they are detected in ethane oxidation reactions. In the case of ethane and propane oxidation it is proposed that multiple reaction pathways exist with the involvement of alkyl radicals which may be a direct consequence of the greater chain length and the action of multiple reaction sites which do not operate in the same way as the proposed dimeric iron site of ZSM-5.

The metal dopant itself, method of introduction into the zeolite and post-deposition treatment were studied in Chapters 3, 4 and 5. It was found that many parameters affected the catalysis and that the CVI technique afforded superior catalysts that could be tuned to produce methanol selectively (from methane) and gave high conversion to useful oxygenates in ethane oxidation. These advantages are thought to be due to the ability to deposit very small nanoparticles (2-4nm) on the zeolite surface and smaller clustered iron species within the zeolite pores. The addition of copper was identified as a suitable way to achieve high methanol selectivity for iron based materials. In depth studies presented in Chapter 4 shows that possibly the unique role of copper is to mediate facile oxidation of methanol to CO_2 *via* surface bound formate species (for the solid copper catalyst) and the selective

transformation of methyl hydroperoxide into methanol. These roles together with the lack of hydroxyl radicals in this system suggest that the iron species cannot operate in exactly the same manner in all zeolite catalysts. These studies (Chapter 4) also led to the discovery that molecular oxygen is involved in the over-oxidation reactions observed with both Cu and Fe/ZSM-5(30) which could be expected if Fenton's type chemistry is in operation.

In a similar manner to the effect of copper it was observed that gold had a positive effect on alcohol selectivity when the catalyst was heat treated under a reducing atmosphere. The Fe-Au combination (prepared by the "hybrid method") requires further study since it was proposed that alternative species exist in this material as observed by UV-VIS and XPS studies. TEM studies on Pd@Au/TiO$_2$ prepared by the "hybrid" CVI@IMP method in other work not reported in this thesis showed that the Pd deposited onto the pre-formed Au nanoparticles to predominantly form a core shell structure. By analogy this may be the case with Fe@Au/ZSM-5 (30) but studies by TEM would be difficult in this case depending on if the Au is on the external surface or internal pores/channels of the material. This material may have major significance in future work as Au is known to activate molecular oxygen which is preferred to instead of hydrogen peroxide.

It is not surprising however that Fe and Cu feature in the most active catalysts studied as nature utilises these metals in enzymatic catalysis in methanotrophic organisms time and time again. The use of lower alkanes as a chemical and energy source in organisms is not restricted to methanotrophic bacterial enzymes like methane mono-oxygenase as there are many P450 enzymes which accomplish the same tasks in varied systems. The key difference offered by the enzymatic systems is the ability to utilise molecular oxygen (with suitable hydrogen donors) for the

244

reaction as opposed to hydrogen peroxide. In terms of commercialisation the requirement of using molecular oxygen with sacrificial hydrogen donors and radical initiators is a strict one due to the high price of hydrogen. This translates into the real need for further work around activation of molecular oxygen and the learning's from ZSM-5 based catalysis presented herein can be transferred into the search for new catalysts. With Fe and Cu/ZSM-5 materials it was shown that molecular oxygen is actually involved in the catalysis but not to produce primary product as desired (i.e. the alcohol). This is likely to be solution phase chemistry or occurs at iron clusters within zeolite pores and not actual activation as iron oxide sites on the external zeolite surfaces since it has been shown that high temperatures are required for activation of oxygen on iron oxide species.

It is envisaged that the catalysts used in this thesis will be studies for *industrial application to ethane oxidation* due to the high yield and selectivity to useful oxygenates obtained. There are a number of work areas which need to be addressed as regards to the ZSM-5 catalysis:

- The study of other metals for the reaction, especially when incorporated by hydrothermal synthesis in an effort to produce more active catalysts.

- The study of the iron species in other ZSM-5 catalysts and other materials such as SiO_2, Zeo Y, Mordenite etc. This work could shed further light on the role of different iron species in the catalysis.

- In depth study of the chemistry of methyl hydroperoxide and the effect of additive and metal species on its chemistry. This area is important as it may pave the way for use of certain organic radical initiator species or organic peroxides for methane oxidation and also show which reactive oxygen species are really involved in the reaction.

- The overall role of radical chemistry for ZSM-5 needs to be probed with classical kinetic analyses using radical clocks/scavengers and radical traps. Such investigations will allow more concrete mechanisms to be postulated.

- The extensive study of the copper species in Cu and Fe-Cu/ZSM-5 must be performed to support the role of copper in the catalysis as copper is essential to high methanol productivity.

- Further characterisation of the iron and gold sites in materials treated under reducing conditions is necessary in understanding how the form of the iron species or presence of gold affects the catalysis in a beneficial manner.

It is also necessary to probe the effect of solvents in this system. This is particularly important as it was found that certain reaction products (methanol, acetone, iso-propyl alcohol) cause catalyst deactivation at relatively low concentration. Thus, as is the case with many catalytic systems, the introduction of an additional solvent to remove the product selectively may improve the reaction yield and selectivity to the desired product. However it is noted that water is essential for the reaction using Fe/ZSM-5(30) but this was not known for Cu/ZSM-5 which may act differently due to the presence of superoxide/ free hydro-peroxy species during the reaction.

The above mentioned work areas do not directly address the issue of oxygen activation. This is another task altogether. There are two strategies which could be adopted based on other work performed by myself in parallel to the studies detailed in this thesis. The first is the use of noble metal nanoparticles to perform the catalysis. It was shown that Au-Pd materials can oxidise methane to methanol selectively but in very low yield (<0.2% conversion) and this can be achieved with a

combination of hydrogen and oxygen in the gas phase or aqueous hydrogen peroxide. Those materials were prepared by wet impregnation methods and use of sol-immobilisation to prepare very small alloy nanoparticles resulted in a lack of catalyst productivity due to facile decomposition of hydrogen peroxide. Though this seems counterproductive it was discovered that CVI materials with similar size particles show very different behaviour to Au-Pd/TiO$_2$ made by IMP or SI. Pd-Pt/TiO$_2$ prepared by CVI and heat treated in H$_2$/Ar showed excellent activity for benzyl alcohol oxidation and moderate activity solvent free toluene oxidation using molecular O$_2$. In these reactions the selectivity and activity was improved versus the IMP catalysts and very different to the SI materials. When used for toluene oxidation with TBHP[a] it was observed that after 24h the utilisation of TBHP practically stopped while the appearance of oxygenated products steadily increased. It was estimated that twice times the amount of oxygen used based on TBHP left after reaction was found in the products. This suggested that oxygen from air could be incorporated into the products and is supported by much lower conversion levels (which matched TBHP disappearance) observed when nitrogen was used to provide an anaerobic environment. ^{18}O$_2$ experiments are required to validate the hypothesis but the data has been reproduced with different batches of catalysts. The idea that molecular oxygen can be activated with TBHP as an initiator by this particular material is amazing. This can be used in a system where toluene oxidation can be coupled with methane oxidation or sole methane oxidation in a different solvent using molecular oxygen and TBHP. There may also be the opportunity to utilise other metal nanoparticles in this way as an extension of the Methane Challenge project[b].

---

[a] Tertiary -butylhydrogen peroxide
[b] 5 PhD theses were submitted based on this project covering methane oxidant by noble metal catalysts, ZSM-5 based catalysts and toluene/benzyl alcohol oxidation using noble metal catalysts.

The second strategy could be based on bio-mimetic catalysis using porphyrin/ phthalocyanine based catalysts incorporated in metal-organic framework materials. This strategy has roots in the ability of isolated metal sites in porphyrins/ phthalocyanines to activate molecular oxygen and perform oxidation, as well as other, reactions. Mention was made in Chapter 1 of an iron phthalocyanine system which oxidises methane to formic acid but was unstable and not re-useable when used with hydrogen peroxide as the oxidant. Similar systems can be rendered more stable through smart catalysts design or by using different oxidants, preferably molecular oxygen. A vast amount of literature exists on this topic and recently advances have been made where the porphyrin units have been incorporated into MOF's. During these PhD studies this was also developed by myself at the CCI labs but not published[c]. The advantage is the ability to have a high concentration of active sites in a porous material which may offer confinement of the substrate or higher localised substrate concentration as MOF's are known high volume storage materials. Further to this MOF's may also confer acidic properties depending on which organic molecules are chosen to link the structure and present and exciting unexplored are for catalyst design and applications. At this stage testing in-house examples has not yet begun but it is envisaged for the future and is indeed a step change in the direction of true molecular design of catalysts. It is this level of design that will help heterogeneous catalysis scientists to conqueror challenging issues such as partial methane oxidation.

---

[c] See Appendix 11 for an example

Appendix 1

TEM images of Pd/TiO$_2$ and Pt/TiO$_2$ catalysts prepared by CVI showing highly dispersed small nanoparticles in support of the hypothesis that all CVI materials made from acetylacetonate precursors have a very narrow size distribution of very small metal nanoparticles as also observed with Fe/ZSM-5(30) of varying Fe loading.
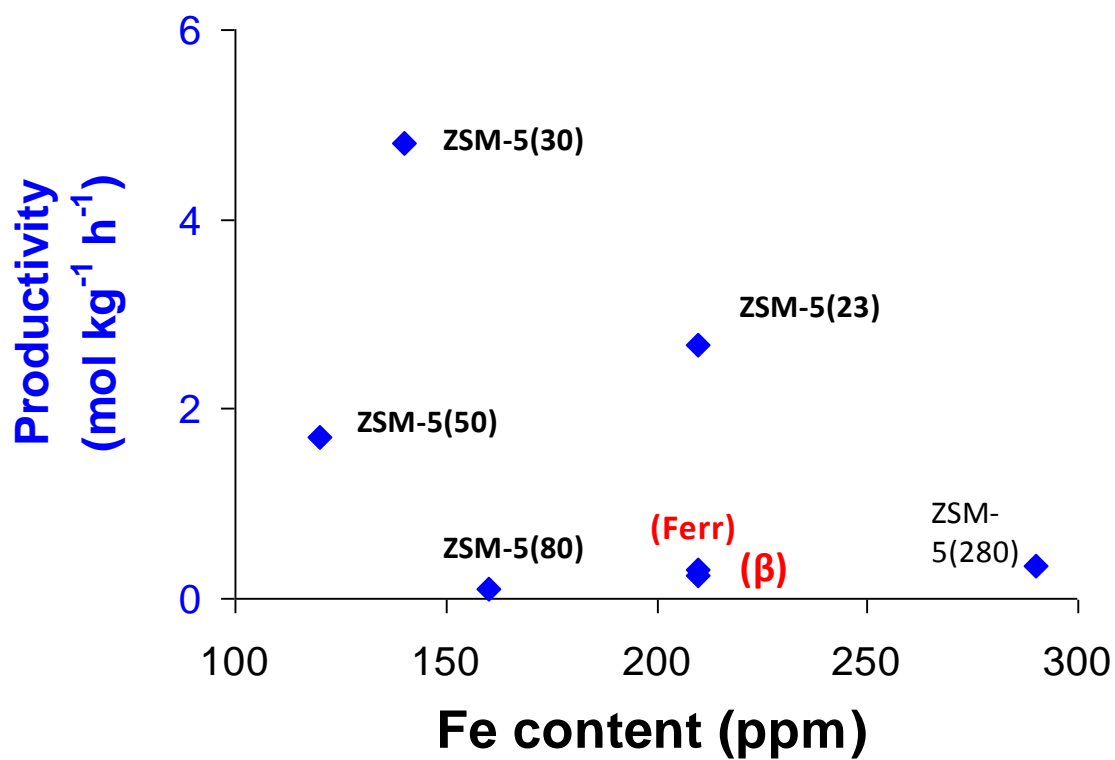
MFA6 – 2.5wt% Pd/TiO2
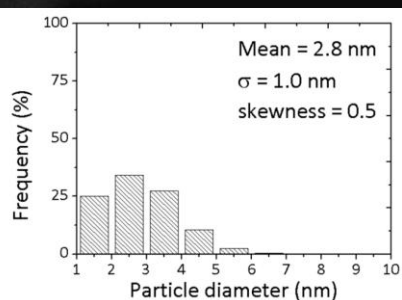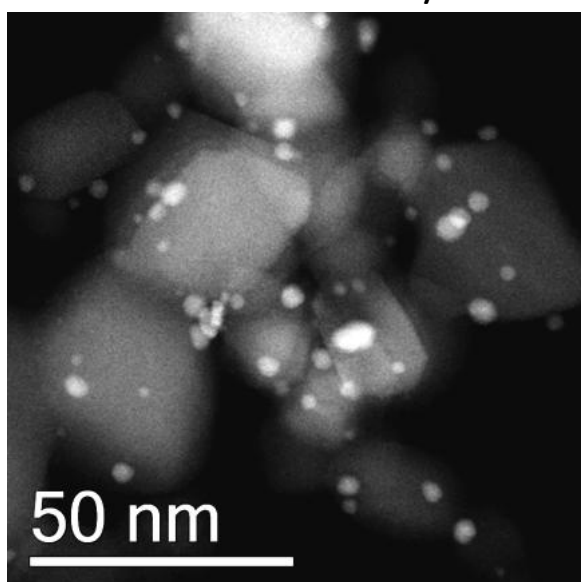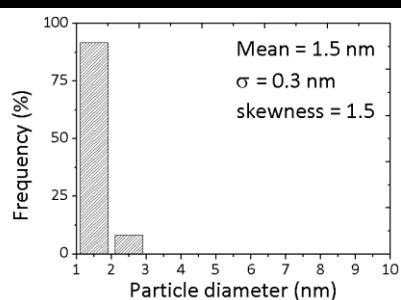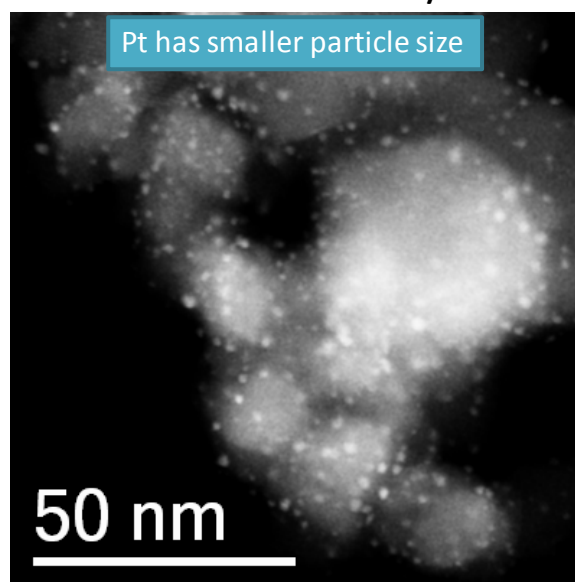

MFA7 – 2.5wt% Pt/TiO2

Fe content and catalytic activity of commercial zeolites tested for methane oxidation under standard conditions. ZSM-5 catalysts are presented along with Ferrerite (Fer) and zeolite beta (β).

Appendix 3

Catalytic activity of commercial ZSM-5(x) versus their $SiO_2:Al_2O_3$ content. Catalysts calcined at 600°C in static air and tested under standard conditions.
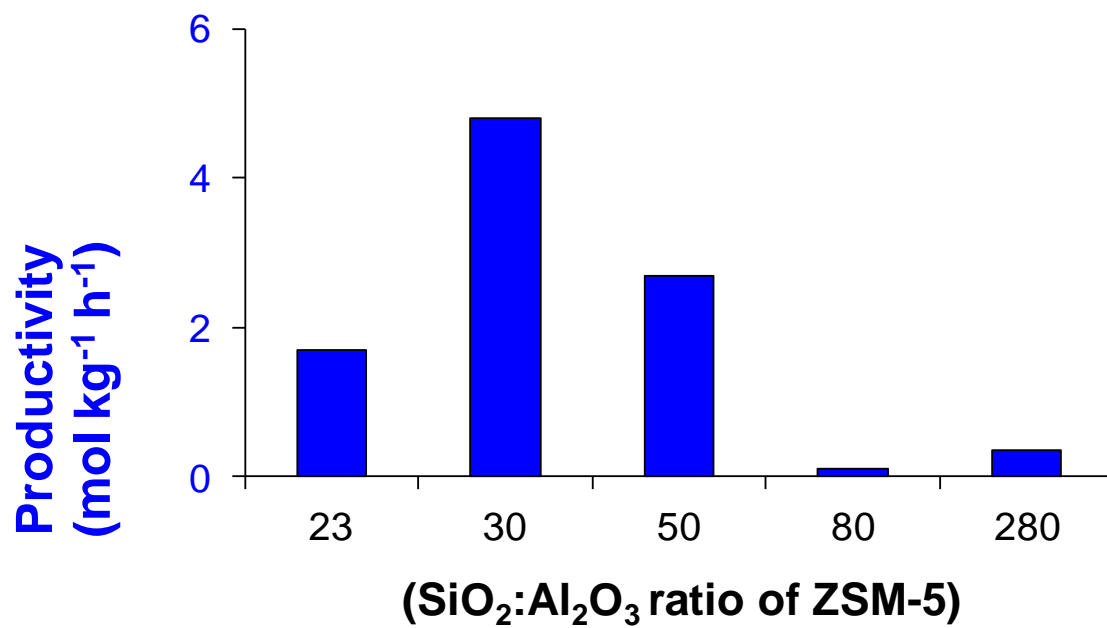
Appendix 4

Effect of heat treatment on the activity of Fe in ZSM-5(30) and the correlation to a shift in Fe $^{3+}$ from tetrahedral to octahedral coordination as observed by XANES spectra (pre-edge feature).
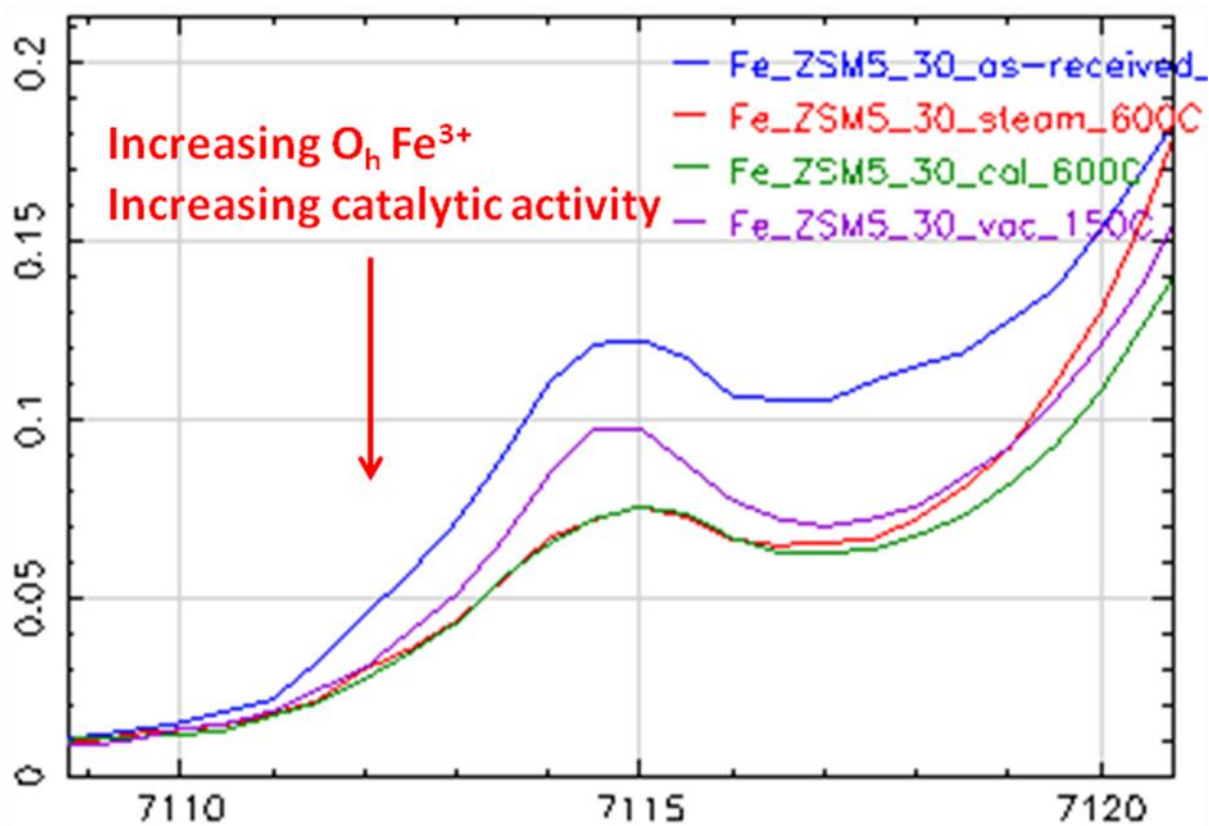
Appendix 5

Assignments of peaks in UV-VIS spectra for Fe containing MFI and SiO_2 materials based on previous studies.

| Peak	Assignment	References
>500nm	Bulky iron oxides	17, 30 in Chapter 3
>400nm	Smaller surface iron oxides	17, 29, 30, 31 in Chapter 3
387nm	Small Fe oligomeric species, mixed O_h/ T_d state	17, 30, 31 in Chapter. 3
333nm	O_h Fe^{3+} in small clusters like iron hydroxides (external)	29 in Chapter 3
~224nm, 278nm	O_h Fe^{3+} in extra-framework species or complexes	29 in Chapter 3
212-218nm , 240nm	T_d Fe^{3+} species in the zeolite channels	29, 35 in Chapter 3
256-258nm	Fe^{3+} in small clusters (oxidic) within the zeolite channels	17, 29 in Chapter 3

Appendix 6

IR spectra obtained the ZSM-5 and iron doped ZSM-5 materials showing the presence of iron oxides but lack of a characteristic 656cm^{-1} stretch for Fe-O-Si unit (Fe $^{3+}$ in T_d coordination in the zeolite framework).
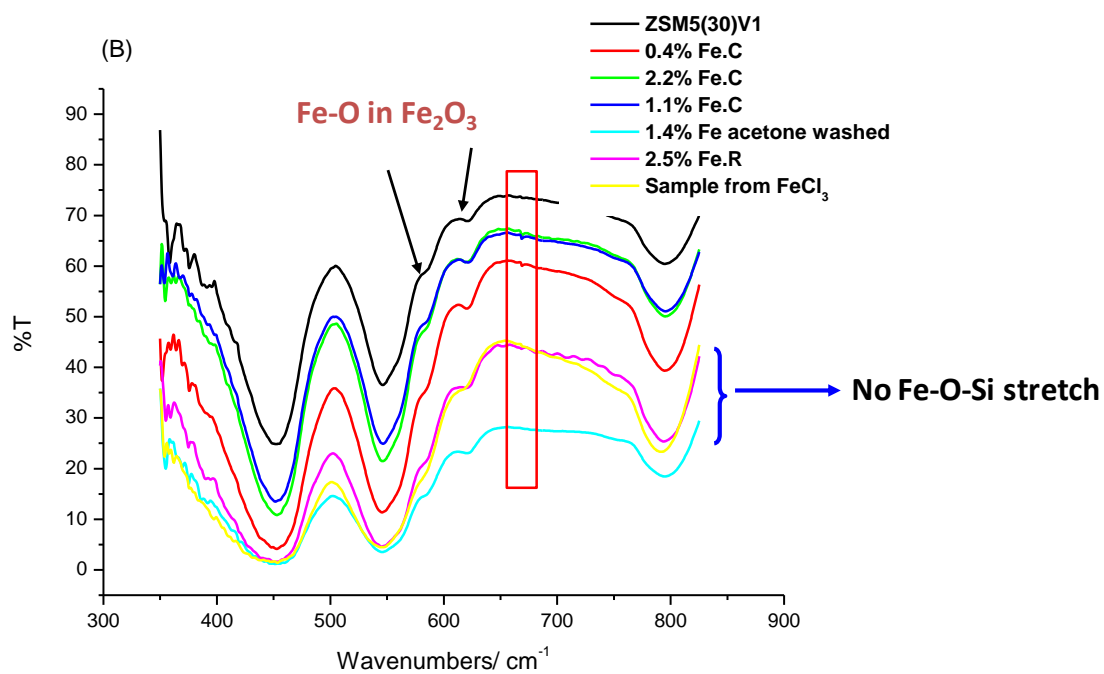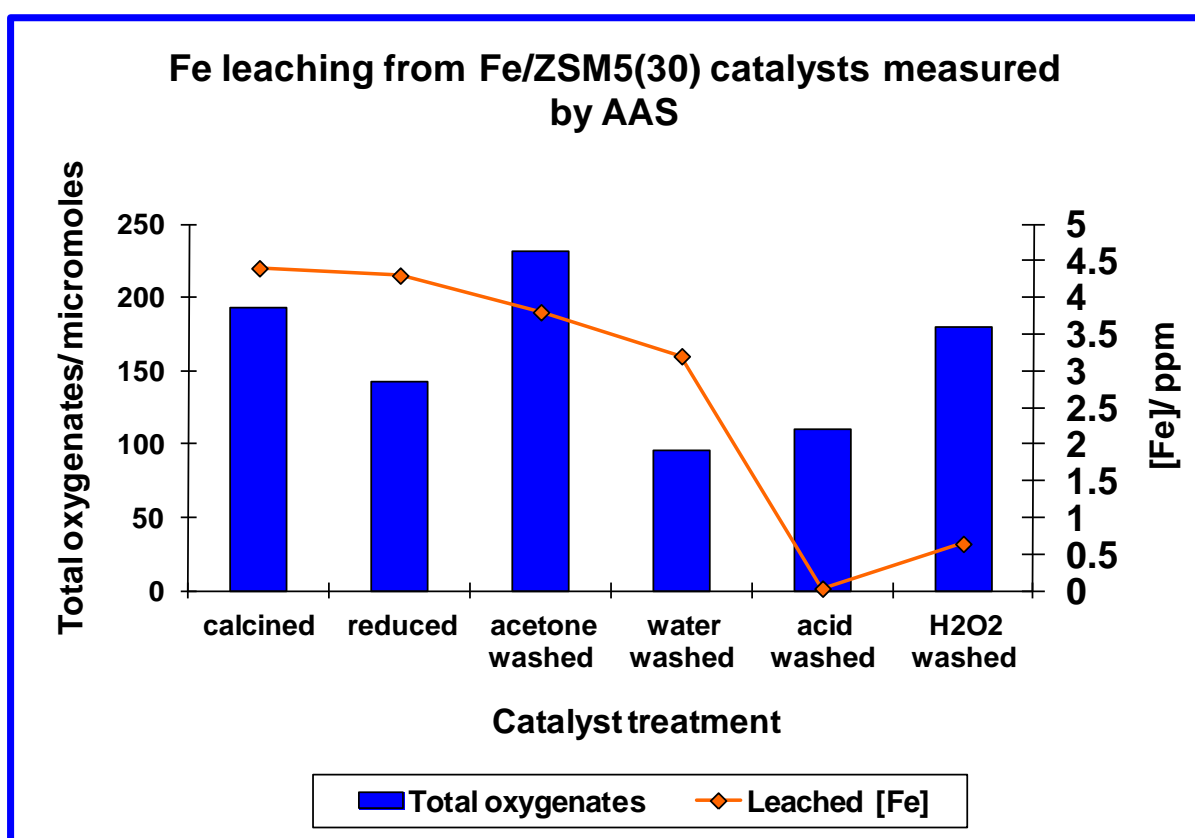
Appendix 7

TEM images of 1.5wt% Fe/ZSM-5(30) prepared by ion exchange from $Fe(NO_3)_3$(aq) showing large surface iron oxide species (circled in red) which is not observed when using the CVI technique to deposit Fe onto ZSM-5(30).
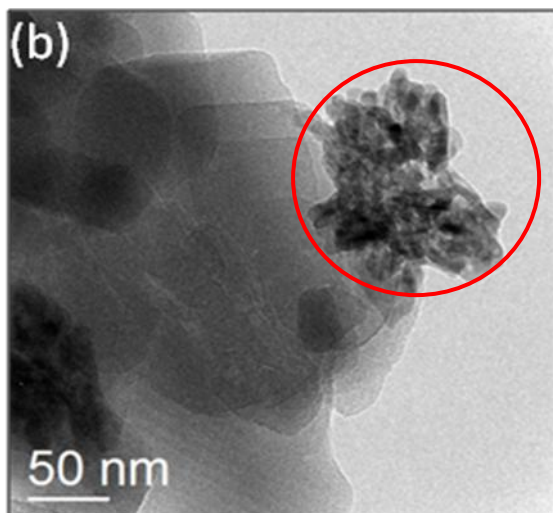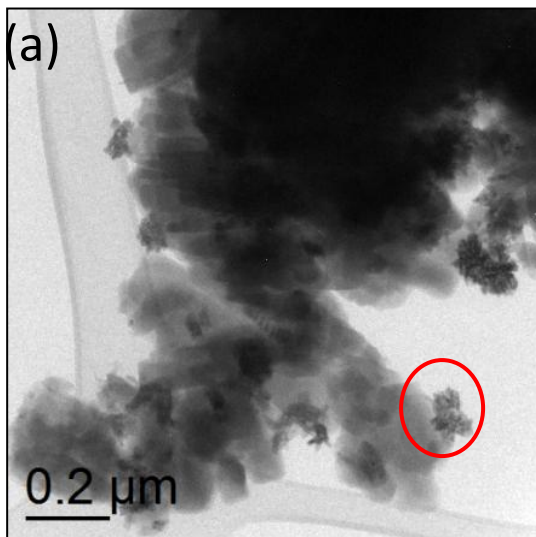
Appendix 8

Leaching measured from Fe/ZSM-5(30) catalysts prepared using the CVI technique. In all cases the maximum leaching observed was less than 5ppm. Catalysts were tested under standard conditions. 5ppm of Fe(aq) cannot account for the observed catalytic activity at 0.5h reaction.
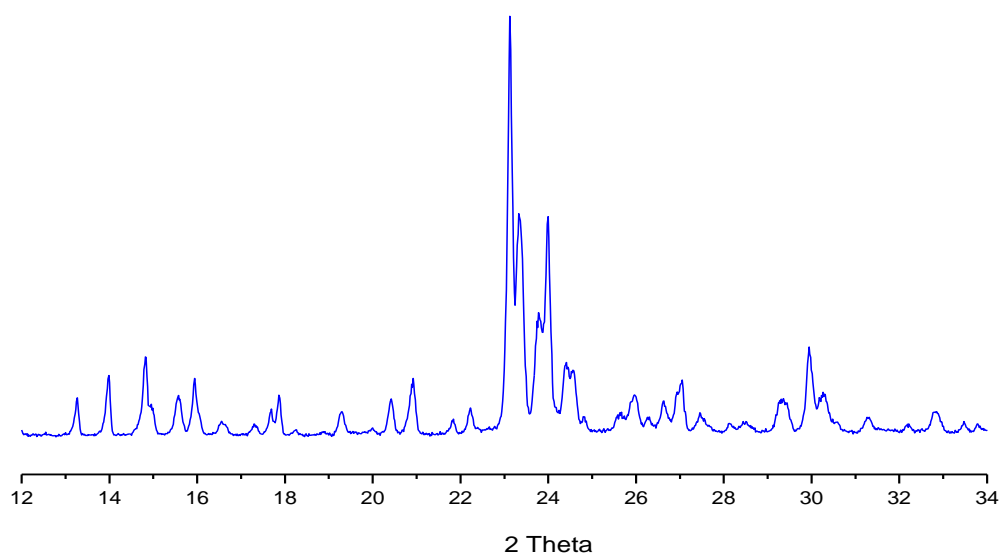

Fe leaching from Fe/ZSM5(30) catalysts measured by AAS

Appendix 9

Confirmation of silicalite-1 structure of Fe/Sil-1 (HTS) via a matching XRD pattern match to authentic silicalite crystalline structure (as TS-1) reported in literature.
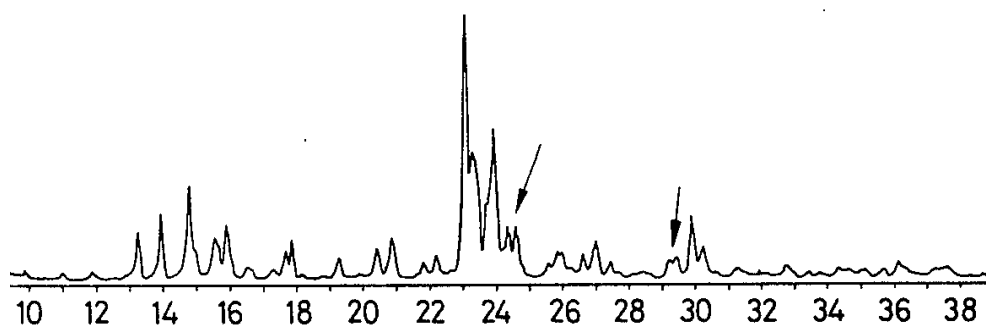
XRD of MFI structure taken from literature (Taramasso,M.; Perego, G.; Notari, B. *US Patent* 4410501 (1983)).

XRD of calcined Fe/Sil-1 prepared by hydrothermal synthesis by C.Hammond.